Loughborough University

Development of Characterisation and Quality Potency Assays for Human Mesenchymal Stem Cells

by

Alexander K. C. Chan

A Doctoral Thesis

Submitted in partial fulfilment of the requirements for the award of

Doctor of Philosophy of Loughborough University

Centre for Biological Engineering

Department of Chemical Engineering

Loughborough University

Abstract

Regenerative medicine and cell therapies hold great potential to treat a variety of medical conditions. Product characterisation of these therapies is particularly difficult as they pose regulatory challenges due to donor heterogeneity and the lack of standardised lot release tests that can reliably predict *in vivo* function. Human mesenchymal stem cells (hMSCs), also called multipotent stem cells or mesenchymal stromal cells, are a viable option in cell therapies due to their immunosuppressive and pro-angiogenic functions. Currently there are no standardised methods or potency assays to quantify these properties.

To address this, five individual hMSCs lines from different donors were created and characterised based upon growth rate, differentiation capability and extracellular surface protein expression. A novel multiparameter flow cytometry method to characterise the cells based upon extracellular surface markers was developed that supports high-throughput and high-content analyses.

Three candidate lines were taken forward and assessed in multiple *in vitro* bioassays that examined the hMSC immunosuppressive response to a defined inflammatory environment, effect on T-cell proliferation, and effect on a mixed lymphocyte population.

Next, the angiogenic properties were assessed using human umbilical vein endothelial cells (HUVECs) tube formation as a model for cardiac regeneration. This involved utilising automated time lapse microscopy techniques coupled with image analysis software to quantify endothelial to tube formation. Further analysis of the hMSC secretome revealed differences in the levels of pro-angiogenic cytokines such as vascular endothelial growth factor, hepatocyte growth factor and IL-8. Significant differences in angiogenic potency were found between the hMSC lines.

This thesis highlights the need to develop specific assays that reflect the intended clinical action. Taken together, these quantitative approaches provide valuable tools to measure hMSC quality and potency, and supports continued efforts to improve characterisation strategies for cellular therapies.

Keywords: Regenerative medicine, human mesenchymal stem cell, characterisation, potency assay, multiparameter flow cytometry, immune suppression, angiogenesis

Acknowledgements

My PhD has been the largest undertaking of my academic career thus far and it would be incomplete without the acknowledgment of the people who have supported me throughout the process.

First and foremost, my appreciation and thanks go to my supervisors, Dr Karen Coopman and Prof Chris Hewitt. Not only have they guided me through the PhD but allowed me to pursue my own ideas and interests to become the scientist I am today.

I could not have done this without the support of everyone at the CBE, not only were they great colleagues but great friends too. A special thanks to Qasim whose guidance gave me a head start in the lab and always provided valuable insights and discussions. Thanks to Andy for his thorough (and often long winded!) advice; Petra for her input and proofreading; and of course to Emma, my work wife, for all of her help and reminding me about the fun side of lab work.

My time at Loughborough would not have been as enjoyable if it wasn't for the all friends along the way: Maz, Nat, Tim, Jen, Jon, Preeti, Matt and Mark. I would also like to thank to the CBE cycling team, Tom, Dave, and Lyness, who provided much needed breaks out of the lab and into the hills of Leicestershire.

My family, especially my parents and brother, have provided constant love, support and encouragement from the very start. I cannot thank them enough.

Finally, I must thank Flo for her love and never ending support through the good times and the bad. I could not have done this without her by my side.

Publications & Presentations

Publications

Chan, A., Orme, R.P., Fricker, R.A. and Roach, P. (2013) 'Remote and local control of stimuli responsive materials for therapeutic applications', Advanced Drug Delivery Reviews, 65(4), pp. 497–514. doi: 10.1016/j.addr.2012.07.007.

Chan, A.K.C., Heathman, T.R.J., Coopman, K. and Hewitt, C.J. (2013) 'Multiparameter flow cytometry for the characterisation of extracellular markers on human mesenchymal stem cells', Biotechnology Letters, 36(4), pp. 731–741. doi: 10.1007/s10529-013-1422-0.

Heathman, T.R.J., Rafiq, Q.A., **Chan, A.K.C**., Coopman, K., Nienow, A.W., Kara, B. and Hewitt, C.J. (2016) 'Characterization of human mesenchymal stem cells from multiple donors and the implications for large scale bioprocess development', Biochemical Engineering Journal, 108, pp. 14–23. doi: 10.1016/j.bej.2015.06.018.

Chan, A.K.C., Neale-Edwards, E., Hewitt, C.J., Coopman, K. (2016) A High-Throughput Angiogenic Potency Assay to Characterise Donor Variation in Human Mesenchymal Stem Cells *(In preparation)*

Conference Presentations

Chan, A. K. C., Coopman, K. & Hewitt, C. J. Multiparameter flow cytometry for the characterisation human embryonic and mesenchymal stem cells. (Invited Oral Presentation). *BD High End Users Meeting, Oxford, UK.* 11th April 2014

Chan, A., Coopman, K. & Hewitt, C. J. Development of an immune modulatory assay for quality and potency characterisation of human mesenchymal stem cells. (Oral Presentation) *ECI Scale-up and manufacturing of cell-based therapies. San Diego, California, USA.* 5th-8th January 2014

Chan, A., Coopman, K. & Hewitt, C. J. Multiparameter flow cytometry assay for human mesenchymal stem cells. (Oral Presentation) *FIRM Symposium. Girona, Spain.* 26th - 29th September 2013

Contents

List of Figures

List of Tables

Chapter 1

Literature Review

Regenerative medicine aims to restore or regenerate the human cells, tissue, or organs back to normal function. This includes the use of cell therapy, tissue engineering and gene therapy. This growing industry of scientific improvement can lead the way to treat currently unmet clinical need and, in future, form part of standardised healthcare treatments.

To pass regulations in the U.S (Food and Drug Administration, FDA) and E.U (European Medicines Agency, EMA) there is a need to fully characterise the cells in terms of identity, purity, safety, and biological activity. Evaluation through potency assays plays a key role in defining the overall quality and efficacy of a cell therapy. Potency assays are designed to produce a quantitative measure of the biological activity and ideally should reflect clinical efficacy. The complexity increases as new discoveries reveal different mechanism of action all of which may be linked to the outcome.

Human mesenchymal stem cells (hMSCs) are a rare population of adult stem cells typically found within the bone marrow niche, they can be readily isolated and expanded *in vitro* to gain a therapeutically relevant dose. Originally hMSCs were utilised in orthopaedic tissue engineering areas as they are able to differentiate into bone and cartilage lineages.

More recently, researchers have discovered they can suppress and modulate the patients' immune system, and secrete bioactive molecules in response to the local environment. These properties have made them an exciting candidate to treat auto-immune disorders; nervous system diseases; and heart and circulatory damage.

However, as hMSCs are a biological entity derived from individual donors there will be inherit variation to how they perform *in vivo*. Therefore there is a requirement to develop tests that can accurately measure their relevant mechanism of action and can be performed in line with the manufacturing process. Potency tests for hMSCs should reflect the intended biological activity and form part of the characterisation/quality panel from isolation, expansion, preservation to patient delivery.

Hence the question, how do we measure quality and determine if the cell product passes an acceptance/rejection criteria?

Addressing these challenges will be key to the overall success of a regenerative medicine product. The aim of this thesis will discuss and present a number of solutions to these challenges.

1.1 Regenerative Medicine & Cell Therapies

Regenerative medicine refers to the methods of repairing and replacing damaged cells, tissue or organs to normal function by the means of cell therapies, tissue engineering or gene therapy. Until recently the healthcare field has relied on three main areas: pharmaceuticals, medical devices, and biologics. Regenerative medicine and cell therapy is set to become the fourth main healthcare area in the upcoming years. The field has been expanding rapidly within the last decade from research laboratories to first in-man trials to late stage clinical trials. By 2008 global sales reached $410 million and was expected to reach $2.7 billion in 2012 and $5.1 billion in 2014 (Mason et al. 2011). More recent

transactions have also demonstrated the growith of the field such as an alliance between Mesoblast and Cephalon, worth $1.7 billion; and Genzyme and Orisis, worth $1.25 billion (Vertès 2016).

Regenerative medicine can be further subdivided into tissue engineering and cell therapies. Typical tissue engineering strategies involves the combination of a scaffold and adequate cells. The scaffold, either a natural or synthetic polymer, provides support and structure to the implanted area and can guide cell proliferation and function in a three-dimensional environment (Mota et al. 2012). Such cell-scaffold constructs have been used successfully for skin and wound healing (Groeber et al. 2011), bladder replacement (Atala 2011), airway reconstruction (Fishman et al. 2014) and cartilage repair (Kuo et al. 2006) to name a few. On the other hand, cell therapies are those without the use of a physical support and are usually just the cells alone. The cells are either delivered locally to the site of injury or delivered systemically. Examples of this include intravenous injection of CAR-T cells (Adusumilli et al. 2014) and expanded adipose-derived mesenchymal stem cells (Ra et al. 2011).

Maintaining cells *ex vivo* requires detailed characterisation methods, most simply these can be cell morphology and/or growth rate. As biochemistry and molecular biology research develops new methods, characterisation becomes more sophisticated from cell morphology, gene analysis to protein production. This allows for more quantitative measures of cell characterisation which are crucial for the development of future cell therapies.

Characterisation of a biological product allows specifications to be established, this enables the development of an acceptance criteria to determine if the cell product is accepted or rejected for release. Ensuring the critical quality attributes (CQA) are maintained throughout the expansion and processing of these cells is essential for a functional deliverable cell therapy product.

Cell therapies require specifications from:

- **Identity:** Confirms the cell is the correct type
- **Purity:** Confirms there are no contaminations from other cell types or reagents
- **Viability:** Current FDA guidelines suggest a minimum viability specification of 70%
- **Potency:** Ensures the product has the intended function for the intended clinical effect
- **Safety:** Ensures the cell preparation does not contain harmful material and there is no tumorigenic potential (Carmen et al. 2012)

This literature review chapter will focus on identity and potency for cell therapies and later more specifically for human mesenchymal stem cells.

1.1.1 Identity & Purity

Identity assays verifies the cells' phenotype from isolation, expansion, storage, to final deliverable product to ensure the product does not adversely change. This is essential to ensure the cells are not changed through manufacturing i.e. phenotypic drift which may affect the function (Freedman 2015).

Identity assays can also measure the purity as the harvested cells from the donor may contain other cell types that are a different lineage or at a different stage of differentiation from the intended cell type. For example, in hematopoietic stem cell (HSC) transplants there will be a mixed population of T-cell, B-cells and other mononuclear cells. The amount of wanted to unwanted cells should be set and an acceptance criterion maintained. In embryonic or induced pluripotent stem cell transplantation, the cells are first differentiated before delivery, the amount of undifferentiated cells should be minimised to avoid tumour formation.

The simplest measure of identity is examining the cell morphology, this method is used in

the release testing of Carticel ® (Genzyme ®) an autologous chondrocyte implantation therapy (Carmen et al. 2012). This method is extremely subjective and results will vary depending on the operator. However, advances in automated high-content image analysis techniques have overcome this problem by quantifying morphology without the need for operator input (Zanella, Lorens, and Link 2010).

Flow Cytometry

A more specific way to identify cell is via the use of flow cytometry, this technique can analyse thousands of events (cells) per second and allows for sorting of cell populations. It is well established in the research community and has translated to good manufacturing process (GMP). In addition, standardised documentation guidelines such as the Minimum Information about a Flow Cytometry Experiment (MIFlowCyt), has increased comparability between researchers (Lee et al. 2008). To further accommodate GMP transfer, automated gating strategies can be applied to improve comparability. Suni et al. (2003) has shown this can be utilised to quantify multiple antigen specific T-cells and reduce operator-induced variability.

In flow cytometry, the cells are suspended in a moving liquid and passed through a wider sheath fluid at a different rate, the two streams of liquid do not mix and form a linear flow termed hydrodynamic focusing. The stream passes over an excitation source, usually a laser, and the cells/particles suspended within the stream causes diffraction and light scatter. Forward scatter is a measure of diffracted light off the axis giving indication to the size, side scatter is a measure of refracted light giving an indication to the granularity of the cell.

For identity analysis the cells are usually labelled with fluorescently bound antibodies, when they are passed over the laser the fluorophores are excited and light is emitted and captured by a set of filters or photomultiplier tubes (PMT). Intracellular proteins can also

be measured by fixing and permeabilising the cells before staining. The antibodies can be specific to a protein or marker which identifies the phenotype of the cell, e.g. when identifying sub-populations of hematopoietic cells researchers will first label either the CD4 or CD8 extracellular surface maker.

More commonly it is now possible to measure multiple markers simultaneously. This is achieved by binding multiple specific fluorescently-bound antibodies that emit light at different wavelengths and using corresponding detection filters that can distinguish between the wavelengths. This method, called multicolour or multiparameter flow cytometry can be used to distinguish distinct cell phenotypes down to rare-population analysis, such as hematopoietic stem cells (HSCs) from the bone marrow niche (Autissier et al. 2010; Nilsson, Bryder, and Pronk 2013).

Cells can be stained and measured within hours, coupled with high-throughput sample analysis, flow cytometry has been widely adopted in the cell therapy field for identity assays. In chimeric antigen receptor T cells (CAR-T cell) therapy flow cytometry is used to ensure expression of the CAR domain following transduction and *in vitro* expansion (Kochenderfer et al. 2014).

Another report by Basford, Forraz, and McGuckin (2010) describes the development of a multiparameter immunophenotyping method for umbilical cord blood cells, the authors demonstrate that using this method the cells could be collected, processed, cryopreserved and immunophenotyped within 5 hours.

The development and use of multiparameter analysis for the characterisation of hMSCs is detailed in Chapter 4.

Gene Expression

Microarray gene expression profiling can also be used to characterise cells. In these types of studies the cells are sacrificed and the RNA is isolated. The RNA are reverse-transcribed into cDNA nucleotides with different fluorescent dyes. Next, the samples are hybridised onto a glass slide with specific spots containing its complementary sequence. The amount of cDNA (and fluorescence) will be proportional to the initial amount of starting RNA (Tan 2003). Microarrays allows the examination of thousands of genes within a small sample and can be used to identify specific biomarkers and gene upregulation (Tarca, Romero, and Draghici 2006). In terms of hMSCs, previous reports have identified multiple adhesion proteins, growth factor receptors and cell motility markers that discriminate them from CD34+ blood cells in the same sample (Silva 2003). Jeong et al. (2007) compared the gene expression of bone marrow hMSCs to peripheral blood mononuclear cells and to umbilical cord hMSCs. They found clear differences between the BM-hMSCs and PBMC, such as collagens, extracellular matrix proteins and growth factors; but when compared to the umbilical cord hMSCs there were over 13,000 common genes.

1.2 Potency Assays for Cell Therapies

Allogeneic therapies, such as hMSC delivery, would require culture expansion *ex vivo* to provide sufficient numbers for multiple doses and patients. Therefore, they are classed as a 'more-than-minimally-manipulated cell and gene therapy' and under rules from the US Food and Drug Administration (FDA) such products require an Investigational New Drug (IND) application. Part of this includes the development of tests to measure potency as part of the final release criteria (Galipeau et al. 2016). This section will focus on the considerations for developing *in vitro* potency assays for cell therapies.

Potency testing is the quantitative measure of biological activity which leads to an ef-

fect. The evaluation of potency plays a key role in defining the critical quality attributes (CQA) of a cell therapy, this allows researchers and clinicians to determine if the product is suitable for delivery to a patient. From these assays a product specification can be developed (e.g. amount of protein produced or expression of marker) that can be used in comparability and stability analysis (Bravery et al. 2013).

1.2.1 Defining Potency and Regulations

In the pharmaceutical and cellular therapy industry, potency is a measure of the strength or effect of a drug or product where the ultimate aim is to identify and measure the key parameters that lead to clinical efficacy. Potency measurement is critical for cell therapies where it forms an essential aspect for quality control and comparability studies.

The European Medicine Agency (EMA) defines potency for a biotechnology/biological product as :

> 'The quantitative measure of biological activity based on the attribute of the product which is linked to the relevant biological properties' - ICH 6B Specifications

The ICH 6B Specifications were published in 1999 and are now superseded by Committee for Medicinal Products for Human Use (CHMP)/410869/06 specifications effective of 2008, with regards to a potency assay states:

> 'In principle the results of a potency assay should provide assurance that the amount of the active ingredient is sufficient to induce a meaningful response and that the amount is consistent from batch to batch. As such, the potency assay should be able to detect clinically meaningful changes in the amount of active ingredient in a human dose of a product.' - CHMP/410869/06

The US Food and Drug Administration (FDA) defines potency as:

> 'The specific ability or capacity of the product, as indicated by appropriate laboratory tests or by adequately controlled clinical data obtained through the administration of the product in the manner intended, to effect a given result.'
> - 21 CFR 600.3(s)

As each biologic will differ, the FDA allows for flexibility in determining what is the most appropriate test and is evaluated on a case-by-case basis. In the early stages of development it states that for some products in pre-clinical, Phase I, and early Phase II, limited quantitative bioactivity information may be sufficient. Later stages, Phase III and beyond, requires an acceptance criteria that can assure a consistently manufactured product.

Potency assays for a regenerative medicine/cell therapy product should therefore quantify the biological activity of the mechanism of action (MoA). From this a pass/fail criterion can be applied to determine the quality of the cells.

It is not uncommon for a single cell therapy product to be used for multiple clinical indications (see Section 1.7), so multiple assays can be developed for a single cell type depending on the treatment.

1.2.2 Considerations and Challenges for Potency Assay Development

Cell therapies, by virtue of their mode of action, are inherently more complex than other pharmaceuticals, and therefore further considerations must be taken into account. This section will summarise the current challenges of potency assay development for cell therapies.

Mechanism of Action and Assay Matrix

The previous section (Section 1.1.1) described characterisation in terms of identity - what the cell is; whereas potency characterisation details what the cell does. The most important aspect of a potency assay is that it must reflect the biological activity of the product and measure the mechanism of action (MoA) for example, immunosuppressive activity, protein secretion or target cell cytotoxicity. Unlike traditional pharmaceuticals where there is a single known MoA, cell therapy is further complicated by possible multiple pathways, many of which may be unknown or not fully understood, therefore a single assay may not provide a full accurate measure of potency. Multiple assays (referred to as an assay matrix), measuring different relevant MoAs can be used together to give a holistic measurement of potency (Galipeau et al. 2016). An assay matrix may consist of various analytical techniques such as flow cytometry, quantitative imaging and protein/cytokine analysis.

Length of Assay

Since there is usually a limited amount of time between the cell process/manufacture and the final delivery, the overall duration of a potency assay can determine its usefulness and implementation. For example, in hematopoietic stem cell (HSC) transplant the goal is to repopulate the patient's hematopoietic niche to produce erythrocytes and immune cells. To examine this *in vitro* a colony forming unit (CFU) assay is used where the HSCs are plated into a semi-solid culture medium and allowed to differentiate over 7-14 days. The colonies are then manually scored. The main drawback for this assay is the length of time, potency assays could be used to determine a pass/fail criteria before transfusion, therefore a delay of several days is not appropriate. Additionally, as the colonies are manually counted there is inherent variation between operators, however image analysis software packages have overcome this to provide quantitative results (Guzman et al. 2014).

Reference Material and Standards

In drug development there is a stringent definition of a drug that can be easily tested. The new drug or iteration can be compared to the reference material for compatibility testing. In an ideal case, this would be similar for cell therapies where there could be central resource to which every new preparation can be compared.

As allogeneic cell therapies will be classed under investigational new drug (IND) preparations, such as hMSCs, for therapy would require the use of a centralised standard or reference material. Basu and Ludlow (2014) suggests that for a cell therapy the reference standard should be the same cell type as the product and ideally be proven in the selected potency assays. For hMSCs it has been suggested the reference material will have details from its optimal culture conditions (ones that are universally accepted), gene expression profile of over 100 genes, a known secretome profile, various *in vitro* assays and performance (including colony forming and differentiation), and finally information regarding genomic stability during passaging and expansion (Tanavde et al. 2015).

The idea of a 'hMSC cell ruler' has been suggested that would serve as a common calibration tool and provide a central data point (Deans 2015). This would require a mixed pool of cells from multiple donors to provide adequate master and working cell banks, adherence to the minimal criteria as suggested by the ISCT and standardised culture conditions. Further functional characterisation assays may include ability to modulate immune function, promote engraftment, clonal assays and key secretome profiling (Viswanathan et al. 2014).

Implementation in a Manufacturing Process

Potency assays can also be utilised in informing process development and manufacturing of cell therapies where the final deliverable product is markedly different from the starting

material. Perhaps the most important role for potency assays within bioprocess is to be able to detect changes in the manufacturing process. As cell therapies develops over time from small-scale Phase I and II trials into large-scale and Phase III trials there will be changes in the manufacturing and processing of the cells. These may include scale-up methods, medium formulation, harvesting, final fill/finish, and even facility changes, such as change in manufacturing centre; as such the cells should be tested throughout the process (in-process testing) and at the end of production (lot release testing) (Stroncek et al. 2007). Due to nature of cell therapies most institutions have built specialised good manufacturing practice (GMP) facilities to produce the cells. These are to ensure that the products are made in a consistent environment, each dose meets a required specification and lot-to-lot variation is minimised.

When these changes do occur, potency assays should be able to reflect if the changes are detrimental to the MoA. As such, potency assays must be reliable and robust enough to ensure the final product is within the specifications of the reference sample.

1.3 Clinically Relevant Cells for Therapy

Cell therapy and regenerative medicine encompasses a variety of cell types that each have different actions and clinical applications. This section shall briefly outline other common cell therapies and their potency assays, following this, mesenchymal stem cells shall be discussed in greater detail.

1.3.1 Hematopoietic Stem Cells

Haematopoietic stem cells (HSCs) are a rare subset of cells found within bone marrow or umbilical cord blood and are responsible for producing all other blood types. They are defined functionally by their extensive proliferation, self-renewal, and differentiation

capability (Pineault and Abu-Khader 2015). HSCs transplants are used to re-establish haematopoietic function in patients where the bone marrow is damaged. They have been used successfully to treat autoimmune diseases such as multiple and systemic sclerosis (Karussis et al. 2013). A successful transplant is dependent on the cells being able to establish in the bone marrow niche, proliferate and differentiate into mature neutrophils, platelets and erythrocytes.

Current accepted potency assays examine the proliferation rate via adenosine triphosphate (ATP) changes or via aldehyde hydrogenase (ALDH) (Sylvester 2011; Veeraputhiran et al. 2011). For greater assessment of functionality the colony forming unit (CFU) assay can determine the ability of the progenitor cells to produce differentiated daughter cells of the blood lineage and number of clonogenic cells. However, due to the qualitative nature of this assay, there is considerable variability in quantification and analysis (Nawrot et al. 2011).

1.3.2 Embryonic Stem Cells & Induced Pluripotent Stem Cells

Human embryonic stem cells (hESCs) are pluripotent cells derived from the inner cell mass (ICM) of an early stage pre-implantation embryo (Thomson 1998). They are able to self renew, show high alkaline phosphatase activity, and differentiate into all cell types of the endoderm, ectoderm and mesoderm lineage, thus making them an ideal cell source for tissue engineering and regenerative medicine. The first patient trial was to be conducted in 2010 by Geron Corporation to treat patients suffering from spinal cord injuries using GRNOPC1 - a oligodendrocyte cell derived from hESCs (Alper 2009). However, after only enrolling four patients the trial was officially ended following safety concerns due to cyst formation. In another case, Advanced Cell Therapy (ACT) initiated Phase I/II clinical trials for the treatment of Stargardt's Macular Dystrophy and Dry Age-Related Macular Degeneration using retinal pigment epithelial cells derived from hESCs (Schwartz et al. 2012).

Several approaches have been used to characterise hESCs including flow cytometry to analyse surface markers, gene microarray studies and multi-lineage differentiation. In 2007, the International Stem Cell Initiative sought to compare 59 different hESCs from 17 different laboratories to examine common markers (Adewumi et al. 2007). The authors found common expression of surface glycolipids SSEA3 and SSEA4, TRA-1-81 along with the pluripotent genes NANOG, OCT4, and SOX2.

It is important to note that hESCs are not implanted in an undifferentiated state as this could lead to teratoma formation (Hentze et al. 2009). This can be avoided by ensuring that all the cells have differentiated and any undifferentiated ones are removed. Therefore, 'potency' of hESCs is generally defined as the ability to differentiate into the required cell type (Hu et al. 2010).

In 2006, Takahashi and Yamanaka (2006) published protocols for the development of induced pluripotent stem cells (iPSCs). These pluripotent cells are derived from fully differentiated adult tissue via the addition of four key transcription factors, Oct4, Sox2, cMyc and Klf4. As they can be derived from the patient's own cells this removes the donor-patient mis-match as seen in other tissue transplants and will remove the need for immunosuppressive medication. Similarly to hESCs, iPSC potency is usually measured by their differentiation capability.

1.3.3 CAR T-Cells

Moving away from stem cells, there has been a tremendous amount of investment into the development of T-cell therapy for cancer treatment. T-cells - so called as they mature in the thymus, are one of two primary lymphocytes, the other type being B-cells. Together they make up the main components of the adaptive immune system, which act to target specific pathogens.

The development of chimeric antigen receptor T-cells (CAR T-cell) has allowed for even more specific targeting of cells. In this process, T-cells are isolated from the patient and modified *ex vivo* to include a targeting domain specific for tumour antigens such as CD19 - an antigen expressed on B-cell cancers. Current second and third generation CAR-T incorporate co-stimulatory domains such as CD28 and OX40 to enhance specification (Sadelain, Brentjens, and Riviere 2013).

To date CAR T-cell therapy has been shown to be effective in patients with B and T-cell malignancies. CD19 is a B-cell surface protein expressed in development and in nearly all B-cell malignancies including chronic lymphocyte leukaemia and non-Hodgkin lymphomas (Scheuermann and Racila 1995). This near-universal expression has made it an attractive target for CAR T-cell therapies. In a recent meta-analysis of 14 recent clinical trials Ghorashian, Pule, and Amrolia (2015) reported that the overall response rate can range from 50-90% in patients with acute lymphoblastic leukemia (ALL). For solid tumours, clinical efficacy is proving to be more challenging as there is no single tumour-specific antigen thus removing the selectivity seen with CD19 leukemias. It has been suggested that CAR T-cells can be modified to recognise multiple antigens that may allow specificity to unique expression found only on tumour cells, for example, Wilkie et al. (2012) reported the generation of a 'split signal CAR' where full activation of the T-cell would be limited to tumours co-expressing ErbB2 and MUC1 in breast cancers.

Characterisation of these cells is relatively simple, typically by flow cytometry analysis of the CD19 targeting domain, CD4 and granulation markers such as CD107a (Kochenderfer et al. 2011). Due to the specific engineered action of the CAR-T, potency assays are based around cytokine production (e.g. IL-2 production) and cytotoxic/lytic activity when incubated with target cells (Lamers et al. 2010).

1.4 Human Mesenchymal Stem Cells

1.4.1 Discovery and Nomenclature

In the late 60's and early 70's Friedenstein and colleagues first described a rare population of non-hematopoietic cells derived from the bone marrow aspirates of mice femurs. *In vitro* these adherent cells were able to form distinct colonies initiated by single cells and were termed colony forming unit fibroblasts (CFU-Fs). These cells could also make bone and reconstitute a hematopoietic microenvironment in subcutaneous transplants. (Friedenstein et al. 1968; Friedenstein, Chailakhjan, and Lalykina 1970).

In vivo transplantation led to the formation of various mesenchyme derived cells such as adipocytes (fat), chondrocytes (cartilage) and osteoblasts (bone) and were termed 'bone marrow stromal cells' (Friedenstein, Chailakhyan, and Gerasimov 1987; Owen and Friedenstein 1988). The term 'mesenchymal stem cell' (MSC) was coined by Arnold Caplan to describe the potential of these cells to give rise to a multitude of mesenchymal tissue along distinct pathways (Caplan 1991). This was rapidly adopted and still is the name of choice. The terms 'mesenchymal stem cell', 'marrow stromal cell' and 'mesenchymal stromal cell' are often used interchangeably.

Pioneering work by Pittenger (1999) (as part of Osiris Therapeutics Inc) demonstrated true multilineage potential and flow cytometry characterisation of hMSCs, this led the way for their use in tissue engineering and regenerative medicine. Due to this rooting in the biomedical field and its potential for regenerative medicine hMSCs are still the most widely published stem cell type when compared to embryonic and induced pluripotent stem cells (Figure 1.1).

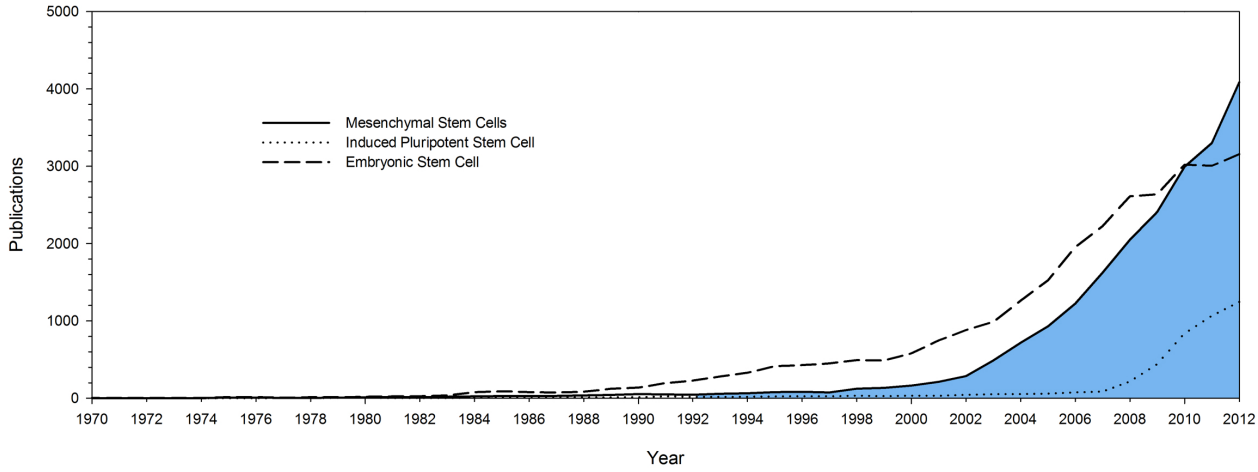

Figure 1.1: Timeline for number of publications per year from 1970 to 2012 of mesenchymal stem cells (solid line, blue fill), induced pluripotent stem cell (dotted line) and embryonic stem cells (dashed line). Data collected from http://www.ncbi.nlm.nih.gov/

1.4.2 Sources of hMSCs

Since the discovery of bone-marrow derived hMSCs, there has since been a number of other tissue from where hMSCs have been isolated. These include both adult tissue such as dental pulp and peripheral blood, and foetal tissue, such as the placenta and umbilical cord blood, other sources are listed in Table 1.1.

Whilst being phenotypically similar and adhering to the International Society for Cell Therapy (ISCT) minimal criteria for an hMSC (see section 1.4.3) there notable differences between the sources. For example in a comparative analysis between bone marrow, adipose and umbilical cord hMSCs, Jin et al. (2013) found all cells exhibited the same extracellular marker profile and showed tri-lineage differentiation. The differences arose from growth rate where UC-hMSCs had the highest rate of proliferation and lower expression of senescence markers such as p53 and p16. In addition, these cells showed greater immuno-suppressive ability by higher secretion of an anti-inflammatory protein, Ang-1, whilst in co-culture with activated macrophages. This is supported by an earlier study

Table 1.1: Sources of human mesenchymal stem cells from adult and foetal tissue

Source	**Abbreviation**	**Reference**
Adult sources of hMSCs		
Bone marrow	BM	Friedenstein et al. (1968)
Articular Cartilage	AC	Alsalameh et al. (2004)
Adipose Tissue	AT	Bunnell et al. (2008)
Peripheral Blood	PB	Tondreau et al. (2005)
Skeletal Muscle	M	Young et al. (2001)
Dental Pulp	DP	Gronthos et al. (2002)
Foetal sources of hMSCs		
Umbilical Cord	UC	Lee (2004)
Placenta	P	inAnker et al. (2004)
Wharton's Jelly	WJ	Wang et al. (2004)

by Kern et al. (2006) who also showed that UC-hMSCs had the highest growth rate. However, these authors were unable to demonstrate adipocyte differentiation from the UC-hMSCs.

Even though there are multiple sources of isolation for hMSCs it is now widely agreed that they all reside with the perivascular niche i.e. surrounding or within blood vessels (Crisan et al. 2008; Silva, Caplan, and Nardi 2008). The pericytes described by Crisan et al. (2008) exhibited all properties of an an hMSC such as tri-lineage differentiation, expression of markers, *in vitro* expansion. This has led to suggestions that all hMSCs are pericytes or a specialised subset of pericyte (Caplan 2008; Caplan and Correa 2011) .

Because they are the most widely studied type, bone marrow derived hMSCs will be the focus of this thesis.

1.4.3 Characterisation

As hMSCs can be obtained from multiple sites one of the major challenges is the presence of a single definitive marker or characteristic which defines a true hMSC. Cell types are commonly characterised by their expression of certain extracellular glycoprotein markers. These cluster of differentiation (CD) molecules are often proteins such as ligand receptors or adhesion proteins that are key for its function. A combination of markers have been suggested by the ISCT to unify characterisation profiles used by different researchers (Dominici et al. 2006). They state that hMSCs must be positive for CD73, CD90 and CD105 and must also lack CD11b or CD14, CD19 or CD79a, CD34, CD45, and HLA-DR as these are representative of haematopoetic cells that may be present due to the initial isolation from the bone marrow. The ISCT minimal guidelines also state that hMSCs must be tissue culture plastic-adherent cells and have the potential to differentiate towards adipocyte, chondroblasts and osteoblasts lineages.

Recently other researchers have suggested a single positive marker for hMSCs. Jones et al. (2010) published a report that described the isolation of hMSCs based upon $CD45^{low}/CD271^{+}$ expression from trabecular bone. These cells possessed the minimal characteristics as suggested by the ISCT but were found to be more immuosuppressive and had strong expression of *Wnt*-associated genes that are linked to oesteoblast-mediated bone formation when compared to $CD271^{-/low}$ cells (Kuçi et al. 2010; Churchman et al. 2012). However, CD271 may only be a suitable marker for bone marrow derived hMSCs as other studies have used this marker to isolate cells from umbilical cord blood and found them to have poor proliferative potential and differentiation capabilities (Attar et al. 2013; Watson et al. 2013).

1.4.4 Potency Assays for hMSCs

Currently there are no standardised potency assays to measure the quality of human mesenchymal stem cells. As potency measurements are designed specifically for a product and its intended use the FDA does not make recommendations for potency assays or propose an acceptance criteria (Galipeau et al. 2016). The vast majority of clinical trials using hMSCs exploit their trophic/paracrine ability, which does not require their tri-lineage differentiation into the adipocyte, chondroblast and osteoblast lineages; however this ability is still included as a preclinical release test for many ongoing trials (Kebriaei et al. 2009; Vaes et al. 2012; Gupta et al. 2013). Characterisation and purity testing can only provide information on the phenotype of the cell population, however this does not reflect their mechanism of action (MoA) for therapeutic action.

As previously discussed in Section 1.2, cell therapies will have a specific test or multiple tests to examine their potency for a given therapy and not a 'one size fits all' approach. Due to the existence of many therapeutic areas for hMSCs (see Section 1.5 and 1.6) there is a need to develop specific, targeted potency assays that reflect the intended MoA on a case by case basis. The next sections will discuss their clinical potential and current assays with focus on their immunomodulatory and angiogenic potential.

1.5 Immunomodulatory Properties of Mesenchymal Stem Cells

The adaptive immune system, which comprises of T- and B-cells, generates specific immunity against pathogens through memory cells; whereas the innate immune system comprises of leukocytes (dendritic cells, eosinophils and macrophages) that act in a non-specific manner. There is a growing interest in the use of hMSCs in treating immunological diseases due to their immunomodulatory properties.

One of the most studied application for hMSC therapy is for the treatment of graft versus host disease (GvHD). GvHD is a rare complication that may occur following allogeneic bone marrow transplant in patients after chemotherapy in which immune cells from the graft (donated tissue) will recognise the host as 'foreign'. This can lead to liver damage, skin rash and inflammation of the gastrointestinal tract (Ferrara et al. 2009).

hMSCs are also being used to treat autoimmune disorders such as Crohn's disease and ulcerative colitis, the two main causes of inflammatory bowl disease (Figueroa et al. 2012). In these conditions chronic inflammation is caused by a weakened mucosal layer and the inability to clear bacteria from the intestinal wall (Baumgart and Sandborn 2012).

This section will outline the immunomodulatory effects hMSCs have on the cells of the immune system followed by potency assays published for hMSC manufacturing.

1.5.1 Immunomodulatory Capacity of hMSCs and Mechanism of Action

T-cells

T-cells or T lymphocytes, (so called as they mature in the thymus) are the primary cellular effector in the adaptive immune system; they are activated following stimulation by antigen presenting cells (APCs) such as dendritic cells or macrophages. They fall into three main categories: $CD8^+$ cytotoxic T-lymphocytes (CTLs) that secrete perforin to induce apoptosis; $CD4^+$ T-lymphocytes that secrete cytokines to assist or influence other immune cells; and $CD4^+/CD25^+/FoxP3^+$ regulatory T-cells (T-regs) which have suppressive functions and are responsible for the resolution of inflammation. An over-stimulated pro-inflammatory T-cell response can lead to diseases such as graft-versus-host disease (GvHD), multiple sclerosis and allotransplant rejection. It is now known that hMSCs are able to suppress or modulate the immune system to resolve the disease

(Duffy et al. 2011).

MSC mediated T-cell proliferation suppression and modulation has been identified across a number of species including in humans, mice (Keyser, Beagles, and Kiem 2007) and baboons (Bartholomew et al. 2002). This effect is independent of major histocompatibility complex (MHC) as it has been observed in both allogeneic and autologous reactions (LeBlanc et al. 2003; Klyushnenkova et al. 2005). The inhibition of proliferation is due to the lymphocytes being held in the G_0/G_1 phase of the cell-cycle (Glennie et al. 2005; Benvenuto et al. 2007).

Studies have shown that the suppressive effects is due to both soluble factors and cell-cell contact, although these are only activated once stimulated within an inflammatory environment and not in a resting state. Several soluble factors have been implemented in T-cell suppression including transforming growth factor-β1 (TGF-β1), hepatocyte growth factor (HGF) and prostaglandin E2 (PGE-2). In mice, Ren et al. (2008) demonstrated inducible nitric oxide synthase (iNOS) is responsible for suppressing T-cell proliferation, whilst in humans Meisel et al. (2004) found indoleamine 2,3-dioxygenase (IDO) has analogous functions. IDO catalyses the conversion of the essential amino acid tryptophan to kynurenine which is a known T-cell suppressor molecule (Terness et al. 2002). While in a resting or unactivated state hMSCs do not produce IDO, when treated with IFN-γ alone or with other pro-inflammatory cytokines IDO gene expression is up-regulated (Krampera et al. 2006). *In vivo* studies have shown that pre-treating the MSCs to first activate them leads to resolution of a GvHD model as mice deficient in the IFN-γ receptor do not show any immunosuppressive function (Polchert et al. 2008).

PGE-2 is a product of arachidonic acid metabolism by the cyclo-oxygenase (COX) family of enzymes. It is another mediator of inflammation that can limit the cytotoxic function of natural killer cells and phagocytosis of macrophages (Kalinski 2011). A study by Najar et al. (2010) has shown that hMSCs derived from bone marrow, adipose tissue and Wharton's Jelly constitutively expressed COX1 and COX2 mRNA and the secretion of

the protein was increased during MSC/T-cell co-culture. The authors also inhibited the synthesis of PGE-2 which allowed the proliferation of T-cells. Mechanistically, PGE-2 is known to induce a FoxP3 T-reg phenotype (see below), induce anergy and prevent cell activation making it powerful indicator for immunosuppression (Sreeramkumar, Fresno, and Cuesta 2011).

In addition to soluble factors, studies have now shown cell-cell contact interactions occur in hMSC-mediated suppression. The first evidence of this was reported by Nicola (2002) in which T-cells were cultured in transwell plates to avoid cell-cell contact with hMSCs and compared to those in direct co-culture. Whist both systems were able to significantly reduce T-cell proliferation, those in direct co-culture had an even greater effect. Further experiments by Ren et al. (2010) suggests the adhesion molecules ICAM-1 and VCAM-1 were essential for this effect as antibody blocking of the molecules resulted in normal T-cell expansion. Due to the multiple pathways of immunosuppression it is likely that hMSCs exert their effect through both direct cell-cell contact and secretion of soluble factors.

Another way in which hMSCs regulate immune function is through the induction of regulatory T-cells (T-regs). T-regs are a subpopulation of T-cells which modulate the immune system by suppressing induction and proliferation of effector T-cells, therefore negatively regulating the immune response (Josefowicz, Lu, and Rudensky 2012). In mouse and human mixed lymphocyte reaction cultures (MLR) Maccario et al. (2005) and Luz-Crawford et al. (2013), both found that MSCs can induce a CD4/CD25/FoxP3 T-reg population from naive T-cells. Further functionality of these cells by English et al. (2009) showed these performed in a similar manner to conventionally derived T-regs.

B-cells

B-cells (B lymphocytes, so called as they were first identified in the bursa of Fabricius in birds) are cells of the adaptive immune system that act by secreting specific antibodies when activated by antigen presenting cells (Cooper 2015). In murine studies, Asari et al. (2009) co-cultured mMSCs with B-cells and found B-cell proliferation was suppressed and the maturation mRNA expression of Blimp-1 was downregulated. Similar effects were seen in human cells where Corcione (2006) reported that hMSCs are able to reduce B-cell proliferation without affecting viability which was mediated through soluble factors. Tabera et al. (2008) showed hMSCs caused the B-cells to arrest in the G_0/G_1 cell cycle phase through phosphorylation of ERK 1/2 MAPK and inhibiting phosphorylation of p-p38, both of which are involved in the regulation of the cell cycle. Taken together these studies suggest MSCs are able not only able to reduce B-cell proliferation but also prevent their maturation into fully functional cells.

Natural Killer Cells

Natural killer (NK) cells are a type of cytotoxic lymphocyte of the innate immune system that play a role in antiviral and anticancer function (Mandal and Viswanathan 2015). In a resting state they recognise self-MHC class I molecule and this prevents their activation. Virally infected and tumour cells often downregulate MHC class I to prevent recognition by T-cells, however this results in vulnerability towards NK cells. When co-cultured with hMSCs, stimulated NK cells do not express the activation marker NKp44. Others have also shown NK proliferation and cytokine release can be inhibited in both direct co-cultures and when separated by transwells suggesting soluble factors play a large role in regulation (Sotiropoulou et al. 2006).

PGE-2 and IDO have both been shown to play crucial roles in hMSC mediated inhibition. Spaggiari et al. (2007) added anti-PGE2 and anti-IDO compounds into hMSC and NK

cell co-cultures and found when added together could fully restore NK cell proliferation.

Dendritic Cells

Immature dendritic cells (DC) reside in tissue and when exposed to stimuli such as pathogens, bacterial DNA or cytokines (such as TNF-α) they undergo maturity into functional antigen presenting cells to activate T-cells (Banchereau and Steinman 1998). In mouse MSC and DC co-cultures English, Barry, and Mahon (2008) demonstrated that mMSCs were able to prevent the migration, maturation and antigen presenting functions of immature DCs. Similar results with human cells have also been previously reported by Nauta et al. (2006) who, by using transwell experiments, also showed these inhibitory effects are mediated by soluble factors.

In addition to IDO and PGE-2 as anti-inflammatory cytokines, interleukin 6 (IL-6) has been shown to modulate DC function. Djouad et al. (2007) showed IL-6 produced by hMSCs in response to co-cultures with monocytes prevented their maturation and differentiation into DCs. Further work by Melief et al. (2013) went on to show IL-6 could induce an anti-inflammatory monocyte phenotype.

1.5.2 Immunogenicity of hMSCs

To first be able to provide therapeutic effects hMSCs must be able to reside within the body whilst not being recognised as a foreign particle that will lead to its removal. Therefore, avoiding recipient recognition and subsequent destruction is the first key to a successful allogeneic cell therapy. hMSCs have long been described as hypoimmunogenic or 'immunoprivileged' as they express a relatively small fraction of the molecules needed to activate T-cells *in vivo* (Potian et al. 2003). For example, they express low levels of human leukocyte antigen (HLA) or major histocompatibility (MHC) class I antigens which are

required for immune recognition. However, this is only true for 'resting' or unactivated hMSCs. When stimulated with pro-inflammatory cytokines such as interferon gamma (IFN-γ) they upregulate expression of HLA-DR (MHC class II).

When infused MSCs are gradually allo-immunised and cleared from the recipient. Nauta (2006) showed repeated transfusion of allogeneic mMSCs into naive mice was sufficient to induce a T-cell response as seen by decreased engraftment. Moreover, Isakova et al. (2010) injected varying doses of allogeneic MSCs intra-cranially into rhesus macaques. Even in this immunoprivileged site there was an allo-graft response that was dose dependent, and this correlated to an increased $CD8^+/CD16^+$ lymphocyte subpopulation.

Therefore, although hMSCs are not as immunogenic as other unmatched cells such as fibroblasts and hematopoietic stem cells, repeated transfusion of unmatched hMSCs may lead to acquired alloimmunisation. To overcome this future hMSC treatments should look to optimise their survival and potency to prevent patient desensitisation (Ankrum, Ong, and Karp 2014).

1.5.3 Current hMSC Immunomodulatory Potency Assays

From the literature it is clear that hMSCs can modulate the immune system in a variety of ways that include secreting soluble factors and by cell-cell contact mechanisms. As such there are many variations of immunomodulatory potency assays, for example, addition of pro-inflammatory cytokines or co-cultures with purified effector cells and MLRs. Due to the many different formats to measure immune suppression there is a large disparity in the claims made by researchers. There have been some attempts for creating a standardised assay to measure the immunomodulatory potential of hMSCs in a clinical or manufacturing setting.

To enhance hMSC response to inflammation Ankrum et al. (2014) first treated hMSCs

with glucocorticoid steroids before addition of IFN-γ to measure IDO response. Here, budesonide was able to induce IDO expression across multiple donors hMSC lines and in late-passage cells. Co-culture with PBMCs also found greater immunosuppression in steroid and IFN-γ treated hMSCs.

As previously discussed in Section 1.4.2, hMSCs can be isolated from multiple areas of adult tissue, previous reports have described the contrast in growth rate and differentiation potential however, there have been very few studies into the differences of immunosuppression. To address this Yoo et al. (2009) isolated bone marrow adipose tissue, umbilical cord blood and Wharton's Jelly hMSCs. To ensure consistency between the different cell lines, the authors maintained the same hMSC seeding density and the same number of purified T-cells. However, there were no differences in the immune suppression potency between the types of hMSCs.

Immunosuppressive potency assays are starting to be implemented as quality control tests for manufacturing of hMSCs. In a multi-centre comparison test Bloom et al. (2015) describes the development of a possible standardised immunopotency assay. Here 11 hMSCs products that were manufactured across three separate sites were assessed using a hMSC/T-cell co-culture proliferation assay. The authors were able to demonstrate a reproducible assay between sites and production runs due to the defined seeding densities and T-cell population. Interestingly, there were varying degrees of immunosuppression ranging from 27% to 88% inhibition of proliferation which may be due to the differences in isolation, culture conditions/medium and cyropreservation formulation.

A report by Luetzkendorf et al. (2015) examined the potency following xeno-free GMP expansion and cryopreservation. Co-cultures of five different hMSCs donors with mismatched PBMCs resulted in an average of 50% proliferation suppression. The degree of suppression varied amongst the donors, however there was no difference between fresh or cryopreserved hMSCs.

The above studies have all used a suppression assay with varying types of immune cells to measure potency. However, there is a lack of cytokine/soluble factor analysis that may give further insights to the immunosuppressive potential of these hMSCs.

The ISCT published a perspective paper on immune functional assays for hMSCs where they suggest 'licensing' or activation via the addition of IFN-γ to prime the cells, IDO response and the use of purified immune cells as a model of immunosuppression. These suggestions stress standardised and common protocols to achieve comparable results for hMSC immunological characterisation (Krampera et al. 2013).

1.6 Angiogenic Properties of Mesenchymal Stem Cells

Within the body the cardiovascular system, a network of blood vessels, provides all cells and tissue with nutrients and oxygen as well as waste removal, this network ranges from large arteries and veins down to smaller capillaries and venules. In embryonic development the cardiovascular system is the first to develop in a process termed 'angiogenesis' or 'neovascularilsation'. In this process, endothelial progenitor cells (angioblasts) differentiate into the mesoderm and then into an early vascular network which undergoes remodelling and sprouting (Breier 2000).

Angiogenesis will also occur in adult life following injury. Wound healing involves four phases: haemostasis, inflammation, tissue formation and tissue remodelling. After injury, different subsets of leukocytes release angiogenic factors into the surrounding site which recruit endothelial cells to the area. Together with fibroblasts, these then undergo remodelling and differentiation to form the new blood vessels (Eming et al. 2007).

Cardiovascular disease (CVD) is still the leading cause of death worldwide, and in the United States of America was estimated to cost $314.5 billion in direct and indirect expenses (Go et al. 2013). After an acute myocardial infarction (MI), the heart has a

limited capacity to repair and will undergo tissue remodelling. This process involves neutrophil invasion, myocyte hypertrophy and eventually fibrosis due to accumulation of collagen. Ventricular remodelling may persist for a number of weeks or even months depending on the size and severity of the attack (Sutton and Sharpe 2000). As a result there is decreased contractility and further tissue necrosis leading to hypotension.

The main goals in the treatment of CVD, such as ischaemic heart disease, is to stimulate vascular repair in order to improve blood flow and perfusion. Pharmacological intervention such as angiotensin-converting enzyme inhibitors (ACE inhibitors) act to cause relaxation of blood vessels and thus reduce blood pressure, it can improve left ventricular dysfunction after 1 week following MI (Sharpe et al. 1991). Other types of medication include thrombolytic drugs that act by activating plasminogen, which forms plasmin. Plasmin then cleaves the cross links between fibrin to reduce the size of blood clots. In the UK, streptokinase is the main thrombolytic agent administered to patients (Gray 2006).

From a regenerative medicine perspective, stem cell therapy for MI and other ischaemic diseases have shown to have potential clinical effects by promoting formation of new vasculature in the damaged area. Authors have described local repair and improved function following hMSC transplantation into affected areas (Hashemi et al. 2007; Jiang et al. 2008; Williams et al. 2012).

1.6.1 Paracrine Mechanisms for hMSC angiogenic effect

It is well documented that hMSCs and other stem cells are able to secrete numerous bioactive and trophic mediators (Haynesworth, Baber, and Caplan 1996; Caplan and Dennis 2006). Although not fully detailed, the therapeutic effect of these cells can be attributed to growth factors and cytokines in the secretome.

It has been demonstrated that conditioned medium from mMSCs is able to improve blood

flow and improve limb function in a mouse model of lower limb ischaemia (Kinnaird et al. 2004). Furthermore, another study reported by Timmers et al. (2011) has shown hMSC-conditioned medium can improve cardiac function in porcine models of MI. This is due to the plethora of pro-angiogenic cytokines produced by the hMSCs and released into the medium. Through high-throughput screening some key factors have been identified as vascular endothelial growth factor (VEGF), fibroblast growth factor-2 (FGF-2), angiopoietin-1 and a number of tissue inhibitor of metalloproteinases (TIMPs) (Park et al. 2009; Bara et al. 2015). Due to the multiple secreted factors it is not clear which ones are the most critical however studies using neutralising antibodies have shown that removing VEGF, IL-6 and CXCL5 can reduce the angiogenic potential of hMSC conditioned medium (Lehman et al. 2012; Kwon et al. 2014).

Given that their therapeutic effect is due to the paracrine mechanism of action, researchers are investigating methods to enhance the hMSC secretome (Ranganath et al. 2012). Kinnaird et al. (2004) showed hypoxic culture at 1% atmospheric O_2 increased secretion of FGF, placental growth factor and VEGF when compared to hMSCs cultured under 20% O_2.

Another approach is to use pharmacological agents or small molecules, these allow for controlled treatment and specific actions. Treating hMSCs with lipopolysaccharide has been shown to not only promote expression of VEGF but also increase post-implantation survival in mouse acute MI models (Yao et al. 2009).

The physiological and pharmacological pre-conditioning strategies allow for simple and controllable modifications to the hMSC secretome. However, as these effects are transient it is likely that these approaches will have limited duration *in vivo*. More permanent enhancements include gene modifications to over express cytokines such as VEGF (Yang et al. 2010).

1.6.2 Differentiation & Engraftment for hMSC angiogenic effect

In addition to the secretion of a large amount of bioactive trophic factors for cardiac repair, there is some evidence that hMSCs are able to differentiate into capillary-like structures to restore blood flow or fuse directly onto the myocardium to improve function. *In vitro* studies by Oswald et al. (2004) and Janeczek Portalska et al. (2012) have both shown that hMSCs are able to differentiate into endothelial cells and form functional capillary-like structures.

In a murine model, Nagaya et al. (2004) found that MSCs would preferentially incorporate into the areas of infarct over non-infarcted areas and improve overall cardiac function. Gene expression analysis of the engrafted MSCs demonstrated upregulation of troponin T and connexin 43, key cardiac genes, suggesting differentiation into cardiomyocytes. Further studies by Quevedo et al. (2009) also reported cardiac commitment by GATA-4 and Nkx2 gene expression but also reduced infarct size and recovery of ejection fraction. More recently, Freeman, Kouris, and Ogle (2015) engineered a Cre/LoxP-based luciferase reporter system so that transplanted hMSCs could be tracked in living mice. The authors show direct fusion of hMSCs to cardiomyocytes for at least 8 days.

Currently there is little evidence to show that hMSCs can differentiate into functional blood vessel structures *in vivo* as most studies demonstrate hMSC engraft to the myocardium rather than undergo cardiac-differentiation. Therefore, it is likely that hMSCs exert their therapeutic properties by a combination of trophic factors and supporting cardiac tissue. This two-way angiogenic approach may make hMSCs a real option for cell therapy following myocardial infarction and ischemia.

1.6.3 Current hMSC Angiogenic Potency Assays

Currently there is no standardised method to determine the angiogenic potency of hMSCs and reported studies use a combination of *in vitro* and *in vivo* assays. The most commonly employed *in vivo* assay is the Matrigel plug assay. Here Matrigel is embedded or infused with the test cells or substance and then injected subcutaneously in to the animal model. After a number of days, typically from 14-21 days, the plug is removed and histologically examined to determine the extent of blood vessel formation. However, this method is low-throughput and time consuming (Auerbach et al. 2003).

An *ex vivo* approach is the aortic ring assay where an explant of a developing chick embryo is plated and supplements are added to the medium. Due to the explant nature it is not possible to determine the starting number of endothelial cells and therefore difficult to have a reproducible and consistent assay (Bahramsoltani et al. 2009).

It is clear from the literature that the main therapeutic effect of hMSCs is via the secretion of relevant pro-angiogenic cytokines, therefore a possible potency assay would be to measure the amount of these factors.

The first true angiogenic hMSC potency assay was published by Lehman et al. (2012) for Athersys's MultiStem multipotent progenitor cell population (MAPC) product. In this study the authors used serum-free conditioned medium to induce endothelial tube formation which reflects the intended MoA. Tube formation mimics the vascularisation process of newly formed capillaries and venules. Proteomic analysis suggested that three key cytokines were related to the angiogenic activity, chemokine (C-X-C motif) ligand 5 (CXCL5), interleukin 8 (IL-8) and VEGF. By selectively depleting these factors the authors were able to determine a necessary lower-limit threshold for endothelial tube formation and therefore a pass/fail criteria.

Overall, this demonstrates a good example of a potency assay as it addresses the points

discussed in section 1.2.2. The endothelial to tube formation reflects the intended MoA and could be attributed to three cytokines. This allowed ELISA to be implemented as a surrogate assay to test the critical quality attributes of the cells during clinical manufacturing.

In a similar assay Hoch et al. (2012) examined the production of VEGF, FGF2 and TGF-β during hMSC to osteoblast differentiation. The authors found under the differentiation conditions there was decreased production of these proteins and increase of osteogenic gene expression such as SP7 and IBSP. Conditioned medium from these samples correlated to a reduced number of branch points and tubule length in endothelial cell tube formation assays.

Although these studies have described angiogenesis assays, there is currently no standardised protocol. There is still a need to develop an assay with defined basement membranes/substrates, quantitative measure of vascularisation and screen for more pro-angiogenic factors. These challenges, and solutions, will be addressed in Chapter 6.

1.7 hMSCs in Clinical Trials

Due to the growing evidence in the therapeutic values of hMSCs the number of clinical trials has grown exponentially in the last decade. As their immune and angiogeneic properties are being revealed trials are moving away from the classical tissue engineering approach of first differentiating hMSCs into bone or cartilage followed by implanting to using the cells as a protein/bioactive delivery vehicle.

ClinicalTrials.gov, a US based database maintained by the National Library of Medicine (NLM) at the National Institutes of Health (NIH) includes information about medical studies conducted in the USA and 187 other countries. The data presented in Figure 1.2 shows only trials which use bone marrow-derived hMSCs. Full figures are presented

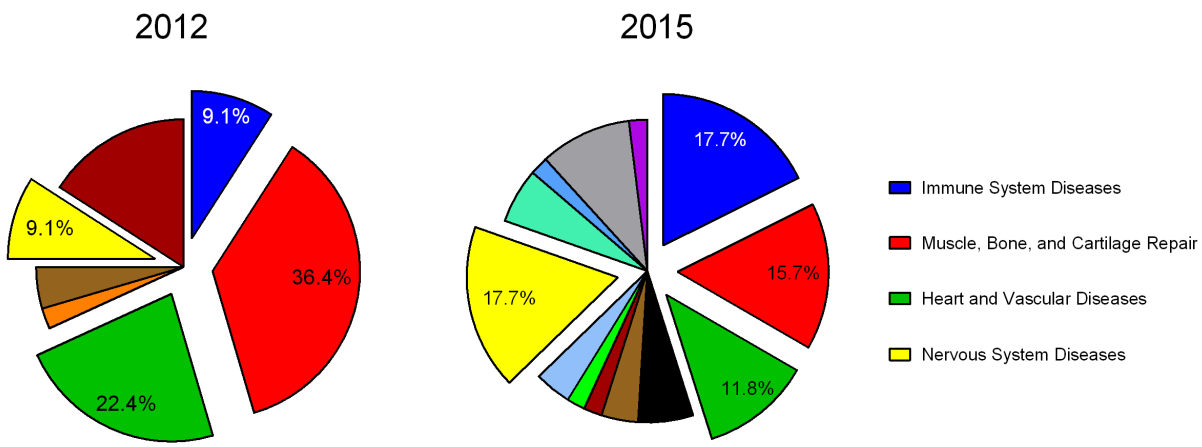

Figure 1.2: Break down of clinical trials involving hMSCs in February 2012 and March 2015 grouped into pathology areas. The main expanded areas show percent in group. Data acquired from www.ClinicalTrials.gov

in Appendix Table A.1. Data acquired from 2012 show treatment for muscle, bone and cartilage disease are the most prevalent accounting for 36.4% of the total number, however, data from 2015 this figure decreases to only 15.7% as other treatment areas such as immune system (17.7%) and heart and vascular diseases (11.8%) account for a greater proportion.

In 2012 only 4 of 44 of trials were for the treatment of immune system diseases, such as GvHD and Crohn's, however, in 2015 this number more than doubled to 9 of 49. Conversely, there has been an overall decrease of muscle and cartilage repair trials for tissue engineering halving from 16 trials in 2012 to 8 in 2015. This change in focus is likely due to the emerging therapeutic properties as previously discussed in Section 1.5 and Section 1.6.

1.7.1 Immune Disorders

The first landmark paper to show hMSCs could be a potent therapeutic was published by Le Blanc et al. (2004) of the Karolinska Institutet at the University of Sweden. In this case report a paediatric patient was treated for severe, acute GvHD using allogeneic

hMSC transplant. Following the first dose of hMSCs there was a clinical response, after the second dose the patient achieved complete remission. Over the next few years, this was followed by a number of cases and Phase II clinical trials which also showed good clinical efficacy in approximately 70% of all patients (Ringden et al. 2006; Le Blanc et al. 2008; Bonin et al. 2008).

Osiris Therapeutics Inc

Osiris Therapeutics Inc is a regenerative medicine company with four main products: Prochymal^{TM}, a pre-manufactured allogenic bone marrow-derived hMSC line; Grafix, a cryopreserved placental membrane; OvationOS, a bone matrix; and Cartiform, a cartilage mesh. Prochymal is being used to target multiple areas of aliments including GvHD, Crohn's disease, acute myocardial infarction and type 1 diabetes.

From the promising academic studies by Le Blanc et al. (2008) Osiris planned to develop Prochymal for the treatment of GvHD. From a single donor they planned to scale-up and expand the number of cells for 10,000 doses, cryopreserve the cells, then thaw and infuse into the patient.

In 2009, they published a press release for the outcome of a Phase III trial, however, in contrast to the earlier reports there was no statistical difference between the treatment group or placebo, thus failing to meet their clinical end-point.

Later in 2011, Osiris published the results of a compassionate use study that looked at the safety and efficacy in children that had developed GvHD (Prasad et al. 2011). All patients in this study had developed grade III-IV acute GvHD and were refractory to standard first-line treatment with corticosteroids and at least one second-line therapy. Two patients received 8×10^6 hMSCs/kg per infusion, the cell dose for the subsequent 10 patients was decreased to 2×10^6 hMSCs/kg. Prochymal was well tolerated as no toxicity was observed. Seven of the patients achieved complete response, two had partial response

and three had mixed responses.

Another larger trial involving 75 paediatric patients was conducted from across seven countries (Kurtzberg et al. 2014). All had acute grade II-IV GvHD and were unresponsive to current immunosuppressive steroids and treatments. Following treatment 43 (63%) patients showed clinical response with a significant chance of survival past 100 days when compared to treated but non-responders.

In October of 2013, Mesoblast Ltd announced the take over of the stem cell division of Osiris and thus acquiring the Prochymal cell line (Waltz 2013).

Mesoblast

Since the 2013 acquisition of Prochymal Mesoblast is expecting to accelerate product approvals in the United States for the treatment of steroid-refractory acute GvHD as an Orphan Drug and Fast Track product. They also expect to complete the current Phase III trial in adult patients with Crohn's Disease in December 2018.

All hMSC clinical trials within Mesoblast are currently ongoing so no further data is available.

Athersys

Similar to Osiris and Mesoblast, Athersys is a biopharmaceutical company aiming to develop an off-the-shelf biological product for a number of different clinical areas. The main focus is proving the utility of MultiStem^{TM}, a proprietary Multipotent Adult Progenitor Cell (MAPC) line. These cells, originally described by Catherine Verfaillie, are a rare population of cells from within bone marrow MSC cultures that are able to undergo prolonged populations doublings but also differentiate into cells of all three germ layers (Jiang et al.

2002). These more embryonic-like cells expressed the classical hMSCs markers (CD73, CD90 and CD105) but did not have MHC Class I or CD140b expression suggesting that they are indeed a distinct cell population.

Athersys are using MultiStem to target several areas such as ischemic injury (myocardial infarction, stroke, and other indications) and conditions involving the immune system (autoimmune disease).

Phase I clinical studies to evaluate safety of single or repeat dose to patients receiving allogeneic hematopoietic stem cell transplantation (HSCT) found that the therapy was well tolerated, and all patients experienced successful platelet engraftment (Maziarz et al. 2012).

Multistem has also been used in clinical trials for the treatment of ulcerative colitis (UC), a form of inflammatory bowl disease (IBD). Recently, in early 2014 a Phase II double-blind, placebo controlled trial the therapy was well tolerated after 8 weeks of administration. However in chronic advanced UC a single dose did not show any improvement. Primary endpoints of safety and tolerance were all met, secondary endpoints for clinical evaluation are expected after long term 16 week post-therapy.

1.7.2 Cardiovascular Disease

Allogeneic hMSCs for the treatment of cardiovascular disease is a growing area that is showing good clinical efficacy. Mesoblast has conducted trials using their allogeneic mesenchymal precursor cell (MPC) to explore if delivery of these cells during left ventricular assist device implantation may assist in myocardial recovery (Ascheim et al. 2014). There was a slight increase in left ventricular ejection fraction (LVEF) in patients who received the cells when compared to controls. In this study there was limited release testing/criteria which was based upon cell viability, karyotyping and surface antigen expression of STRO-

1, CC-9 and HLA class I and II.

Hare et al. (2009) performed the first major trial using allogeneic Prochymal for patients after acute myocardial infarction. This was a randomised, double-blind, placebo-controlled study involving 53 patients receiving 0.5 - 5 million cells/kg through a single intravenous infusion. Similar to the Mesoblast study, release testing only involved cell surface profiling of CD105, CD166, and negativity for CD45, however, there was no documentation of potency or quality measurements. Nonetheless, this study found the treated group demonstrated improved LVEF and experienced fewer arrhythmic events. This resulted in a further phase I/II study involving 30 patients with ischemic cardiomyopathy (The POSEIDON-Pilot Study) (Hare et al. 2012). Here patients were treated with either autologous or allogeneic hMSCs and the cells were delivered directly into the infarcted area through a procedure called transendocardial stem cell injection (TESI). The release criteria for this trial involved cell viability, surface expression of CD105 and CD45, growth assay using CFU-F and sterility testing.

The patients in the POSEIDON and another ongoing study to compare the effects of allogeneic versus autologous hMSCs for treatment of nonischemic dilated cardiomyopathy were retrospectively enrolled for further functional tests (Mushtaq et al. 2014; Premer et al. 2015). In an *in vitro* examination, conditioned medium from allogeneic hMSCs were able to induce HUVEC endothelial tube formation to a greater degree than autologous hMSCs. In addition, flow-mediated vasodilation, a measure of blood vessel response to physical stimuli, was improved in the allogenic group whereas there was no improvement found in the autologous-hMSC treated group. This was explained due to the donor age of the hMSCs, in the allogenic group the donors were typically from a healthy donor aged between 20 - 35, however, those treated with autologous hMSCs were typically older (45 - 75) and had underlying chronic disease.

1.7.3 Lessons from Clinical Trials

Over the last few years there has been a great increase of early stage clinical trials demonstrating the safety and tolerance of hMSCs. The use of cryopreserved, unmatched allogenic hMSCs for treatment of GvHD has been successful in early stage European trials (Le Blanc et al. 2008; Kebriaei et al. 2009). This is in contrast to the disappointing Phase III results from Osiris that failed to meet its clinical outcome. It has been suggested that donor variance, culture expansion and senescence, immunogenicity, and cryopreservation could underlie the discrepancy between the academic and industrial trials (Galipeau 2013)

This failure could be due to a few important causes. Culture expansion of the cells may play a role in the immuno-suppressive ability. In the successful Kebriaei et al. (2009) early phase Prochymal trial, the cells were expanded to a total of 5 passages, in contrast, for the phase III trials the cells were expanded into large lot doses as 163 patients were treated with 16 million cells over the period of 4 weeks. To get this amount of cells it would have been necessary to perform large scale *in vitro* expansion to obtain the require cell volume. A previous study by Bahr et al. (2007) patients suffering from acute GvHD were treated with early passage (Passage 1-2) had one year survival rate of 75% compared with those given cells at later passages (passage 3-4) who had a survival rate of 21%. It was also noted that this difference was only apparent *in vivo* and not *in vitro*. As the full details on Osiris's Phase III Prochymal trial has not been published it is not possible to fully compare it to the more successful trials.

Large scale allogeneic cell therapies would require cyropreservation, storage and transport of cells to the patient. Upon delivery the cells would be thawed and infused into the patient. A report by François et al. (2012) shows that cyropreservation could negatively affect the hMSCs in an *in vitro* immunosuppression assay due to the upregulation of heat shock proteins. This was later supported by Moll et al. (2014) who also demonstrated a reduced IDO expression response to IFN-γ exposure. The authors also retrospectively

analysed 44 hMSCs infusions. They found patients who received early-passage fresh hMSCs showed a 100% response rate whereas those who received later-passage thawed cells showed only 50% response rate.

Some attempts have been made for incorporating potency assays in clinical trials, for example, Kebriaei et al. (2009) used TNFR1 expression on hMSCs and inhibition of IL2Rα as surrogate markers for potency and as an acceptance criteria for lot release. In this study 77% (24/31 patients) had a complete recovery following 28 days of treatment suggesting these could be possible makers for hMSC to treat GvHD. These few studies have highlighted the limited release testing and lack of quality criteria for allogeneic hMSC treatment for various cardiomyopathies and immune diseases.

This highlights the need for appropriate potency assays to serve as a release criteria before lot release. Aspects such as donor variability and cryopreservation of cell therapies cannot be avoided and will likely have an impact on the efficacy of the product, therefore, the extent to which they effect the MoA will need to be determined. Ideally a potency assay will be linked to a clinical endpoint and the results can be used to determine a product specification and a pass/fail criteria.

1.8 Aims & Objectives

Cell therapy can potentially provide treatment for currently unmet clinical needs. hMSCs in particular can be a platform for treatmenting cardiovascular and immune diseases such as stroke, infarction, ulcerative colitis, and Crohn's disease. For successful translation from the research laboratory into the clinic there is a need for development of robust quality and potency assays that accurately reflects the *in vivo* mechanism of action. Currently there are no standards to the 'quality' or potency required for hMSCs.

This work seeks to address these problems by developing standardised assays that can be

employed to characterise multiple donor hMSCs and be used in a manufacturing setting. This will be achieved by first performing full physiological characterisation of hMSC followed by developing assays that will analyse their immunomodulatory and angiogeneic potential.

The aim of this work is to:

- Isolate and characterise multiple hMSC donors in terms of growth rate, nutrient/metabolite consumption, extracellular marker expression, and differentiation capability.

- Develop an identity assay using markers as described by the ISCT *via* a multiparameter flow cytometry approach

- Develop an *in vitro* inflammation assay to examine the immunomodulatory properties of hMSCs and measure known effectors

- Investigate the pro-angiogenic effect of hMSCs by induced *in vitro* endothelial vessel formation and screen for known angiogenic cytokines

Chapter 2

Materials & Methods

2.1 hMSC Cell Culture

2.1.1 Cell Source

Human mesenchymal stem cells were isolated from Lonza (UK) from Bone Marrow Mononuclear Cells (BMNCs) for healthy donors after informed consent. The local Ethical Committee approved the use of samples for research. Five donors are used for the studies, Table 2.1 denotes the naming convention and background regarding each donor.

Table 2.1: hMSC donor details including age, sex and race

Name	Donor Lot	Age	Gender	Ethnicity
M1		20	Male	Black
M2	071313B	19	Female	Black
M3	071150B	24	Male	Caucasian
M4	0000327825	25	Female	Hispanic
M5		59	Female	

2.1.2 hMSC isolation

Plastic Adherence

The peripheral blood mononuclear cells (PBMCs) were thawed into 10ml of complete growth medium (see below, Section 2.1.3) and a sample was taken for counting (see Section 2.7 Cell Counting). Cells were centrifuged for 5 minutes at 220xg, the supernatant was aspirated and cell pellet was re-suspended into 10ml of medium. Cells were seeded at 80,000 cells/cm^2 in multiple T-225 flasks and placed into a humidified incubator at 37°C with 5% CO_2.

After 48 hours the medium and any cells in suspension was aspirated and washed with phosphate buffered saline (PBS, Lonza, Cat No. 17-516F). Subsequent media changes were performed every 2-3 days and check regularly for colony formation for the next 3 weeks. Once at 80-90% confluence the cells were passaged as described in Section 2.1.4 Cell Growth and Sub-Culture.

CD271 MACS

Magnetic activated cell sorting (MACS) was performed using a CD271 MicroBead Kit (Miltenyi Biotec, UK, Cat No. 130-099-023)) according to the manufacturer's instructions. Thawed PBMCs were passed through a 30μm mesh to remove clumps of cells and centrifuged at 300xg for 10 minutes and the supernatant was removed. The cell pellet was re-suspended in buffer (PBS, 0.5% bovine serum albumin, and 2mM EDTA), FcR blocking reagent and labelled with CD271 microbeads. The cells were incubated for 15 minutes at 4°C followed by dilution with buffer and an extra wash step.

The MACS column was prepared by wetting it thoroughly with buffer and placing onto the MACS stand. The labelled cell suspension was applied to the column and the flow

through was collected. After the cell suspension had been passed through, the column was removed from the magnetic stand and buffer was pushed through the column to elute cells. These cells were then placed into prepared T-Flasks for further culture.

2.1.3 Medium Formulation

hMSCs were cultured in Dulbecco's Modified Eagles Medium (DMEM, 1g/L glucose; Lonza, UK, Cat No. BE12-707F) containing 10% foetal bovine serum (FBS, Hyclone, Belgium) and 2mM UltraGlutamine (Lonza, UK. Cat No. BE17-605E/U1). Once complete the medium was stored at 4°C and used within one month. Before use the medium was warmed to 37°C.

2.1.4 Cell Growth and Sub-Culture

Cells were seeded at 5000 cells/cm^2 into pre-warmed growth medium. Cells were then transferred to a humidified incubator set at 37°C with 5% CO_2. After 72 hours of culture the growth medium was completely replaced.

Following a further 72 hours the cells were passaged. Existing medium was aspirated and an equal amount of PBS was used to wash the surface of the cells. The PBS was then removed and 0.25% trypsin/EDTA (Gibco, UK, Cat No. 25200) was added to the surface of the T-flask to detach the cells. Volumes for each T-flask size are listed in Table 2.2. The flask was then placed back into the incubator for five minutes. Cells were then detached by gently tapping the sides of the flask. The trypsin/EDTA was quenched using the appropriate volume of fresh pre-warmed media. A sample of the cell suspension was taken for cell count and viability determination (see section 2.7).

The cell suspension was transferred to a centrifuge bottle and centrifuged at 200xg for 5 minutes. The supernatant was aspirated and the remaining pellet resuspended at 1 x 10^6

Table 2.2: Tissue culture flask size and reagent volumes

T- Flask Size	Medium Volume (ml)	Trypsin/EDTA Volume (ml)	Quench Volume (ml)
T25	5	1	4
T75	15	3	7
T175	30	7	13
T225	45	12	18

cells/ml before seeding into a new flask.

2.1.5 Cryopreservation and Thawing

Once confluent, cells were trypsinised as in section 2.1.4 and resuspended in 90% v/v FBS and 10% v/v Dimethyl sulfoxide (DMSO, Sigma, UK, Cat No. 472301). 1 x 10^6 cells were aliquoted into a cryopreservation vial in 1ml of freeze mixture. The filled vials were transferred into a CoolCell (BioScion, USA, Cat No. BCS-405) and placed into a -80°C freezer which allows the suspension to cool at a rate of -1°C/minute. After 24 hours the vials were transferred into the vapour phase of a liquid nitrogen cyrostore.

For thawing and revival the vial was removed from the cryostore and placed into a water bath at 37°C until a trace of ice remained - approximately 3 minutes. The 1ml of cell suspension was then transferred into 9ml of pre-warmed growth medium and centrifuged for 5 minutes at 220xg. The supernatant was removed and the cell pellet was reseeded to tissue culture flasks as required.

2.2 Differentiation and Staining

Differentiation and staining of the hMSCs into the three lineages are described below.

2.2.1 Adipocytes

Cells were seeded in a 12 well plate at 1x10^4 cells/cm^2 with Invitrogen StemPro Adipogenic medium (Invitrogen, UK, Cat No. A1007001). The medium was changed every 3–4 days. After three weeks in culture, cells were washed and fixed in 2% (v/v) paraformaldehyde (Sigma, UK, Cat No. F8775) for 30 mins at room temperature. For adipogenic staining, cells were washed three times with PBS and incubated with 0.3% (v/v) Oil Red O (Sigma, UK, Cat No. O1391) in 99% 2-propanol for 30 minutes at room temperature. Cells were washed three times in distilled water and visualised under a light microscope.

2.2.2 Chondroblasts

To induce chondrogenic differentiation, cells were sub-cultured and re-suspended at 1.6 x 10^2 cells/ml. Micromass cultures were generated by seeding a six well plate with 2μl droplets of cell suspension and allowed to attach to the tissue flask surface in a humidified atmosphere for 30 min before adding pre- warmed Invitrogen StemPro Chondrogenesis medium (Invitrogen, UK, Cat No. A1007101). The medium was changed every 3–4 days. After 14 days in culture, cells were washed and fixed in 2%(v/v) paraformaldehyde for 30 min at room temperature. Chondrocytes were stained with 1% (v/v) Alcian Blue (Sigma, UK, Cat No. B8438) in 0.1 M HCl solution for 30 minutes, washed three times with 0.1 M HCl, diluted with distilled water and visualised under a light microscope.

2.2.3 Osteocytes

To induce osteogenic differentiation, cells were seeded into a 12 well plate at 5 x 10^2 cells/cm^2 with Invitrogen StemPro Osteogenesis medium (Invitrogen, UK. Cat No. A1007201). The medium was changed every 3–4 days. After four weeks in culture, cells were washed and fixed in 4% (v/v) paraformaldehyde for 5 min at room temperature. For calcium

staining, 2.5% (w/v) silver nitrate was added and cells were incubated for 30 min at room temperature under UV light. Counterstaining for alkaline phosphatase (ALP) was carried out with a solution containing Fast Violet B Salt with 4% (v/v) naphthol AS-MX phosphate alkaline solution (Sigma, UK. Cat No. N4875) for 45 min at room temperature in the dark. Cells were washed three times in distilled water and visualised under a light microscope.

2.3 Flow Cytometry

2.3.1 Cell Labelling

Detached cells were re-suspended at 0.5 x 10^6 cells/ml in growth medium and loaded onto a 96 well plate. The plate was centrifuged for 5 minutes at 220xg. The aspirate was removed and the cells re-suspended and washed in flow cytometry staining buffer (BD Biosciences, UK, Cat No. 554656) and the centrifugation cycle repeated. The cells were stained for 30 min in the dark at room temperature with fluorescent monoclonal antibodies against CD34 (PE-CY5), CD73 (PE-Cy7), CD90 (APC), CD105 (PE) and HLA-DR (FITC, all from BD Biosciences, UK) in addition with the corresponding isotype controls. After incubation, the cells were washed twice with staining buffer as before. Finally, 200μl of staining buffer was used to re- suspend the samples before analysis.

2.3.2 Data Acquisition

Flow cytometry data was acquired using a Merck Millipore guava easyCyte^{TM}HT or a BD Biosciences FACs Jazz as indicated in the text. Excitation lasers and band pass filters are detailed in Table 2.3.

Table 2.3: Flow cytometer excitation and band pass filters

Flow Cytometer	**Excitation wavelength**	**Filters**
guava easyCyteHT	488nm	525/30 (Green)
		583/26 (Yellow)
		690/50 (Red1)
		785/70 (NiR1)
	635nm	690/12 (Red2)
		785/70 (NiR2)
BD FACs Jazz	488nm	530/40
		585/29
		670 LP
	640nm	660/20
		750 LP
	405nm	450/50

2.3.3 Data Analysis

A minimum of 1000 events was recorded for each sample. Compensation was performed using BD CompBeads (BD Bioscience, UK. Cat No 552843). Data analysis was performed using FlowJo version 7.6.5 or version 10 (TreeStar Inc, USA).

2.4 *In Vitro* Pro-inflammatory Stimulation of hMSCs

hMSCs were seeded at 5000 cells/cm^2 and cultured for 3 days as described in Section 2.1.4. On day 3 of culture the media was aspirated and the cells were washed once with PBS. Media was replaced with standard culture media containing the pro-inflammatory cytokines interferon-γ (IFN-γ) (10ng/ml) and tumour necrosis factor-α (TNF-α) (10ng/ml, both from Gibco, UK. Cat No. PHC4031 and PHC3015 respectively) for a further 3 days or as described in the text.

2.5 CD4$^+$ Cell Culture

2.5.1 Cell Source

Peripheral blood CD4$^+$ cells were obtained from Lonza (UK). The donor was 33 year old, male, Caucasian.

2.5.2 Medium Formulation

$CD4^+$ T-cells were cultured in RPMI 1640 (Lonza, UK. Cat No. 12-167F), 2mM Ultra-Glutamine, 10% FBS and 55mM beta-mercaptoethanol (Gibco, UK. Cat No. 21985023). Before use the medium was warmed to 37°C. 30U/ml of recombinant human Interleukin-2 (IL-2, Gibco, UK. Cat No. PHC0021) was added separately.

2.5.3 Cell Growth and Sub-Culture

$CD4^+$ T-cells were stimulated and expanded using CD3/CD28 DynaBeads (Gibco, UK. Cat No. 111.31D). DynaBeads were transferred with a 1:1 bead:cell ratio to a centrifuge tube and washed with 1ml of PBS then placed into a magnetic DynaMag holder. The PBS was removed and resuspended for use in culture medium.

Cells were seeded into a new flask at 0.5 x 10^6 cells/ml along with prepared DynaBeads. The cells were then transferred to a humidified incubator at 37°C with 5% CO_2.

Once the cells reached a density of 2.5 x 10^6 cells/ml the cultures were reduced back down to 0.5 x 10^6 cells/ml by the addition of fresh medium.

2.6 hMSC & CD4 Co-Culture

hMSCs were seeded at either 10,000 cells/cm^2 or 15,000 cells/cm^2 in a 12 well plate and allowed to attach for 24 hours. hMSC-medium was removed and the surface of the cells were washed with PBS. CD4 cells, with DynaBeads, were added at 1:2, 1:5, 1:10 or 1:20 hMSC:CD4 ratio in RPMI complete medium for 72 hours.

Following the co-culture the CD4 cells were gently resuspended and sampled for cell counting. Media samples were taken for kynurenine analysis (see Section 2.13).

2.7 Cell Counting

All cell counts and viability were performed using either a NC-100 or a NC-3000 Nucelo-Counter (Chemometec, Denmark), based on propidium iodide (PI) and PI/acridine orange respectively. For the NC-100, a non-viable cell count was obtained first by drawing cell suspension into a NucleoCassette and the reading would give a non-viable cell count as viable cells would exclude the PI stain. Total cell counts was then obtained by mixing an equal volume of cell suspension to NucleoCounter Buffer A (Chemometec, Denmark) to permeabilise the cells. NucleoCounter Buffer B was added to stabilise the solution, then analysed with a NucleoCassette as before. The value would be multiplied by three to take into account the dilution due to the buffers. Total live cells was calculated by subtracting the non-viable cells from the total cell count.

On the NC-3000 a cell suspension of approximately 200μl was drawn into a Via-1 Cassette. This stains the cell with acridine orange and propidium iodide to discriminate between live and dead cells respectively.

2.8 Cell Vitality

Apoptosis and cell health was determined by the levels of free thiols in the cells using cell vitality protocol on the NC-3000 NucleoCounter. VitaBright-48, PI, and acridine orange solution was added to a cell suspension and the samples were imaged on the NC-3000. VitaBright-48 reacts with thiols becoming a fluorescent product that has peak excitation at 405 nm and emission at 475/25 nm. PI/acridine orange allow for live/dead staining as described above.

2.9 Cell Cycle

Cell cycle was determined by DAPI nuclear staining. Cells were first washed with PBS then fixed with 70% ethanol for two hours on ice. The ethanol was removed and the cells were again washed in PBS. Then the cells were resuspended in a solution containing 1μ g/ml DAPI and 0.1% triton-X100 in PBS (Chemometec, Denmark) for 5 minutes at 37°C. The samples were then loaded onto slides for analysis on the NC-3000.

2.10 Nutrient/Metabolite Analysis

Nutrient and metabolite was determined using a BioProfile FLEX (Nova Biomedical, UK). Medium samples (1ml) were taken from cultures and stored at -80°C until analysis. Glucose concentration is based on the level of ammonia (H_2O_2) produced during enzymatic reaction between glucose and oxygen is the presence of glucose oxidase enzyme. Similarly lactate measurement is based on H_2O_2 production between lactate and oxygen under lactate oxidase enzyme. Both values are displayed as g/L and were converted to mmol/L.

The yield of lactate from glucose was calculated from the following equation:

$$Y_{Lac/Gluc} = \frac{\Delta Lac}{\Delta Gluc} \tag{2.1}$$

Where:

- $Y_{Lac/Gluc}$ = Yield of glucose from lactate
- ΔLac = Lactate production over time
- $\Delta Gluc$ = Glucose consumption over the same time period

The cell specific glucose consumption rate was calculated from the following equation:

$$q_{gluc} = \frac{\mu}{c_x 0} \times \frac{C_{gluc(s)} - C_{gluc(e)}}{e^{\mu t} - 1} \tag{2.2}$$

Where:

- q_{gluc} = Specific glucose consumption
- μ = Specific growth rate
- $c_x 0$ = Cell number at the start
- $C_{gluc(s)}$ = Glucose concentration at the beginning
- $C_{gluc(e)}$ = Glucose concentration at the end
- t = time in hours

2.11 Protein Quantification

2.11.1 Enzyme-linked Immunosorbent Assay (ELISA)

Supernatant from cell cultures were taken and stored at -80°C. IL-6 levels were measured by sandwich ELISA using a BD OptEIA^{TM}reagent kit (BD Biosciences, UK. Cat No. 550799). Anti-human IL-6 monoclonal antibody was coated to the surface of a 96-well Maxisorp plate (NUNC, UK) and left overnight at 4°C. The plate was then washed 3 times with wash buffer containing PBS and 0.05% Tween-20. The wells were then blocked with Assay Diluent containing 10% FBS at room temperature for 1 hour, during this time media samples and IL-6 standards were prepared. Following further washing the samples and standards were loaded onto the plate and incubated for 2 hours at room temperature. The plate was washed 5 times before incubation of Working Detector (Biotinylated Anti-human

IL-6 monoclonal antibody + Streptavidin-HRP reagent) for 2 hours at room temperature. This was then aspirated and washed 7 times. Substrate solution (Tetramethylbenzidine (TMB) and Hydrogen Peroxide) was added for 30 minutes followed by addition of Stop Solution (1M H_3PO_4).

Immediately after adding Stop Solution the absorbance was read at 450nm using a FLUOstar Omega plate reader (BMG Labtech, Germany).

2.11.2 Luminex

In order to quantify the angiogenic paracrine growth factors 48 hours conditioned medium from hMSCs were analysed using multiplex assay Luminex MAGPIX kits (R&D Systems, UK) according to the manufacturers instructions. Standards were prepared by reconstituting a premixed cocktail with Calibrator Diluent and preparing a 3-fold dilution series. Capture microparticle cocktail was added to each well of a 96-well assay plate. Samples or standards, prepared in duplicates, were added to each well, sealed with foil and incubated for 2 hours at room temperature on an orbital shaker. The plate was washed three times then incubated with Biotin Antibody Cocktail for 1 hour at room temperature. Wash steps were repeated and the plate was incubated with Streptavidin-PE for a further 30 minutes. Beads were captured and analysed using a Bio-Plex®MAGPIX^{TM}Multiplex Reader. Array data was quantified using Bio-Plex Data Pro software.

2.12 Real-Time Quantitative Polymerase Chain Reaction (PCR)

2.12.1 RNA Extraction

Total RNA extraction and clean-up was performed using a RNeasy Plus kit (Qiagen, Germany. Cat No. 74134) as follows according to the manufacturer's guidelines. Following cytokine incubation hMSCs were trypsinised as described in section 2.1.4. Buffer RLT (350μl) was added to the cell pellet and vortexed for 30 seconds. The resulting lysate was transferred into a QIA shredder spin column and centrifuged for 2 minutes at 8,000xg. A further 350μl of of 70% ethanol was added to the homogenized lysate. The sample was transferred to an RNeasy spin column and centrifuged for 15 seconds at 8,000xg. The column was rinsed by addition of 700μl of Buffer RW1 and centrifugation for 15 seconds at 8,000xg, the flow through was discarded. Next, 500μl of Buffer RPE was added to the column and centrifuged for 2 minutes at 8,000xg to wash the spin column membrane. To fully dry the membrane, the column was placed into a new 2ml collection tube and centrifuged for 1 minute at 8,000xg. RNA was eluted by adding 30μl of RNase-free water directly to the spin column membrane and centrifuged for 1 minute.

RNA concentration and ratio of absorbance at 260nm to 280nm (A_{260}/A_{280} ratio) was quantified using a NanoDrop 2000c Spectrophotometer (Thermo Scientific). Samples were frozen at -80°C.

2.12.2 PCR

RNA samples were subject to reverse transcription using EXPRESS One-Step Superscript qRT-PCR kit (Invitrogen, UK. Cat No. 11781200) according to the manufacturer's instructions. cDNA products were amplified on an Applied Science StepOne Plus machine

(Invitrogen, UK) in a 20μl reaction mixture containing 360ng of sample RNA, One-Step SuperScript®III Reverse Transcriptase, ROX dye and Platinum®Taq DNA Polymerase with forward and reverse primers (Table 2.4). Each amplification cycle consisted of an initial holding step at 50°C (15 minutes), followed by 40 cycles of denaturation at 95°C (15 seconds) and annealing at 60°C (1 minute). Quantification of the levels of gene expression for each sample was calculated using the comparative C_T method ($\Delta\Delta C_T$). Glyceraldehyde 3-phosphate dehydrogenase (GAPDH) was chosen as a reference gene.

Table 2.4: Primer Sequences for PCR

Gene	Forward Primer	Assay ID	Reporter Dye
IDO	TTCTGCAATCAAAGTAATTCCTACT	Hs00984148_m1	VIC
GAPDH	CAAGAGGAAGAGAGAGACCCTCACT	Hs03929097_g1	FAM

2.13 Kynurenine Assay

IDO catalyses the conversion of tryptophan to N-formylkynurenine which is further catabolised to kynurenine. Kynurenine concentration in the medium is directly proportional to IDO activity. Media supernatants from inflammatory treated cells were analysed. Cell medium (150μl) was incubated with 50μl of 30% (vol/vol) Trichloroacetic acid (Sigma-Alridch, UK. Cat No. T0699) for 10 minutes at 50°C, vortexed and centrifuged at 10,000g for 5 minutes. Supernatant (75μl) was transferred to a 96 well plate followed by addition of equal volume of Ehrlich's reagent (1% w/v p-dimethylbenzaldehyde in glacial acetic acid) (Sigma-Aldrich, UK. Cat No. 156477) for 10 minutes at room temperature. Optical absorbance was measured at 492nm. The amount of kynurenine was determined using a standard curve from 0-100μM.

2.14 HUVEC Culture

2.14.1 Cell Source

Human umbilical cord endothelial cells (HUVECs) were purchased from Gibco, Life Technologies (UK). The donor was a newborn male.

2.14.2 Medium Formulation

HUVECs were cultured in Medium 200PRF supplemented with low serum growth supplement (LSGS) (all from Life Technologies, UK. Cat No. M200PRF500).

2.14.3 Cell Growth and Sub-Culture

Cells were seeded at 2.5x10^3 cells/cm^2 T75 culture flasks. The medium was changed every 48 hours until the cells had reached 80% confluency. Once the cells had reached 80% confluency the medium was removed completely and 0.025% trypsin/EDTA was added to cover the flask surface and incubated for 1-3 minutes at room temperature. Trypsin neutraliser solution was added to the cells and pipetted until a single cell suspension was produced. The suspension was transferred to a centrifuge tube and centrifuged at 180xg for 7 minutes. The supernatant was removed and the cells resuspended in culture media, reseeded and placed into a humidified incubator at 37°C with 5% CO_2.

2.14.4 HUVEC Tube Formation

HUVECs were harvested and seeded at 2.3 x 10^4 cells/cm^2 or as stated in text. For positive controls HUVECs were cultured in supplemented Medium 200PRF.

To compare coating strategies multiple approaches were taken:

1. GelTrex 100%: 50μl/cm^2 of GelTrex (Life Technologies, UK. Cat No. A1413202) (kept on ice) was added in the centre of a 24-well plate and spread evenly with the back of a sterile pipette tip. The plate was then placed in a 37°C incubator for 30 minutes.

2. GelTrex 75%: GelTrex was mixed with cold PBS at a 3:1 ratio and applied to the well as before.

3. GelTrex 50%: GelTrex was mixed with cold PBS at a 1:1 ratio and applied to the well as before.

4. Gelatin 2%: 50μl/cm^2 of Gelatin solution 2% (Sigma, UK) was added in the centre of a 24-well plate and spread evenly with the back of a sterile pipette tip and allowed to coat at 4°C overnight. Before use the well was washed once with PBS.

5. Gelatin 1%: Gelatin was diluted at 1:1 ratio with PBS and applied to the well as above.

6. Gelatin 0.5%: Gelatin was diluted at 1:2 ratio with PBS and applied to the well as before.

7. Matrigel Layer: 50μl/cm^2 of reduced-growth factor Matrigel (Corning, US. Cat No. 356231) (kept on ice) was applied in the centre of a 24-well plate and spread evenly with the back of a sterile pipette tip. The plate was then placed in a 37°C incubator for 30 minutes. Before use the layer was wash once with serum-free DMEM.

8. Matrigel Coating: Matrigel was diluted to a protein concentration of 3mg/ml with cold serum-free DMEM and added to each well to cover the surface. The plate was then placed in a 37°C incubator for 30 minutes to coat. Before use the solution was removed and washed once with serum-free DMEM.

HUVEC tube formation was imaged using a Nikon Biostation CT in 20 minute intervals over 24 hours. This allowed live-image time lapse recordings of the cells undergoing tube formation. To obtain a representative view of the well a 4 x 4 tiling observation was set covering a 60.84mm^2, or 56% of the well.

2.14.5 Tube Analysis

Following tube formation, the images were downloaded from the main computer to be analysed using either ImageJ or CL-Quant software packages. ImageJ is an open-source image processor that allows the use of external user-created plugins, for tube analysis the images were scaled-down to 70% of the original size and analysed using the Angiogenesis Analyzer for ImageJ plugin as developed by Chevalier et al. (2014). CL-Quant is analytical software designed to be used in conjunction with the Nikon Biostation CT. Similar to ImageJ, image analysis is performed by applying recipe macros.

2.15 Hypoxic Culture of hMSCs

For the angiogenesis study hMSCs were cultured into flask as described in Section 2.1. For hypoxic conditioning the cells were thawed and cultured in a Galaxy 170r incubator (New Brunswick Scientific, UK) set at 5% CO_2, 5% O_2 O2, and 90% N_2 for one passage before the experimental harvest. After another passage the cells were cultured as before with a full medium exchange at 72 hours. The cells were cultured further for another 48 hours before the conditioned medium was harvested and the cells passaged. Control cells were cultured in a standard cell culture incubator containing atmospheric air and 5% CO_2.

2.15.1 Generation of hMSC Conditioned Medium

For experimental hMSC-conditioned medium, hMSCs were cultured as described in Section 2.1.4. The cells were seeded at 5,000 cells/cm^2 and placed into an incubator. After 72 hours the spent medium was removed and fresh hMSC-medium was added. Following a further 48 hours of conditioning the medium was harvest and stored at -20°C until

required. The cells were then passaged into new flasks.

2.16 Equations

The following equations were used to calculate the various parameters:

Cumulative population doubling level (PDL)

$$PDL = x + 3.322(logY - logI) \tag{2.3}$$

Where:

- x = Initial population doubling
- Y = Final cell count
- I = Initial cell number seeded

Population doubling time (PDT)

$$PDT = \frac{T \times \ln 2}{\ln\left(\frac{Y}{I}\right)} \tag{2.4}$$

Where:

- T = Time (hours or days)

Specific Growth Rate

$$\mu = \frac{(ln\,(Y/I))}{\Delta T} \tag{2.5}$$

Where:

- μ = Specific Growth Rate (h^{-}1)

Fold Increase

$$FoldIncrease = Y/I \tag{2.6}$$

Table 2.5: Level of significance

Symbol	Meaning
n.s	$P > 0.05$ (not significant)
*	$P \leq 0.05$
**	$P \leq 0.01$
***	$P \leq 0.001$
****	$P \leq 0.0001$

2.17 Statistical analysis

Statistical analysis was perform using one-way analysis of variance (ANOVA) to determine significance at P >0.05. GraphPad Prism 6 was used for all statistical analysis. Levels of significance are indicated in Table 2.5

Chapter 3

Establishment and Characterisation of Human Mesenchymal Stem Cell Lines for Cell Therapy Manufacture

3.1 Introduction

The use of hMSCs and other potentially therapeutically cells hold a great potential to treat a variety of unmet medical conditions. Developing cells for human clinical application starts with tissue/cell donation followed by processing, release testing, and finally, transplantation (BSI PAS 83, 2012).

For autologous therapies, where the cells are isolated, processed and transplanted back into the same patient, establishing a master cell bank is not required especially for 'minimally manipulated' cases where the cells are enriched and separated before returning to the patient. Examples of near bedside or point-of-care processing include Celution®(Cytori Therapeutics Inc.) or Icellator®(Tissue Genesis) both of which isolate, enrich and re-deliver the patients own adipose-derived stem cells; these systems have been used in

wound healing and for critical limb ischemia (Fraser et al. 2014). The main advantage of autologous therapies is the lack of immune rejection as it is the same patients cells being used. This avoids the need for HLA-matching or the use of immunosuppressive medication. However, due to being patient specific cells they require isolation and lengthy *in vitro* expansion before administration which leads to longer treatment times and impacts on cost. Autologous expanded hMSCs have been used for cartilage repair and ischemic cardiomyopathy (Haleem et al. 2010; Hare et al. 2012).

In contrast, allogeneic therapies are cells that are sourced from one donor and transplanted into a different recipient. Once the donor cells are isolated they can be expanded *in vitro* and cryopreserved until required. For this to be achieved it is vital to start with a well characterised master cell bank that is amenable for scale-up production to the required dose. As previously discussed in Chapter 2, hMSCs can be used for multiple therapeutic areas including treatment of stroke and GvHD due to their innate ability to evade the immune system by low expression of MHC class I and negative expression of MHC class II and thus do not require immunosuppressive medication. For these reasons they have emerged as an ideal 'off the shelf' allogeneic cell therapy product (Glennie et al. 2005; Kwon et al. 2014). Current clinical examples include MultiStem for ischemic stroke and Prochymal for GvHD (detailed in Table 4.1).

Before manufacturing of an allogeneic cell therapy product it is necessary to characterise multiple starting donor lines to determine which is amenable for manufacturing. It is known that donor variation plays a large role in growth potential and osteogenic differentiation capability of hMSCs (Phinney et al. 1999; Siddappa et al. 2007). This work will detail the variation on multiple hMSC donor lines in terms of growth rate, nutrient/metabolite consumption, extracellular marker expression, and differentiation capacity. Later chapters will look at developing functional assays that relate to their intended clinical function for immunosuppression (Chapter 5) and angiogenesis (Chapter 6).

Growth and culture of adherent cell lines is traditionally performed in two-dimensional,

monolayer tissue culture flasks. This system allows for easy observations of the cells during culture with simple medium exchange regimes and passaging. Cell culture variables include medium formulation (basal media, supplements and serum), medium exchange regimes, culture surface substrate, cell seeding densities and passage length. Standardisations of cell culture techniques and widely accepted protocols have played key roles in the development of consistent and robust cell lines.

This chapter focuses on the variation of input material in the derivation and establishment of five individual hMSC lines from separate donors to provide a comprehensive, parallel characterisation of hMSC lines.

The aims of this chapter were to:

- Isolate hMSCs from bone marrow mononuclear cells taken from multiple donors
- Determine the growth kinetics over several passages
- Measure nutrient consumption and metabolite production
- Analyse extra-cellular surface markers
- Perform differentiation into adipo-, osteo-, and chrondrocyte lineages [1]

3.2 Isolation of hMSCs

3.2.1 Plastic Adherence

As previously discussed in Chapter 2, the mesenchymal stem cell population represents a small fraction (0.01 - 0.001%) of nucleated cells found within adult bone marrow fraction

[1]Experimental procedures and data collection from this chapter was performed in conjunction with Thomas Heathman and Qasim Rafiq

(Pittenger 1999). Traditionally and still widely performed, hMSCs have been isolated from bone marrow aspirates by their adherence to tissue culture plastic. Other non-adherent haematopoietic cells are removed by aspiration during the first medium exchange. Five individual mononuclear cells (MNCs) donor vials were purchased from Lonza (see Chapter 2 Table 2.1) and the cells were plated (p0) into T-225 flasks until the appearance of adherent cell colonies, typically within 14 days of seeding. Each individual donor cell line was denoted M1 through to M5. All five donor MNCs gave rise to adhered cell colonies that readily expanded in culture. Once approximately 80-90% confluency was achieved the cells were passaged into new flasks for banking and experimentation.

hMSCs are identified *in vitro* by their ability to adhere to tissue culture plastic and proliferate in culture with a fibroblastic, elongated morphology (Pittenger 1999). Throughout the culture period the cells exhibited long branching protrusions and as the culture length progressed the cells packed closely together and aligned next to each other. Figure 3.1 shows the morphology of M2 cells throughout a 6 day passage taken every 24 hours from seeding. Initially the cells are evenly dispersed across the flask (24 - 72 hours). As they proliferate the cells align closer together (120 - 144 hours). hMSCs are growth contact inhibited and were sub-cultured when reaching approximately 90% confluency (Krinner et al. 2010).

Visual examination of the cells showed slight morphological differences between the cell lines. Figure 3.2 shows the morphology of each cell line at passage 3, day 3 of culture. M2 and M4 displayed the typical elongated structure with either two or three extensions from the main body. In contrast, M3 displayed a flattened appearance with a larger central body and multiple extensions. Morphological characterisation has been used as a quality assurance test for cell therapy, Regenexx®have used culture-expanded autologous hMSCs for various orthopaedic conditions and were graded using a morphology scale published by Katsube et al. (2008), where it was shown that thicker cells (larger cell body) correlated to a higher growth rate. As such, it is expected that flatter cells, such as M3, will exhibit

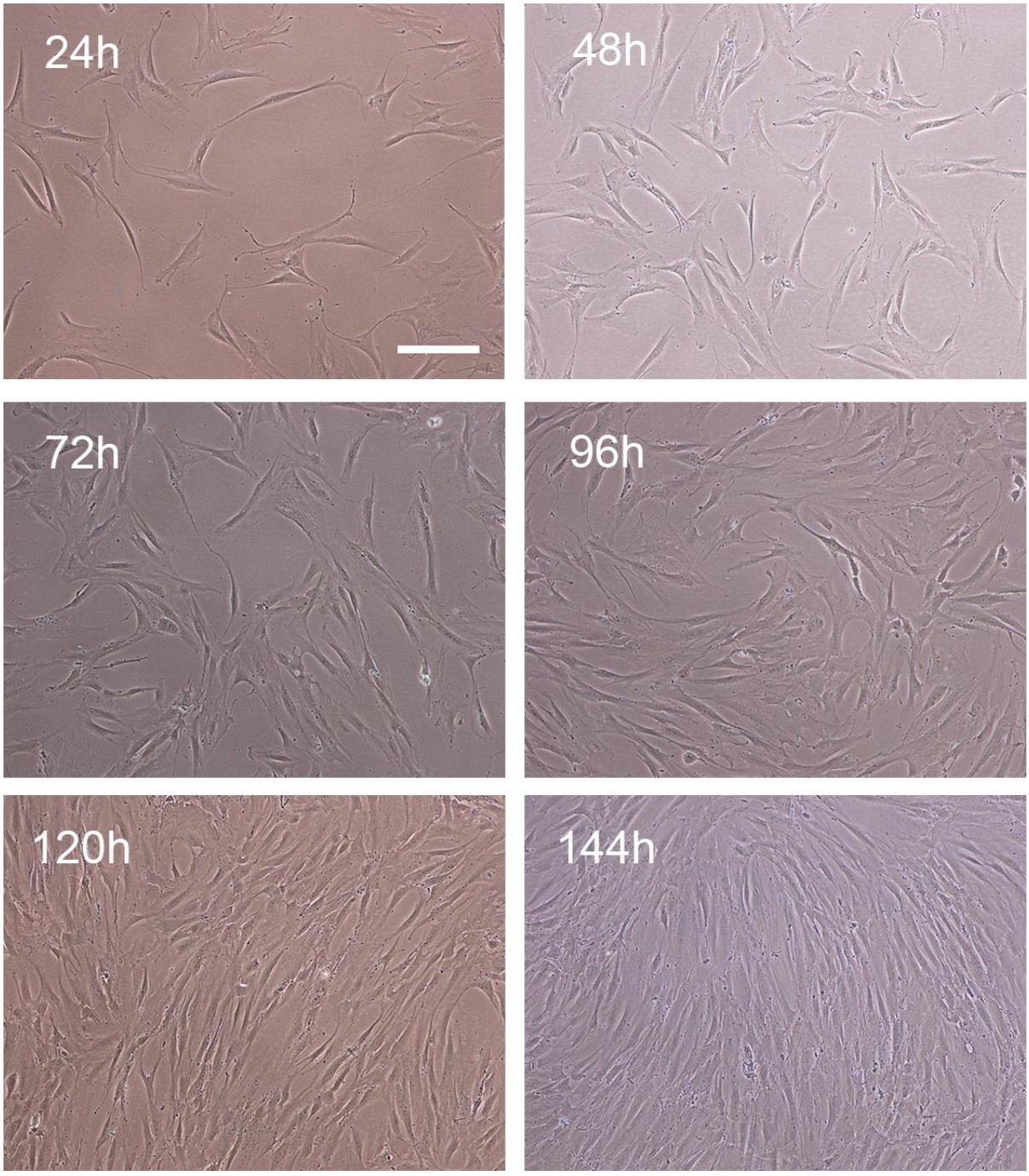

Figure 3.1: Representative M2 hMSC line morphology from multiple flasks. Images taken every 24 hours over passage 3. At 144 hours (day 6) the cells were sub-cultured into new flasks. Scale bar = 200μm

a slower growth rate.

Figure 3.3 shows the morphological changes seen in M2 hMSC line at p3 (left image) and at p7 (left image). Early passage cells had an elongated fibroblast morphology with two to three main protrusions from the cell body as shown by the red arrow. Late passage hMSCs became much larger, flatter and irregular with a more granulated cytoplasm. Similar changes were observed across all five hMSC lines suggesting reduced proliferation and senescence at the later passages. Growth senescence of hMSCs has previously been widely reported by others. Wagner et al. (2008) reported similar phenotypic abnormalities at similar passages (7 through to 9), further gene expression studies by Noh et al. (2010) and Schallmoser et al. (2010) found up-regulation of cell death related genes and down-regulation of genes related to mitosis and proliferation.

3.2.2 CD271 Isolation

Studies by Jones et al. (2002) and Jones et al. (2010) have suggested a novel mesenchymal stem cell population isolated from within the intramedullary cavity of long bones. This hMSC population was found within the $CD45^{-/low}/CD271^{+}$ fraction of bone marrow aspirates. $CD271^{+}$, also known as low-affinity nerve growth factor (LNGFR), cells have been isolated from the trabecular bone niche and found to exhibit a more efficient colony forming unit fibroblast (CFU-F) ability compared to cells isolated from the iliac crest bone marrow. In addition to this, $CD271^{+}$ cells also express the classical hMSC markers such as CD73, CD90 and CD105; with the ability to differentiate into the adipogenic, osteogenic and chondroblast lineages (Cox et al. 2012).

In terms of functional capability the $CD271^{+}$ hMSC subset Kuçi et al. (2010) showed these to secrete more growth factors and significantly inhibit the proliferation of allogeneic T-lymphocytes when compared to $CD271^{-}$ hMSCs . For these reasons, hMSCs were then isolated using magnetic activated cell sorting (MACS) based upon CD271 expression as

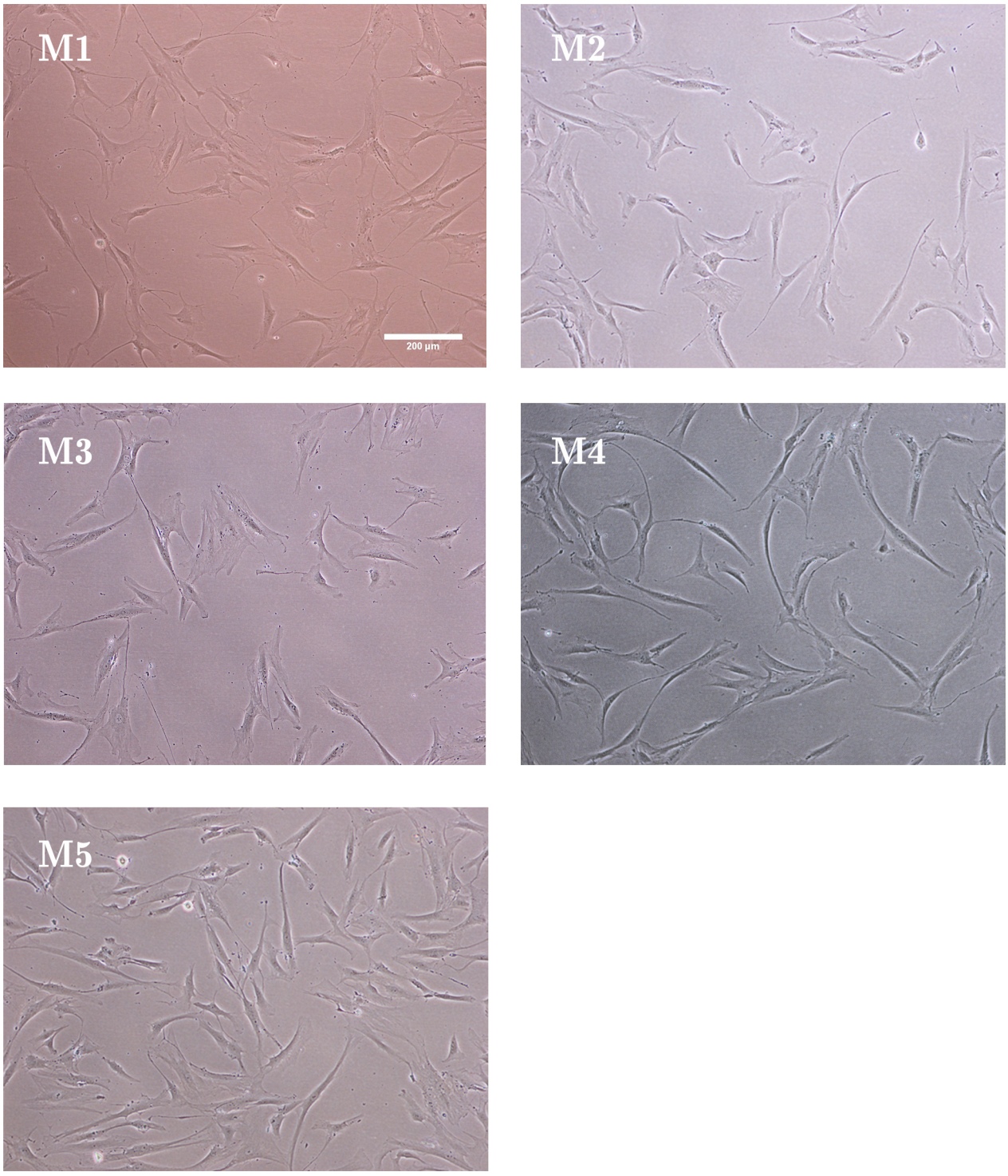

Figure 3.2: Representative cell morphology of M1- M5 cell lines at passage 2, day 3 of culture. Scale bar = 200μm

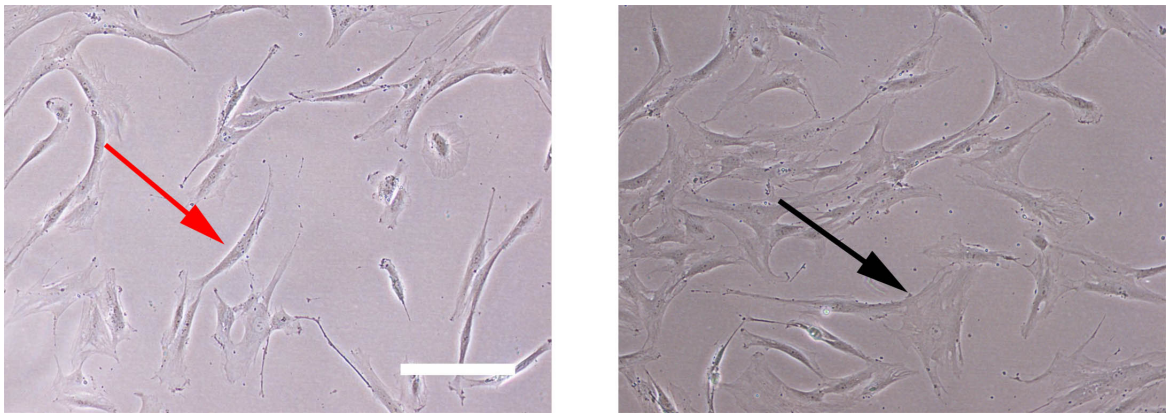

Figure 3.3: Morphological changes over passage. Left images shows M2 at passage 3, red arrow indicates a typical hMSC. Right image shows M2 at passage 7, black arrow indicates an hMSC with a larger and flatter morphology. Scale bar = 200μm

detailed in Materials & Methods 2.1.2.

After 21 days following the CD271$^+$ MACS procedure there was no evidence of cells observed in the culture flask from the CD271$^+$ flow through fraction (Fig 3.4a). However, there were cells in the CD271$^-$ flow through fraction (Fig 3.4b). Cells from this fraction had the classical hMSC morphology with long spindle-like protrusions and alignment when reaching confluency (Fig 3.4b) suggesting these cells were potentially hMSCs.

To further characterise the cells from the CD271$^-$ fraction, flow cytometry was performed to evaluate the extracellular surface marker expression and were found to be positive for CD73, CD90 and CD105; and negative for CD34 and HLA-DR suggesting this fraction of cells were hMSCs (Figure3.4c).

As there was no evidence of a CD271$^+$ sub-population following three weeks after MACS it was decided to analyse thawed MNCs via flow cytometry using the same staining and gating strategy as described by Cox et al. (2012). In this method, MNCs were dual stained for CD271 and CD45 - a hematopoietic marker found on leukocytes. A gate was placed in the CD271$^+$/CD45$^-$ area to examine the frequency of CD271 hMSCs (Fig 3.4d). Similar to the MACS technique there was little to no expression of CD271$^+$ cells (0.16 $\pm$ 0.02%)

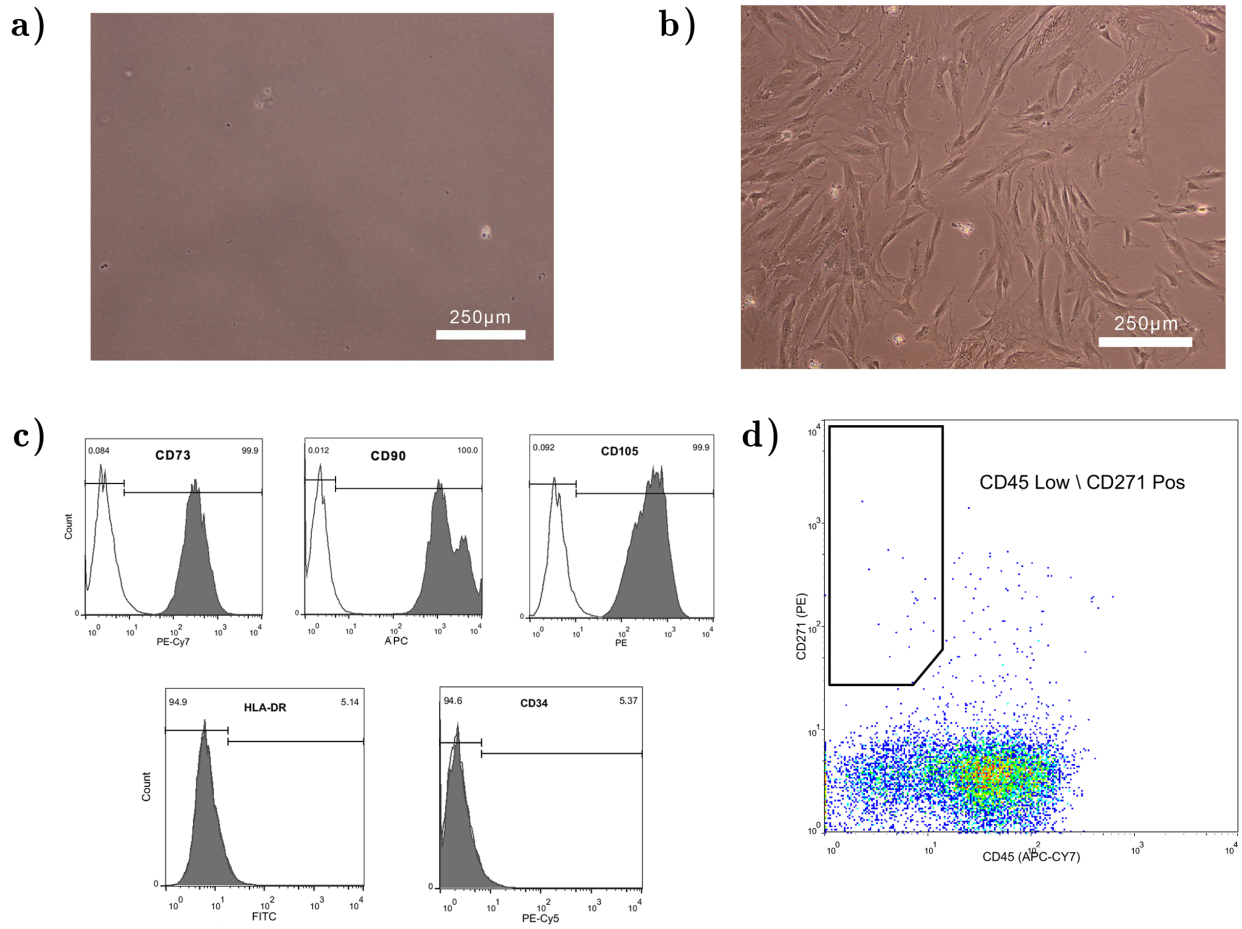

Figure 3.4: hMSC isolation on CD271 a) Image of the T-flask following 21 days after CD271$^+$ sorting showing lack of cells b) CD271$^-$ fraction showing adherent cells c) Flow cytometry analysis of cells from the CD271$^-$ fraction for CD73, CD90, CD105, CD34 and HLA-DR d) Dual staining of MNCs with CD271 (PE) and CD45 (APC-Cy7) n = 3

or the presence of a discrete population in the $CD271^{+}$/ $CD45^{-}/^{l}ow$ gate.

The lack of $CD271^{+}$ from these samples may be due to the source or isolation of the MNCs. The original reports by the Academic Unit of the Musculoskeletal Diseases Group, Leeds, UK described cell isolation following enzymatic digest of trabecular bone fragments from the pelvic area whereas the MNCs in this study were isolated from bone marrow aspirates (Jones et al. 2010).

CD271 expression may be specific to bone marrow hMSCs as also suggested by Attar et al. (2013) and Alvarez-Viejo (2013) who have both failed to find expression on cells isolated from umbilical cord and Wharton's Jelly samples. However, the absence of CD271 did not relate to the ability to isolate hMSCs from these areas suggesting it is not an adequate marker for hMSCs sourced from the umbilical cord or the Wharton's Jelly. Therefore, it could be argued that the ISCT definition of an hMSC can be used as an 'umbrella term' for all hMSCs. Typically there are site-specific markers to identify cells sourced from different niche locations i.e. CD271 for bone (Jones and Schäfer 2015). Due to the negative findings of a $CD271^{+}$ hMSC sub-population in the MNCs this method was not considered for future studies. It should also be noted that due to master MNC vial limitations it was not possible to perform MACS isolation multiple times and further repeats are necessary.

3.3 Growth Rate

Following plastic adherence isolation and first passage, each cell line was sub-cultured into four T75 flasks and passaged for a further five consecutive passages. A single passage consisted of 6 days in continuous culture with a 100% medium exchange on day 3. The cumulative population doubling and population doubling time for each hMSC line is presented in Figure 3.5. Previous studies have described the differences in hMSC prepa-

rations, including seeding density, culture length, media formulations and description of *in vitro* age (Schellenberg et al. 2012; Siegel et al. 2013). Therefore, in this study the culture variables will remain constant.

M2 and M4 showed the highest cumulative population doubling level (PDL) over the five passages, 12.09 ± 0.34 and 11.42 ± 0.2 respectively (Figure 3.5a). M1 initially demonstrated comparable growth kinetics until passage 6 where the cumulative population doubling significantly decreased when compared to M2 and M4. M3 and M5 showed the lowest cumulative population doubling over the 30 days with a final value of 7.82 ± 0.32 and 8.35 ± 0.29 respectively. Li et al. (2015) showed similar growth kinetics with bone marrow derived hMSCs to the M2 and M4 lines, however the authors demonstrated adipose derived hMSCs had a higher PDL over five passages. Bonab et al. (2006) performed cultures over 150 days, at day 15 the authors showed a PDL between 6-8 and at day 30 a PDL around 10-12. Compared to results shown here, there was a higher initial PDL but later time points showed similar results to M2 and M4 hMSC lines.

Population doubling time represents the number of hours required for doubling the cell number (Figure 3.5b). M2 and M4 both had a consistent doubling time of around 55 - 60 hours over the 30 day culture. M5 also showed a consistent doubling time but was slightly longer at 89.5 ± 17.8 hours. Up to passage 7, M1 (70.5 ± 17.5 hours) and M3 (79.0 ± 8.09 hours) both had comparable doubling times. However at passage 8 both hMSC lines significantly increased to 207.69 ± 72.7 and 229.55 ± 97.89 hours respectively.

This is also represented in Figure 3.5c where the specific growth rate for M1 decreased from $8.2\text{x}10^{-3} \pm 1.2\text{x}10^{-3}$ h^{-1} to $3.7\text{x}10^{-3} \pm 1\text{x}10^{-3}$ h^{-1} at p8. A similar effect is observed in M3. This sudden increase in doubling time suggested the cells were undergoing senescence. The specific growth rate of M2 remained high throughout the passages starting from $1.3\text{x}10^{-2} \pm 4\text{x}10^{-4}h^{-1}$ at p4 to $1.0\text{x}10^{-2} \pm 5\text{x}10^{-4}h^{-1}$ at p8.

M4 had the same specific growth rate at p4 and p5 ($1.25\text{x}10^{-2} \pm 1\text{x}10^{-4}h^{-1}$) this then

dropped to $9.5\text{x}10^{-3} \pm 9\text{x}10^{-4}\text{h}^{-1}$ at p6 and remained consistent throughout the remaining time points. The increased doubling time of M3 and M1 was mirrored by the sudden decrease of specific growth rate where it decreased to approximately half.

The sudden increase of doubling time and decrease of population doubling at passage 8 (day 30) of M1 and M3 could be linked to cellular senescence as the cells reach the Hayflick limit. The findings here correlate to published work by Wagner et al. (2008) who found similar growth patterns after 30 days in culture representing 10-12 cumulative population doublings. Similar changes in hMSC morphology were also described and linked to upregulation of genes responsible for cell membrane and lysosome integrity. Further microarray analysis by the authors demonstrated senescence associated gene expression was not restricted to certain passages, but increased continuously during expansion. A similar effect could be seen in this study where M1 and M3 cell lines showed a decreasing specific growth rate over the five passages (Figure 3.5c), therefore genetic analysis of these cells maybe required.

For a bioprocess examining the growth kinetics is a simple way to determine product consistency. Having a more consistent but slower growth growth rate may be advantageous as this limits the variation during the production of cells. By examining different donor hMSC sources it was possible to identify potential cell lines that are amenable for scale-up and can be taken further for characterisation and potency testing.

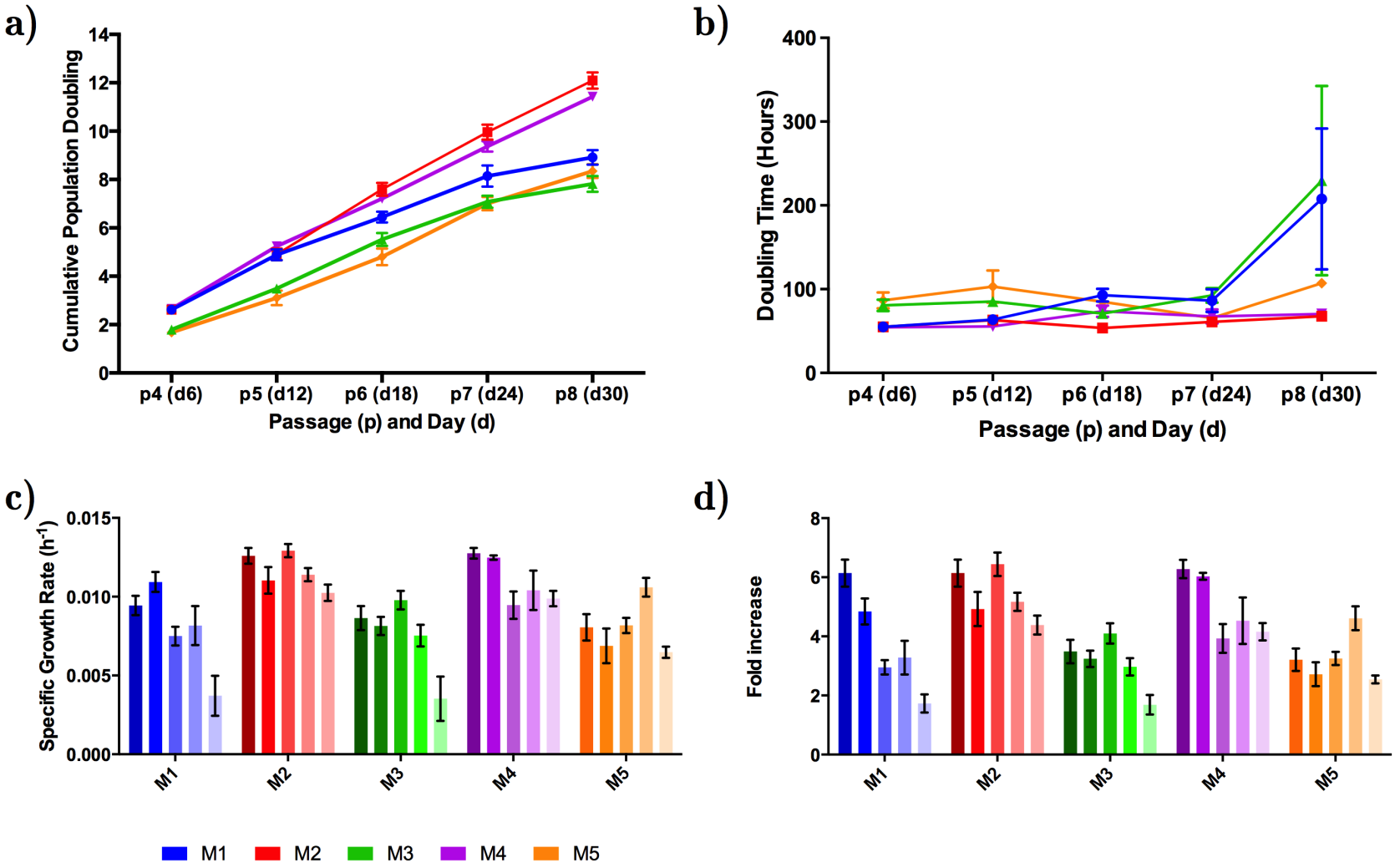

Figure 3.5: Growth characteristics of each hMSC line, M1 - M5. a) Graph of cumulative population doublings over 5 consecutive passages b) Doubling time for each MSC line over 5 passages c) Specific growth rate d) Fold increase. Each bar represents a passage, values presented as mean ± SD (n = 4)

3.3.1 Implications for Cell Therapies

Current published cell therapy doses of hMSC transfusion remain high, typically over $5x10^7$ cells per treatment and are administered as either a single transfusion or over multiple times. Table 3.1 shows the number of cells for each dose and the total for each treatment ranging from $6.4x10^7$ to $1.2\ x10^9$ cells. The exemplified treatments were chosen as they are currently in Phase II or III clinical trials. Extrapolating from the fold change in each passage from Figure 3.5d, the lower part of Table 3.1 shows the theoretical number of days needed in continuous culture - to produce enough cells for each treatment, assuming the starting point is $1x10^6$. As expected the faster growing lines, M2 and M4, would yield enough cells after 13-14 days in culture for a full treatment of Prochymal (Osiris) for the treatment of GvHD. This correlates to just over two passages. In contrast, M5, the slowest growing line would take a minimum of 21 days, or 3 passages, for the same treatment. Having an extended manufacturing time would impact on the overall cost due to increased personnel time, media, serum and other reagent usage.

Serum is a crucial component of hMSC culture and current stocks and production rate is not enough to sustain a growing cell therapy industry (Brindley et al. 2012). To overcome this challenge manufacturers and researchers are looking at serum-free media formulations, an early study by Agata et al. (2009) showed hMSC expansion was greater in serum-free medium (STEMPRO MSC SFM) when compared to FBS-containing media. In the context of this chapter future work could examine the growth kinetics of these lines under serum-free conditions. More recently Tan et al. (2015) screened multiple serum-free media and found there was no single optimal formulation that worked across seven individual hMSC donor lines suggesting further development or optimisation is required.

The implications of growth rate is clear when considering a treatment such as MultiStem where a single dose of $1.2x10^9$ cells is required. For M2 and M4 this number of cells is reached within 25-26 days or approximately 4 passages. However, the other three lines

have a significantly longer production time of 38-40 days, or approximately 6 passages.

Table 3.1: hMSC doses for three commercial cell therapy trials showing the total number of cells transfused. Extrapolated culture time (days) for each cell therapy treatment for each hMSC line assuming an initial starting number of $1x10^6$ cells

Cell Therapy	**Treatment**	**Dose**	**No. of doses**	**Total no. of cells**	**Reference**
MultiStem	Ischemic Stroke	1.2 $x10^9$	1	1.2 $x10^9$	Hess et al. (2014)
Stempeucel	AMI	$2x10^6$	64	1.28 $x10^8$	Chullikana et al. (2014)
Prochymal	GvHD	$2x10^6$	32	$6.4x10^7$	Kurtzberg et al. (2014)

	Time in culture (Days)				
	M1	**M2**	**M3**	**M4**	**M5**
MultiStem	38.1	25.1 ± 0.11	40.4	26.4 ± 0.06	38.1
Stempeucel	21.3 ± 0.55	16.2 ± 0.32	24.8 ± 0.40	17.0 ± 0.20	25.3 ± 0.31
Prochymal	16.1 ± 0.88	13.5 ± 0.39	19.9 ± 0.70	14.1 ± 0.25	21.4 ± 0.55

3.4 Nutrient, Metabolite and Electrolyte Analysis

Each day a medium sample was taken for analysis to determine the concentration of glucose, lactate and ammonia (Figure 3.6). Each passage lasted 6 days (represented by the vertical dashed line) and a 100% medium exchange (represented by the vertical dotted line) was performed on day 3. As expected, as the glucose (black line) was taken up the concentration of lactate (red line) and ammonia (green) increased due to the metabolic requirements of the proliferating hMSCs.

M2 and M4 lines consumed the most glucose over the 30 day culture. Starting at 5 mmol/L, at day 6 (3 days after the medium exchange) the cells had consumed 1.78 ± 0.19 mmol/L in all cases. Similarly for the M4 line there was a consumption of 1.88 ± 0.19 mmol/L over the same time period.

For the most part M1 and M3 lines showed a comparable consumption of glucose, consuming 1.38 ± 0.16 mmol/L and 1.21 ± 0.10 mmol/L per passage. However, during the last two passages of M3 there was a larger consumption of glucose and equally an increased production of lactate indicating a faster metabolic rate.

M5, showed the slowest population doubling time and least cumulative population doubling, consumed the least amount of glucose and produced the least amount of lactate. During the second passage it consumed a total of 0.96 ± 0.28 mmol/L of glucose, compared to M4 which consumed 2.66 ± 0.34 mmol/L over the same culture period. The slow division rate could explain the requirement for less energy (Schneider, Marison, and Von Stockar 1996).

As cells consume glucose and glutamine for energy they produce lactate and ammonia as waste byproducts, shown by the red and green lines in Figure 3.6. Excessive accumulation of lactate can lead to changes in the pH and osmolarity of the culture medium whereas ammonia can lead to reduced growth rate as it crosses the cell membrane and effects

intracellular enzymatic reactions. All hMSCs show an increase of lactate concentration as the passage proceeded, towards the end there is a higher concentration of lactate as the cells proliferate (Figure 3.6 red lines).

As with the glucose, M2 and M4 showed the highest concentration of lactate and remained consistent throughout. The small utilisation of glucose in M5 is reflected by the production of lactate. In later passages the concentration does not exceed 2 mmol/L, which is less than half of that seen in M2 for example.

During the culture of the cells the concentration of glucose was maintained above the Monod constant (K_s) of 0.1 - 0.4 mmol/L, the lowest value seen here was 2.875 mmol/L (M3 at 720 hours), suggesting growth was not inhibited by the lack of glucose (Acosta et al. 2007; Eibes et al. 2010). Additionally, the maximum lactate concentration observed was 5.67 mmol/L (M4 at 288 hours), lower than the inhibitory values known for hMSCs (24 mmol/L) (Schop et al. 2009). This is in part due to the regular medium exchange regime every 3 days and the use of low-glucose (1g/L) medium.

This data, in conjunction with the cell growth kinetics allows for the calculation of specific glucose consumption (pmol/cell/day) and the yield of lactate from glucose (mol/mol). The specific glucose consumption was calculated from the specific growth rate and glucose concentrations (Figure 3.7a). M2 and M4 showed comparable specific glucose consumption at around 19 - 20 pmol/cell/day and was consistent throughout the five passages. Overall M3 had the highest specific glucose consumption with an average rate of 17.4 $\pm$ 9.41 pmol/cell/day across all passages.

The yield of lactate from glucose was calculated over the same time period. The maximum theoretical yield of lactate from glucose is 2 mmol/mmol. A higher yield will indicate a more effective metabolism. Figure 3.7b shows yields of lactate from glucose calculated for the five different hMSC lines. M1 initially had a yield of 1.123 $\pm$ 0.08 mmol/mmol at p4 and declined to 0.70 $\pm$ 0.03 mmol/mmol at p8. The significant decrease appeared from

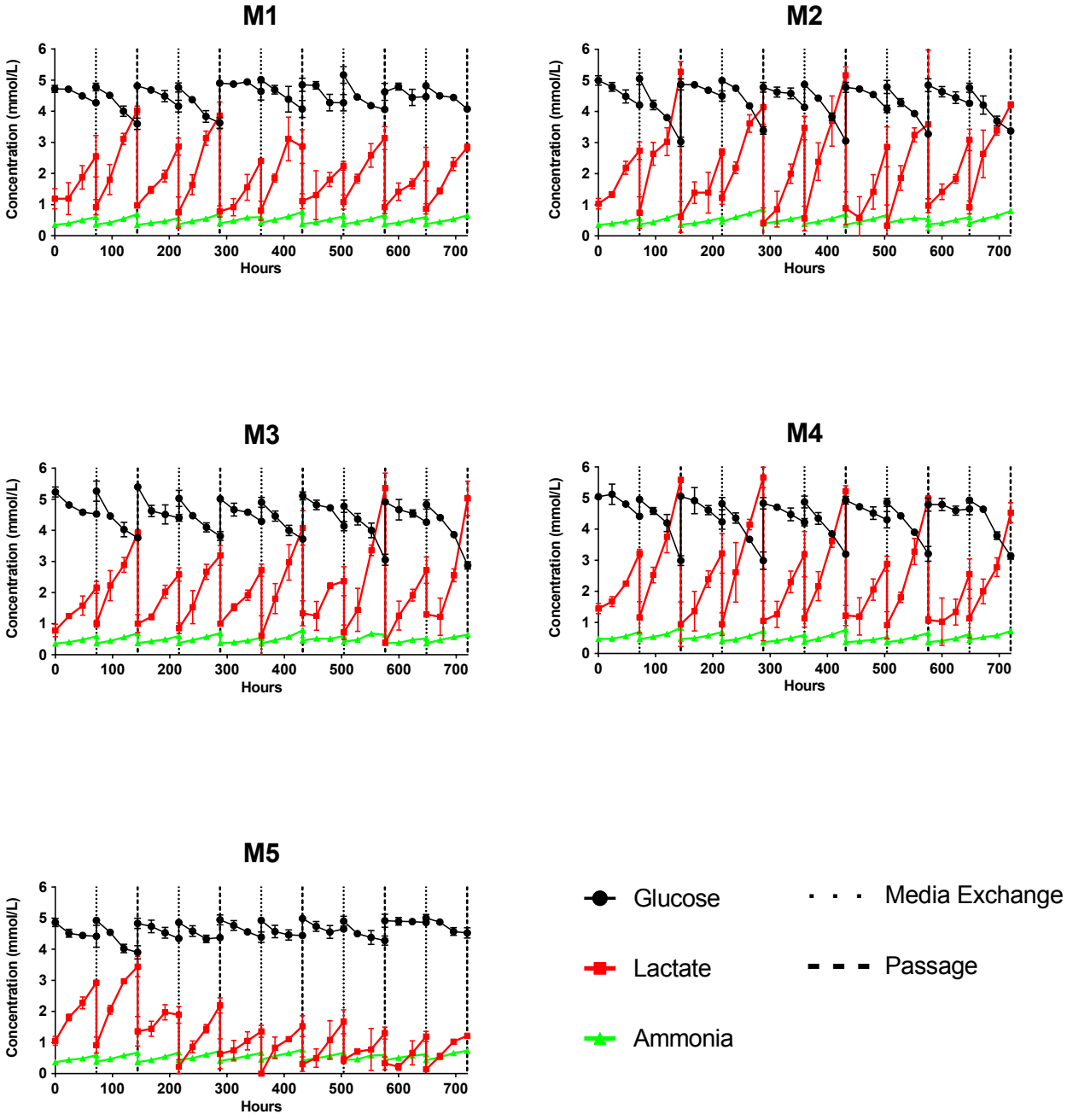

Figure 3.6: Nutrient and metabolite data for each hMSC line over 5 consecutive passages. Dots indicate 100% media exchange on day 3 of culture. Dashed lines indicate passage on day 6 of culture. Mean ± SD (n = 4)

p5 to p6 suggesting an *in vitro* limit for expansion. The faster growth rate of M2 and M4 are mirrored by efficient yield of glucose into lactate.

Of all lines M5 showed the least efficient conversion starting at 0.89 ± 0.27 mmol/mmol at p4 and steadily dropping to 0.12 ± 0.01 mmol/mmol at p8. This also correlates the decrease specific glucose consumption and growth rate.

For all cell lines the yield of lactate from glucose did not exceed the theoretical value of 2 mol/mol indicating the cells utilised the glycolysis metabolic pathway. The yield of ammonia from glutamine is not reported here as Ultra-glutamine, a stable form of L-glutamine, was used to supplement the medium and could not be measured with the Flex analyser.

3.5 Cell Surface Marker Analysis

Identity assays are intended to verify the the product quality in the master cell bank, working cell bank, and finally of the deliverable product. This ensures the product contains the cell population of interest and the manufacturing process did not produce unwanted contaminants. Cells undergoing extended long-term expansion *in vitro* are more prone to developing undesirable characteristics such as the gain or loss of a marker that may relate to an unwanted functional effect (Wang et al. 2013). Changes to the manufacturing process, such as culture methods or serum removal, may lead to phenotypic drift in the final product (Carmen et al. 2012). Therefore regular identity testing should be performed regularly in order to identify any changes and ensure a consistent product at the end of the manufacturing process.

To confirm the identity of the hMSCs they were assessed using a panel of extracellular markers as proposed by the ISCT was employed and this states the cells must express CD73, CD90, and CD105 whilst lacking expression of CD34, CD45, and HLA-DR (Do-

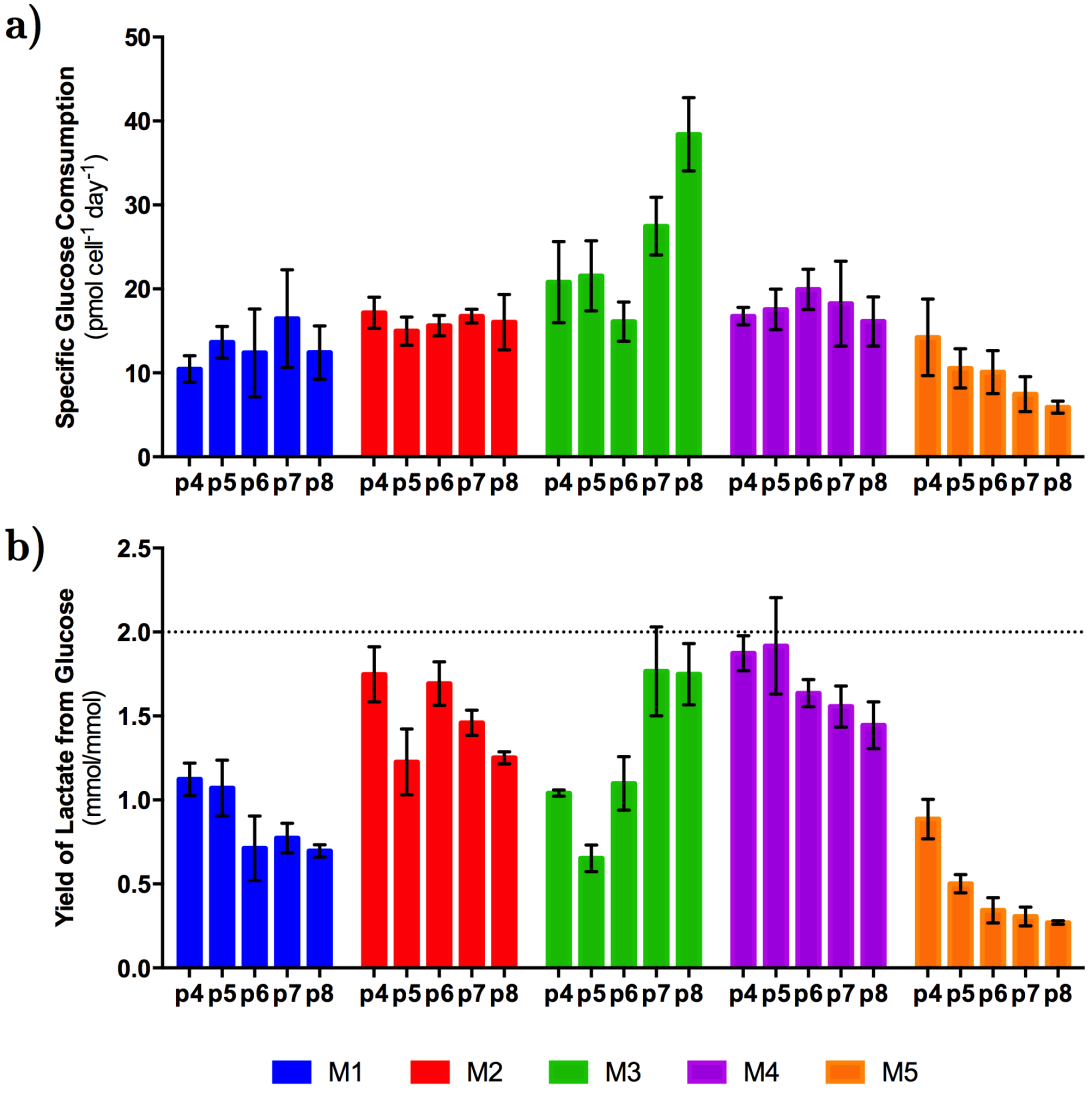

Figure 3.7: Nutrient and metabolite analysis showing a) Specific glucose consumption for five hMSC lines at the end of each passage b) Yield of lactate from glucose, dotted line indicates theoretical maximum glucose to lactate yield. Mean ± SD (n = 4)

minici et al. 2006). The ISCT guidelines further state that the cells must express $\geq 95\%$ of the positive markers and ≤ 2 % of the negative markers.

A multiparameter flow cytometry method, detailed in Chapter 4, was used to confirm the identity of the cells at the start (passage 3) and at the end of the experiment (passage 7). Figure 3.8 shows the representative flow cytometry diagrams of each hMSC line at passage 3 based upon the serial gating method (Chapter 4) and Table 3.2 details the full percent of the $CD73^+/CD90^+/$ $CD105^+/CD3^-/HLA\text{-}DR^-$ expression phenotype. The first gating shows the co-expression of CD105 and CD90 (red boxed quadrant), followed by CD90 and CD73. This is then finally gated on the two negative markers CD34 and HLA-DR to give a full phenotype value.

At passage 3 all hMSC lines expressed the full marker expression greater than 96% except for M4 ($93.60 \pm 2.51\%$). However at passage 7 it recovered expression to $95.56 \pm 0.42\%$. On the other hand M1, M2 and M3 lines were able to retain their phenotype expression throughout the passages whereas the M5 line started at $98.14 \pm 0.94\%$ then dropped to $93.17 \pm 1.60\%$. Loss of these markers over long term culture has also been previously reported by Otte et al. (2013), however, the authors did not find a correlation between the loss of markers and loss of differentiation capacity over long-term culture.

3.6 Differentiation

The final ISCT minimal criterion to demonstrate hMSCs identity is tri-lineage differentiation into the adipogenic, osteogenic and chondrogenic pathways (Figure 3.9). The ability of hMSCs to differentiate into these cell types have made them an ideal candidate for tissue engineering and regenerative medicine strategies and has become a key criterion to demonstrate the activity of hMSCs.

Cells cultured under adipogenic conditions for 14 days produced large lipid vacuoles

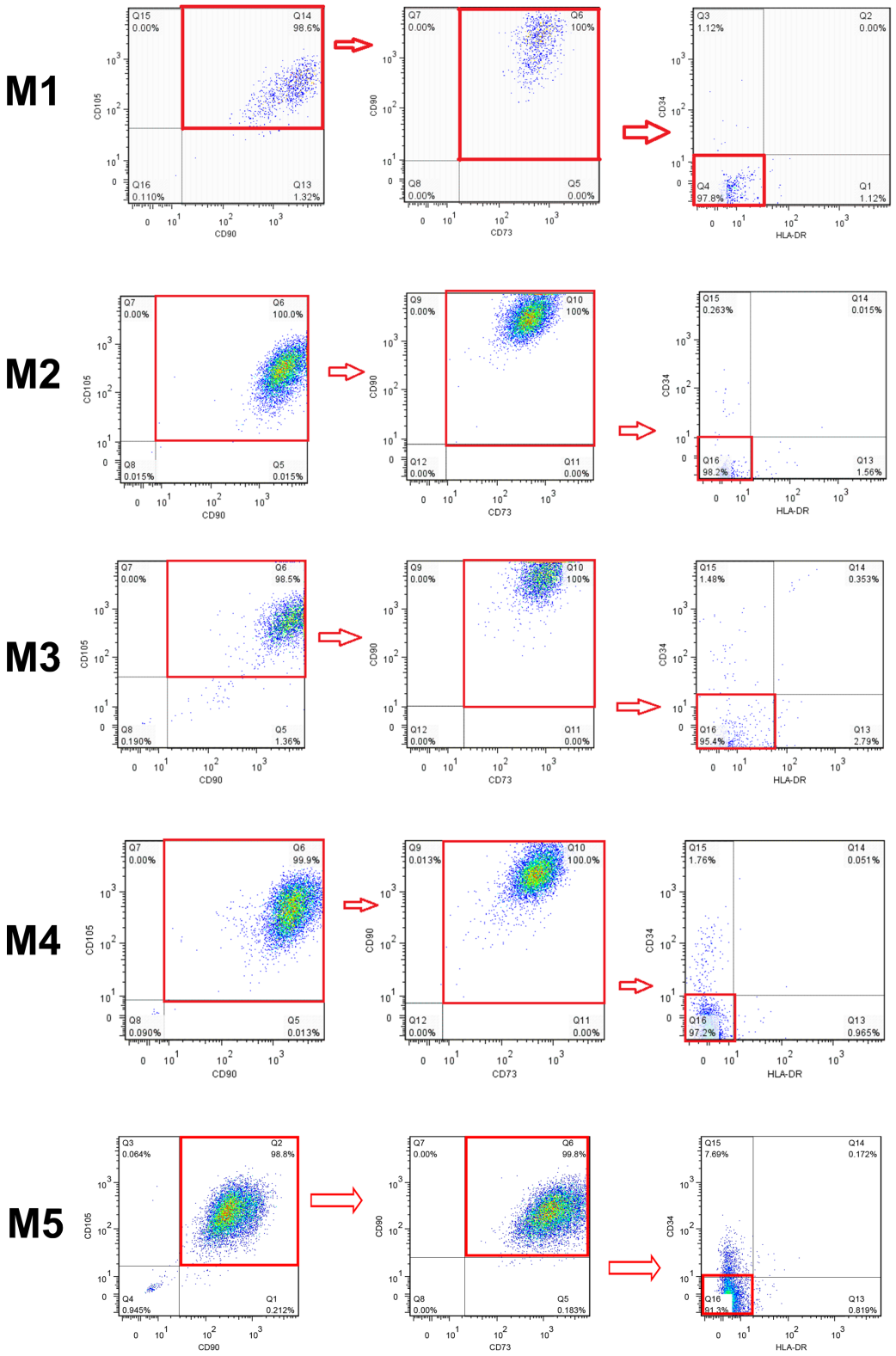

Figure 3.8: Representative plots for multiparameter analysis of the five hMSC lines using the serial gating strategy.First column CD105/CD90, second column CD90/CD73, third column CD34/HLA-DR

Table 3.2: Percent expression of the $CD73^+/CD90^+/$ $CD105^+/CD3^-/HLA\text{-}DR^-$ extracellular markers expression of hMSCs using the multicolour flow cytometry serial gating analysis as described in Chapter 4 for all cells lines at the end of passage 3 and passage 7. Mean value ± SD, 10,000 events were acquired per test, n = 4

hMSC Line	Day 0 (p3)	Day 30 (p7)
M1	98.97 ± 0.19%	97.78 ± 2.26%
M2	96.21 ± 0.22%	95.97 ± 0.42%
M3	98.19 ± 0.09%	95.13 ± 2.53%
M4	93.60 ± 2.51%	95.56 ± 0.42%
M5	98.14 ± 0.94%	93.17 ± 1.60%

throughout the cell cytoplasm. These lipids also stained positive for Oil Red O, a fat soluble dye thus showing differentiation into the adipogenic lineage.

Cells cultured under osteogenic conditions for 21 days stained positive for alkaline phosphatase (ALP) and silver nitrate. ALP demonstrates the presence of the alkaline phosphatase enzyme by reducing 5-bromo-4-chloro-3-indolyl-phosphate/nitro blue tetrazolium (BCIP/NBT) substrate into a dark blue precipitate. Calcium present in the mineral deposits generated during bone formation is reduced by light and replaced with silver deposits when silver nitrate staining is performed.

To demonstrate chondrocyte differentiation the hMSCs were plated in high-density micromass droplets in chondrogenic medium and cultured for 21 days. They were then stained with Alician Blue a polyvalent basic dye that is used to stain acidic polysaccharides such as glycosaminoglycans (GAGs). Under these conditions all five cell lines retained their micromass structure and showed positive staining for chondrogenic differentiation.

Under the differentiation conditions all five hMSC lines were able to differentiate into the respective types confirming that these all meet the ISCT guidelines to be classified as

'multipotent mesenchymal stromal cells'.

3.7 Conclusions

This chapter investigated the differences in growth rate, metabolism, extra-cellular marker expression, and differentiation of five separate hMSC lines derived from five individual donors. As there is no standard baseline definition for a 'good' hMSC line, each must be considered separately. By considering all these attributes it is possible to speculate which hMSC line could be a good candidate for further development into a cell therapy.

Before a cell manufacturing process can begin it is important to fully characterise the selected cells lines in order to avoid changes to the critical biological parameters. *In vitro* batch-to-batch variation comes from a number of sources, including the tissue/location of isolation, donor age, or isolation technique. Therefore choosing a good starting cell batch is critical for before further upstream processing can begin. Only then can considerations and control in culturing protocols, media formulation and passage number could be determined to maintain a consistent product.

By considering the growth rate, M2 and M4 lines showed the highest cumulative population doubling along with the highest specific growth rates. M1 initially showed a comparable growth rate but this significantly decreased towards later passages. From a manufacturing perspective it is advantageous to have a consistent cell expansion rate to be able to accurately predict the final yield. M3 and M5 lines had a consistent expansion profile similar to that of M2 and M4, however the final cumulative population doubling was significantly lower and thus limiting their potential for scale-up. These differences in donor variation will impact on autologous therapies where many cells maybe required within a limited time period. From the examples described here the slower growing cell lines such as M3 or M5 may not generate sufficient numbers of cells to be administered.

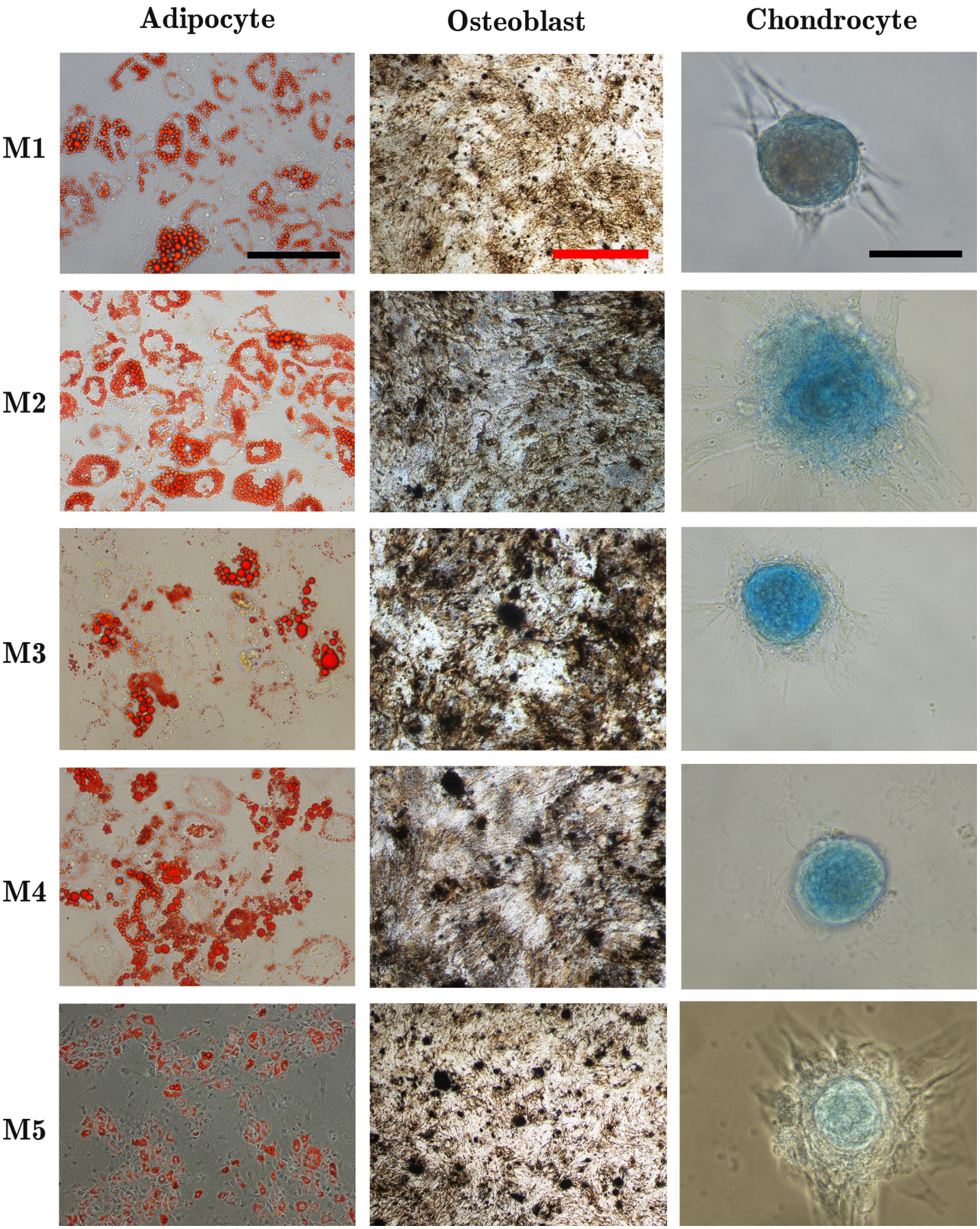

Figure 3.9: Phase contrast images of differentiated MSCs into the adipocyte (stained with Oil Red O), osteoblast (stained with Alkaline phophatase and silver nitrate solution) and chondrocyte (stained with Alician Blue) lineages. Black scale bar = 1000μm Red scale bar =100μm

This problem can be overcome in allogeneic therapies where multiple cell lines can be characterised, expanded and preserved until administering to the patient.

Differences in the nutrient consumption requires customised medium exchange regimes. In all cases the glucose consumption and the production of lactate/ammonia did not reach inhibitory levels. Regular medium exchanges would also remove unwanted byproducts not measured here. Unlike cell counting, media sampling is a non-destructive and non-invasive measurement of the culture process and provides valuable information on the cell environment. Determining a feeding regime that allows proper utilisation of the nutrients aids the optimising of the culture parameters.

The plastic adherence, expression of extra-cellular phenotype markers and tri-lineage differentiation demonstrate all hMSC cell lines meet minimal criteria as outlined by the ISCT.

In this chapter, the plastic adherence, expression of extra-cellular phenotype markers and the tri-lineage differentiation demonstrated that all selected hMSC lines meet the minimal criteria as outlined by the ISCT demonstrating the identity of a mesenchymal stromal stem cell. However, these assays does not characterise the supposed *in vivo* therapeutic effects that is essential for its application as a cell therapy. Chapters 5 and 6 will consider the hMSC potency in terms of immunosuppression and angiogenic potential.

Chapter 4

hMSC Characterisation via Multiparameter Flow Cytometry

4.1 Introduction

A robust identity assay ensures the master cell bank, working cell bank, and delivered product are the intended cells to be delivered to the patient. It verifies the manufacturing process was successful in producing the correct cell type and does not cause phenotypic drift, which is essential if there are changes in the manufacturing process, such as technology transfer or changes in medium formulation. Directives from the European Medical Agency (EMA) list identity testing as the first step in product characterisation (EMEA/CHMP/410869/2006).

The first hMSCs line was derived from bone marrow but other sources were also identified including adipose tissue, dental pulp and umbilical cord (Kern et al. 2006). Due to the varying sources of hMSCs and diversity of the isolation techniques employed, it is imperative to ensure the isolated cell population is homogeneous and has the correct cell surface marker phenotype.

Bone marrow derived hMSCs are distinct from the haematopoietic niche in that they express a very different set of cell surface antigens. hMSCs were shown to lack CD34 and CD45, markers typically expressed by red bloods cells and leukocytes respectively. As hMSCs were firstly isolated from the bone marrow stroma there may be a heterogeneous mixture of cell populations including cell types from the hematopoietic lineage. Therefore, it is imperative to ensure that the isolated population of cells are truly hMSCs and are not contaminated with other cell types.

As there is a lack of single definite marker for an hMSC identity, a combination of markers is needed to describe a population, this often leads to an inability to compare results. In an effort to develop a standardised criterion for defining a hMSC population, the International Society for Cell Therapy (ISCT) published a positional paper outlining the minimal criteria required (Dominici et al. 2006). This included the expression of certain cell surface antigens such as CD73, CD90 and CD105, whilst lacking others such as CD45, CD34, CD14, CD79α and HLA-DR. CD73, also called ecto-5'-nucleotidase, is an enzyme that converts AMP to adenosine and is a regulatory factor in hMSC osteo-/chondrogenic differentiation (Ode et al. 2012). CD90 (Thy-1) is a cell surface protein that mediates adhesion of leukocytes and monocytes to endothelial cells. Downregulation of CD90 has been associated with decreased immunosuppressive function(Campioni et al. 2009). Finally, CD105, an auxiliary receptor for the TGF-β receptor complex is associated with improved angiogenesis and vascular remodelling (Duff et al. 2003). As each marker/protein has a distinct function and is also found on other cell types, the simultaneous expression is required to identify a hMSC population.

4.1.1 Flow Cytometry

Flow cytometry is a laser-based technology that allows analysis of cells by suspending them in a stream of liquid and passing them directly over an excitation source. For cell characterisation, a single cell suspension is usually first incubated with fluorescently

bound antibodies before analysis. This allows discrimination for cells either having the antigen/protein of interest to those that do not. Flow cytometry offers the ability to rapidly examine thousands of cells individually in a short amount of time (seconds) and due to the high specificity also allows the discrimination of discrete subpopulations based on morphology and/or marker expression. These advantages make flow cytometry a valuable method for identity testing within a manufacturing process. However, this is an offline method which requires lengthy preparation steps and skilled personnel so maybe a disadvantage if the analysis requires rapid turnover.

In most stem cell literature single colour (or single parameter) flow cytometry has been used where a single marker was examined at one time. Therefore, to obtain a full expression phenotype each marker must use a separate sample. For hMSCs, this would require analysis of the three positive and at least one negative marker. This leads to an increased preparation time and requires more cells/reagents, and is thus not ideal when handling a limited numbers of cells. This is particularly important in cell therapies if the cells are to be transfused into a patient and there are limited quantities available for analysis.

To overcome this limitation, it is necessary to develop a more efficient method of cell characterisation. Multiparameter flow cytometry could be a viable option as it applies a cocktail of antibodies, each with their own discrete fluorophore, allowing multiple targets to be analysed simultaneously. This measurement of multiple parameters allows for detailed co-expression studies that may be lost during single staining (O'Donnell, Ernst, and Hingorani 2013). More commonly used in haematology and immune cell therapies to analyse mixed cell populations of blood samples. To date, multiparameter flow cytometry has rarely been utilised for stem cell applications.

This technique does require a greater understanding of the technical aspects of flow cytometry as there must be considerations to the excitation sources, band pass filters and fluorophore emission properties.

For multi-site manufacturing of cells, identification and comparability are key. In re-distributed manufacturing there is a shift to smaller-scale local manufacturing sites and quality assurance must be consistent across the sites. As different sites may have different flow cytometers the developed protocol was transferred to another machine to test for comparability and ease of protocol transfer.

The work described in this chapter was aimed at developing a novel flow cytometry analysis for hMSCs that goes beyond the current widely used techniques. More specifically, the objectives of this chapter were:

- Confirm marker expression of hMSCs using standard single staining flow cytometry techniques
- Develop a panel of antibodies that can be used in conjunction with each other
- Develop a post-acquisition analysis strategy that fully defines a hMSC population
- Transfer the method to a different cytometer

4.2 Single Colour Flow Cytometry

The cells were first singly stained for the markers of interest to ensure the panel was valid. All positive markers CD73, CD90 and CD105 gave 100% positive expression compared to isotype gating. Additionally, there was little expression of the negative markers with HLA-DR being 3.24% positive and CD34 being 3.42% positive (Figure 4.1). Due to being outside of the suggested ISCT range ($> 2\%$ expression) the cells were then analysed via the multiparameter flow cytometry method.

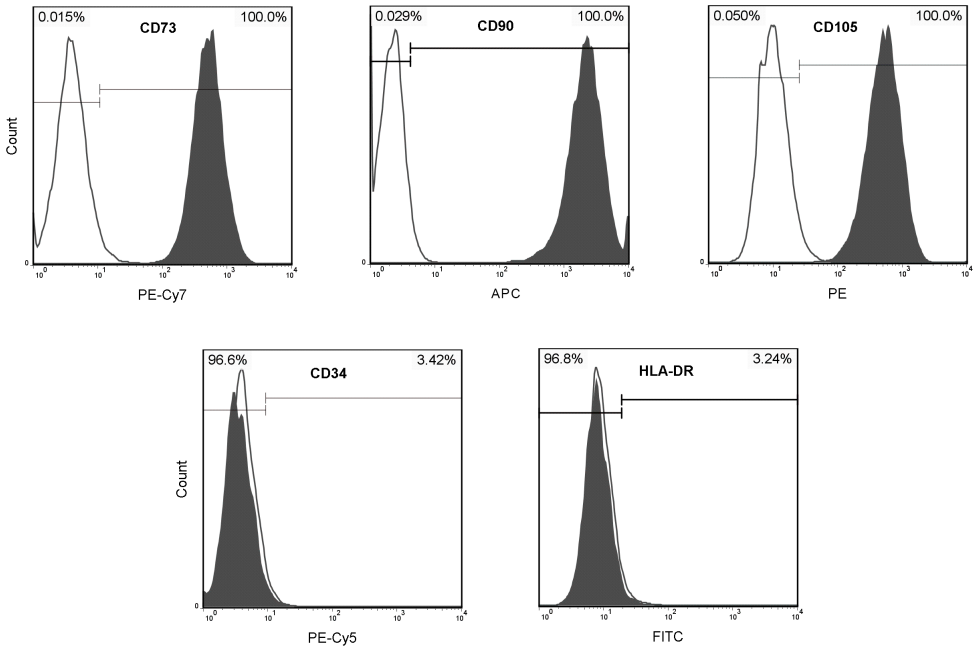

Figure 4.1: Single colour flow cytometry results for expression of selected markers of hMSCs (filled). Isotype gating (outline) was set to 95%. Positive markers CD73 (PE-Cy5), CD90 (APC), CD105 (PE) compared to negative markers CD34 (PE-Cy7) and HLA-DR (FITC). Graphs are representative of four separate experiments

4.3 Multiparameter Flow Cytometry

To further analyse the cell population and gain a greater understanding of cell marker expression, a multiparameter flow cytometry method was developed. In this set of experiments the cells were incubated with a mixture of antibodies conjugated to distinct fluorophores. This allows the simultaneous analysis of multiple extracellular targets on a single cell.

The number of markers that can be measured is limited by the number of filters and excitation sources available with each flow cytometer. With the Millipore Guava 8HT, it was possible to use all four filters from 488nm excitation and one from the 635nm excitation (Figure 4.2). Due to the nature of fluorophores and emission spectra, spectral overlap is most likely present. The fluorophores employed in this study were chosen on the basis of giving the least amount of spectral overlap which was achieved by selecting one fluorophore for each bandpass filter and ones that have narrow emission spectra as to avoid overlaping into the adjacent filters. As spectral overlap is most likely present, compensation must be applied. Compensation is a procedure that subtracts non-specific electronic signal from fluorochrome spillover. These values were determined using antibody capture beads and applied post-acquisition. The matrix was automatically defined by FlowJo software based on the emission from the beads. The final compensation matrix is shown in Table 4.1.

Two-dimensional dual plots of each marker combination confirmed the results of the previous single staining. The cells showed $\geq$ 99.9% dual positivity for CD73/CD105, CD105/CD90, CD90/CD73 combinations and >90% negative for CD34/HLA/DR expression (Figure 4.3). This pairwise analysis confirmed the validity of the panel combination and the compensation was effective.

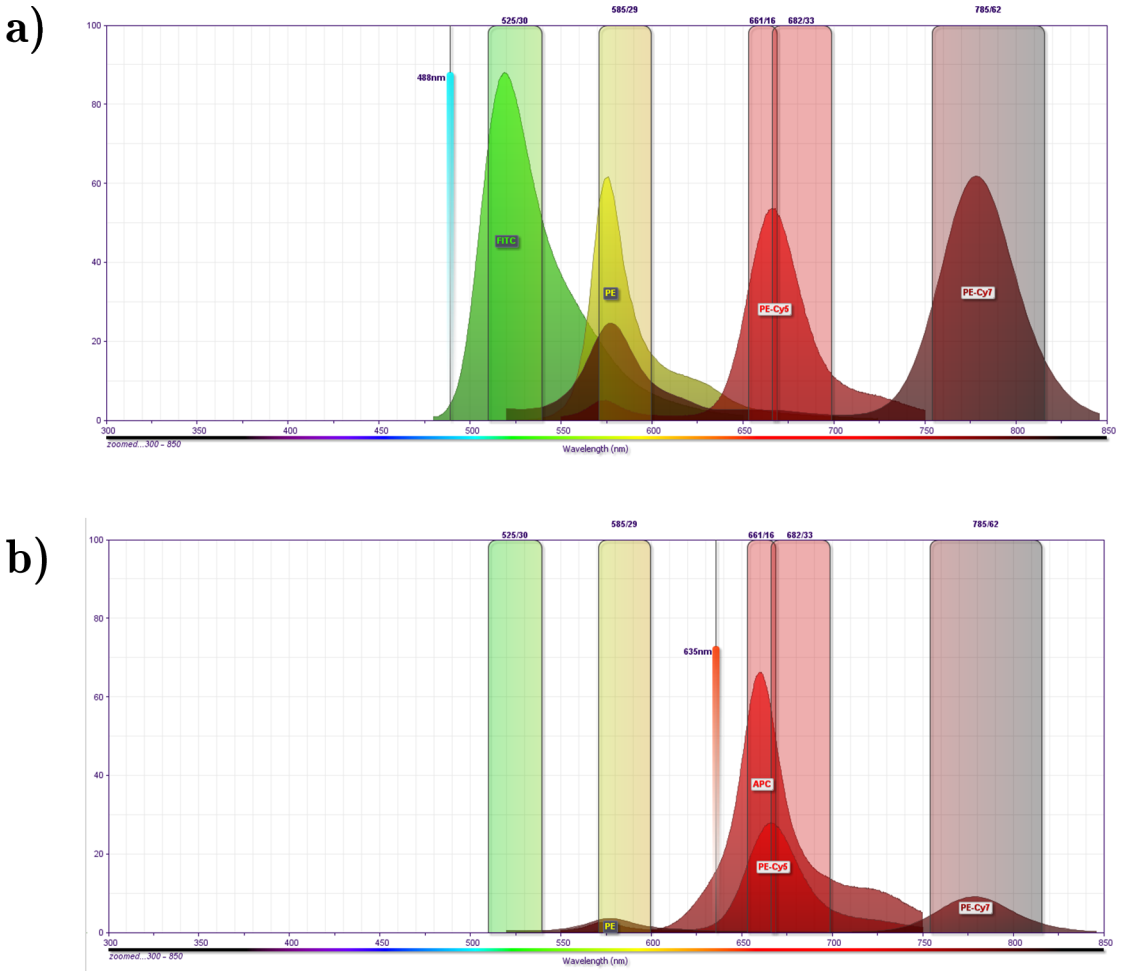

Figure 4.2: Filters and selected fluorophores for the multiparameter panel for the Millipore Guava 8HT. a) Excitation and filters for the 488nm laser b) Excitation and filters for the 635nm laser.

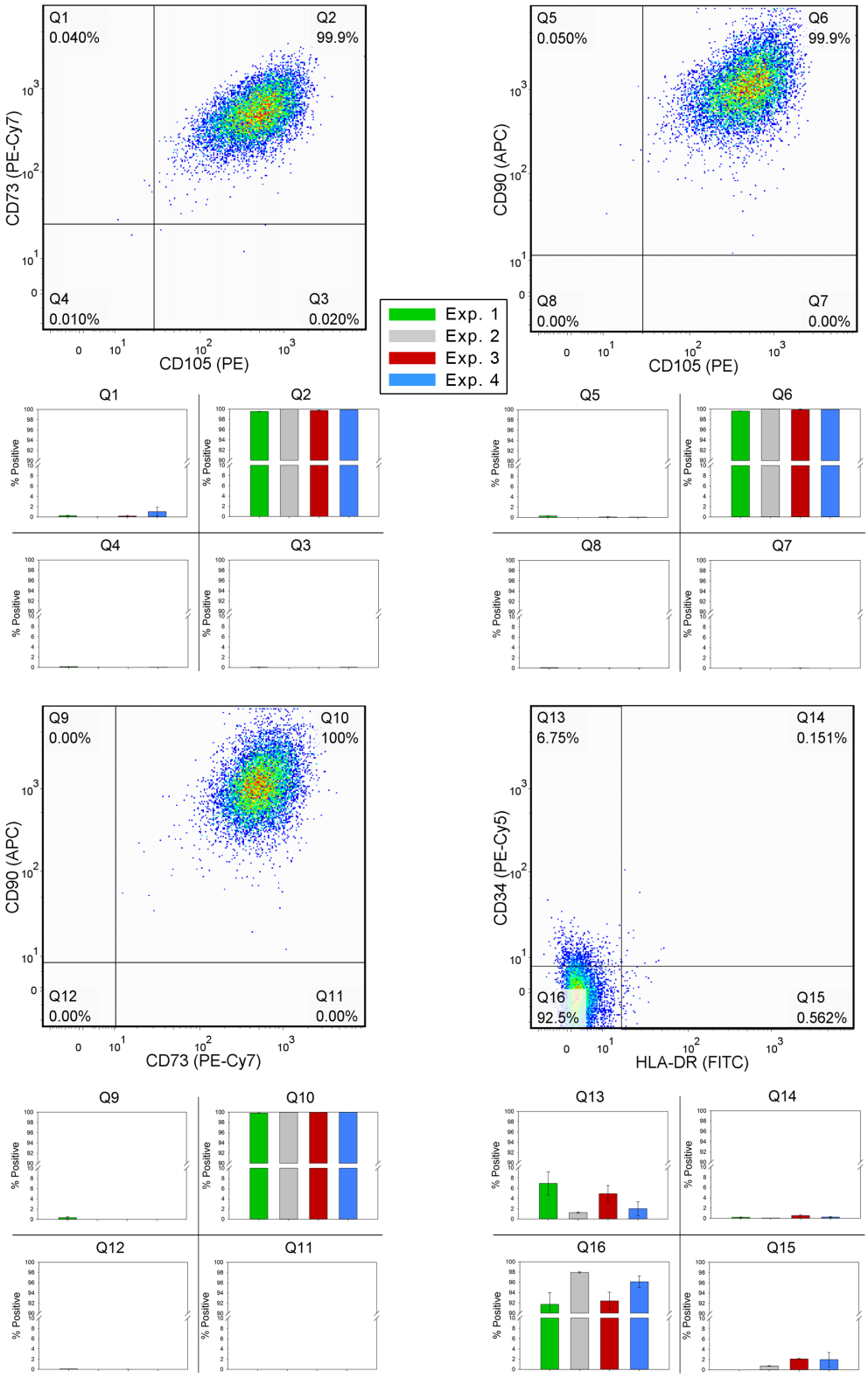

Figure 4.3: Multiparameter flow cytometry analysis of hMSCs using CD37, CD90, CD105, HLA-DR and CD34 markers. Dot plots show representative analysis of four independent repeats. Graphs correspond to the percentage of cells in each quadrant.

Table 4.1: Compensation values for multiparameter flow cytometry. Values were acquired using CompBeads (BD Biosciences) and applied post-analysis.

	GRN-HLog	NIR-HLog	RED-HLog	RED2-HLog	YEL-HLog
GRN-HLog		0.094%	0.440%	-0.001%	3.22%
NIR-HLog	0.270%		0.160%	0.007%	0.853%
RED-HLog	0.150%	0.100%		2.50%	1.51%
RED2-HLog	0.080%	0.273%	1.30%		0.005%
YEL-HLog	0.900%	1.82%	6.00%	-0.001%	

4.4 Serial Gating Strategy

By applying serial gating analysis to the population of interest it is possible to fully determine the full expression phenotype (Figure 4.4). Starting with the forward and side scatter the population of cells is initially analysed for CD73 and CD105 as before. Then the CD105$^+$ CD73$^+$ quadrant is further gated for CD90 and HLA-DR. The CD90$^+$ HLA-DR$^-$ quadrant was then finally gated for CD34 and HLA-DR expression.

Using this analytical method, essentially multiple steps are sieved down, thus making it possible to determine the full CD73$^+$/CD90$^+$/ CD105$^+$/CD73$^-$/HLA-DR$^-$ expression phenotype. Table 4.2 displays results from the serial gating experiments; the average percentage of cells with the full phenotype was 94.49% $\pm$ 1.3%. As this is just below the level suggested by the ISCT this adds greater justification for using the multiparameter approach over single staining flow cytometry as it does not overestimate the population purity and provides a much greater depth of data.

The results shown here using the multicolour staining and serial gating analysis gives a full phenotype expression that is lower than the values given *via* the single colour method, 94.49% and 100% respectively. As the obtained value is just below the level suggested by the ISCT, using the multiparameter approach over single staining flow cytometry does

not overestimate the population purity and provides a much greater depth of data.

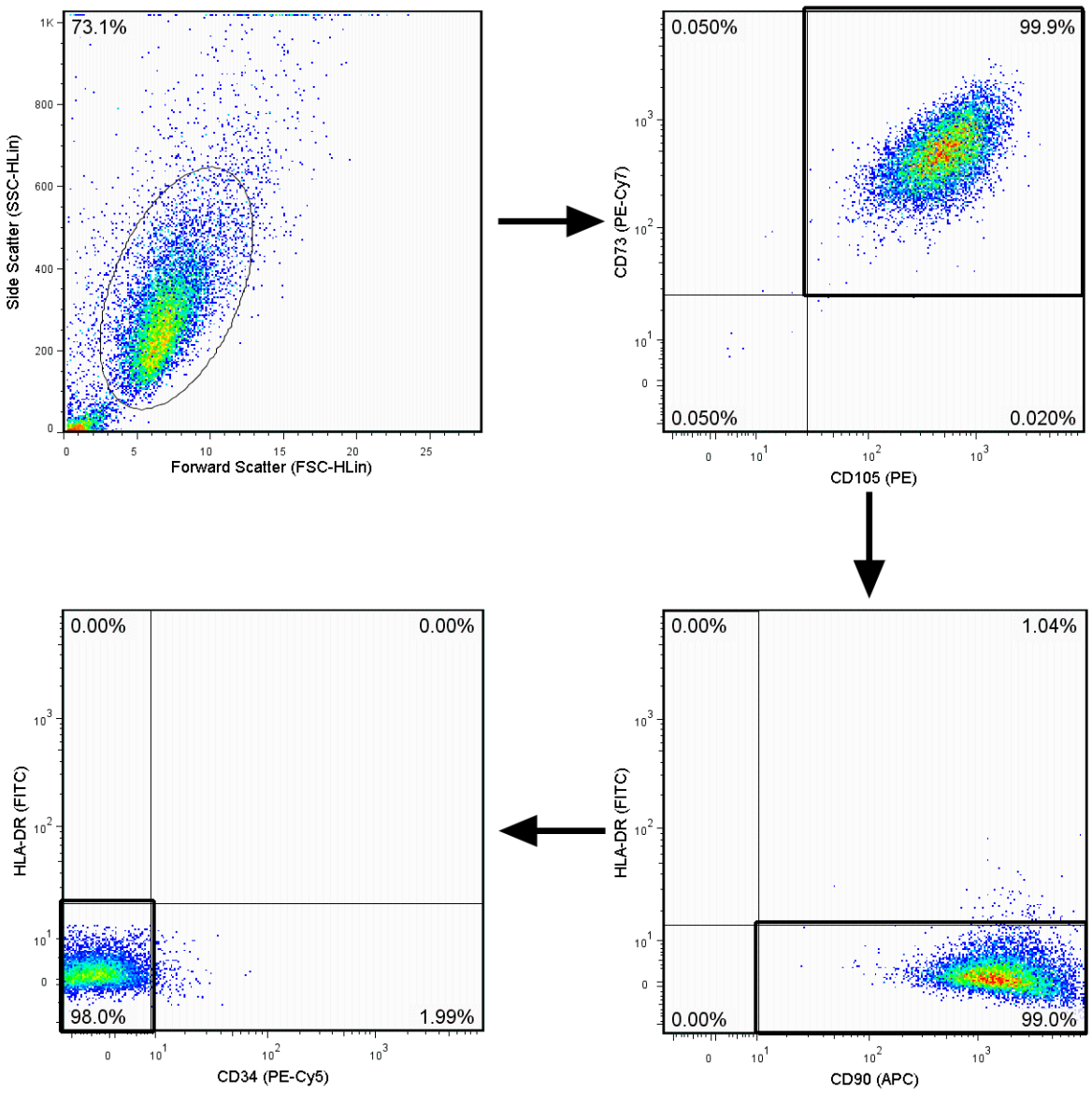

Figure 4.4: Serial gating of hMSCs showing co-expression of the selected surface markers. The initial analysis region used forward and side scatter to determine the population of interest. This was then gated for the $CD73^+$ and $CD105^+$ cells. Sequential gating was used to determine the $CD90^+$/HLA-DR^- and finally the HLA-DR^-/$CD34^-$ population. From the initial gate 95 percent of cells had the $CD73^+$/$CD105^+CD90^+$/HLA-DR^-CD34^- cell surface expression phenotype

Table 4.2: Gating strategy for the multiparameter experiment. The samples were initially gated on the single cell population followed by expression of CD105/CD73. This was then further gated on HLA-DR/CD90 and HLA-DR/CD34 respectively to assess, from the starting population, the percent of cells with the $CD105^{+}/CD73^{+}/CD90^{+}/HLA\text{-}DR^{-}/CD34^{-}$ phenotype. ± values represent the SE, n≥ 3 in all cases.

% Expression from Multiparameter Data									
	Subset 1: CD105 / CD73		→	Subset 2: HLA-DR / CD90		→	Subset 3: HLA-DR / CD34		% with full phenotype
Exp 1 (n=3)	CD105- / CD73+	0.24±0.06		HLA-DR-/CD90+	98.80±0.05	→	HLA-DR-/CD34+	7.06±2.31	91.32±2.04%
	CD105+/ CD73+	99.53±0.03	→	HLA-DR+/CD90+	1.22±0.05		HLA-DR+/CD34+	0.00±0.00	
	CD105+/ CD73-	0.06±0.02		HLA-DR+/CD90-	0.00±0.00		HLA-DR+/CD34-	0.05±0.02	
	CD105-/ CD73-	0.16±0.02		HLA-DR-/CD90-	0.00±0.00		HLA-DR-/CD34-	92.87±2.28	
Exp 2 (n=4)	CD105- / CD73+	0.00±0.00		HLA-DR-/CD90+	99.37±0.06	→	HLA-DR-/CD34+	1.14±0.03	98±0.09%
	CD105+/ CD73+	100.00±0.00	→	HLA-DR+/CD90+	0.61±0.05		HLA-DR+/CD34+	0.01±0.00	
	CD105+/ CD73-	0.00±0.00		HLA-DR+/CD90-	0.00±0.00		HLA-DR+/CD34-	0.19±0.03	
	CD105-/ CD73-	0.02±0.01		HLA-DR-/CD90-	0.00±0.00		HLA-DR-/CD34-	98.63±0.02	
Exp 3 (n=4)	CD105- / CD73+	0.01±0.00		HLA-DR/CD90+	97.37±0.12	→	HLA-DR-/CD34+	5.46±2.20	91.90±2.40%
	CD105+/ CD73+	99.80±0.16	→	HLA-DR+/CD90+	2.60±0.13		HLA-DR+/CD34+	0.00±0.00	
	CD105+/ CD73-	0.21±0.14		HLA-DR+/CD90-	0.00±0.00		HLA-DR+/CD34-	0.00±0.00	
	CD105-/ CD73-	0.01±0.01		HLA-DR-/CD90-	0.02±0.01		HLA-DR-/CD34-	94.57±2.20	
Exp 4 (n=4)	CD105- / CD73+	0.05±0.00		HLA-DR/CD90+	99.10±0.05	→	HLA-DR-/CD34+	0.00±0.00	96.72±0.68%
	CD105+/ CD73+	99.0±0.00	→	HLA-DR+/CD90+	0.91±0.05		HLA-DR+/CD34+	0.00±0.00	
	CD105+/ CD73-	0.02±0.00		HLA-DR+/CD90-	0.00±0.00		HLA-DR+/CD34-	0.00±0.00	
	CD105-/ CD73-	0.04±0.01		HLA-DR-/CD90-	0.00±0.00		HLA-DR-/CD34-	97.7±.065	

4.5 Protocol Transfer to BD FACs Jazz

The process was then repeated using a BD FACs Jazz flow cytometer to examine protocol transfer capability and fluorophore combination of the assay. Due to the different combination of filters CD34 (PE-Cy5) was not included due to the lack of filter that was previously available on the Millipore Guava 8HT. PE-Cy5 has an emission maximum at 670nm and is detected on the Red1 (692/46nm) filter. The measurement of PE-Cy5 on the BD Jazz is not possible due to having three filters on the 488nm excitation laser with PE-Cy5 overlapping on the PE-Cy7 670LP filter (Figure 4.5). However, as CD34 is a marker for red blood cells that are usually found and cultured in suspension, it was assumed that no traces would be left following multiple passages of the adherent hMSCs.

4.5.1 Single Colour Flow Cytometry

As previously, single parameter flow cytometry showed the expected expression of CD73, CD90 and CD105 (>99.9% in all cases) as shown in the blue-filled peaks in Figure 4.6. Likewise, there was no expression of HLA-DR. Red filled peaks on the same figure show the isotype controls used for each extracellular marker.

4.5.2 Compensation

A new compensation matrix was then produced due to the differences in the bandpass filters and excitation sources between the Millipore Guava 8HT and BD FACs Jazz flow cytometers. As such, the compensation was performed the same way as in section 4.3 where BD CompBeads were single stained with each antibody and the resulting fluorescence acquired. Figure 4.7 shows the bead plots with the main fluorophore emission on the left and the spillover into the other channels shown by the smaller plots on the right. From the FITC fluorophore, a clear spillover into the PE channel can be observed.

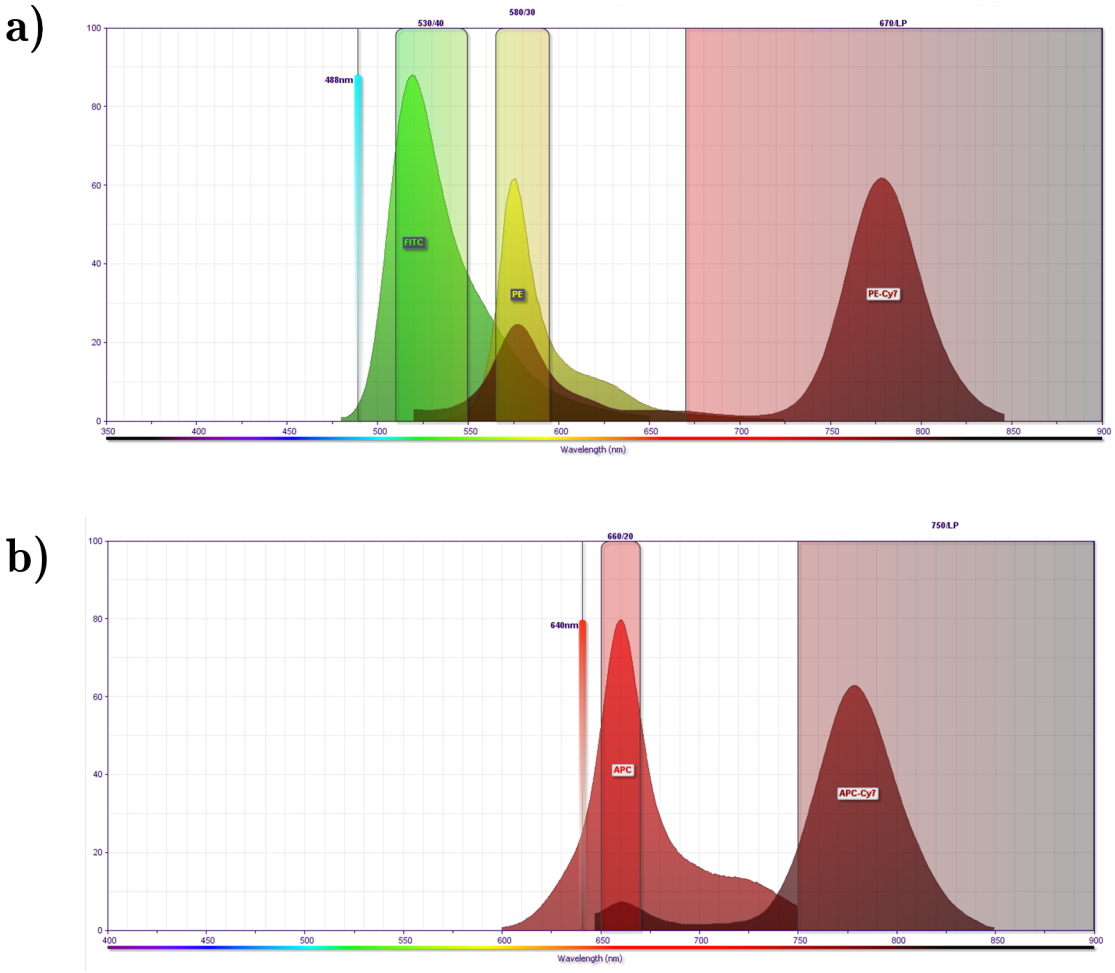

Figure 4.5: Excitation and filter configuration for BD FACs Jazz a) 488nm excitation source with three bandpass filters b) 640nm excitation with bandpass filters.

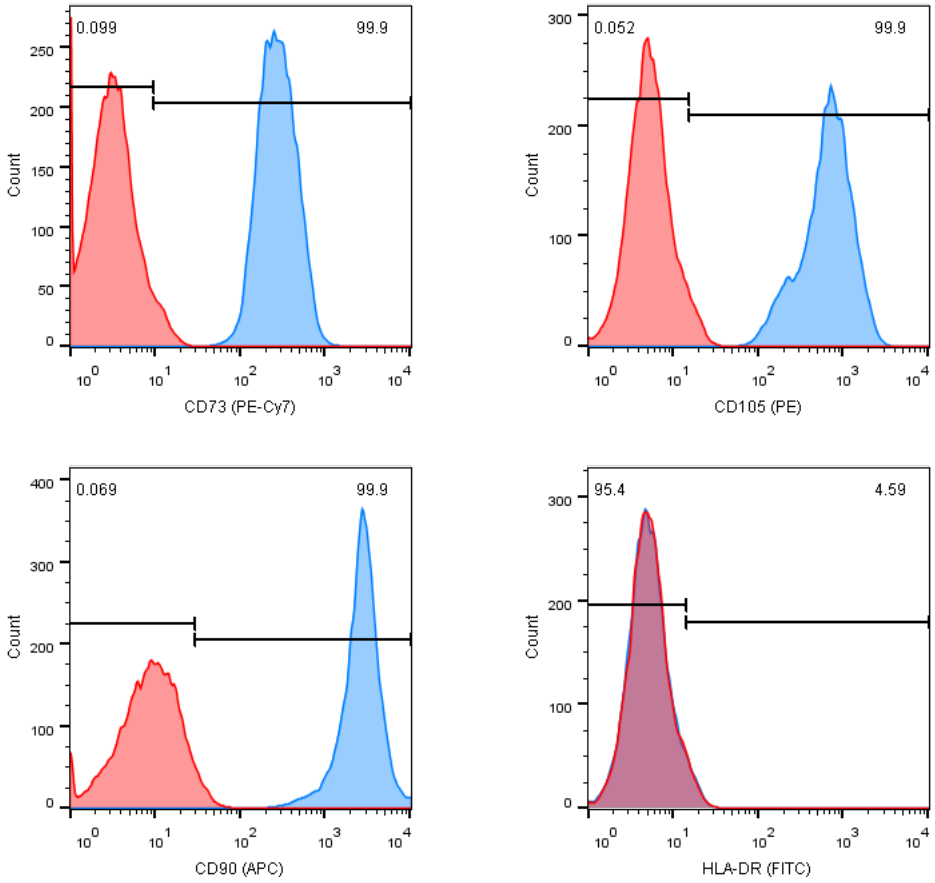

Figure 4.6: Single colour staining of MSCs as analysed by BD FACs Jazz. Red filled peaks indicate isotype controls, blue filled peaks indicate stained cells. Gating was set to 95% of isotype.

Likewise, PE spills over into the PE-Cy5 channel.

Based on these observation a new compensation matrix was calculated by the BD FACS Sortware analysis software (Table 4.3) and applied during cell acquisition.

4.5.3 Fluorescent Minus One (FMO)

The same gating strategy was used as previously described in section 4.4, dot plots for CD73/CD90 and CD105/HLA-DR were plotted and gating boundaries were determined from the isotype at 95%. Figure 4.8 shows the resulting plots. From these results there

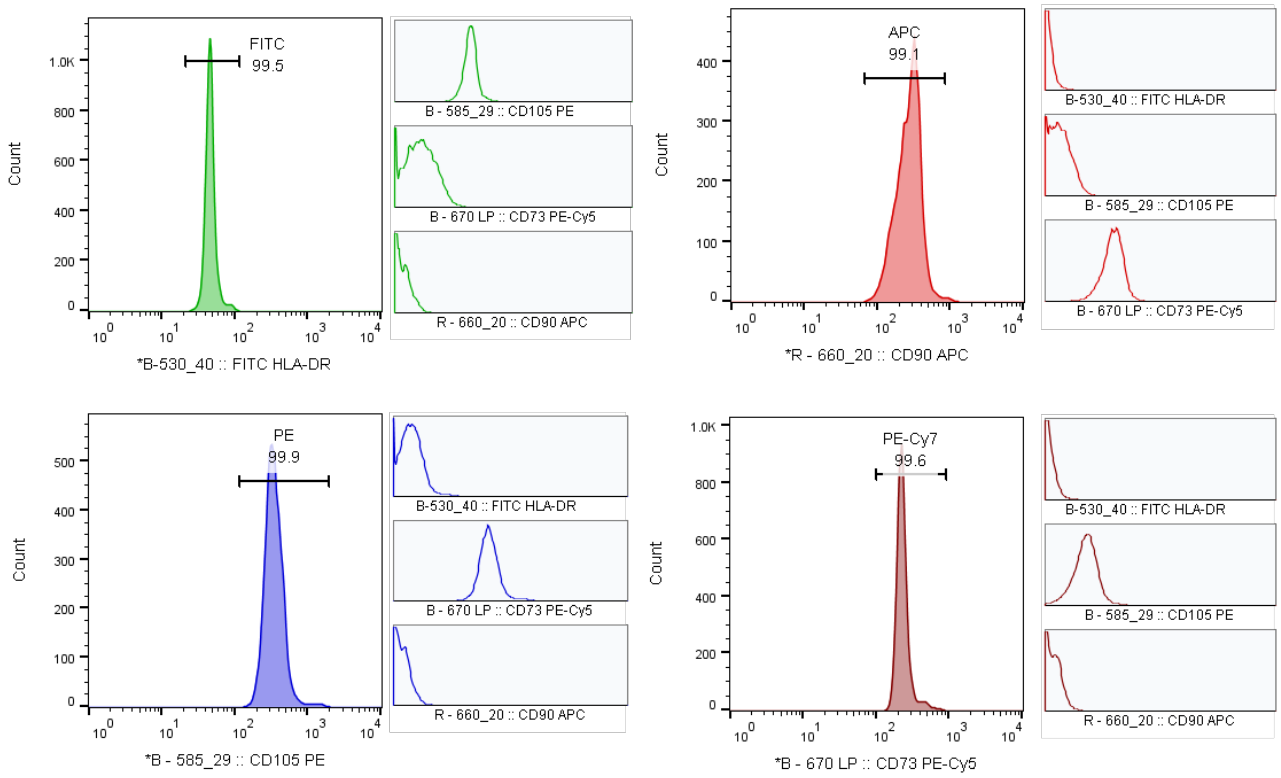

Figure 4.7: CompBeads plots for each of the fluorophores. Smaller plots show the fluorescent spillover into the other channels.

Table 4.3: Compensation matrix for multiparameter flow cytometry on the BD FACs Jazz. Values were acquired using CompBeads and applied during analysis.

	530/40 :: FITC	585/29 :: PE	670/LP :: PE-Cy5	660/20 :: APC
530/40 :: FITC		22.4%	1.16%	0%
585/29 :: PE	0.94%		8.7%	0%
670/LP :: PE-Cy5	0.24%	1.99%		0%
660/20 :: APC	0%	0%	0.84%	

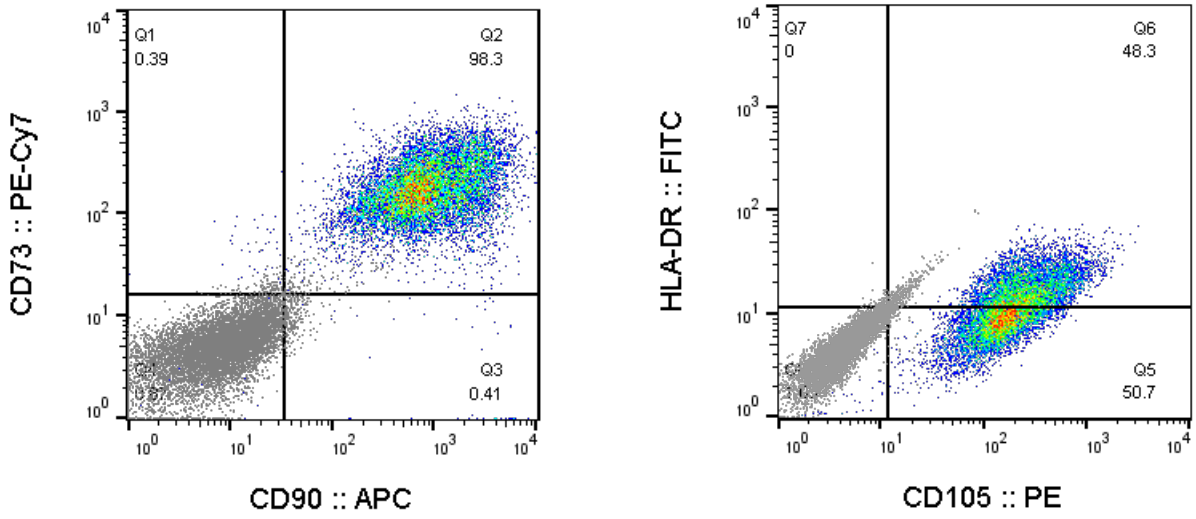

Figure 4.8: Multicolour plots from BD Jazz following compensation. Stained hMSCs are shown in the pseudocolor plots, isotypes are overlayed in grey.

was the expected positive expression of CD73, CD90 and CD105. However, HLA-DR was also shown to be expressed in approximately 50% of the population. This error must arise from the gating or the compensation as there was no expression of HLA-DR as shown via single colour staining in Figure 4.6.

To overcome the improper gating, Fluorescent Minus One (FMO) controls were used. In FMO controls the cells are stained with all the antibodies in the panel, except for the one that is being measured. This ensures that any fluorescence in this channel is due to the spectral spillover from the other channels and allows for correct gating.

Figure 4.9a shows the new gating strategy for each channel. For each image the original 95% isotype control (left plot) is shown by the horizontal blue line. The central image shows the plot for the FMO gate with the red line showing the revised gating level. The right most plot shows the fully stained hMSC population. Both the HLA-DR (FITC) and CD105 (PE) gate was increased as the isotype channel underestimated the boundary. Conversely, the CD90 (APC) gate was reduced as the isotype did show a small amount of fluorescence.

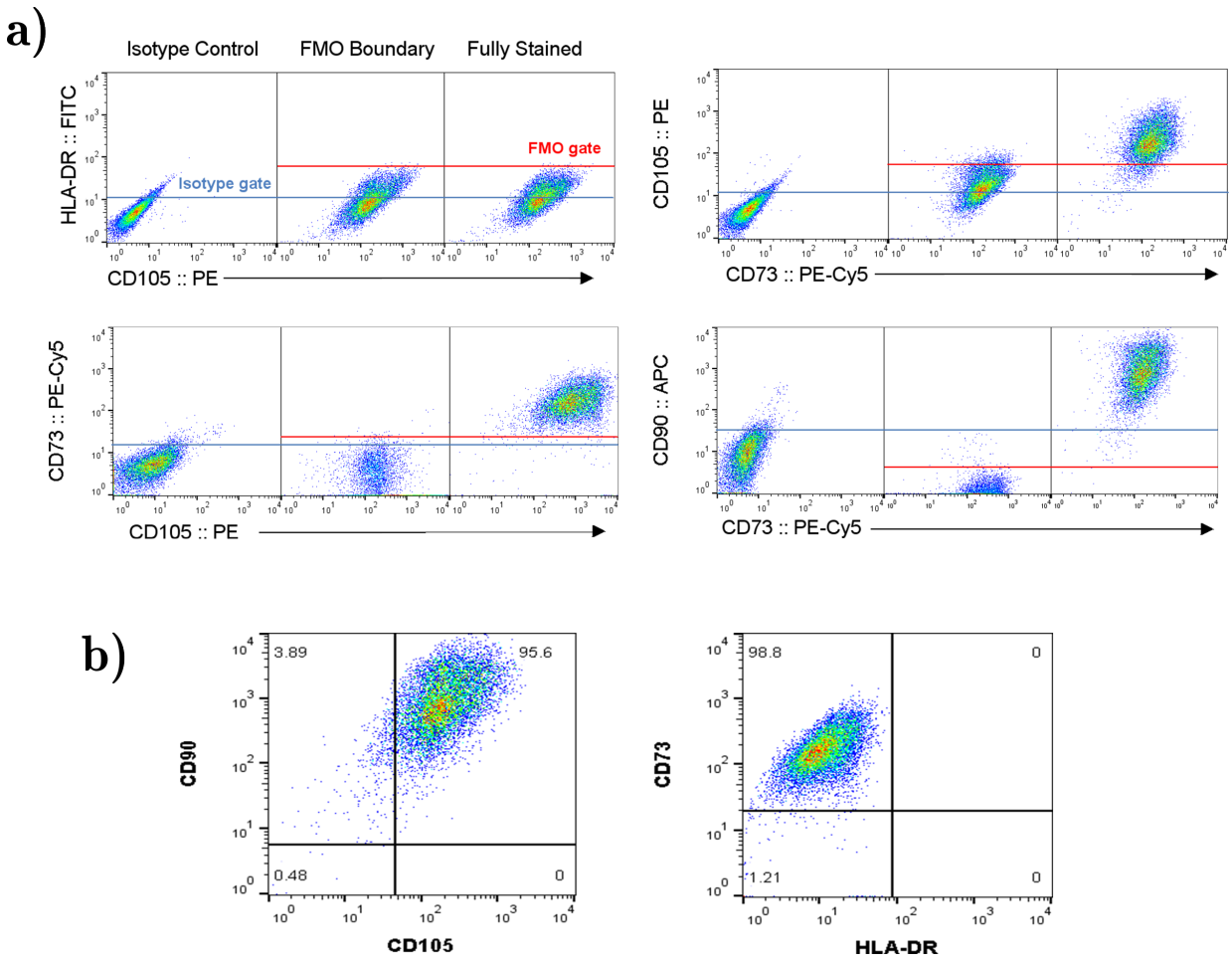

Figure 4.9: Fluorescent Minus One (FMO) analysis for improved gating controls. a) hMSCs are initially stained with the isotype (left panel). The 95% gate is shown by the horizontal blue line. Middle panel shows FMO boundary with the red line. Right panel is the fully stained sample. b) Final gating strategy on the BD FACs Jazz with the updated FMO gating parameters.

Following the refined gating strategy from the FMO controls the cells were re-plotted onto the dual dot plot graphs (Figure 4.9b). Dual expression of CD90 and CD105 was over 95% as expected, with CD73 expression over 98.8%. Importantly, there was no HLA-DR expression, thus removing the error seen previously as shown in Figure 4.8. This demonstrates that FMO controls results in more accurate gating for hMSCs characterisation.

4.6 Conclusions

Human MSCs are costly to isolate and culture, therefore by taking a multiparameter approach, the phenotype analysis requires fewer cells and reagents, as well as a decreased operator time representing a real cost saving for laboratories. For the multicolour assay, fewer samples of cells than the usual single staining were prepared, one 5-isotype control, one unstained tube and four multicolour test samples with an additional six wells for the compensation beads. In contrast, the conventional single staining flow cytometry method would require at least twice this number to achieve less stringent characterisation. This is important for autologous cell therapies, especially for older patients, where cell quantity may be limited and fewer cells are available for analysis. While the multicolour approach is still not routinely applied in stem cell research, it is becoming increasingly popular (Zimmerlin et al. 2010; Zimmerlin et al. 2013).

Single-staining flow cytometry provides a simple and robust method to analyse the phenotype of cells. For a multicolour analysis, there must be more considerations in the design and execution of the assay. Fluorochromes must be selected based on the least spectral overlap as possible in order to later simplify compensation. Detection of the fluorochromes requires the appropriate filters and there must be clear emission into the filter but as little from other fluorochromes. In practice, the optimal fluorochrome/filter set will be different depending on the instrument hardware and it requires alterations to the panel. In this work, a comparison between the Millipore Guava 8HT and BD FACS Jazz

flow cytometers was performed and it was demonstrated that the same fluorochromes can be used, but with appropriate controls and compensation optimised for each flow cytometry instrument.

The use of flow cytometry in stem cell research requires robust technique since the numbers of cell populations to be analysed is relatively small compared to other fields such as immunology. As such, it is advantageous to utilise newer techniques and instruments to obtain maximum possible information from the cells. In this chapter, five extracellular markers were analysed from one sample of cells, effectively reducing the number of cells to a fifth, to gain the same information if analysed using single colour flow cytometry. Reducing the number of sample preparations also reduces the amount of reagents thus representing a cost-saving method. In a bioprocess or scale-up manufacturing environment where the cells are to be used in a therapy it is important to retain as many for the patient. Therefore, each analytical stage throughout the process should use the least number of cells possible.

Multiparameter flow cytometry is a standard technique used in immunology to decipher sub-populations within a larger sample. This method has been proven invaluable to identify B-lymphocytes from peripheral blood (Blimkie et al. 2010) and dendritic cell from spleen and Peyer's patches (Duriancik and Hoag 2009). Whist multiparameter flow cytometry is still not widely performed in the stem cell community some authors have used this technique to identify multiple populations of stem/progenitor cells from within an adipose tissue sample (Zimmerlin et al. 2010; Zimmerlin et al. 2013).

For cell therapy characterisation, identity and purity are the first two aspects that must be satisfied for an ATMP (BSI PAS 93). In this chapter, the work has focused on proving the identity of hMSCs so that they are within the ISCT minimal criteria guidelines. However, physical testing alone does not demonstrate the biological activity or the potency. The following chapters will characterise the cells in terms of the properties that will lead to a clinically functional cell therapy product.

Chapter 5

Immuno-modulatory properties of hMSCs

5.1 Introduction

The previous chapters have examined ways to characterise hMSCs based on their physiological characteristics such as growth rate, metabolism, differentiation capability (refer to Chapter 3) and extracellular surface marker expression (refer to Chapter 4). These properties are crucial quality control assessments when developing a manufacturing and expansion process but do not reflect the therapeutic value of the hMSCs. A growing body of literature shows that hMSCs possess anti-inflammatory and immunosuppressive capabilities that precede their reparative function in injury models (Uccelli, Moretta, and Pistoia 2006; Blanc et al. 2007; Jones and McTaggart 2008). High-profile hMSC clinical studies, such as Prochymal® (Mesoblast) for the treatment of GvHD and Multistem® (Athersys) for the treatment of ulcerative colitis, are utilising this innate property for hMSC cell therapy in Phase II and Phase III clinical trials.

Potency assays that predict the therapeutic effect are critical to their success in regener-

ative medicine. Currently, patients are receiving cells with unproven potency which may result in suboptimal clinical responses (Samsonraj et al. 2015). Therefore, producing a robust potency assay is vital to ensuring that hMSCs possess and retain their clinical efficacy through from isolation, expansion and delivery. Many previous reports aimed to develop an immune potency assay have used a mixed lymphocyte reaction (MLR) to measure proliferation and gene expression (Prevosto et al. 2007). However, due to MLR requiring a heterogeneous population of cells it is not possible to retain consistency between runs and batches. To overcome this problem, this chapter will first examine the hMSCs under a chemically defined induced inflammatory environment and measure known hMSC response such as release of immunomodulatory proteins and upregulation of effector genes (Section 5.2). Having a defined system will allow direct comparison between the hMSC lines without the need for other cell types thus maximising the comparability and consistency. Following this, a co-culture assay will be developed using purified CD4 T-cells, and it will examine the anti-proliferative effects induced by the hMSCs. Also, again known immunomodulatory aspects will be compared across the selected hMSC lines (Section 5.4). Finally, this chapter will examine the hMSC cultured in a MLR as they are known to induce a regulatory T-cell phenotype (Section 5.5).

When considering the quality and potency of a cell therapy there must be considerations into the *in vivo* mechanism of action. It is unlikely that a biological product, such as a stem cell, will have a single mode of action, rather it will be a combination of different factors that lead to the therapeutic effect. Throughout this chapter multiple aspects will be evaluated. These varied analyse employed here can determine which properties reflect the potency and which can be taken forward to the development of a holistic assay.

The aims of this chapter were to:

- Culture individual hMSCs in a defined inflammatory environment
- Measure and compare known immuno-modulatory effectors produced by the hMSCs

- Develop a CD4 T-cell/hMSC co-culture assay
- Measure CD4 T-cell proliferation, cell cycle, and vitality under co-culture conditions
- Co-culture hMSCs with peripheral blood mononuclear cells (PBMCs) to assess T-reg differentiation capability

5.2 Defined Inflammatory Environment Culture

The initial set of experiments examined the response of M2, M3, and M4 hMSC lines in a defined inflammatory environment by the addition of pro-inflammatory cytokines. This allowed for a reproducible and consistent assay that did not require co-cultures with other cell types. M2 and M4 hMSC cell lines were chosen due to their potential for a cell therapy as they exhibited fast growth rate and consistent performance into later passages (refer to Chapter 3). M3 cell line were also examined as an example of a potentially 'poorer' cell line due to its slower growth rate and metabolism.

To examine the cells response to an inflammatory environment the selected hMSC lines were incubated with pro-inflammatory cytokines (10ng/ml IFN-γ and 10ng/ml TNF-α) for 72 hours as previously described by English et al. (2007) and Prasanna et al. (2010).

5.2.1 Morphological Changes and Upregulation of HLA-DR Expression

After 72 hours in culture with IFN-$\gamma$and TNF-α, changes in cell morphology were observed in the hMSCs. The treated cells were larger in size, had high amounts of cytoplasm granularity and displayed an irregular flattened shape when compared to untreated control cells (Figure 5.1). The cells were then analysed for changes in phenotype via the

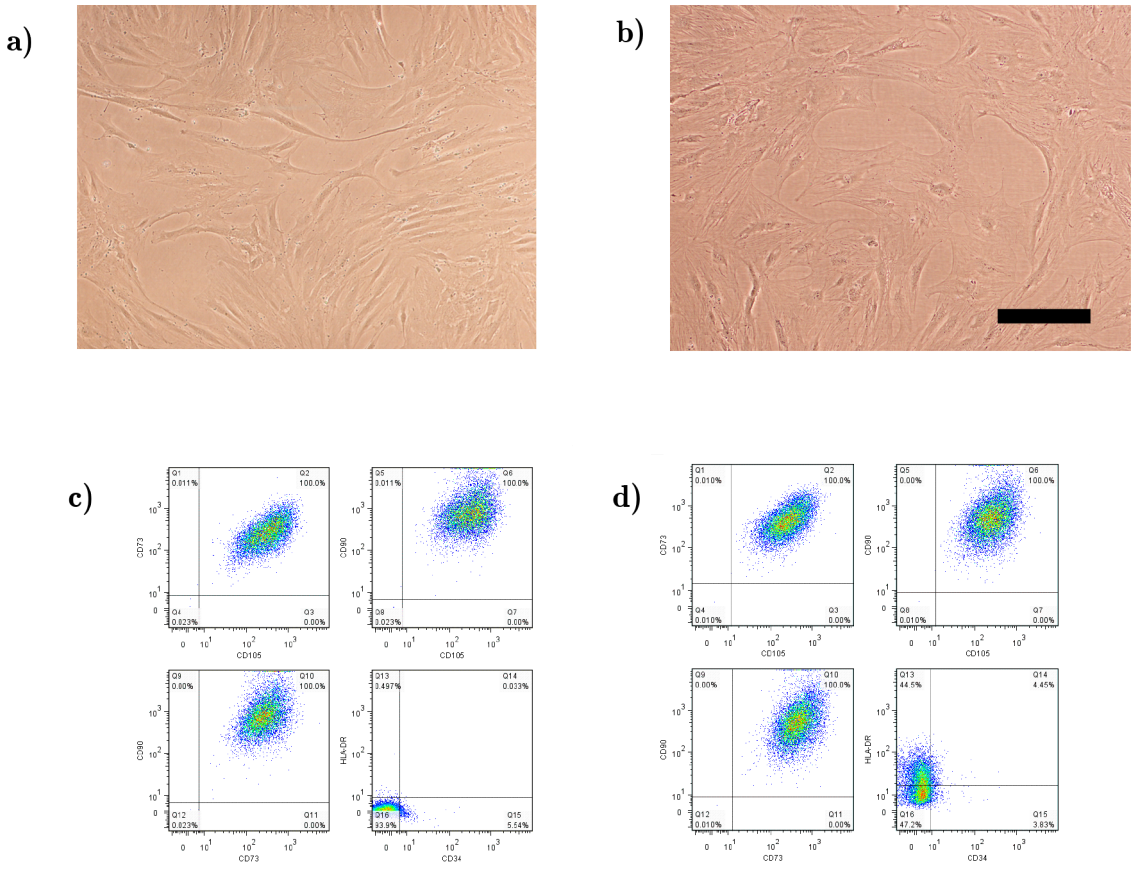

Figure 5.1: M2 hMSC line cultured within an inflammatory environment a) Untreated control b) Treated with TNF-α and IFN-γ. Representative plots (n = 5) for multicolour flow cytometry analysis of: c) untreated control and d) treated cells. Scale bar = 250μm

multiparameter flow cytometry approach as developed in Chapter 4. Positive markers CD73, CD90 and CD105 remained unchanged and the cells continued to express these in the same manner as control cells. Similarly, the negative marker, CD34 was not expressed. However, there was a 44% increased expression of HLA-DR (Figure 5.1 c and d, lower left quadrant). HLA-DR is a MHC class II cell surface receptor expressed on the surface of antigen presenting cells. Its usual function is to display peptide antigens to other immune cells, such as T cells, to elicit an immune response. A previous study has also reported hMSC expression of HLA-DR following treatment with IFN-γ and have suggested this plays a role in antigen presenting properties of hMSCs within an inflammatory environment (Chan et al. 2006).

To further investigate HLA-DR expression M2, M3 and M4 cell lines were cultured under an increasing severity of inflammation by changing the concentration of TNF-α and IFN-γ. After three days in culture the cells were harvested and the expression of HLA-DR protein was measured (Figure 5.2a). The expression is shown by the mean fluorescent intensity (MFI) - a measure of fluorescent intensity due to marker expression.

Throughout all concentrations of cytokines, M2 and M3 cell lines showed an increase of HLA-DR expression. In contrast, M4 cell line did not increase expression of HLA-DR throughout any of the cytokine concentrations tested. This may indicate that M4 has a weaker response to the inflammatory environment and may not possess any further immunological properties.

At the highest concentration (10ng/ml), M2 gave the highest MFI at 94.6 $\pm$ 0.35 compared to a slightly lower expression by M3 at 82.8 $\pm$ 1.46. However, M4 showed the weakest expression at 10.7 $\pm$ 0.81. As the severity of inflammation decreased M2 and M3 lines continued to show high HLA-DR expression (Figure 5.2b) whereas M4 continued to express low levels throughout.

Inducing HLA-DR expression is a simple way to examine if hMSCs are responsive under inflammatory conditions, but nonetheless as is it a responsive assay it still requires 72 hours to complete. Here it is shown that M2 upregulated the expression proportionally to the severity of inflammation whereas M3 exhibited the same amount throughout. Surprisingly, M4 a probable candidate for cell therapy due to its high growth rate and consistent performance, may not be suitable as an immunotherapy therapy due to the lack of response.

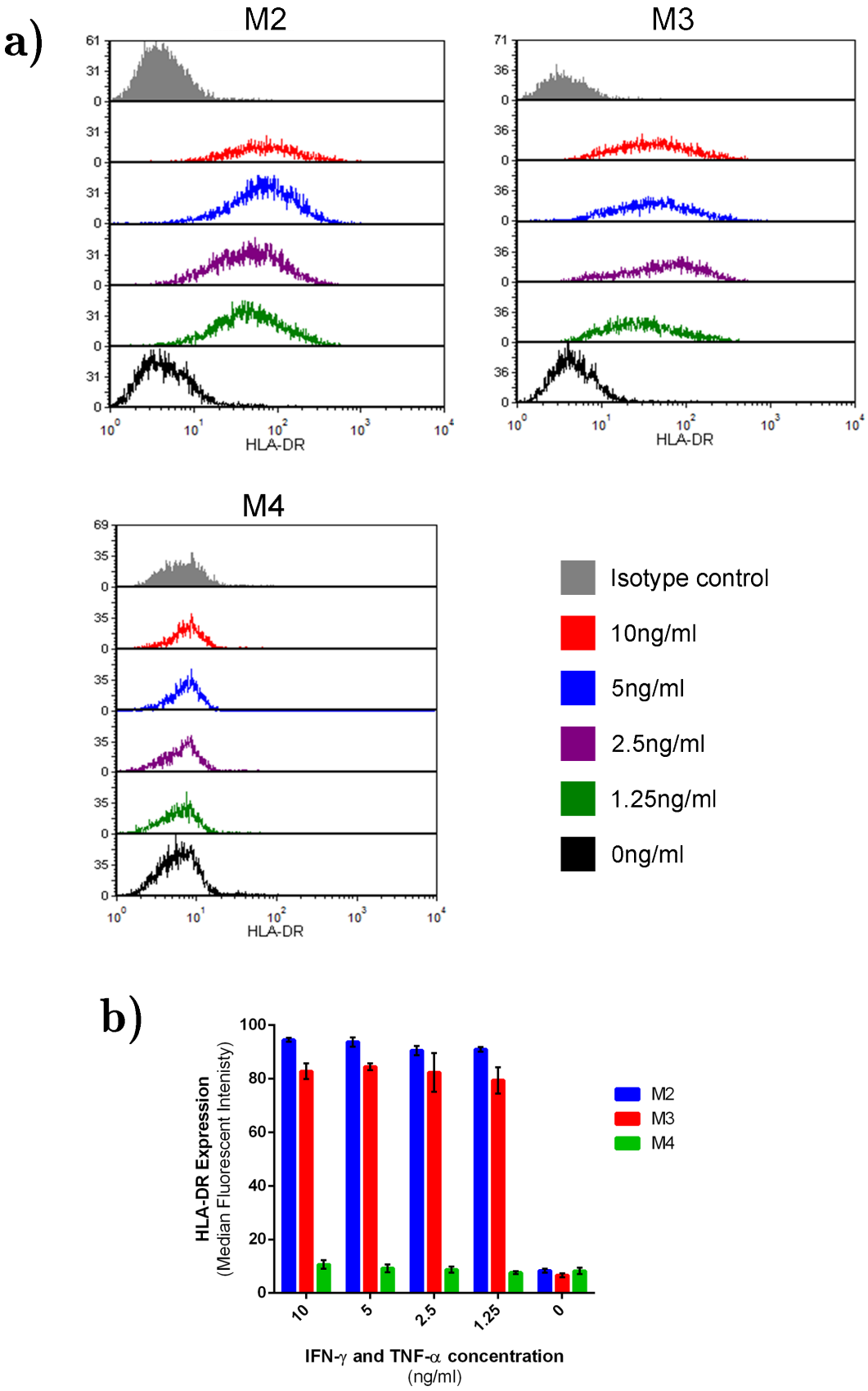

Figure 5.2: Each selected hMSC line was cultured with varying amounts of pro-inflammatory cytokines (IFN-γ and TNF-α) for 72 hours. a) Expression of HLA-DR in M2, M3 and M4 measured by flow cytometry. b) Median florescent intensity (MFI) for each hMSC line and cytokine concentration. Values presented as mean $\pm$ SD (n = 4).

5.2.2 IL-6 Production

The expression of HLA-DR in response to stimulation indicates the cells are able to respond to the severity of inflammation. The next investigation would therefore be to determine the soluble factors that are associated with immunomodulation. Interleukin-6 (IL-6) is an anti-inflammatory protein and mediator for the acute phase of inflammation (Gabay 2006). Previous reports using IL-6 gene knock-out mice have shown that it is required to stimulate the production of acute phase proteins and for controlling the levels of pro-inflammatory cytokines (Fattori et al. 1994; Xing et al. 1998). IL-6 secretion by hMSCs has previously been confirmed when cultured with allogeneic splenocytes causing a decreased proliferation (Djouad et al. 2007). For the next set of experiments IL-6 was chosen as an exemplary protein for immunomodulatory potency. Other possible proteins might include PGE-2, COX-2, or TGF-β1 (Ryan et al. 2007).

As previously described, the hMSC lines were cultured for three days with varying concentrations of the pro-inflammatory cocktail and media samples were harvested at day 3 in culture for IL-6 analysis. The values were normalised per cell (Figure 5.3).

In contrast to the HLA-DR expression results, M4 cells showed the most IL-6 production at the highest level of severity (0.79 $\pm$ 0.078 pg/cell) compared to M2 (0.15 $\pm$ 0.014 pg/cell) and M3 (0.19 $\pm$ 0.02 pg/cell) lines. As the concentration of pro-inflammatory cytokines were decreased the levels of IL-6 yield also decreased proportionally indicating the cells were able to respond to the environment and produced anti-inflammatory molecules accordingly.

On the other hand, M3 production was not significantly different between the 10ng/ml and 1ng/ml pro-inflammatory cytokine concentrations indicating a maximum response level and suggesting that an increase in the severity will not result in an increase of the response.

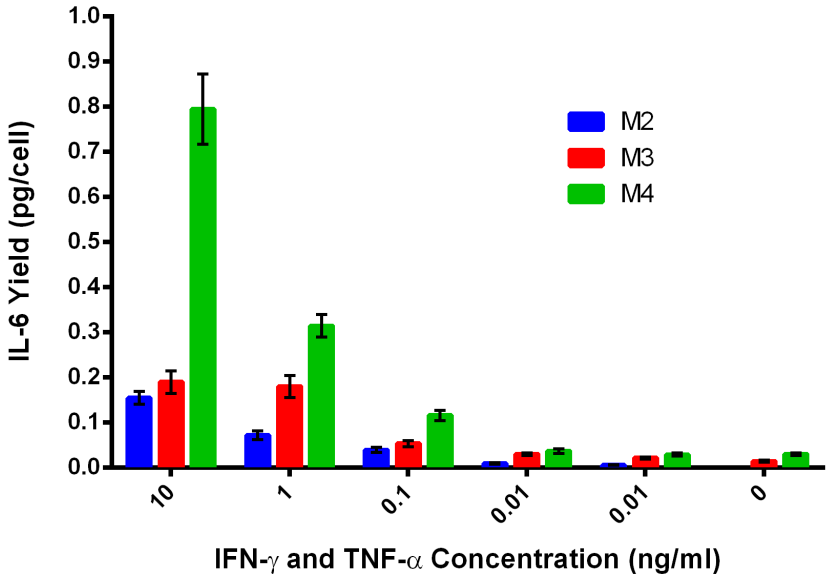

Figure 5.3: IL-6 yield per cell from individual hMSC lines within varying severity of inflammation. Values represented as mean ± SD (n = 6)

The M2 cell line showed the least amount of IL-6 production throughout with 0.15 ± 0.01 pg/cell at the maximum (10ng/ml) concentration and 0.071 ± 0.001 pg/cell at the minimum (1ng/ml) concentration.

The results here contrast to those seen in section 5.2.1 where M2 and M3 lines exhibited the highest HLA-DR expression and therefore led to the conclusion that these cell lines may be more responsive to the inflammatory environment. However, the secretion of cytokines, such as IL-6, have the potential to give a better indication to the cell lines immunomodulatory potential due to it being directly responsible for hMSC immunomodulatory properties.

5.2.3 Indoleamine 2,3-dioxygenase Function

Indoleamine 2,3-dioxygenase (IDO) is an immunomodulatory enzyme produced by antigen presenting cells (APCs) under stimulation by IFN-γ. It has also been shown to be a key factor in both human and mouse MSC immunomodulation (Meisel et al. 2004; English

et al. 2007). IDO is the first rate-limiting step in the catabolism of the essential amino acid L-tryptophan to N-formylkynurenine, followed by further conversion to kynurenine via the enzyme kynurenine formamidase (Equation 5.1) (Moffett and Namboodiri 2003). The depletion of tryptophan causes reduction of T-cell proliferation. Measuring the concentration of resulting kynurenine in the media could be an indicator to the upregulation of IDO and the immuno-inhibitory potency of different hMSC lines.

$$L-tryptophan \xrightarrow{IDO} N-formylkynurenine \xrightarrow{kynureninef ormamidase} kynurenine \quad (5.1)$$

Under normal culture conditions hMSCs do not express IDO or deplete tryptophan. When TNF-α was added alone there was no significant kynurenine production when compared to the controls (Figure 5.4). However, kynurenine production could be induced by the addition of IFN-γ alone, where all cell lines produced an average of 0.007145 $\pm$ 0.0016 nM/cell with no significant differences between the hMSC lines. When IFN-γ and TNF-α were added together there was a synergistic effect and kynurenine production increases significantly in all three hMSC lines. M2 produced the most kynurenine at 0.015 $\pm$ 0.0026 nM/cell, but was not significantly different to M4 at 0.013 $\pm$ 0.0038 nM/cell.

Therefore, both IFN-γ and TNF-α were required to effectively induce IDO gene expression. This is detailed further in section 5.3.2.

5.2.4 Metabolism

Media samples were collected from cells treated with the inflammatory cytokines and compared to untreated controls. Figure 5.5 shows the glucose consumption and lactate production for each hMSC line.

Glucose consumption was greater in cells that were being treated with the inflammatory

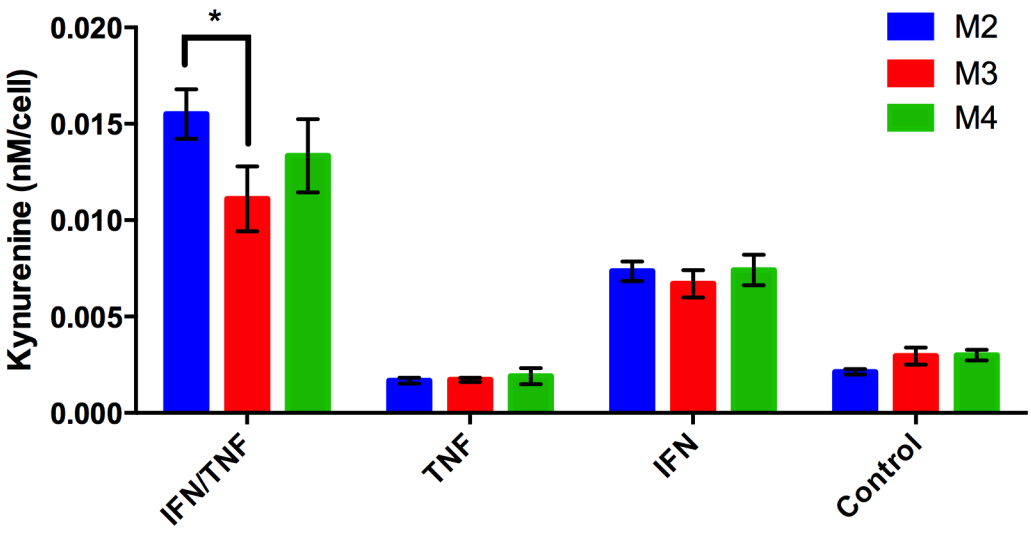

Figure 5.4: Induction of IDO activity and subsequent kynurenine production in M2, M3, and M4 by addition of IFN-γ, TNF-α, or IFN-γ/TNF-α (10ng/ml each) for 72 hours. Data are presented as mean $\pm$ S.D (n = 6)

cytokines as shown by the solid bars. The largest differences was seen in both M2 and M4 cell lines where the final concentration was 0.91$\pm$ 0.74 mmol/L and 0.61$\pm$ 0.56 mmol/L respectively. M3 lines had a higher final glucose concentration of 1.52 $\pm$ 0.30 mmol/L indicating a lower rate of glucose uptake.

As expected, lactate concentration was higher in those cells in the inflammatory environment. Similarly to the glucose results, M2 and M4 lines both produced similar lactate concentrations, whereas M3 produced the least.

Under normal culture conditions the untreated cells consume glucose and produce lactate at different rates, Table 5.1 shows the differences between the treated and untreated concentrations to account for this effect. The glucose difference was higher in M2 and M3 lines when compared to M4. This can be accounted to the usually high glucose demands of M4 line as seen in Chapter 3.

The increased metabolism of the selected hMSCs lines when treated indicate a response to the environment and possible utilisation of the nutrients for the production of anti-

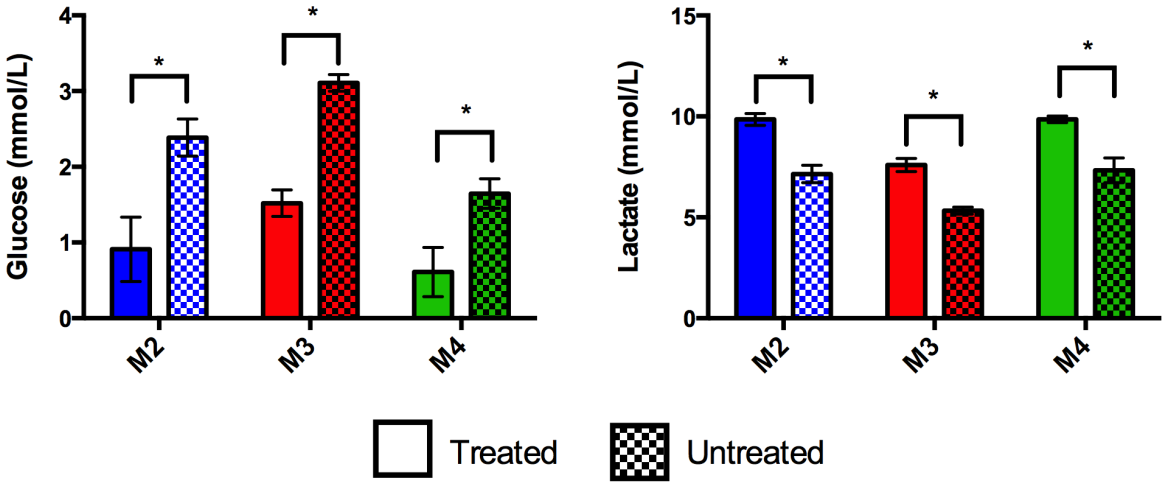

Figure 5.5: Glucose and lactate analysis from media samples taken from hMSCs in the inflammatory environment (treated, solid bar) or control (untreated, patterned). Values presented as mean ± SD (n = 3)

Table 5.1: Difference of glucose consumption and lactate production in treated and untreated hMSCs. Values presented as mean ± SD (n = 3)

hMSC	Glucose (mmol/L)	Lactate (mmol/L)
M2	1.48 ± 0.32	2.70 ± 0.60
M3	1.59 ± 0.11	2.26 ± 0.74
M4	1.04 ± 0.40	2.52 ± 0.62

inflammatory proteins and other functions. Currently, there are no other reports of the metabolism of hMSCs in similar conditions.

5.3 Inflammatory Response Over Multiple Passages

Next, the cell lines were compared over extended passage when treated with the 10ng/ml TNF-α and IFN-γ concentration. As mentioned previously in Chapter 3, scale-up is required to generate a sufficient number cells for a complete treatment, as continuous passaging and expansion is required. Here the cells were tested from passage 3 to 7 to

determine if long-term culture affects the immunomodulation potential of selected hMSC lines. Therefore, the cells were analysed at p3, p5 and p7; with sacrifice at 24 hours, 48 hours and 72 hours following treatment.

5.3.1 IL-6 Production

Each hMSC line was able to produce IL-6 in response to the inflammatory environment (Figure 5.6). Over the three days there was a steady increase in the production, for example in passage 5, M4 produced 24.6 ± 2.0 ng/ml at Day 1, 49.7 ± 9.0 ng/ml at Day 2, and 80.8 ± 15.6 ng/ml at Day 3 in culture.

When the individual cells lines were compared, M2 and M3 lines showed consistent IL-6 production throughout all the passages with no significant changes. This behaviour suggested that these two cell lines could be expanded *in vitro* for up to passage 7 without any loss of potency. However, M4 line showed a higher production of IL-6 compared to M2 and M3. This may be important for cell dosing as the patient will require fewer cells than M2 and M3 for the same therapeutic benefit. However the production was less consistent as an increase was recorded during passage 5, followed by a decrease at passage 7. The decrease at later passages might be an *in vitro* culture limit as it is believed that older cells might exhibit a reduced potency.

5.3.2 IDO Gene Expression and Function

The expression of IDO was measured via PCR with untreated samples serving as baseline controls (Figure 5.7). M2 and M4 cell lines showed a significantly greater increase of gene expression when compared to M3, this higher gene expression was observed throughout all passages and tested time points. M2 showed a maximum fold change of $1.4x10^5$ at p3 day 3, and only decreased at passage 7. M4 showed a slightly higher fold expression of

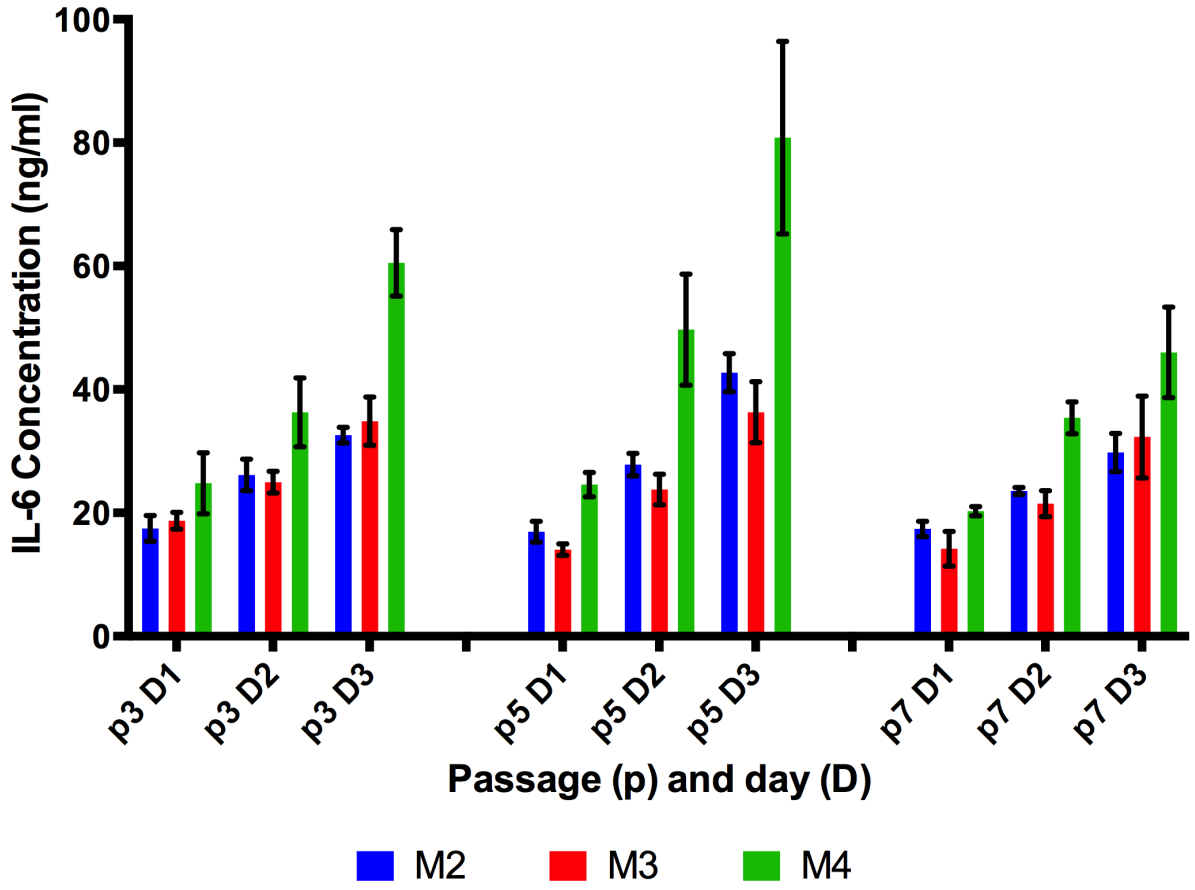

Figure 5.6: IL-6 production over three passages (p) and three days (D) following culture in the presence of 10 ng/ml IFN-γ and TNF-α. Individual hMSC lines are shown in blue (M2), red (M3), and green (M4). Values presented as mean $\pm$ SD (n = 6)

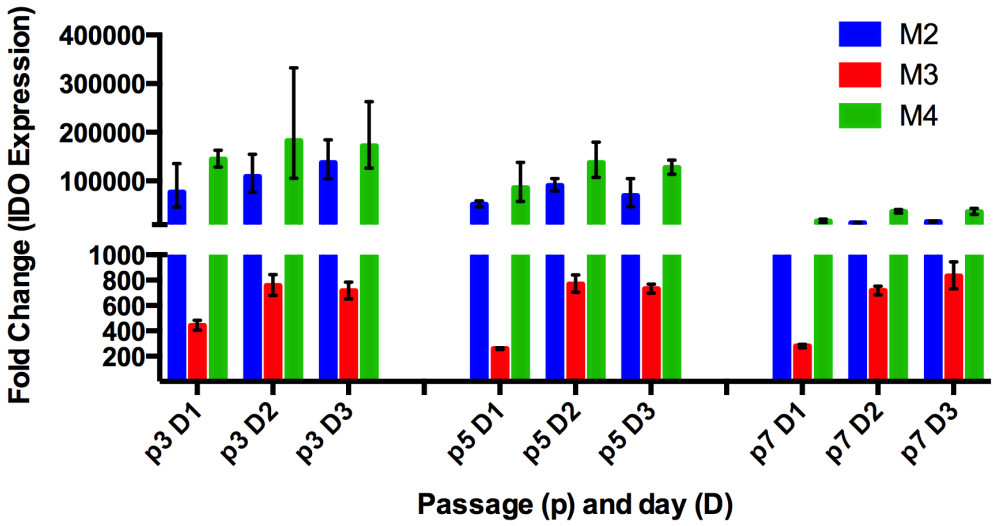

Figure 5.7: hMSC lines after treatment with 10ng/ml TNF-α and 10 ng/ml IFN-γ. Samples were taken over passages 3 to 7 at days 1, 2 and 3 after culture with cytokines. Bars indicate fold change (RQ) from untreated controls, error bars show maximum and minimum RQ values. The housekeeping gene was Glyceraldehyde-3-Phosphate Dehydrogenase (GAPDH) n = 3

$1.8x10^5$.

For M3, gene expression was lower, at p3 day 1 being 442 $\pm$ 38, while at day 2 and day 3 it reached the maximum level of 760 $\pm$ 82. In contrast, M2 and M4 both reached maximum gene expressions within the first day.

Along with the gene expression, the enzyme activity of IDO was measured by the production of kynurenine. In the first 24 hours of treatment there was little metabolism of tryptophan (5.96 $\pm$ 1.56μM) despite the gene expression suggesting a lag phase between gene expression and protein function. After 48 hours of treatment, kynurenine was detected indicating enzyme function, with only slightly higher concentration at 72 hours . Throughout all passages the final concentration of kynurenine was the same showing that all tryptophan was metabolised.

Next, all the cell lines were assayed for tryptophan to kynurenine metabolism over three

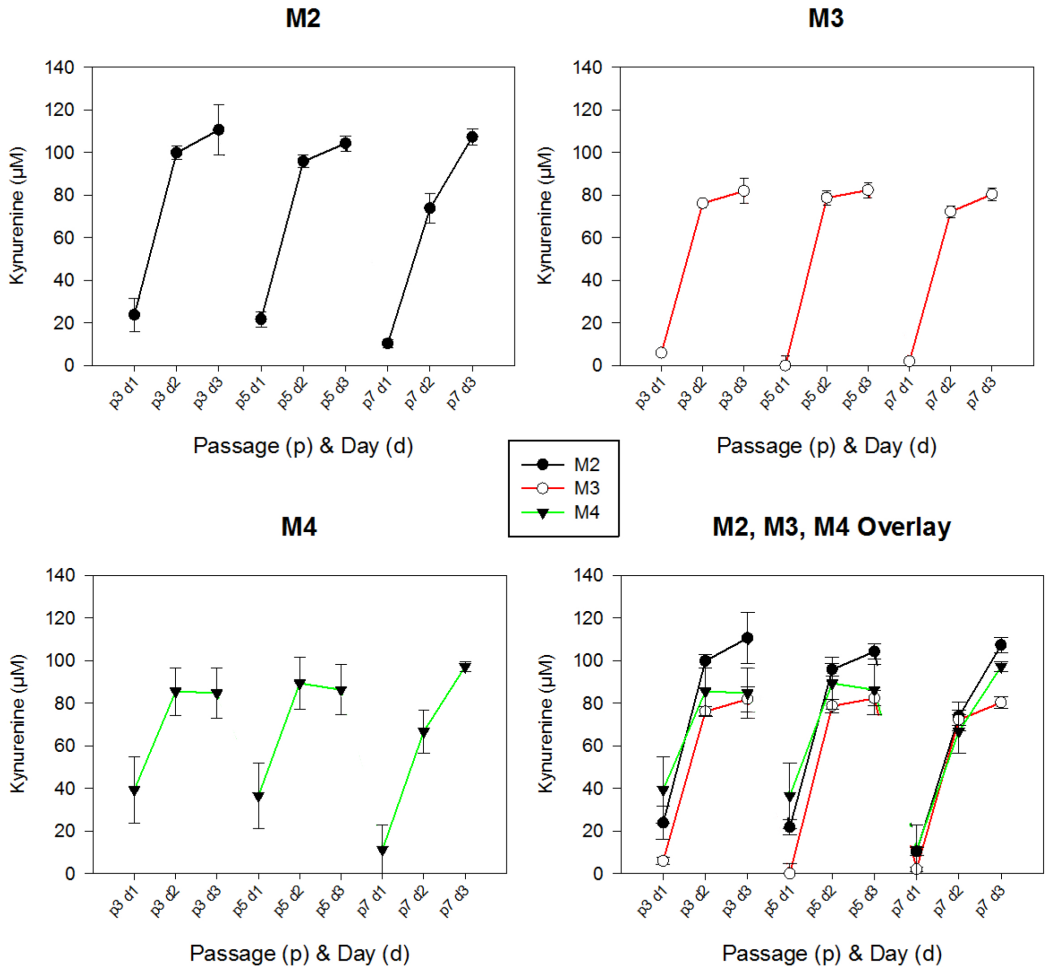

Figure 5.8: Kynurenine production by three individual hMSC lines over three days (d1-3) within five passages (p3-7) cultured under defined inflammatory conditions with 10ng/ml TNF-α and 10 ng/ml IFN-γ. Points represent mean $\pm$ SD, n = 3

days throughout the 7 passages (Figure 5.8). Similar patterns were observed in all three cell lines as there was little to no metabolism of tryptophan over the first 24 hours but increased over the next 48 hours. M4 cell line showed the fasted response as determined by the highest initial amount of conversion, but this dropped in the later passages. Similar patterns in loss of potency were observed with the M2 and M4 cell lines, where at p7 the rate of conversion was significantly lower, although total kynurenine concentration was the same after 72 hours. Over the 7 passages, M3 cell line converted less tryptophan than M2 and M4, but showed a more consistent pattern.

These results suggested that M2 and M4 cell lines possess a higher inhibitor potential of T-cell proliferation, as a result of the faster conversion of tryptophan to kynurenine observed during culture and also due to the final higher amounts of kynurenine produced, suggesting more efficient depletion of tryptophan. Tryptophan conversion to kynurenine closely follows that of IDO gene expression with the maximal expression at day 2 that is retained until day 3. As there was little conversion in the final day, this might indicate that gene expression does not always give a true representation to function.

5.4 hMSC and CD4$^+$ T-cell Co-Culture

5.4.1 Culture and Expansion of CD4 Cells

The lymphocyte population is comprised of thymus-derived lymphocytes (T-cells), bone-marrow-derived lymphocytes (B-cells), and natural-killer cells (NK cells). CD4$^+$ and CD8$^+$ cells make up the majority of the T-cell population. The main purpose of the CD4$^+$ T-cells is to secrete cytokines that activate the adaptive immune system and mediate its function (Luckheeram et al. 2012). However, in autoimmune cases such as multiple sclerosis (MS) these cells are thought to promote inflammation by recognising nerve myelin as 'foreign'. In other cases such as GvHD following allogeneic tissue transplant, the graft recognises the host as foreign and targets the host's cells.

A seminal study by Nicola (2002) showed that hMSCs are able to suppress both CD4 and CD8 T-cell proliferation and activation in a dose-dependent manner, therefore making them a potential cell therapy treatment for autoimmune and inflammatory diseases. The next set of experiments will detail the development of an hMSC:CD4 T-cell co-culture assay to examine the immunosuppressive function of different hMSCs lines.

To create a working bank of CD4$^+$ T-cells, it was first necessary to expand the number of

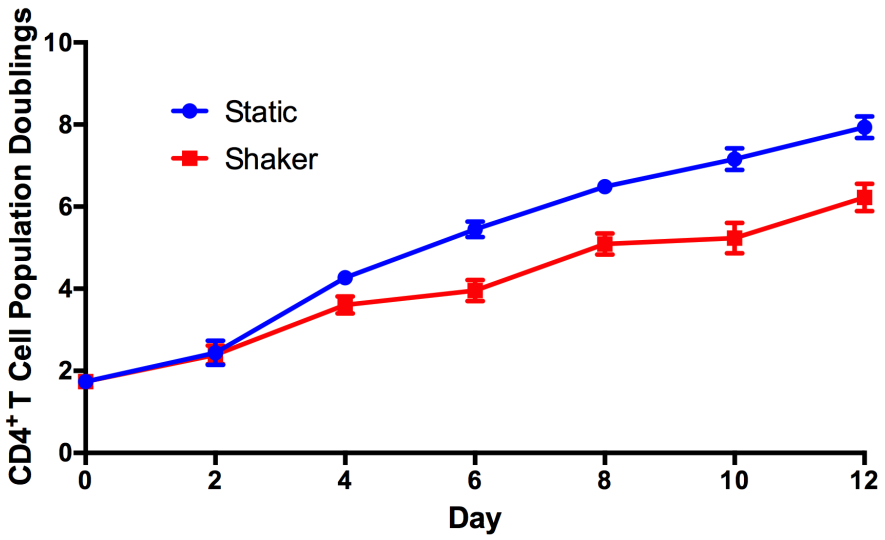

Figure 5.9: Population doubling of suspension CD4 T-cells cultured under static (blue) or shaker (red) conditions for 12 days. Points represent mean ± SD, n = 8

cells *in vitro*. Unlike hMSCs, T-cells are grown in suspension and therefore can be cultured under static, shaker, or spinner flask conditions. In this initial study T-cell expansion was performed on an orbital shaker in flat bottomed culture plates and compared to standard static culture. Cell counts were taken every two days over a 12 day culture period.

After 12 days in culture, cells under static conditions reached a population doubling level of 7.93 ± 0.27 whereas in the shaker conditions reached only 6.23 ± 0.33 population doublings (Figure 5.9). The circular motion of the orbital shaker caused the cells to aggregate in the middle of the well, resulting in reduced nutrient/waste transfer and gas exchange to cells in the centre therefore reducing proliferation.

For the remaining study T-cells were expanded in standard tissue culture flasks.

5.4.2 hMSC Growth Comparison in CD4 and hMSC Medium

For the co-culture experiments both cell types, hMSCs and T-cells cells had to be cultured in the same complete medium. For this set of experiments T-cell complete medium was

chosen (see Chapter 2, Materials & Methods, Section 2.5). As hMSCs are not routinely cultured in RPMI it was necessary to ensure that they can survive, at minimum, over three days. RPMI was developed specifically for hematopoietic cells and supports growth of suspension cultured cells, whereas DMEM is a standard basal media for adherent cells with high concentrations of amino acids and vitamins. In these experiments both were supplemented with 10% FBS.

hMSCs were cultured in T-cell complete medium for three passages from p3 to p6 (Figure 5.10a). Those in standard complete DMEM (blue) exhibited over double the population doubling (3.55 ± 0.29) compared to hMSCs cultured in complete RPMI (red) (1.72 ± 0.13). Images taken on the last experimental days showed no obvious morphological change (Figure 5.10b).

Multicolour flow cytometry revealed cells cultured in T-cell medium showed a significant increase of both HLA-DR and CD34. expression. HLA-DR expression can be a marker for a 'stimulated' hMSC or one that is primed (Dominici et al. 2006). CD34 expression was also highly expressed, from 20.3 ± 6.13% to 50.0 ± 6.86%. Although CD34 is a negative marker for hMSCs previous research has suggested this is due to culture on tissue culture plastic and the cells may originally express CD34 due to proximity to the vascular niche (Lin et al. 2012).

5.4.3 Optimising Co-Culture Conditions

Cell Culture Ratios and Length

To investigate the immunosuppressive effects of the selected hMSC lines the ratio of hMSCs to CD4 T-cells the initial seeding density and time in culture were first examined.

hMSCs were seeded at normal seeding densities (5,000 cells/cm^2) and allowed to adhere

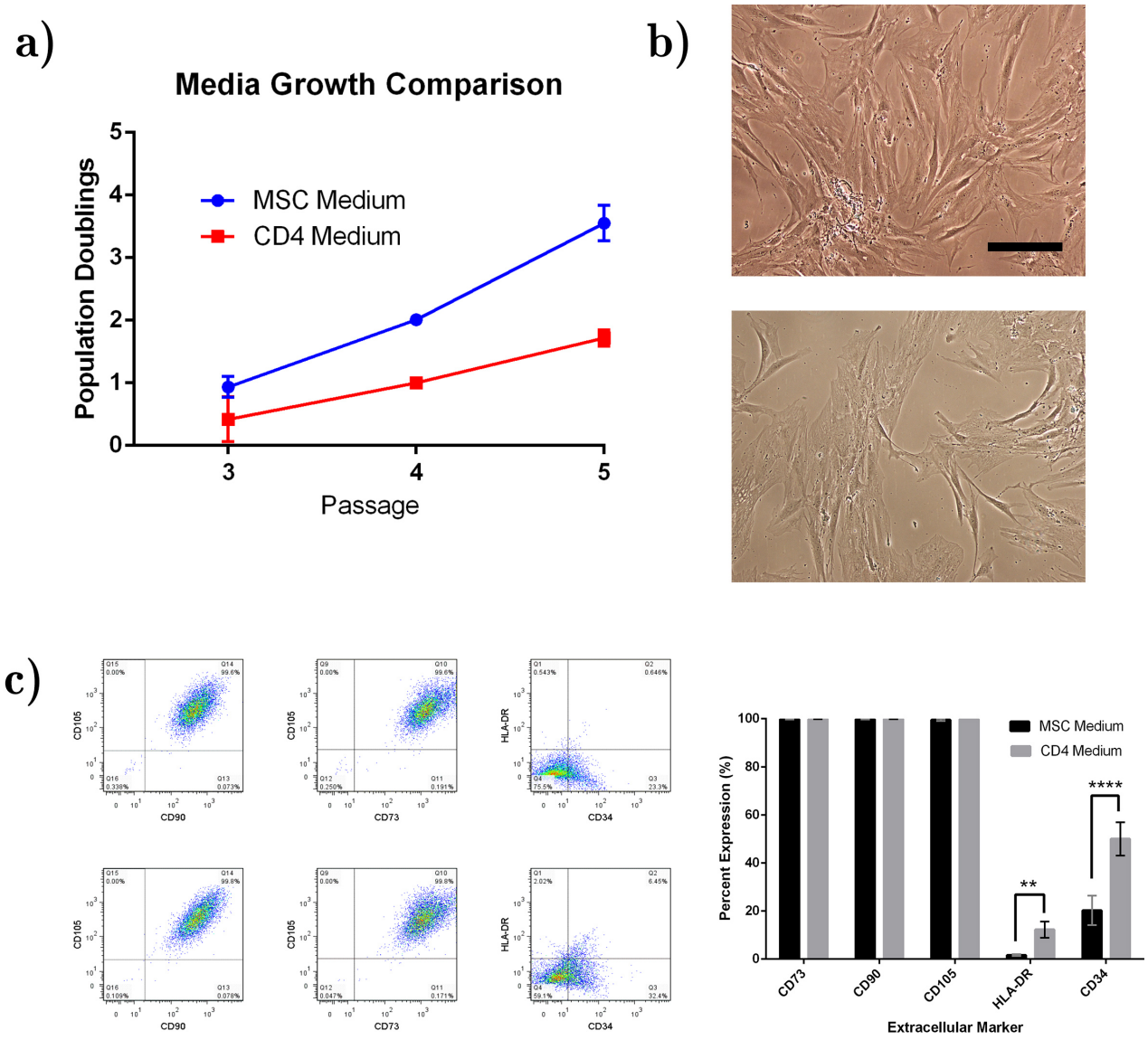

Figure 5.10: hMSC cultured in standard hMSC medium or CD4 medium a) Population doubling over 3 consecutive passages b) Morphology at day 3; hMSC medium (top image), CD4 medium (bottom image) c) Multicolour flow cytometry plots; hMSC (top), CD4 (bottom). Graph of percent expression for each marker. Scale bar = 250 μm. Points represent mean $\pm$ SD, n = 6

overnight. T-cells were added at 1:2, 1:5, 1:10 and 1:20 ratios (hMSCs:CD4 T-cells) and cultured together for either 3 or 5 days as previously described by Nold et al. (2013), Glennie et al. (2005), and Ryan et al. (2007)

At the 1:2 ratio the T-cell number was below the accurate limit of detection therefore any cell count may be erroneous. In the higher co-culture ratios (1:10 and 1:20) the CD4 T-cells proliferated rapidly and caused hMSC death where very few hMSCs could be seen (Figure 5.11 c and d, black arrows), therefore these ratios were not included in future experiments.

At the 1:5 ratio, the CD4 T-cells could be accurately counted, the hMSCs remained viable and there was no significant difference in cell counts between day 3 and day 5. Ideally when developing a potency assay reducing the overall time would beneficial as rapid readouts can inform the manufacturing and processing. As there was no difference between the two culture times, 3 days will be used for the remaining experiments.

hMSC Priming and Pre-treatment

Previous studies by Ryan et al. (2007) and Cuerquis et al. (2014) have shown that pre-treatment or priming of hMSCs with IFN-γ can increase the immunosuppressive effect by stimulating the release of other cytokines such as HGF and TGF-β1. As shown in Section 5.2.3, IDO expression can be induced by treating hMSCs with IFN-γ. This priming may enhance the immunosuppressive function of the hMSCs. Therefore, the cells were primed with 10ng/ml IFN-γ for 48 hours before the co-culture.

The impact of cyropreservation is widely debated in the current literature. Some reports have argued that it does not alter the function, whereas others have shown impaired immunomodulatory potential following cryopreservation and thawing (François et al. 2012; Luetzkendorf et al. 2015). To address this, hMSCs were thawed and left in a 37°C water bath for 60 minutes to determine if thawing and DMSO toxicity, due to the prolonged

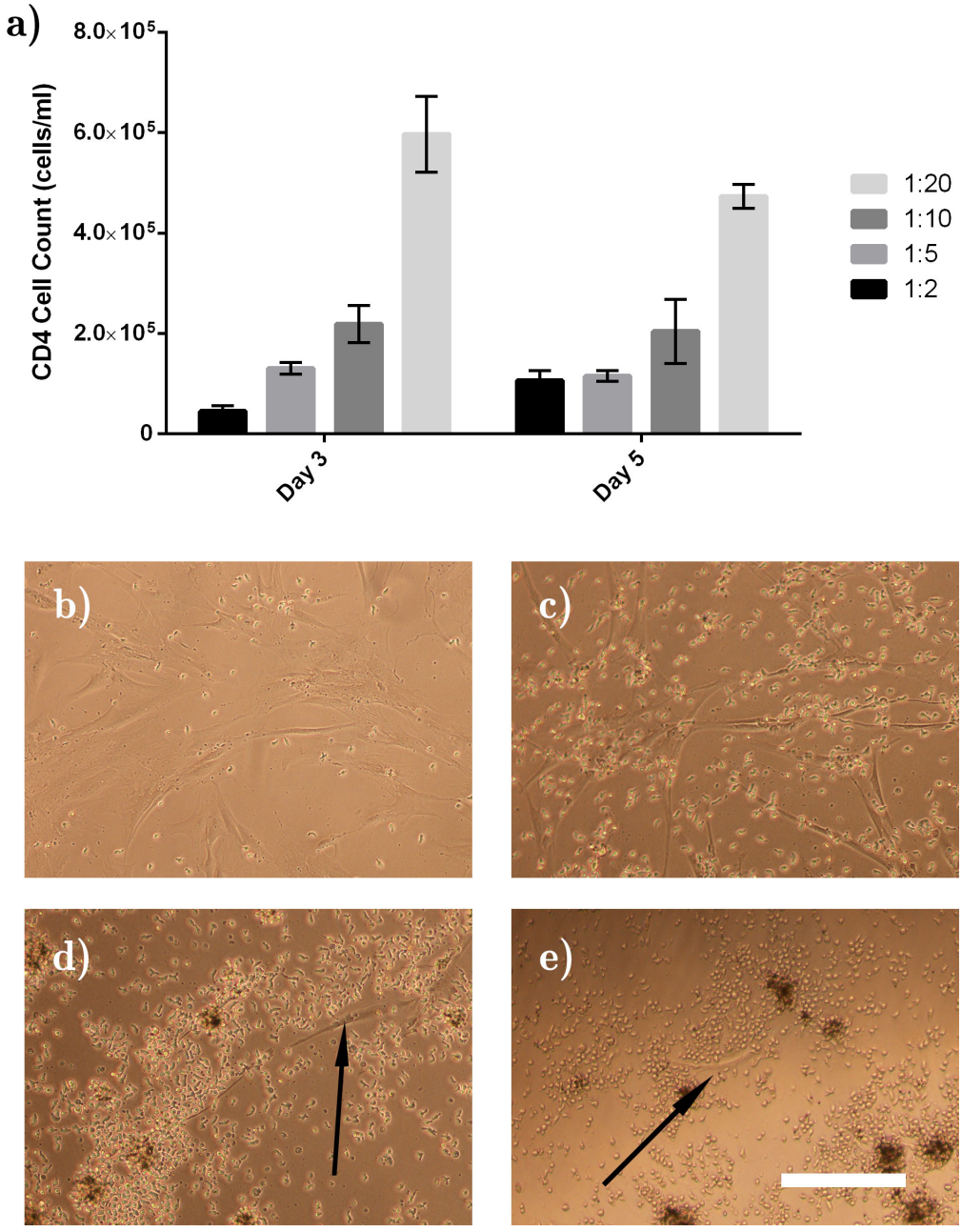

Figure 5.11: Co-culture of hMSCs with CD4 T-cells a) CD4 T-cell counts when varying the hMSC:CD4 T-cell co-culture ratios and time lengths (3 days or 5 days). Representative images at day 3 for b) 1:2 c) 1:5 d) 1:10 and e) 1:20 ratios. Black arrows indicate hMSCs. Values presented as mean ± SD, n = 6

exposure, impacted the immunosuppression properties of the selected hMSC lines. In addition, a human osteosarcoma cell line (HOST85) was also included as an adherent non-functional control.

Images of the cells in each co-culture condition are shown below in Figure 5.12. Regardless of the conditions tested, hMSCs exhibited a typical long spindle-like morphology, whereas the HOST cells exhibited a shorter and denser cell body. CD4 T-cells could be observed in suspension around the hMSCs, as smaller, rounded clusters.

Figure 5.13 shows the cell counts and kynurenine concentration after 72 hours of co-culture. hMSCs under either normal conditions, pretreated with IFN-γ or following DMSO exposure showed the same level of proliferation inhibition (Figure 5.13a). Cell counts from the HOST85 and CD4 T-cell only control were not significantly different, demonstrating that the immunosuppression effect is caused by the hMSCs and not due to the co-culture system employed here or due to the presence of another adherent cell type.

The kynurenine concentration was also measured (Figure 5.13b). Surprisingly, pre-treatment of the hMSCs with IFN-γ did not significantly increase the final kynurenine concentration when compared to the control. In the other conditions tested, hMSC/DMSO, HOST and CD4 T-cell control, the same amount of kynurenine was produced and it was lower when compared to the other tests. These findings agree with those previously reported by François et al. (2012) who found that freshly thawed hMSCs exhibited low levels of IDO expression and therefore low levels of tryptophan to kynurenine conversion. Even though the hMSC/DMSO group did not significantly increase the concentration of kynurenine it did show a reduction of T-cell proliferation suggesting other factors play a role in the immunosuppression effect of hMSCs.

With current hMSC allogeneic therapies the cells are thawed and delivered directly to the patient without time for *in vitro* recovery. The data shown suggests this is a viable

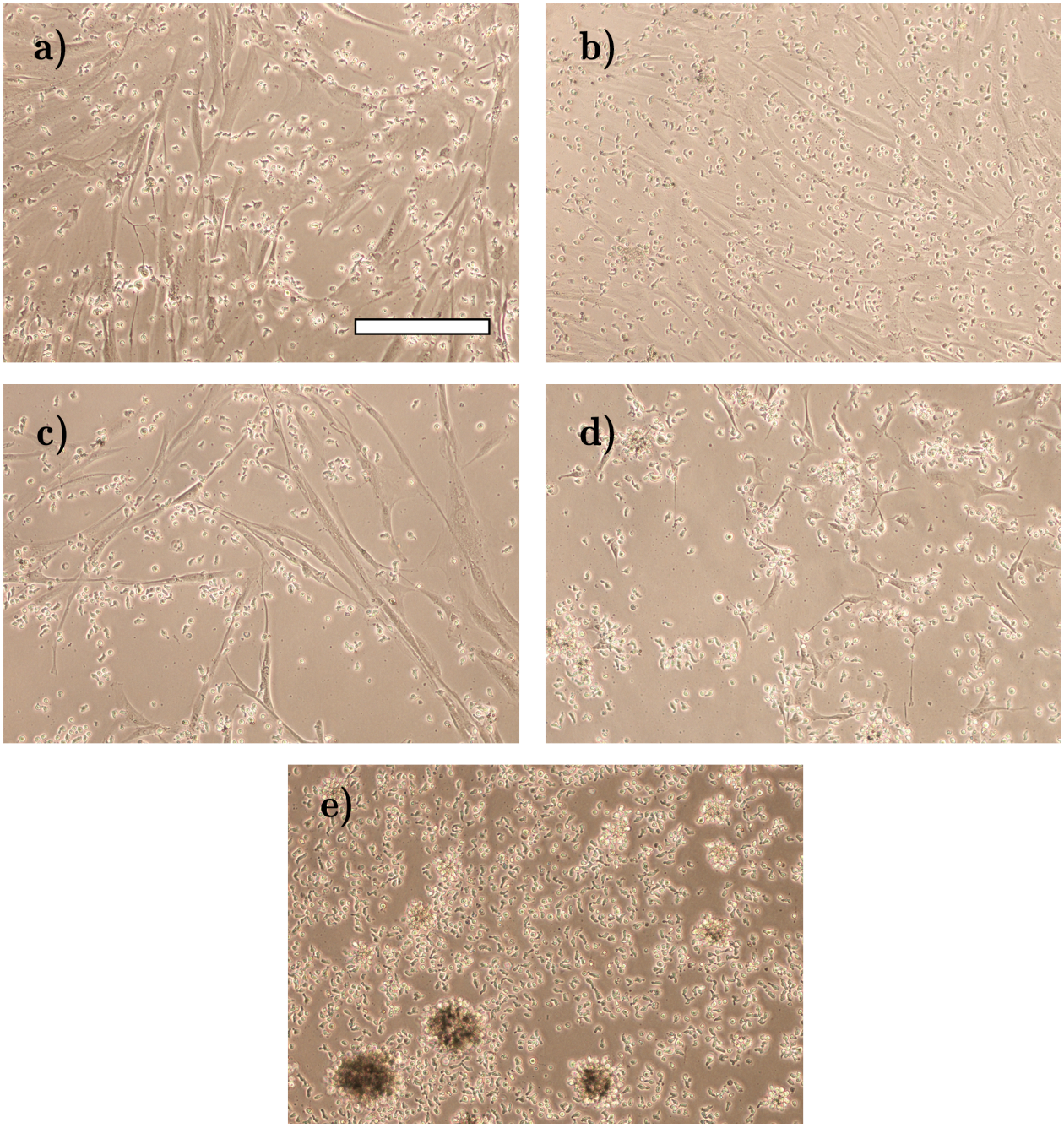

Figure 5.12: Representative images of pre-treated hMSCs and controls in the co-culture with CD4 T-cells a) hMSC b) hMSC/IFN c) hMSC/DMSO d) HOST85 e) CD4 only Scale bar = 250μm

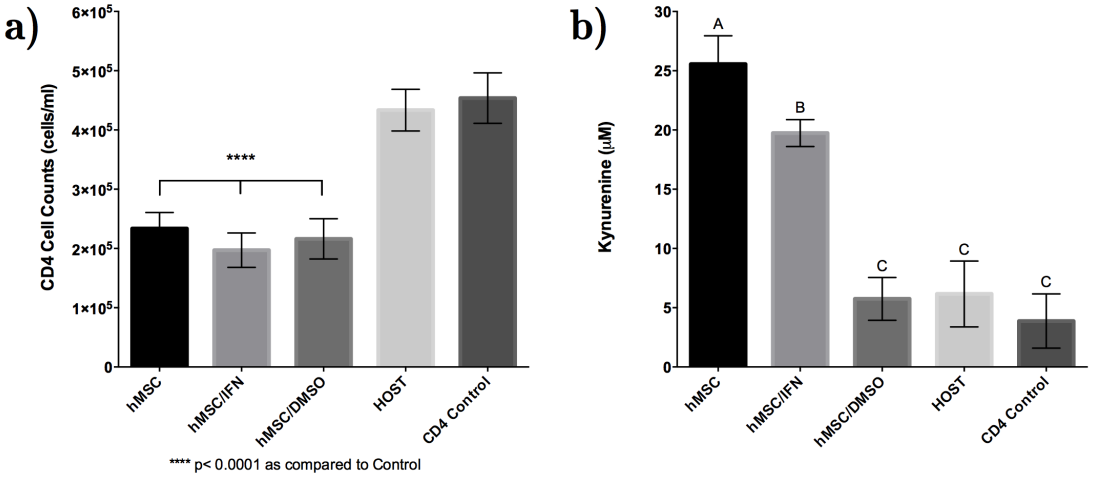

Figure 5.13: hMSC and CD4 T-cell co-culture pre-treatment screening under normal conditions, pre-treatment with 10ng/ml IFN-γ, thawed and left in freeze mix (90% FBS, 10% DMSO) for 60 minutes, HOST, and CD4 only control a) CD4 cell counts after 72 hours b) Kynurenine concentration. Values presented as mean $\pm$ SD (n = 6)

option as there was no significant difference from the standard cultured hMSCs compared to the DMSO-exposed hMSCs in terms of CD4 T-cell suppression. However, others have reports shown that freshly-thawed hMSCs perform worse in a similar T-cell proliferation assay (François et al. 2012).

Due to the inhibition of proliferation and the high concentration of kynurenine produced, the remaining experiments will focus on the hMSC only group with no IFN-γ pretreatment.

Taken together, these results showed the optimal assay would be a 3 day co-culture with a ratio of 1:5 hMSC to CD4 T-cells.

5.4.4 hMSCs reduce CD4 T-cell proliferation and viability

Next, the co-culture assay was examined using M2, M3, and M4 hMSC lines to assess donor variability and the effect on hMSC potency.

Figure 5.14 shows the CD4 cell counts following the co-culture. All selected hMSC lines were able to inhibit the proliferation of CD4 T-cells, with M2 and M3 cell lines showing the same level of inhibition as seen by the cell count and percent suppression. However, M4 cell line showed the most suppression (87.2 ± 1.52%) when compared to M2 (76.0 ± 5.74 %) and M3 (67.0 ± 2.51%) lines.

In addition to the proliferation suppression effect, hMSCs can induce apoptosis in activated T-cells (Plumas et al. 2005). Therefore, the viability of the CD4 T-cells was measured by measuring intra-cellular reduced glutathione (GSH). The decrease of GSH is an early indicator of cell death (Franco and Cidlowski 2012). Figure 5.15 shows a representative result where apoptotic cells are in the top half stained by propidium iodide (PI). Lower right quadrant indicates healthy cells, while low vitality cells are present in the lower left quadrant. As shown in Figure 5.15, there is an inverse correlation to the apoptotic cells and healthy cells. However, across all tested conditions, there were statistically insignificant differences in the number of low viability cells. M2 cell line induced the most cell death with 46.8± 6.0% undergoing apoptosis and 41.2 ± 2.3% healthy cells, In contrast M4 cell line induced the least CD4 T-cell apoptosis (22.8 ± 6.1%) and showed 70.1± 4.0% healthy cells. This apoptotic effect has been previously reported (Plumas et al. 2005) and since shown to be partly due to contact-dependent mechanisms such as the FAS ligand (Akiyama et al. 2012).

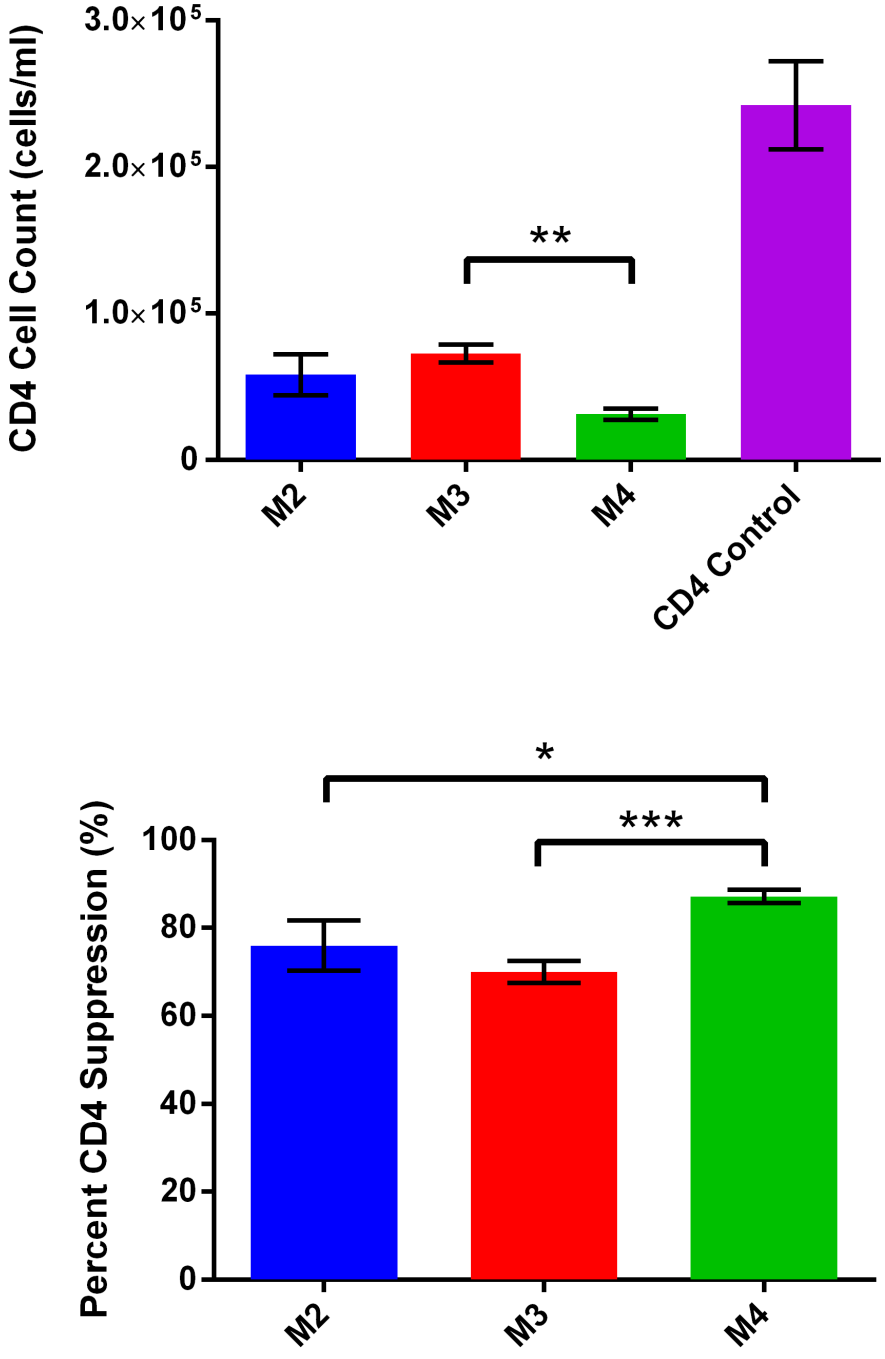

Figure 5.14: CD4 T-cell counts and percent of proliferation suppression following co-cultures with three hMSC lines. Values presented as mean ± SD (n = 6)

5.4.5 hMSCs produce kynurenine

In response to the CD4 cells, the hMSCs converted tryptophan into kynurenine *via* IDO as seen previously when cultured in the defined inflammatory environment (section 5.2.3). There was no significant difference in the final kynurenine concentration between the three hMSC lines (Figure 5.16). As expected there was little to no kynurenine found in the CD4 T-cell only control. The medium used in these experiments (RPMI 1640) contains 25μM of tryptophan, with a full conversion this would produce an equal amount of kynurenine.

5.5 hMSC and Peripheral Blood Mononuclear Cell (PBMC) Co-Cultures

The previous section has examined the ability of hMSCs to inhibit proliferation of purified CD4 T-cells. This next section will investigate if hMSC can affect the phenotype of T-cells from a mixed population of peripheral blood mononuclear cells (PBMCs). Earlier reports by Maccario et al. (2005) have shown that hMSCs can specifically inhibit dendritic cell differentiation whilst favouring T-reg cell activation. More recently, Selmani et al. (2008) and English et al. (2009) have shown this effect can be attributed to soluble factors produced by hMSCs such as HLA-G5 and through direct cell-cell contact mechanism.

Regulatory T-cells (T-regs) are a specialised sub-set of CD4 cells that are identified by their expression of CD25, FoxP3 and CTLA-4 amongst other markers. They were originally defined as preventing autoimmune diseases, but other functions include maintenance of self-tolerance and immune homoeostasis by suppressing activation and proliferation of other immune cells (Sakaguchi et al. 2009). Inducing a differentiated T-reg phenotype from naive T-cells is one of the other immunomodulatory functions thought to be possessed by hMSCs.

5.5.1 PBMC Culture

PBMCs were thawed and cultured for 4 days to examine if proliferation would occur spontaneously or require the CD3/CD28 DynaBeads as previously with the CD4 T-cell culture.

Figure 5.17a shows PBMCs cultured with or without CD3/CD28 bead stimulation. Both contained a mixed population of suspension blood cells including lymphocytes (L) (CD4 and CD8 cells), granulocytes (G) and monocytes (M). After four days in culture the cells were counted and there was clear proliferation of those cultured with the beads (Figure 5.17b).

The cells were also analysed by flow cytometry, Figure 5.17c shows the initial characterisation of the cells. The forward and side scatter plots showed typical PBMC characteristics with clear distinction between the smaller lymphocytes to the larger and more granular monocytes. Further analysis on the lymphocyte population revealed high CD4 expression but no expression of CD25 or FoxP3 suggesting that within the unstimulated and naive state there were no regulatory T cells present.

5.5.2 hMSC and PBMC Co-Culture

As previously with the CD4 T cells, the hMSCs were co-cultured with PBMCs. After 72 hours, the PBMCs were sampled for counting, viability testing and for T-reg induction.

Figure 5.18 shows the cell counts and viability as measured by acridine orange and DAPI staining. Similarly to the CD4 co-cultures, all the individual hMSC lines were able to inhibit proliferation of the PBMCs, when compared to controls. There was no difference in the inhibition between the selected hMSC lines. Viability analysis shows that M4 cell line induced the most apoptosis (68.23 $\pm$ 5.98 % live cells) , whereas the M2 cell line induced

the least (77.80 ± 1.82% live cells). However, all recorded values were significantly lower than the PBMC only control.

The next aim of this study was to examine if hMSCs could induce a regulatory T-cell phenotype following direct co-culture. After the co-culture the PBMCs were harvested and stained with CD4, CD25 and intracellular FoxP3.

Figure 5.19a shows that hMSCs were able to induce a small population of T-regs from naive PBMCs as analysed via flow cytometry. The full expression of the CD4/CD25/FoxP3 taken from the upper right quadrant (Q2) is given in Figure 5.19b. No significant difference between M2 cell line and the control was observed, whereas M3 and M4 cell lines were able to generate 21.4 ± 5.80% and 15.4 ± 2.43% T-regs respectively. M2 cell line generated high CD25 positive cells, but only a small number of cells had FoxP3 expression. This phenotype is indicative of an activated T-cell, but not necessarily a fully differentiated T-reg (Corthay 2009).

Also, IDO activity by the hMSCs was measured by the concentration of kynurenine present in the spent medium. Figure 5.20 shows that in all hMSC/PBMC co-cultures there was full conversion of tryptophan into kynurenine. There was no significant difference found between each of the selected hMSC lines. In PBMC-only controls there was little to no conversion. This shows that the inhibition of proliferation by the hMSCs is partly due to the IDO activity and supports previous findings by Krampera et al. (2006) and Gieseke et al. (2007).

To summarise, this data shows that bone marrow derived hMSCs possess the potential to alter the phenotype of naive T-cells into specific regulatory T-cells. Initially, hMSCs can inhibit proliferation, reflecting the effect seen previously with the purified CD4 T-cells. This finding was in agreement with previous reports as by Gieseke et al. (2007) and Jones et al. (2007) who have also described the inhibition of PBMCs with adipose and umbilical cord-derived hMSCs.

Moreover, inducing a T-reg phenotype could be considered a standard for the measurement of the immunomodulatory properties of hMSCs. Here, it was shown that M3 and M4 hMSC lines were able to effectively cause T-reg induction, whereas M2 cell line did not possess the same potential as it has only induced the expression of CD25 and not FoxP3. Unlike previous studies, here it was shown that there are marked differences in the immunomodulatory properties of hMSCs, which were previously determined to have similar characteristics. Producing a reliable and reproducible immunomodulatory potency assay could potentially be the key to develop these cell lines for diseases such as GvHD or ulcerative colitis. It is not sufficient to measure hMSC potency by growth rate or marker expression, for example. Instead, functional assays that measure the intended *in vivo* biological function should be required.

Measuring kynurenine concentration is a quick and simple way to assess hMSC reaction to an inflammatory environment. However, the data shown here does not indicate any significant differences between the individual cell lines, unlike what is seen when measuring the T-reg phenotype change. Therefore, given the sensitivity of the flow cytometry method, it makes it a better choice to determine hMSC potency by determining the immunomodulation potential.

5.6 Conclusions

The aim of this chapter was to develop an immunomodulatory potency assay that could measure key known MoAs of hMSCs. This chapter has examined the hMSCs under three separate inflammatory culture conditions to analyse the response and effect. In order to reduce inconsistency with co-culture assays, the hMSCs were first cultured in a hostile environment by the addition of pro-inflammatory cytokines. This allowed for the analysis of known modulators such as IL-6 secretion, IDO gene expression and tryptophan to kynurenine conversion. Next, in order to determine if these metrics could be applied

to measure the immunosuppressive ability of the cells, the selected hMSC lines were co-cultured with purified CD4 T-cells. Here, it was found that all the hMSC lines could effectively suppress proliferation and induce apoptosis in the CD4 T cells. In particular, M4 cell line showed the greatest level of suppression, when compared to M2 and M3 lines. However, M2 line induced the most cell death. Following this study, the hMSC lines were then co-cultured with PBMCs to again determine their proliferation suppression ability. In addition, the PBMCs were further analysed for differentiation into a regulatory T-cell phenotype. As such, the M3 cell line was found to significantly induce this T-cell subset when compared to M2.

These assays considered both the effector cells (*i.e.* hMSCs) and the responder cells (either CD4 T cells or PBMCs) and examined key mechanistic pathways that are known to be responsible for their clinical activity. The use of these QC assays take a much needed step towards standardising potency assays of hMSCs to ensure an effective cell therapy is delivered.

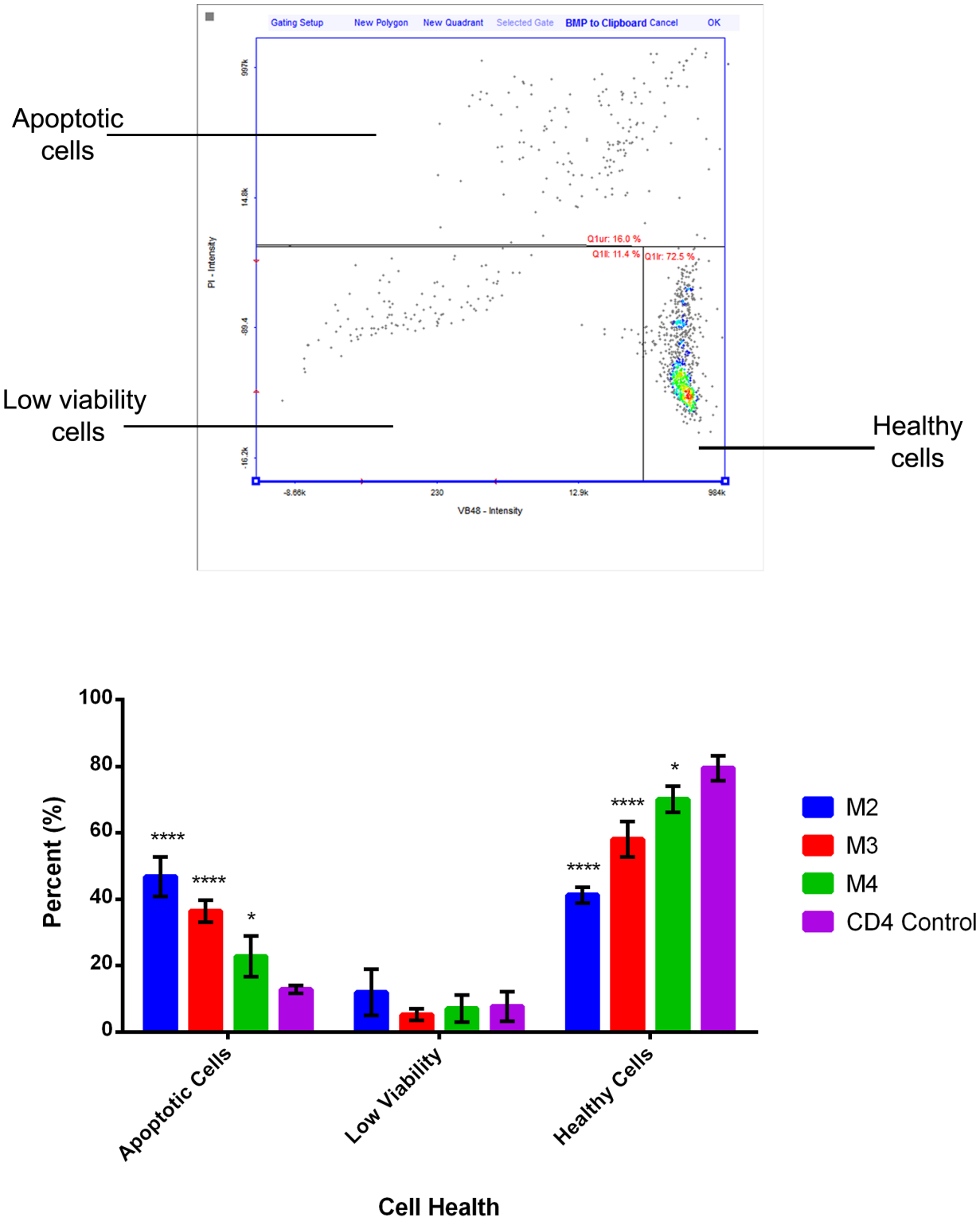

Figure 5.15: CD4 T-cell health following co-culture. Top plot shows representative image, top quadrant indicates propidium iodide (PI) positive cells (dead/apoptotic); lower left indicates low viability (VB48 low) and lower right indicates healthy cells (low PI, high VB48). Graph presents CD4 analysis after co-culture with each hMSC line as a percentage in each quadrant. Values presented as mean ± SD (n = 6)

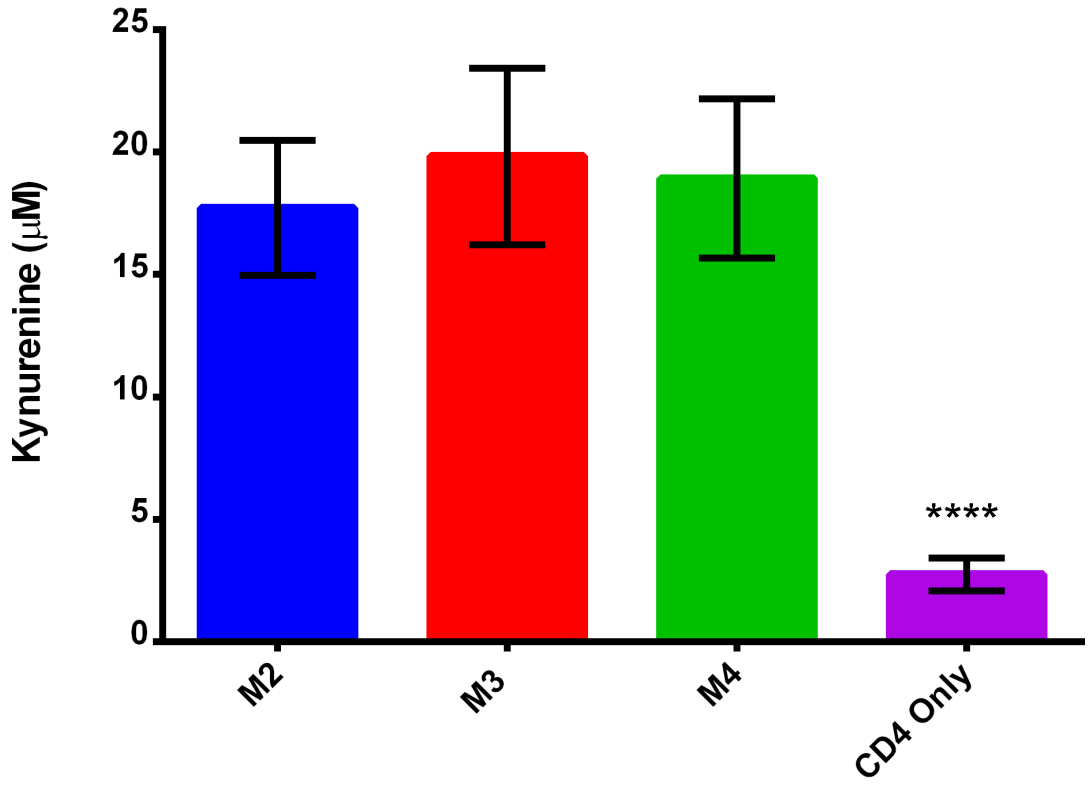

Figure 5.16: Kynurenine concentration following hMSC and CD4 T-cell co-culture for three days. Values presented as mean ± SD (n = 6)

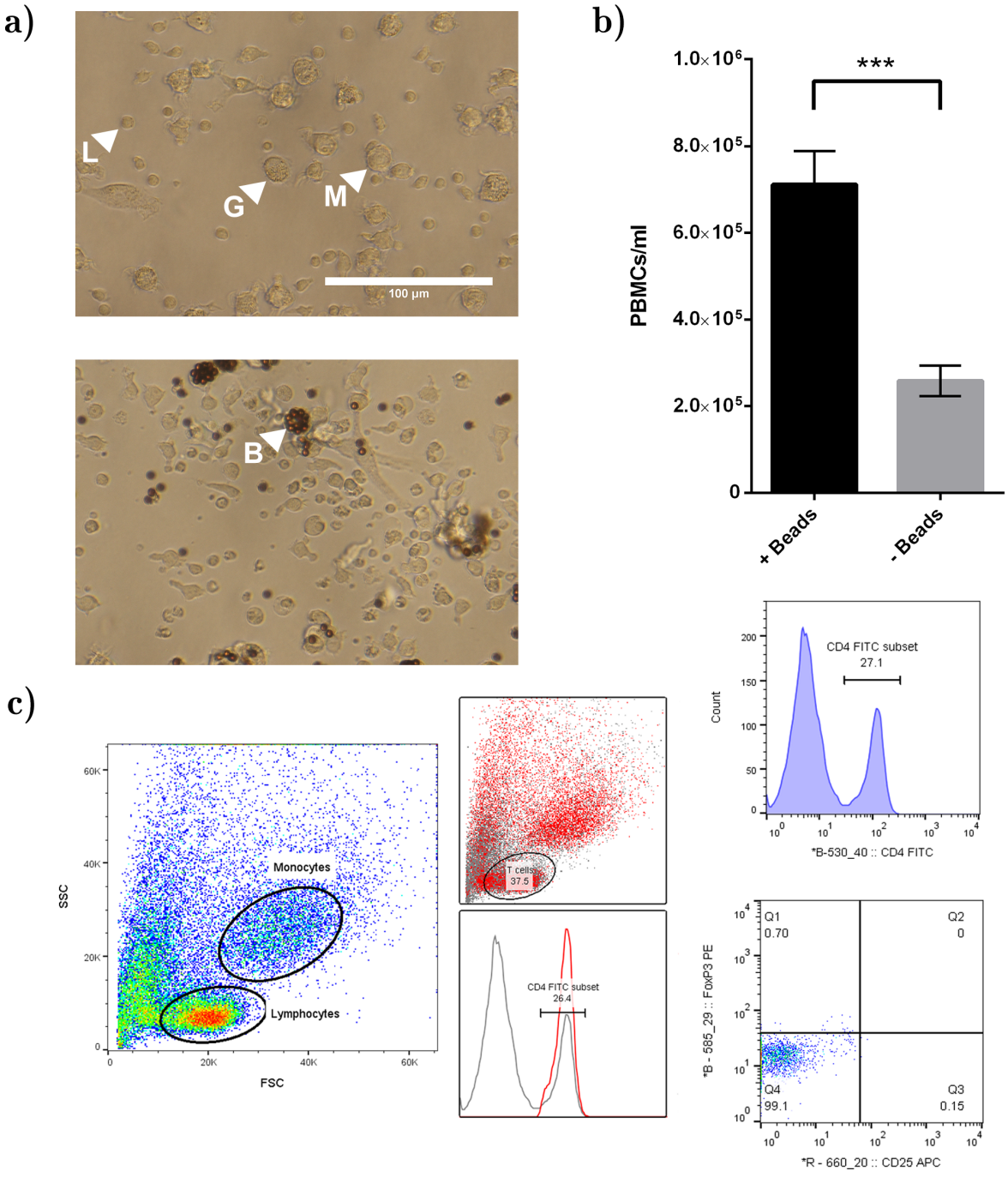

Figure 5.17: Culture of PBMCs over 4 days. a) No stimulation (top), with CD3/CD28 DynaBead stimulation (bottom). L = Lymphocytes, G = Granulocytes, M = Monocytes, B = CD3/CD28 DynaBeads. Scale bar = 100μm. b) Cell counts following 4 days of culture. c) Flow cytometry plots of fresh PBMCs and analysed for the CD4/CD25/FoxP3 T-reg sub-population. Values presented as mean ± SD (n = 3)

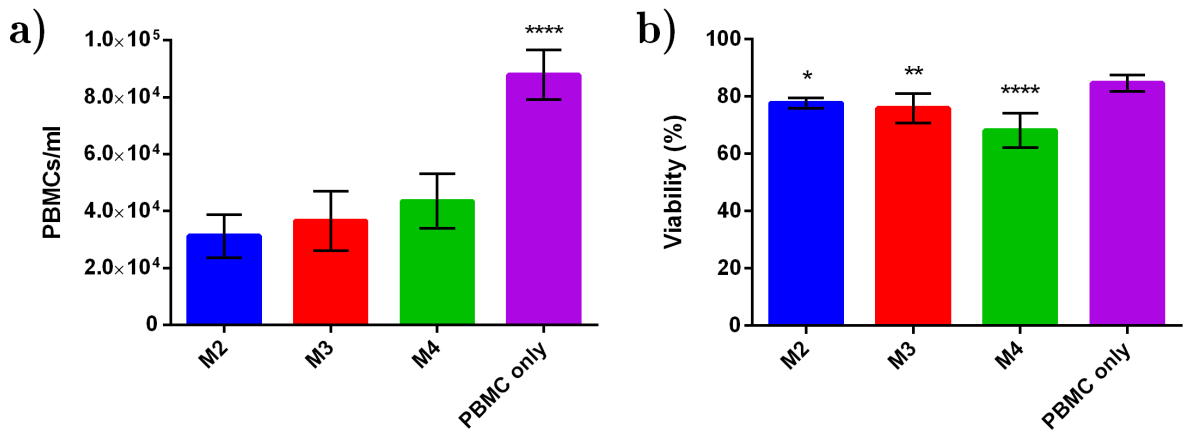

Figure 5.18: Co-culture of PBMCs with hMSCs after 72 hours a) Cell counts b) Viability. Significance as compared to the PBMC control. Values presented as mean ± SD (n = 6)

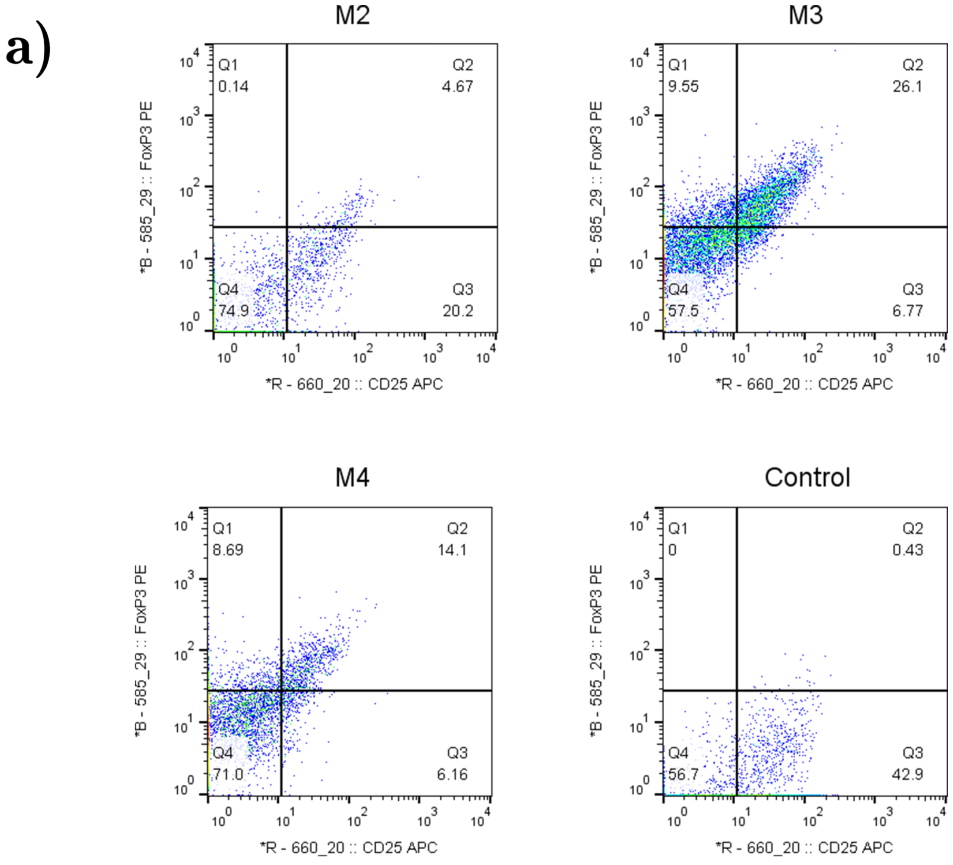

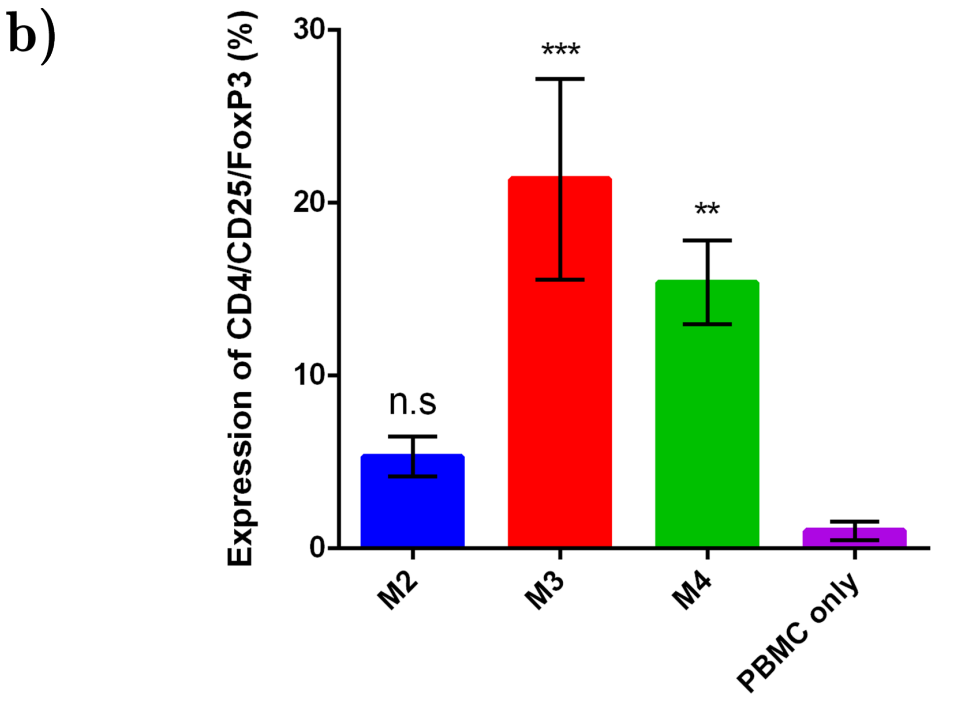

Figure 5.19: Regulatory T-cell phenotype expression from PBMCs following co-culture with hMSCs. a) Representative flow cytometry plots of CD25 and FoxP3 subgated from CD4 b) Graph of T-reg full expression phenotype compared to PBMC only control. Values presented as mean ± SD (n = 4)

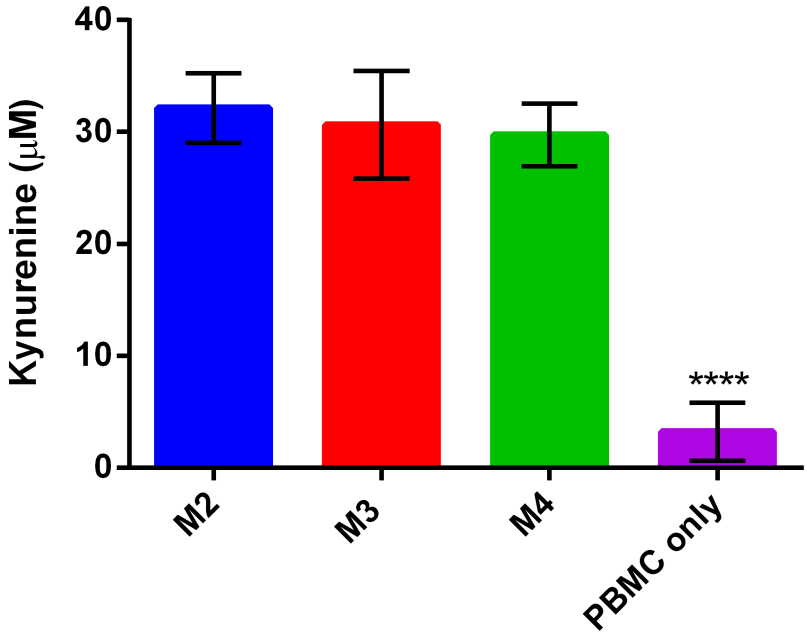

Figure 5.20: IDO activity as measured by kynurenine concentration following 72 hours of hMSC and PBMC co-culture. Values presented as mean ± SD (n = 6)

Chapter 6

Development of an Angiogenesis Assay

6.1 Introduction

In 2013, ischaemic heart disease was the leading cause of death in England and Wales accounting for 15.4% of death in males (ONS 2015). Heart failure following myocardial infarction (MI) remains one of the leading causes of death and disability worldwide, while treatment still remains a major challenge for cardiovascular medicine. Reperfusion therapy is a medical treatment that acts to restore blood flow to the ischaemic tissue and organs. For large to medium sized vessels an angioplasty or bypass surgery is required, for smaller sized vessels it may be possible to utilise stem cell treatment to induce angiogenesis (Williams and Hare 2011). Others have shown growth factors such as vascular endothelial growth factor (VEGF) and placental growth factor (PIGF) can also induce small vessel angiogenesis (Luttun et al. 2002).

Angiogenesis, or neo-angiogenesis, is the formation of blood vessels from existing vasculature or creation of new vasculature. It is a key stage in embryo development, growth,

and wound healing in adult life. Wound healing occurs as part of the repair and regeneration mechanism after injury to aid removal of dead cells and restore blood flow to the surrounding tissue. The process of angiogenesis involves endothelial cells invading a fibrin wound clot and reorganising into a microvascular network throughout the tissue. This dynamic interaction occurs due to angiogenic cytokines such as fibroblast growth factor (FGF), VEGF, and angiopoietin released by activated macrophages and endothelial cells (Tonnesen, Feng, and Clark 2000).

In vitro hMSC are able to induce endothelial tube formation due to the broad range of cytokines they release into the local area (Bronckaers et al. 2014). In addition, delivery of hMSC conditioned medium has been shown to improve blood flow and function in murine hind limb ischaemia (Deuse et al. 2009; Lee et al. 2013). Therefore, investigating the secretome will be essential to determine the molecular mechanisms through which hMSCs exert their pro-angiogenic effect. It is likely that they release multiple cytokines, therefore identifying the factors that relate to efficient angiogenesis will be crucial to developing in-line quality control checks during hMSC manufacturing.

There are a number of assays that can be used to determine angiogenic potential (described in Chapter 1 Section 1.6.3). The most reproducible *in vitro* assay is the HUVEC/endothelial tube formation assay and will be used in this chapter (Auerbach et al. 2003). By seeding a known number of cells onto a basement membrane matrix, the spontaneous formation of capillary or tube-like structures can be observed. By allowing the tubes to form on a two-dimensional surface, the level of angiogenesis can be quantified using computer based image analysis and allows for high-throughput screening. Therefore, this assay will be utilised in this chapter as it is suitable in a bioprocess and manufacturing environment. Researchers using this method typically choose an endpoint between 16-24 hours, however as tube formation is a dynamic process occurring over short time period it is possible that key time points are missed (Dao et al. 2013; Bara et al. 2015). To overcome this problem time lapse imaging will be used to record the full formation

and degradation of the tubule structures.

The objectives of this chapter were:

- Verify and consistently perform an *in vitro* angiogenesis assay
- Compare and evaluate analysis software
- Investigate the use of hMSC-conditioned medium to enhance angiogenesis and compare different donor lines
- Screen and quantify known pro-angiogenic cytokines produced by hMSCs

6.2 Establishing Critical HUVEC Tube Formation Parameters and Analysis

The most specific *in vitro* assessment for angiogenesis is the measurement of endothelial cells to form three-dimensional tube structures (Auerbach et al. 2003). Human umbilical vein endothelial cells (HUVECs) are cells isolated from the endothelium of veins from the umbilical cord and they are typically used in wound healing, angiogenesis, and migration assays (Vailhé, Vittet, and Feige 2001). For this set of experiments pooled multiple donor HUVECs were purchased at p0 and plated onto standard tissue culture treated plastic for 7 days. They exhibited small, rounded cobblestone/endothelial-like morphology from thaw until confluent and cryopreservation (Fig. 6.1).

6.2.1 Inducing HUVEC Tube Formation

Under the correct conditions HUVECs can undergo extensive morphological changes from a flat monolayer to form high organised, three dimensional tube/capillary-like structures

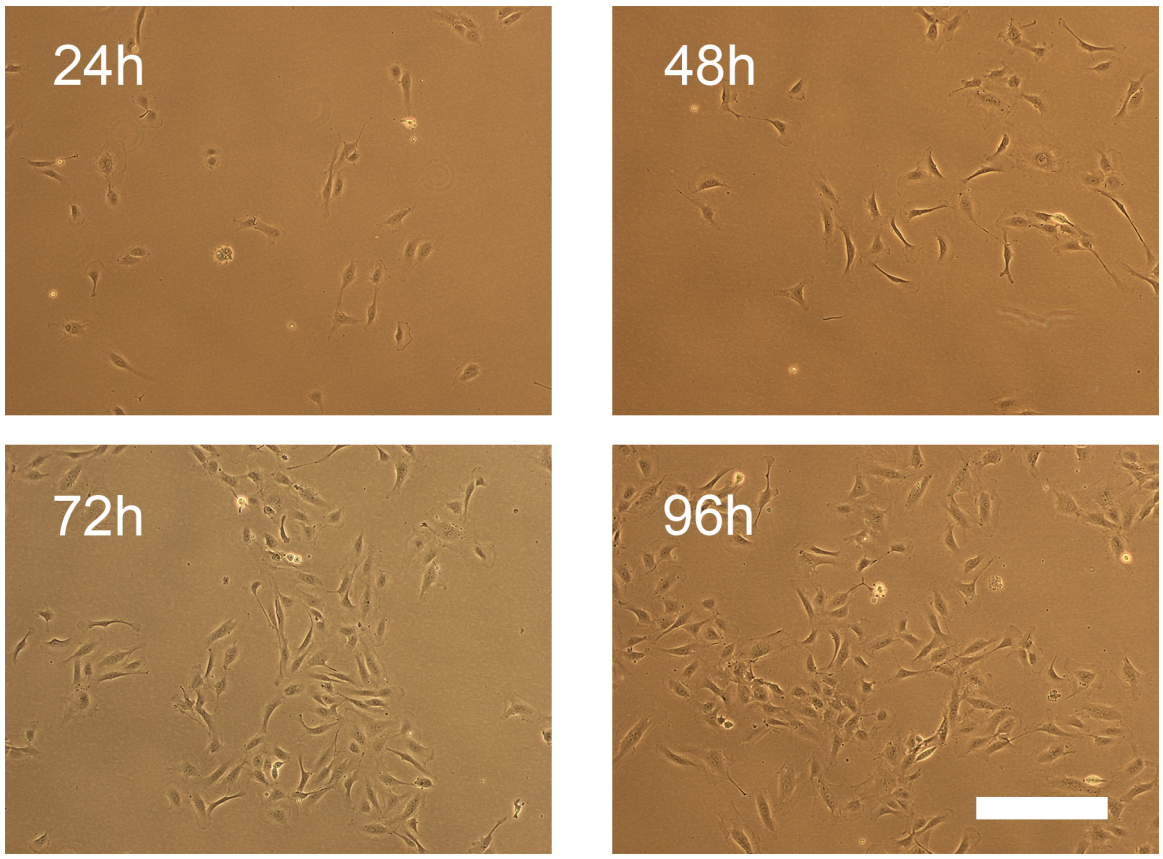

Figure 6.1: Representative images of HUVECs from initial thaw and seeding for 96 hours. Scale bar = 250μm

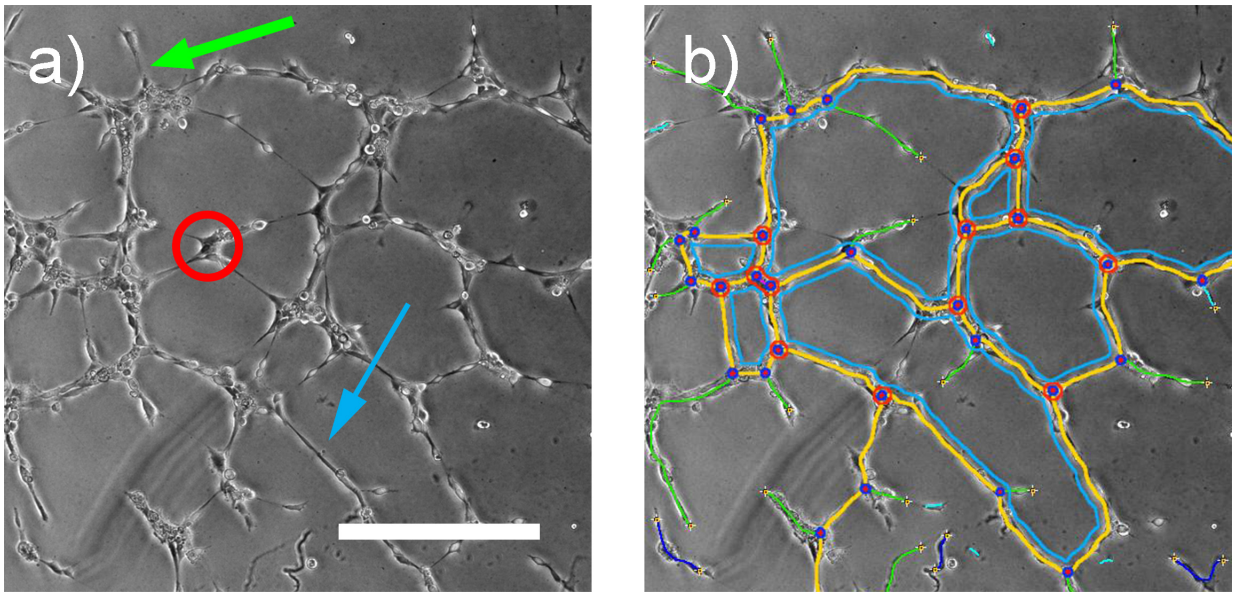

Figure 6.2: Example of HUVEC analysis following tube formation. a) Raw image with nodes (red circle), branches (blue arrow) and extremities (green arrow). b) The same image following ImageJ processing overlaid with the analysis skeleton. Scale bar = 250μm

thus mimicking angiogenesis *in vitro*. The extent of angiogenesis can be determined by a number of different characteristics (Staton, Reed, and Brown 2009; Arnaoutova and Kleinman 2010). Nodes are the central branching point from which branches sprout, branches (and their total length) are the tubes connecting between nodes, and extremities are branches that connect to only one node (Figure 6.2). Branch and node analysis methods are detailed later in Section 6.2.3.

Positive differentiation of HUVECs into tubules was performed with Medium 200PRF on a GelTrex basement membrane layer, Figure 6.3 shows the formation of tubules after 24 hours. Tube formation was observed only in the GelTrex coated wells that contained either Medium 200PRF (Positive Control) or hMSC conditioned medium (hMSC-CM) (Figure 6.3a and b). No significant difference was found in the number of nodes from the two conditions, 35.25 $\pm$ 5.68 and 47.50 $\pm$ 6.36 ($p = 0.05$) respectively. Similarly, the total branching length did not show any significant difference 2320 $\pm$ 213px and 2803 $\pm$ 734px. However, the total number of branches was found to be significantly different than the positive control at 10 $\pm$ 1 and hMSC-CM at 39 $\pm$ 2.

There was no observed tube or node formation when HUVECs were seeded without a GelTrex layer with hMSC-CM. Cells in these conditions retained their undifferentiated cobblestone-like appearance (Figure 6.3c). Finally, a negative control was also included by the addition of 30μM of suramin, an anti-angiogenic compound and as expected there was no tube formation (Fig 6.3d).

To conclude, in order for HUVECs to initiate tube formation a basement membrane is required and the efficiency was found to be enhanced by the use of hMSC-CM. However, use of hMSC-CM alone was not sufficient to cause tube formation.

6.2.2 Optimising Basement Matrix Choice

Previous studies have used various coatings, including GelTrex and growth factor reduced Matrigel, to induce HUVEC tube formation (Faulkner et al. 2014; Kwon et al. 2014). Both matrices contain purified extra-cellular proteins from the Engelbreth-Holm-Swarm (EHS) tumour. The major components of these matrices include laminin, collagen IV, entactin, and heparin sulphate proteoglycan. The main role is in the physical support and compartmentalisation of tissue. Specifically for angiogenesis it supports the role in cell/tissue organisation as it affects cell adhesion, migration and proliferation (Grant et al. 1994). Previous studies have also shown that gelatin hydrogels can support the implantation and survival of cardiomyocytes in myocardial infarction mouse models (Dreesmann, Ahlers, and Schlosshauer 2007; Nakajima et al. 2015). Gelatin was therefore included in the screening test to assess if it could promote angiogenesis. The basement membrane layers were prepared as described in Chapter 2 Section 2.14.4.

At 6 hours of formation the cells were fixed, imaged, and analysed. GelTrex 100% was found to be the most potent inducer of angiogenesis (Figure 6.4a) Left image and b) Blue bar) with 41 $\pm$ 19 nodes and 16969 $\pm$ 6750 px of branching length. The dilutions of GelTrex (75% and 50%) also showed node and tube formation however at a much lower

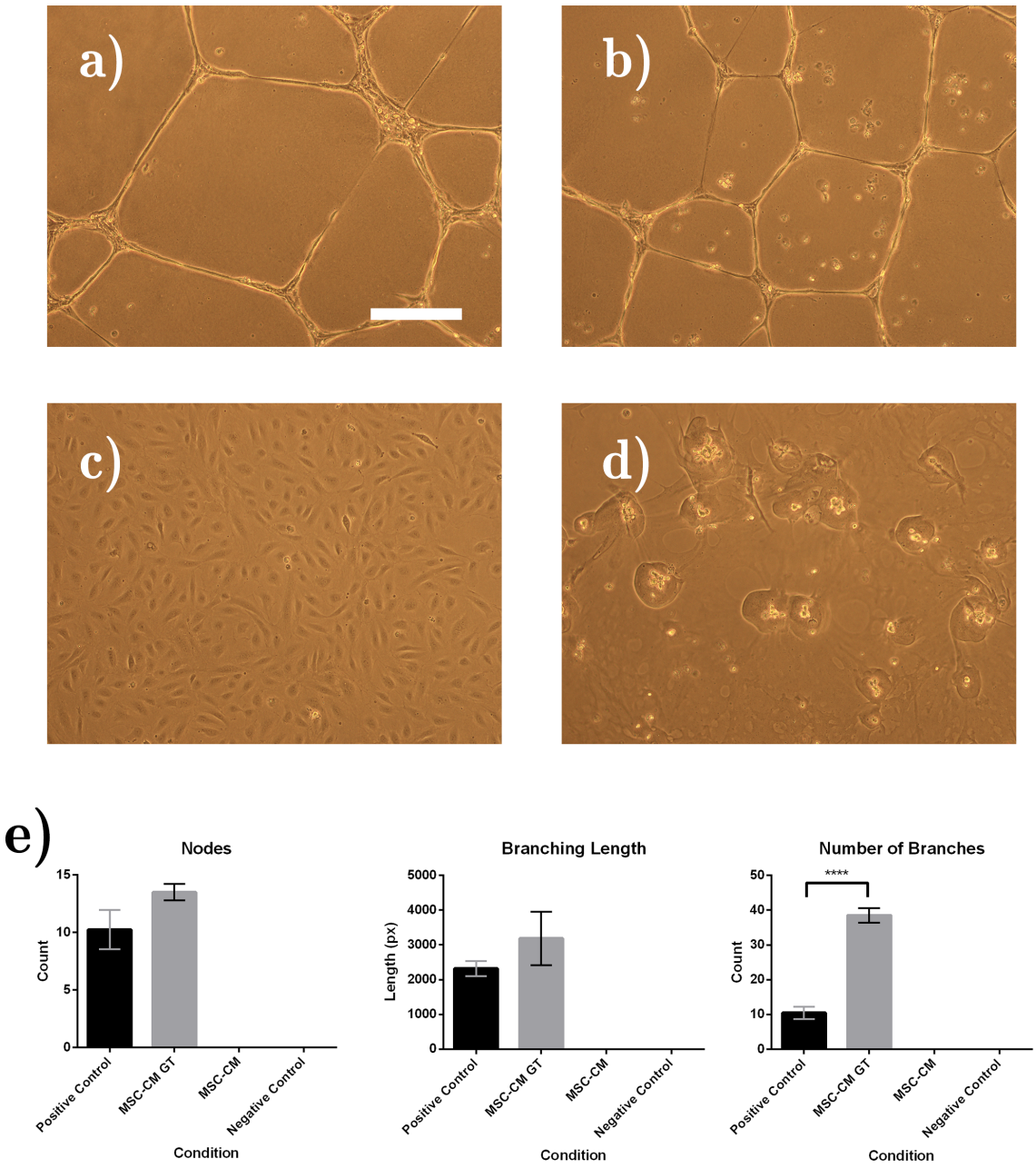

Figure 6.3: Critical parameters for HUVEC tube formation a) Positive control with GelTrex b) GelTrex and hMSC conditioned medium c) HUVEC and hMSC conditioned medium only d) Negative control by the addition of 30μM Suramin e) Graphs from analysed images. Values presented as mean ± SD (n = 4). Scale bar = 250μm.

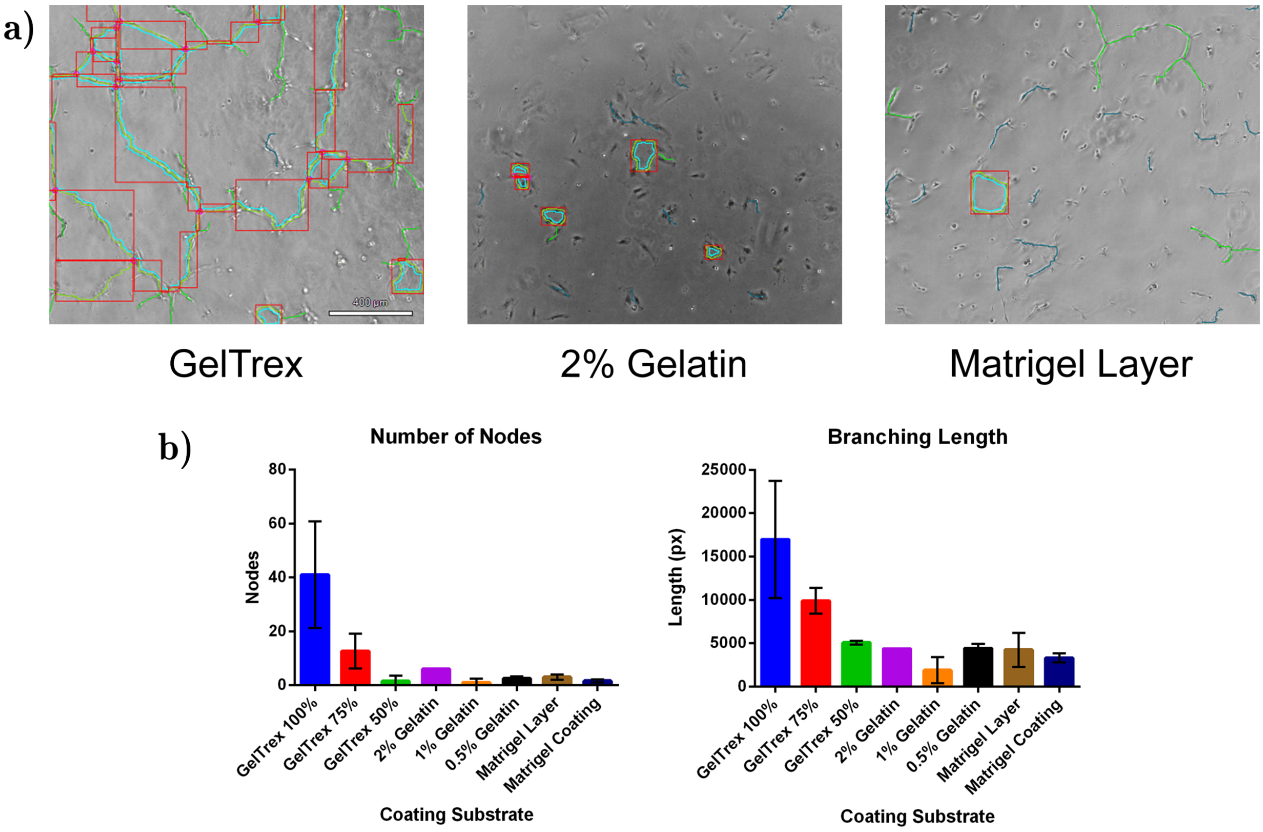

Figure 6.4: Basement membrane coatings for HUVEC tube formation a) Representative images for 100% GelTrex, 2% Gelatin, and Matrigel Layer. Regions of interest are shown in red boxes, branches in green. b) Graphs of number of nodes and branching length taken after 6 hours of formation. Values presented as mean ± SD (n = 3). Scale bar = 400μm.

efficiency. Both Matrigel preparations had similar branching lengths and nodes.

Gelatin was the worst performer at all concentrations demonstrating 2-3 nodes per field of view and 3386 ± 1421 px branching length. Previous studies that used gelatin to induce HUVEC tube formation also incorporated VEGF into the hydrogels to induce angiogenesis (Del Gaudio et al. 2013; Li et al. 2015). This may explain the lack of tubes formed from these preparations of gelatin.

To study HUVEC tube formation a relatively large volume of basement membrane is required, typically around 50μl/cm^2. As well as increasing the overall cost per assay, thicker gel preparations can lead to uneven surfaces making image analysis more prob-

Table 6.1: Cost of each surface matrix/basement membrane per cm^2 for the HUVEC tube formation assay

Surface Matrix	**Volume per cm^2 (μl)**	**Cost per ml (£)**	**Total cost per cm^2 (£)**
GelTrex 100%	50	23.18	1.16
GelTrex 75%	37.5	23.18	0.87
GelTrex 50%	25	23.18	0.58
Gelatin 2%	50	0.38	0.02
Gelatin 1%	37.5	0.38	0.01
Gelatin 0.5%	25	0.38	0.01
Matrigel Layer	50	43.95	2.20
Matrigel Coating	1.22	43.95	0.54

lematic. Table 6.1 outlines the cost for each matrix preparation per cm^2. For bioprocess and quality control assays the ease of use, reproducibility, throughput, and total cost per test will play a factor in deciding its usability.

Overall the Matrigel layer preparation was the most expensive at £2.20 per cm^2 whereas as the gelatin solution was the cheapest at £0.01 per cm^2. GelTrex 100% represented a middle price point with the maximum cost at £1.16 per cm^2.

Due to the best tube formation efficacy resulting from the GelTrex at 100% and being more cost effective than both the Matrigel Layer and Coating methods, GelTrex was selected to be used for further experiments.

6.2.3 Analysing HUVEC tube formation

In this chapter, the level of angiogenesis was determined by the efficiency of tube formation in HUVECs. The interpretation of this assay was quantified by software packages that could determine key angiogenic characteristics. ImageJ is an open-source image analysis

software with the ability for users to develop specific plugins to fulfil specific requirements (Schneider, Rasband, and Eliceiri 2012). For part of this work an Angiogenesis Analyser plugin was used in conjunction with ImageJ (Chevalier et al. 2014).

For time-lapse culture, images were analysed using a custom recipe (macro) developed for the Nikon CL-Quant software. Both ImageJ and CL-Quant software packages were able to output nodes (branching points), number of branches, and branching length. These outputs are shown in Figure 6.5a. The left image shows the original image overlaid with the analysed skeleton or outline. The middle image shows the skeleton only with the background removed. The right image shows an enlarged section of the skeleton, for each of the numbered triangles, annotation "1" indicates an extremity branch, connected to one node only, "2" depicts a full mesh loop, while "3" shows a branch connected between two separate nodes and "4" shows a node. Each image was analysed individually and the results were collated over the time points.

As both software packages were used in conjunction they were compared to determine if there were any significant differences from the outputs. For this, a sample of 125 images were randomly selected and processed. The number of nodes and total tube length were plotted. Figure 6.5b shows a linear regression plot for the number of nodes while Figure 6.5c shows a plot for the branching length. The r^2 value was 0.965 for the number of nodes and 0.957 for branching length. Therefore, as both software packages gave the same output within a 95% confidence interval, it was concluded that both can be used alongside each other with confidence.

In all experiments the formation and degradation of the tubes were imaged every 20 minutes for 24 hours. By using a live-imaging system it was possible to follow the formation and degradation of the tubes over this time. Figure 6.6 shows a representative point in a well of HUVECs undergoing tube formation. The cells rapidly organised between 0 to 1.5 hours of seeding to form connecting networks of tubes. This effect continued for a further 4.5 hours. After approximately 6 hours the mesh network began to degrade and there

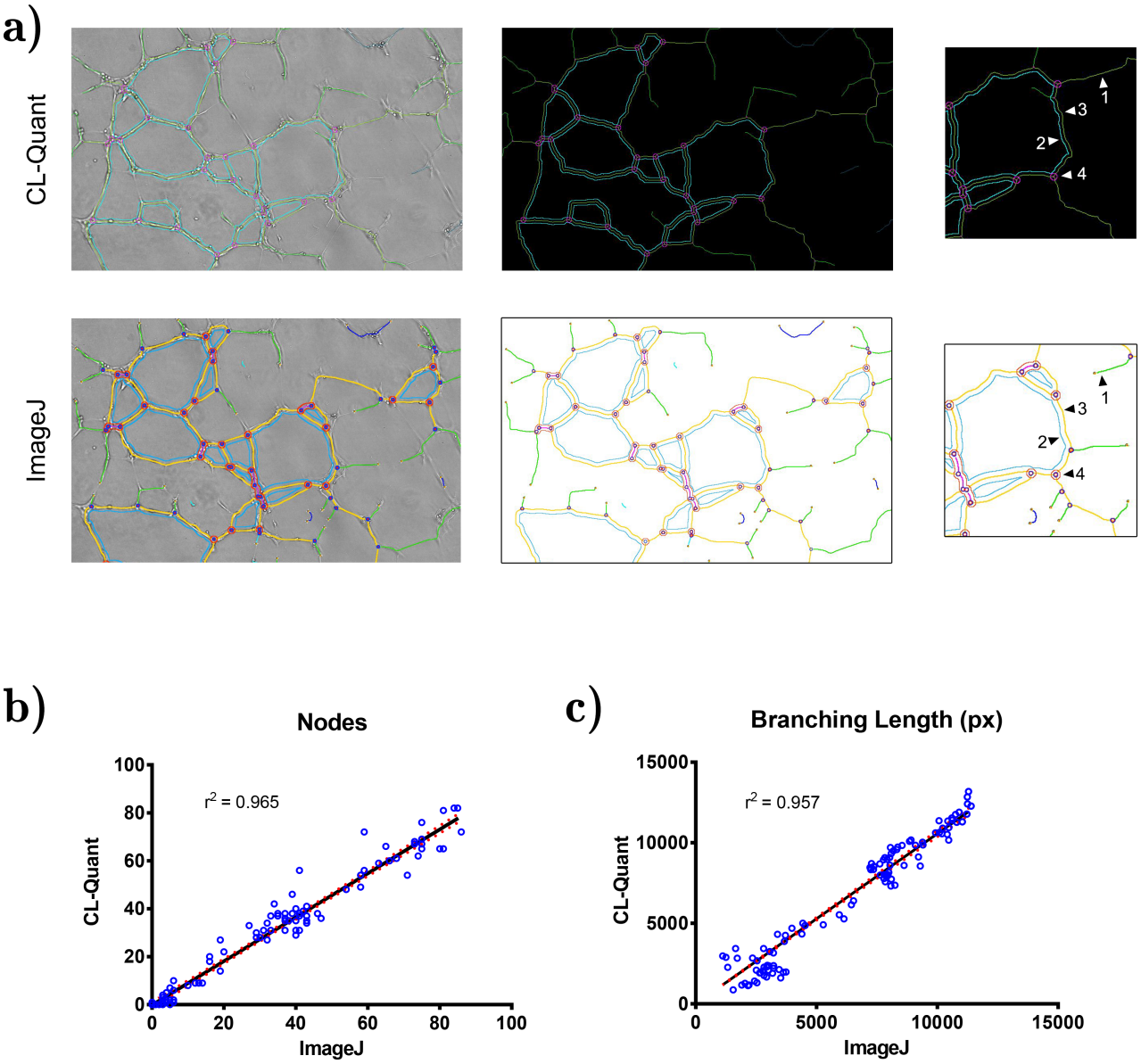

Figure 6.5: Comparative analysis of ImageJ Angiogenesis Analyzer plugin and CL-Quant software a) Analysis of the same image, left shows the original with overlay, middle shows the skeleton map, right displays a section of the image 1. extremity branch, 2. mesh loop, 3. branch between two nodes, 4. nodes. Regression plots of 125 images for b) Nodes and c) Branching length

were fewer branches and nodes. The slow degradation continued until 20 hours where there were only a few remaining branches observed.

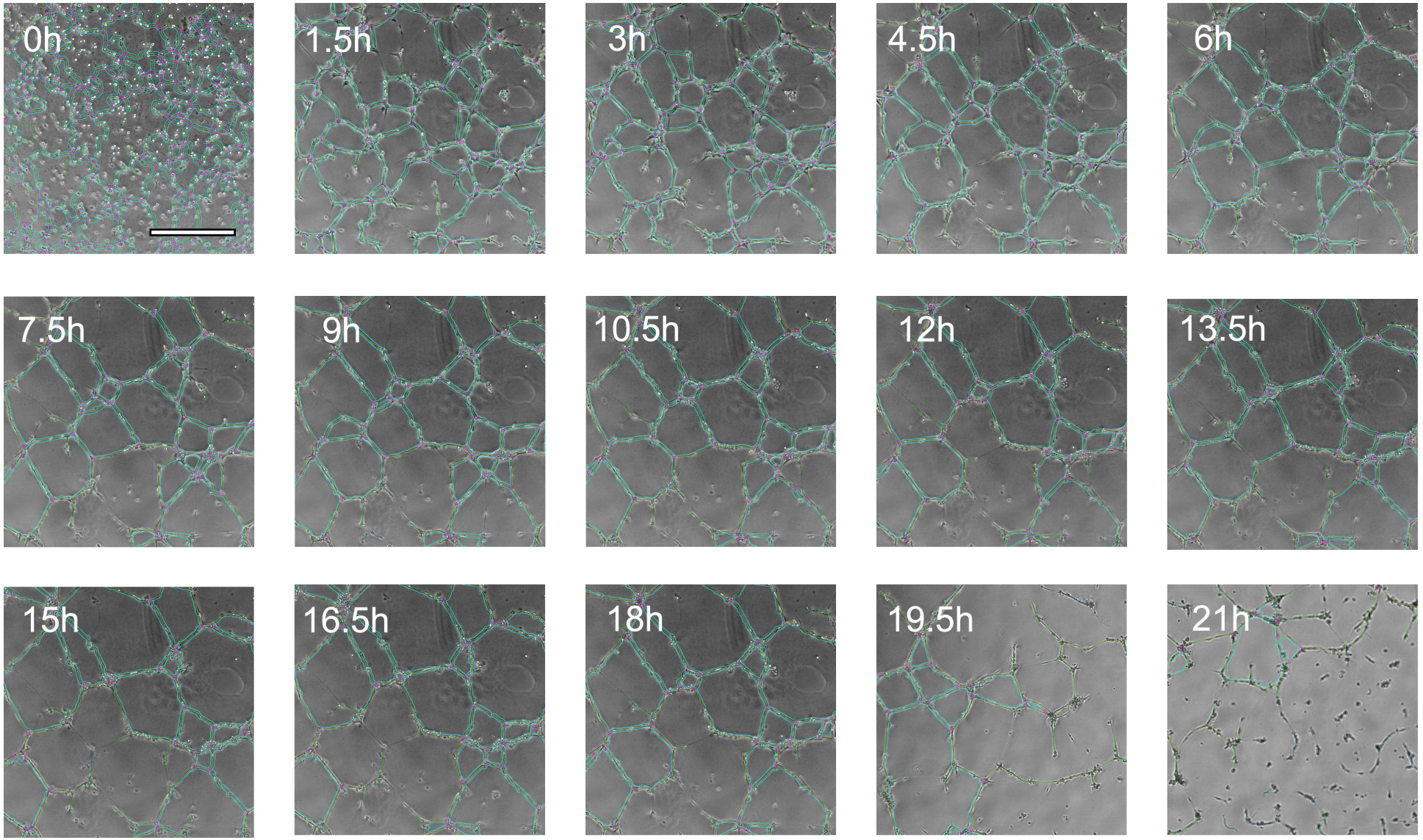

Figure 6.6: Representative time lapse imaging of HUVEC tube formation/degradation over 21 hours. Overlaid analysis showing tubes marked in blue and nodes marked in purple. Scale bar = 400μm

Once all images were collected they were then analysed via the CL-Quant software and plotted to show nodes or branching length. Figure 6.7 shows the plots of nodes (top) and branching length (bottom) for HUVEC tube formation from the M2 and M3 cell lines conditioned medium. The highest value for node or branch length at the time point is shown by either a dashed line (M3) or dotted line (M4).

For the M2 cell line, the number of nodes increased to 192 at 420 minutes, while for the M3 cell line the maximum nodes was 87 at 320 minutes. Similarly for branching length, the maximum shown by M2 was 8034 px at 400 minutes compared to M3 which gave a maximum of only 4679 px at 300 minutes. From the maximum value and time the rate of node/branch formation can be given by the following equations:

$$Rate of node formation = \frac{Nodes_{start} - Nodes_{end}}{Time_{minutes}} \tag{6.1}$$

$$Rate of branch formation = \frac{BranchLength_{start} - BranchLength_{end}}{Time_{minutes}} \tag{6.2}$$

From the example given in Figure 6.7, M3 cell line exhibited a node formation rate of 0.46 nodes/min whereas M4 cell line had a rate of 0.27 nodes/min. Likewise for branch length formation M3 had a rate of 20 px/min while M4 had a rate of 15.6 px/min.

In a similar manner the rate of degradation can also be calculated. For this the difference between the value at the maximum point and at the end of 24 hours was divided over the time. As such, it was found that the node degradation for M3 and M4 were -0.1 nodes/min and -0.05 nodes/min respectively. Branch degradation was similar in both lines at -2.27 px/min and -2.26 px/min respectively. However, as M3 had a higher starting value for nodes and branches the final values at the end of 24 hours were still higher than those of M4. Due to the differences of the starting value, comparing the degradation rate does not give a clear indication to the angiogenic potency but to the stability of the nodes and branches. This may correlate to *in vivo* stability however further investigation is required. As both values start at zero then comparing the formation rate up to the highest point

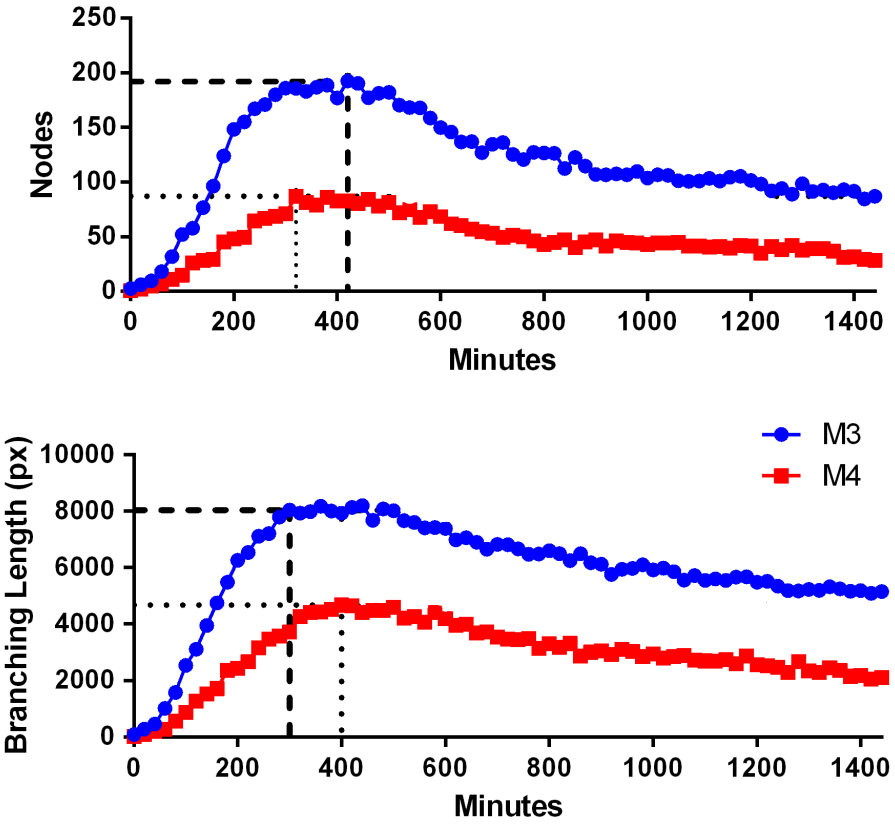

Figure 6.7: Example from a single sample showing rate of node formation from M3 (blue) and M4 (red) conditioned medium. Dashed lines show the maximum observed value from M3 cell line, dotted line from M4 cell line.

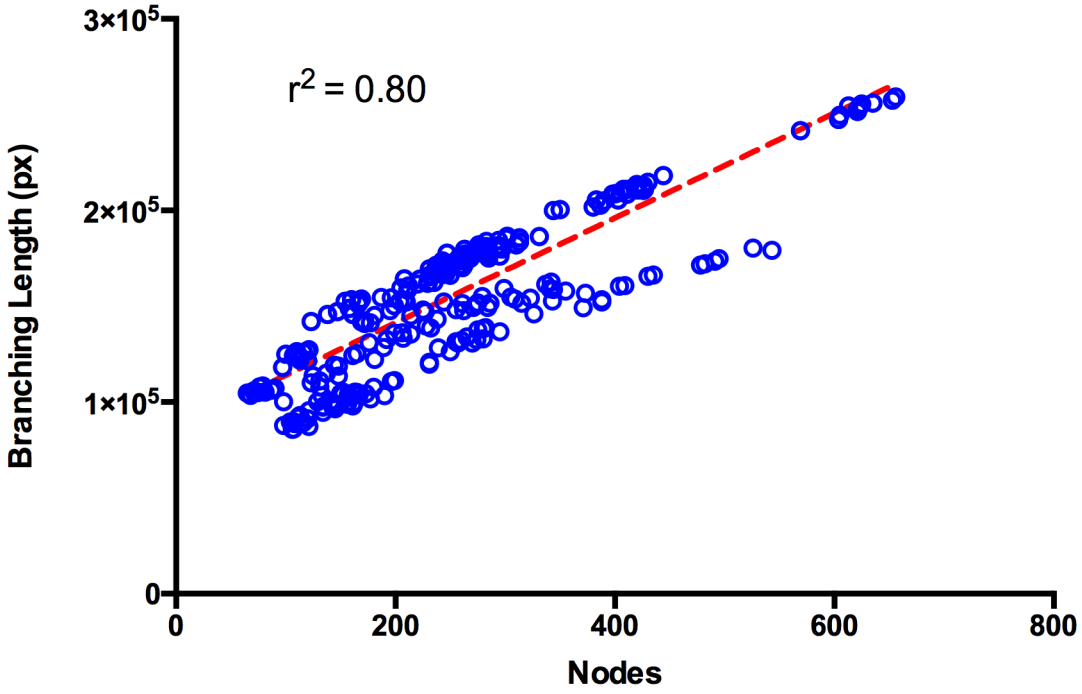

Figure 6.8: Correlation of branching length (px) to number of nodes. $r^2 = 0.80$. Sample of 375 images.

will be more indicative of potency, therefore for the remaining work the rate of formation will also be given.

Nodes represent the origin for branch formation, therefore as more nodes are formed the number of branches should increase and thus the total branching length should also increase. To test this theory a sample of 375 images were taken at peak formation, between 5 to 7 hours, and branch length was plotted against the number of nodes (Figure 6.8).

The r^2 value was 0.80, suggesting a moderately good correlation between the number of nodes and branching length. As both are important characteristics of angiogenesis and the mostly widely described in the literature, both aspects will be reported here (Bahramsoltani et al. 2009; DeCicco-Skinner et al. 2014). Other characteristics include mesh area (a loop of connecting networks of branches) and segments, however, these parameters are both dependent on nodes and branches.

Previous studies that have reported a similar assay to determine angiogenesis have anal-

ysed the cells after 12 hours (Shen et al. 2015), 16 hours (Hoch et al. 2012), or 24 hours (Bara et al. 2015). According to the results shown here, these time points will not be suitable as most of the branches would have degraded by then and any experimental differences would not be as pronounced. By examining the cells throughout formation it has been possible to gather a greater depth of data than previously reported and allowed for optimisation of the assay.

This study has also highlighted that the maximum formation time was approximately 5 to 6 hours following seeding makes this a rapid assay to determine hMSC angiogenic potency, an advantage previously discussed in Chapter 1.

6.2.4 Serum Free and Hypoxic Pre-Conditioning of hMSCs

hMSCs are generally cultured under 'normoxic' oxygen conditions (21% O_2 and 5% CO_2). However, *in vivo* the cells exist within a physiological perivascular niche and are subjected to a much lower (2-8% O_2) concentration that is thought to maintain the hMSCs in an undifferentiated state (Mohyeldin, Garzón-Muvdi, and Hinojosa 2010). Previous studies have shown that hypoxic pre-conditioning and culture of adipose-derived hMSCs were able to enhance the angiogenic potential by increased secretion of VEGF and other pro-angiogenic cytokines (Liu et al. 2013). Therefore investigations were undertaken to determine if hypoxic culture (5% O_2, 5% CO_2, supplemented with nitrogen) could enhance the angiogenic potency of bone-marrow derived hMSCs.

Serum is classically used in protein expression systems such as Chinese Hamster Ovary (CHO) cells and HEK 293 for maintenance and expansion. For protein production and purification the medium is then switched to serum-free formulations for ease of downstream purification. It was therefore tested to determine if culturing hMSCs without serum in basal medium could alter angiogenesis by increasing the secretion of pro-angiogenic cytokines/proteins.

hMSCs were cultured under either normoxic or hypoxic conditions in medium with or without serum for two consecutive passages. During the second passage the medium was harvested at 48 hours post exchange. The conditioned medium was then used to induce HUVEC tube formation.

Tube formation was tracked by imaging the cells every 20 minutes for 24 hours (Figure 6.9a and b) and analysed using the Angiogenesis Analyser plugin for Image J. Normoxic conditions were found to induce the highest number of nodes over time. The maximum number of nodes was 248 $\pm$ 37.61 and the branching length was found to be 10725 $\pm$ 541.2 px at 5 hours (300 minutes) (Figure 6.9c and d, blue bars). This finding also correlated to having the longest total branching length throughout the culture when compared to the other conditions. For node formation both the serum-free oxygen conditions showed the same number throughout (shown in green and purple) with no significant difference. However, the overall branching length was significantly longer in the normoxic condition (6213 $\pm$ 625.2px) at 5 hours when compared to hypoxic (1469 $\pm$ 339.1px). On the other hand, hypoxic serum-free conditions showed the shortest branching length, but was not found to be significantly different when serum was introduced.

The worst overall performing condition was seen with the hypoxic culture with serum. Node formation did not exceed the value of 45 and the branching length was the shortest (Figure 6.9a and c, red).

The serum-free media that was used in these studies comprised of DMEM supplemented with Ultra-Glutamine and without the addition of FBS. However, this formulation is not ideal for growth or expansion of hMSCs. Therefore, other fully defined serum-free media, such as StemPro MSC SFM (Invitrogen) or Mesencult-XF (StemCell Technologies) should be considered instead (Jung et al. 2012).

Taken together, these results showed that conditioned medium from standard culture conditions of hMSCs in normoxic culture with serum-containing media enabled HUVECs

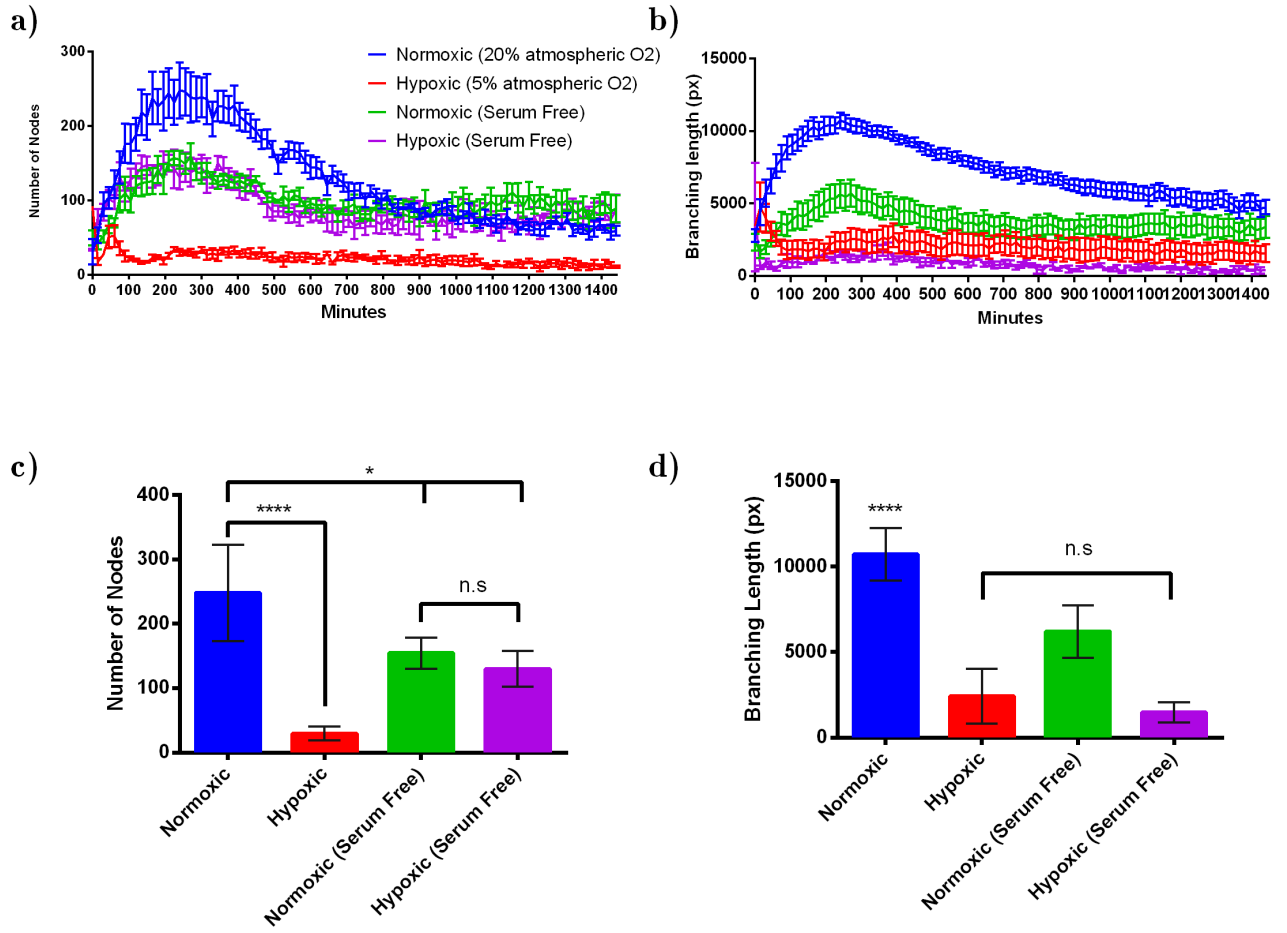

Figure 6.9: Node and total branching length from hMSC conditioned media cultured in normoxic (20% atmospheric O_2, blue), hypoxic (5% atmospheric O_2, red), normoxic (serum free) (green), and hypoxic (serum free) (purple) conditions. a) Number of nodes b) Total branching length c) Number of nodes at 5 hours of formation d) Total branching length at 5 hours of formation. All graph values presented as mean ± SEM (n = 4)

to effectively form tubules and retain them over time. The formation period was also recorded over 24 hours as the peak time may differ and imaging after 12 hours did not give a clear representation of the angiogenic properties of hMSC-CM (Figure 6.9a). Other culture parameters such as serum removal and low oxygen adversely affected the angiogenic potency of the hMSCs so will not be considered in the remaining experiments, however further studies are needed to fully explore these conditions.

The next experiments investigated the potency differences from the individual hMSC lines as previously done in Chapter 5. The *in vitro* age in terms of passage was also examined to determine if the potency changed as passage ages increased. As a result of the optimisation experiments performed, the following conditions were selected to be used further:

- GelTrex layer coating at 100%
- hMSC-CM from 48 hours of culture in normal conditions i.e. with serum at normoxic O_2 conditions
- HUVECs allowed to form for 24 hours and analysed via Nikon CL-Quant software

6.3 Angiogenic Properties of hMSCs

Following the optimisation of the assay parameters the angiogenic potency of the individual hMSCs lines was investigated. Conditioned media from M2, M3 and M4 cell lines between passage 3 to 7 was collected after 48 hours and stored at -20°C until use. By examining multiple lines across the *in vitro* age it may be possible to determine if there are differences in the angiogenic potency and if this changes with time in culture.

Figure 6.10 shows representative images of HUVEC tube formation at 6 hours following seeding. The analysis skeleton is overlaid over the original image. Clear differences in

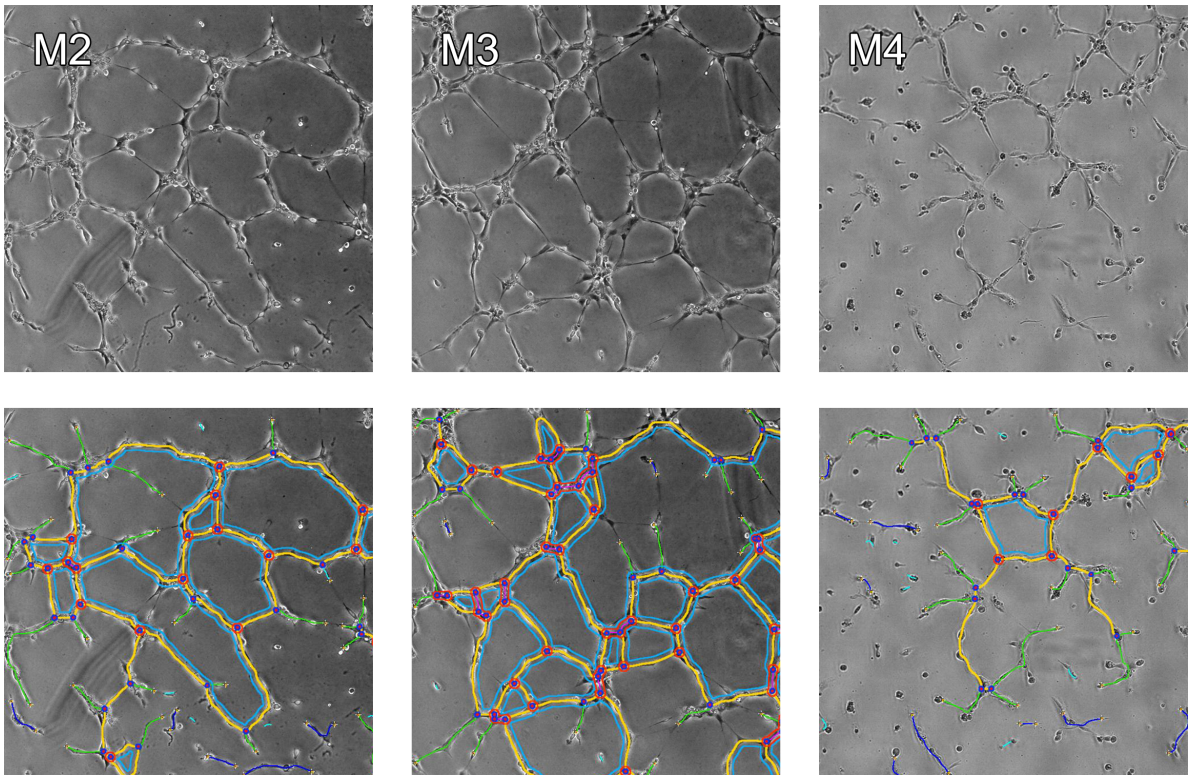

Figure 6.10: Visual comparison of HUVEC tube formation at 6 hours using hMSC conditioned medium from M2, M3, and M4. Top row: raw images; bottom row: analysis overlay

the angiogenic potency between the hMSC lines was observed. M3 cell line showed the most node appearance (purple dots) and the most number of connecting branches (yellow lines), thus giving a higher overall branching length. This also resulted in the largest mesh area shown in blue. Comparatively, M4 cell line showed the fewest number of nodes and branches, due to the lack of connecting points it displayed the most extremities and isolated branches, highlighted in dark blue.

The clear differences between the hMSCs lines warranted further investigation, therefore, the formation and degradation of HUVEC tubes were analysed over 24 hours using time lapse (Figure 6.12). Each graph represents an individual hMSC line with p3 (purple), p4 (blue), p5 (red), p6 (green) and p7 (orange) plotted as three separate lines. The top row shows the number of nodes, and the bottom row shows the total branching length. Some points at the start were omitted as they produced erroneous results.

M2 produced a maximum of 145 ± 14 nodes at p3, which increased at p4 and p5 where it produced a maximum of 562 ± 107 and 387 ± 70 nodes respectively. At p6 there was a significant reduction in the number of nodes with a maximum of 177 ± 21. Very few nodes were observed at p7 with an average of 7 nodes over 24 hours. A similar behaviour was also observed across all three hMSC lines employed. As such, M3 demonstrated the highest number of nodes at p4 with a maximum of 838 ± 177 at 420 minutes. A high number of nodes was also observed at p5 (820 ± 43) with the maximum number occurring early at 240 minutes. However, M4 produced the fewest number of nodes across all passages with the highest reaching 393 ± 33 at p4.

Similar patterns were seen in the total branching length where earlier passages showed longer tubes (Figure 6.11 bottom row). Across the passages, M2 showed similar tube lengths with the only significant difference at their maximum point between p4 (2.26x105 ± 3.61x103 px) and p6 (1.22x105 ± 2.50x103 px) at 440 minutes.

M3 showed the longest tube formation at p4 with a length of 2.88x105 ± 2.58x103 px, however it reduced over the next passages. Similarly to the nodes, M4 shows lower, consistent branching length across all passages (1.74x105 ± 1.5x104 px) except for p7 where the maximum observed length was 4.31x104 ± 1.2x102 px.

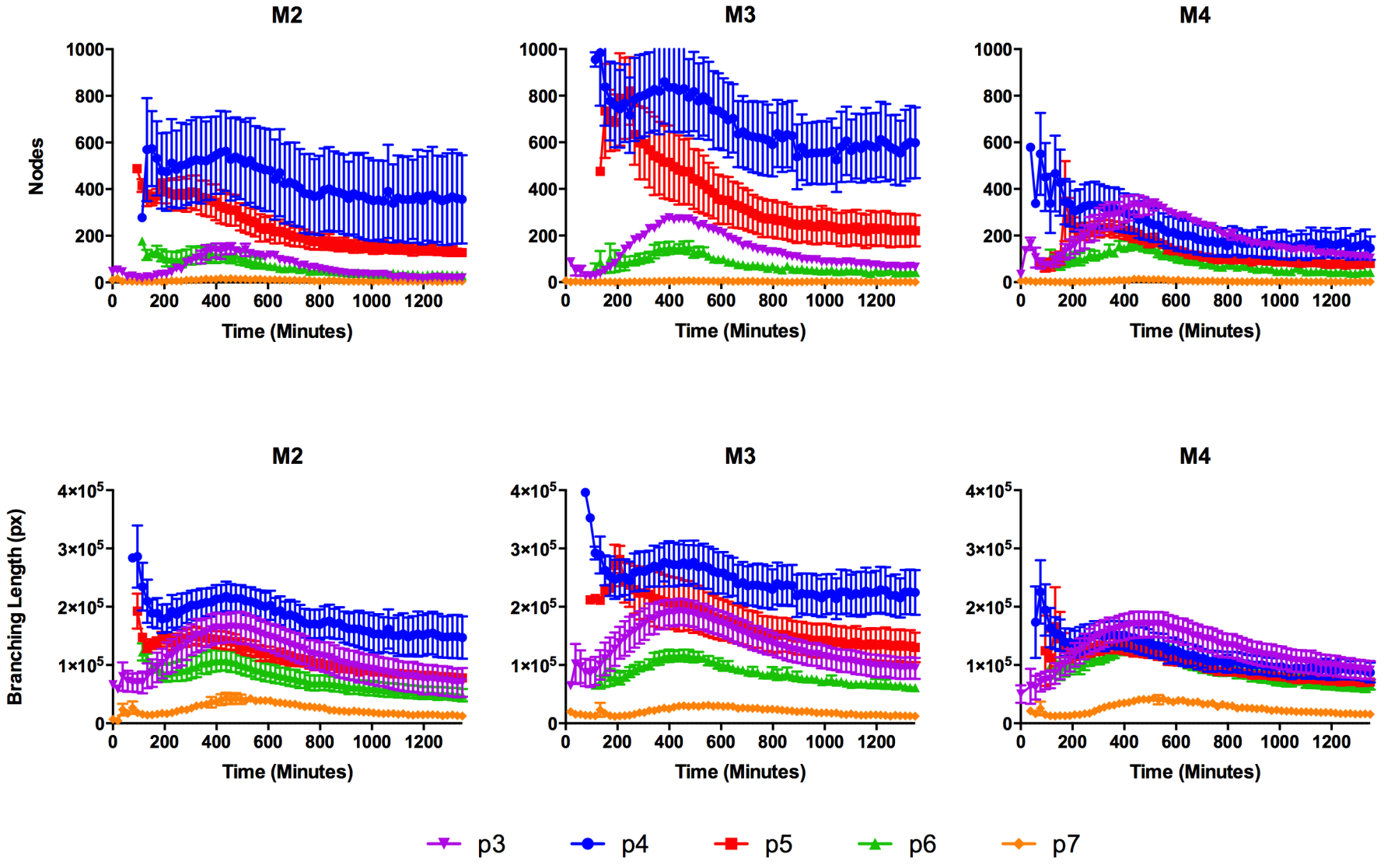

Figure 6.11: Comparison of number of nodes (top row) and total branching length (bottom row) over 24 hours (1440 minutes) for each hMSC line over 5 consecutive passages. Each line indicates a different passage. Values reported as mean ± SEM (n = 4)

Next, the plots were grouped on the basis of passage number to assess a comparison of the three different cells lines selected at the same time points. Figure 6.12 shows the same data but grouped based on passage number. At p3, M2 and M3 cell lines showed similar node formation characteristics were the same as the unconditioned medium control. However, M4 cell line developed fewer nodes when compared to the other lines. The branching length at p3 was the same for all conditions and not statistically different.

At p4 and p5, the differences were more apparent. M3 developed the most nodes and had the longer total branching length, which were significantly higher than M4 and the control. At p6, the loss of angiogenic potency was noticeable as all conditions produced fewer nodes and shorter total branches, when compared to p4 or p5. Finally, at p7, all the hMSC lines showed poor angiogenic potency as the maximum number of nodes and branching length were less than the control.

As before in Figure 6.7, the rate of node and tube formation was calculated per passage from zero minutes until the maximum value was reached (Figure 6.13). Node formation gives a clear indication to the differences in potency. At p4, M2 and M4 had the same node formation rate, 1.32 $\pm$ 0.40 nodes/min and 1.00 $\pm$ 0.28 nodes/min respectively. In contrast, M3 showed the fast rate at 2.40 $\pm$ 0.50 nodes/min. At p5, the rate for M4 decreases to 0.7 $\pm$ 0.11 nodes/min whereas M2 and M3 continued to show the same rates as before.

However, the differences in branch formation rate is less clear with significant differences only seen with M3 at p5 when compared to M2 and M4. The node and branching formation rate was the same for all lines at passages 6 and 7.

This assay offers the ability to determine the efficiency and rate of *in vitro* angiogenesis, and it is not possible with *in vivo* assays. Whilst not simulating the complete process, it demonstrates two main steps: the migration and the potential to differentiate into endothelial tubes. The data described here shows the potency of hMSC conditioned

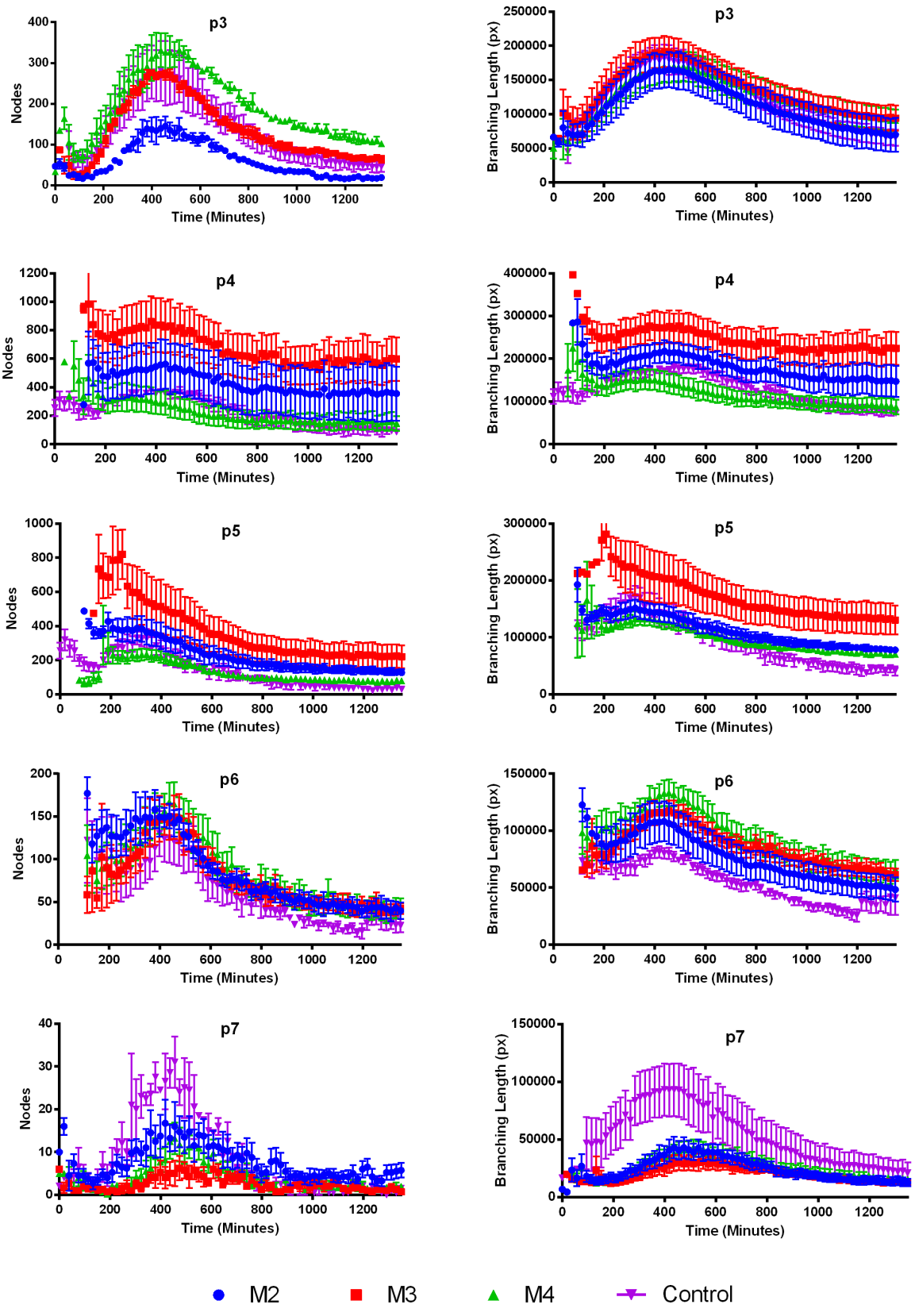

Figure 6.12: Number of nodes (left column) and total branching length (right column) for each passage. Each line represents a different hMSC line, M2 (blue), M3 (red), and M4 (green). Values reported as mean ± SEM (n = 4)

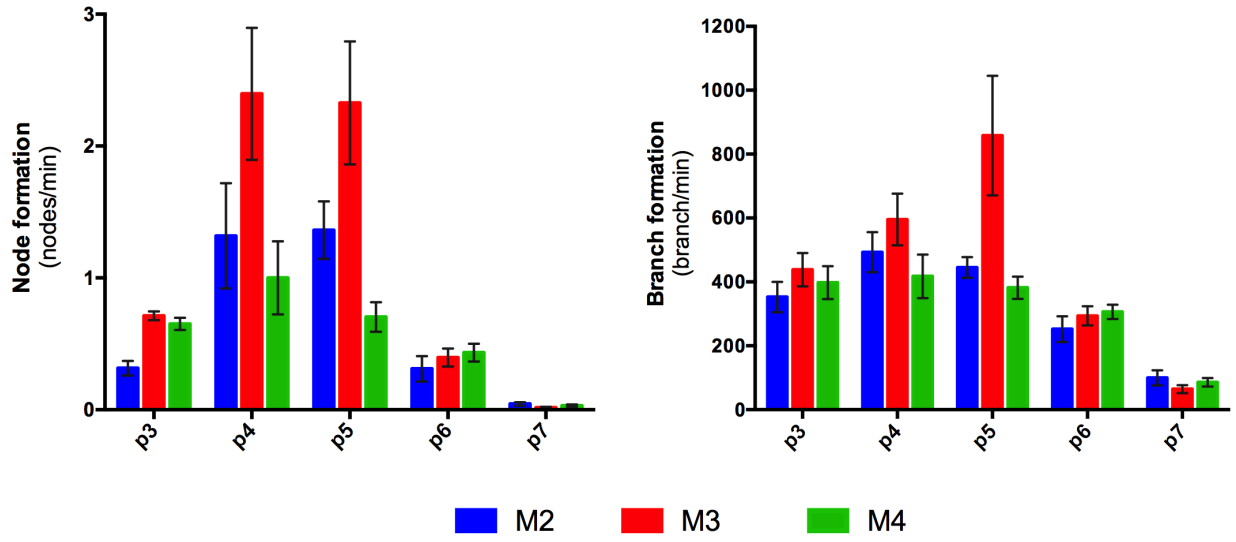

Figure 6.13: Rate of node and branch formation for hMSC lines. Values reported as mean ± SD (n = 4)

media to induce this effect. By using only spent/conditioned media to measure angiogenic potency, there is no requirement to harvest any cells. For a bioprocess this is an advantage as it is a non-invasive procedure that does not lose any product.

Significant differences were found not only between cell lines but also over multiple passages. M3 was found to be the most effective at inducing node formation at p4 and p5. This also correlated to the longest overall tube length, and is reflected in Figure 6.13 showing the higher rates during these passages.

Passage, or *in vitro* age, had the most profound effect on angiogenic potency. In all cases, later passages (p6 and p7) showed a significant reduction in the total number of nodes and branching length along with a reduction in formation rate. This decline in potency, and ultimately quality, suggests that for a more effective cell therapy, hMSCs at lower passages (p4 - 5) should be used.

6.4 Screening of Pro-Angiogenic Cytokines Produced by hMSCs

As conditioned medium from the hMSC lines was able to enhance angiogenesis in HUVECs there must be secreted products/cytokines present in the medium that causes this action. There is a growing body of evidence that transplanted hMSCs are able to produce soluble factors that contribute to cardiac repair and regeneration is one of the proteins of interest. (Gnecchi et al. 2008).

Next, known angiogenic proteins were screened and analysed using Luminex MAGPIX technology. VEGF, a potent mediator of angiogenesis which is know to induce growth of blood vessels and stimulate migration of endothelial cells (Ferrara, Gerber, and LeCouter 2003). Another protein of interest is hepatocyte growth factor (HGF), a regulator of cell growth, motility and morphogenesis, it was first identified as a mitogen for hepatocytes (Nakamura and Mizuno 2010). More recently, the specific receptor, c-met, was found on cardiac myocytes and studies have demonstrated its therapeutic use in treatment of cardiovascular diseases (Morishita et al. 2004). IL-8 is another member of the chemokine family and can induce endothelial cell proliferation and tube formation. It is also included one of the three cytokines in the Athersys Multistem QC tests for stroke treatment (Li et al. 2003; Lehman et al. 2012). Fibroblast growth factor (FGF), is acts in a similar way to VEGF by binding to tyrosine kinase receptors and mediating proliferation, migration and differentiation of endothelial cells. VEGF and FGF together act synergistically to promote angiogenesis (Cross and Claesson-Welsh 2001; Kano et al. 2005). Platelet derived growth factor (PDGF) is mitogenic in early developmental stages, while later in development it is involved in tissue remodelling for angiogenesis (Andrae, Gallini, and Betsholtz 2008).

The same multi-passage hMSC conditioned medium used to induce tube formation was used for this analysis. Results of the cytokine screen are shown in Figure 6.14, where the total concentration per ml is shown on the left and normalised per cell value is shown on

the right.

VEGF was the most highly secreted cytokine by all hMSC lines ranging from a total concentration of 329 ± 96.2pg/ml (M3 p3) to 647 ± 5.85 (M3 p6). The per cell production of VEGF remained constant over the passages by all cell lines with M3 only significantly higher at passages 4 and 7. Hung et al. (2007) reported concentrations between 250 - 100 pg/ml in cells cultured under normoxic conditions, but with an increase to 600 pg/ml when cultured in hypoxic conditions, which more closely reflects what is seen here. Kwon et al. (2014) reported VEGF concentrations from 336 - 428 pg/ml, slightly lower than the concentrations reported here. Through immunodepletion and re-addition, Lehman et al. (2012) found the minimum concentration of VEGF required for tube formation to be 34 pg/ml, much lower than the observed value here.

HGF was only found to be produced by M3 mostly during passages 3 to 5. The highest concentration occurred at passage 4 with 142.9 ± 4.16 pg/ml or 1.82 ± 0.00047 fg/cell. At passages 6 and 7 the concentration decreased to 27.1 ± 2.13 fg/cell and 15.4 ±1.51 fg/cell. On the other hand, M2 and M4 did not show any production of HGF throughout the experimental passages. This suggests that HGF secretion maybe donor specific, however Kwon et al. (2014) found concentrations ranging from 169 - 283 pg/ml across three hMSC donors. Furthermore, the production of HGF also correlated to the improved angiogenic potency as seen in Figure 6.11 suggesting that HGF may enhance potency alone or synergistically with another cytokine. Indeed, a previous study by Xin et al. (2001) found that the addition of both HGF and VEGF improved angiogenesis when compared to either growth factor alone.

M2 showed a steady decrease of IL-8 production from passage 3 to 7 in both the total and per cell concentration. On a per cell level, M3 produced the most throughout culture. Regardless of cell line, there was an increased production of IL-8 at passage 5. Similar to the results found here, Chen et al. (2014) found IL-8 at 240 pg/ml in conditioned medium and found an increase to 320 pg/ml when cultured in hypoxic conditions. As before,

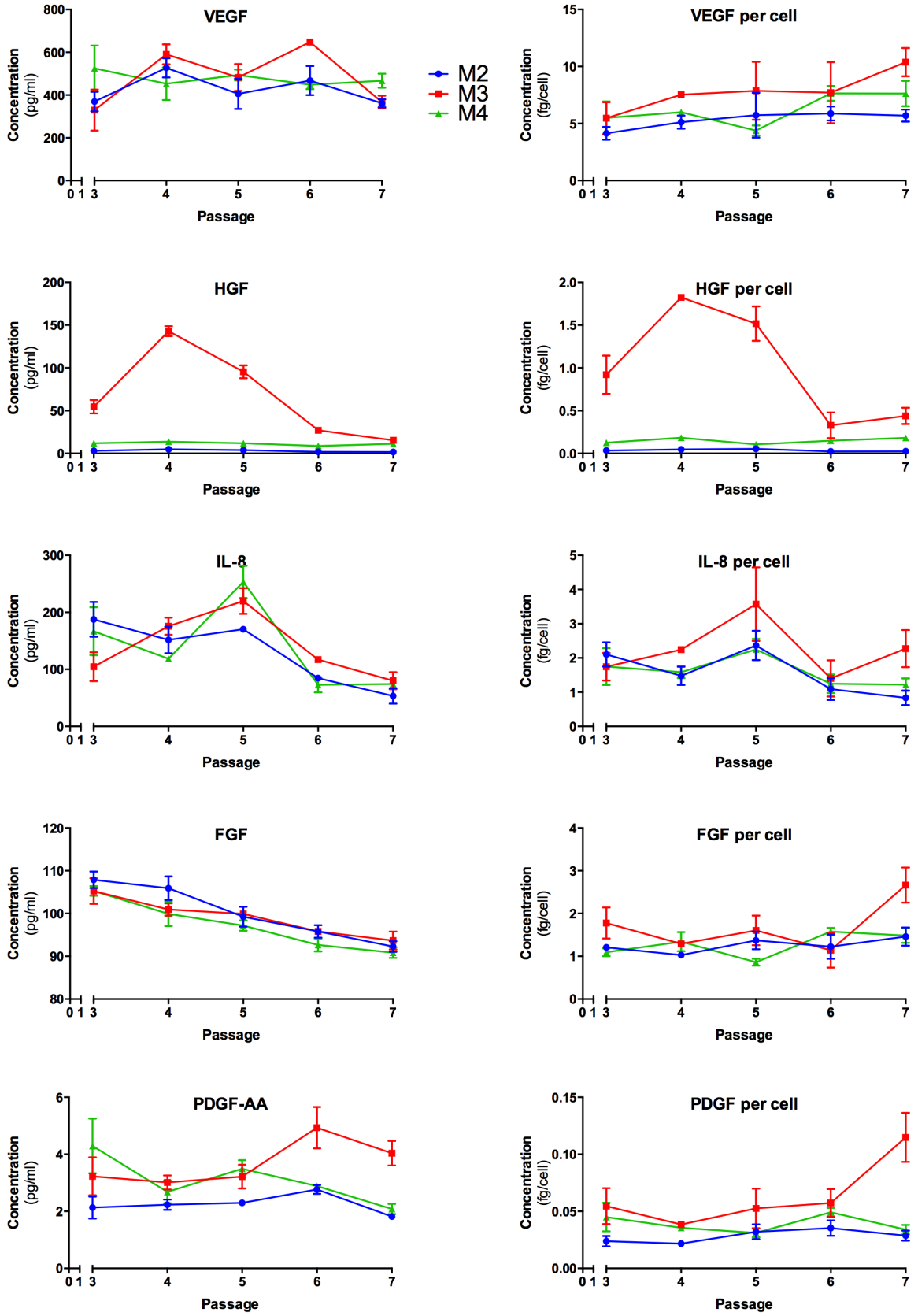

Figure 6.14: Cytokine screening results from hMSC lines: M2 (Blue), M3 (Red), and M4 (Green) from passage 3 to 7. Left column shows protein concentration in pg/ml, right column are results normalised to per cell. Values presented as mean ± SD (n = 4)

Lehman et al. (2012) found 112 pg/ml of IL-8 was the minimum concentration to induce tube formation. Along with VEGF and IL-8 these three cytokines form part of a surrogate potency assay that must be met for a pass/fail lot release of Athersys MultiStem MAPC product (Chapter 1, Section 1.6).

FGF was produced most consistently and equally by all hMSC lines throughout all culture points. At passage 3, the total concentration was not significantly different by M2 (107.9 $\pm$ 1.59 pg/ml), M3 (105.3 $\pm$ 2.47 pg/ml) or M4 (105.28 $\pm$ 0.933 pg/ml). There was a steady loss of overall total production over the passages at a rate of 2.77 $\pm$ 0.09 pg/passage seen across all three hMSC lines. When taken on a per cell basis the concentration remains steady throughout (1 - 2 fg/cell). The decline of total FGF was possibly due to the slower proliferation rate of cells at higher passages.

Finally, the concentration of PDGF was also measured. It was found that this cytokine was the lowest measured cytokine regardless of the cell line or passage number, ranging from 2 to 5 pg/ml. However, these values were registered below the lower limit of detection and any signal may be erroneous.

By using a high content screening technique, it was possible to compare the proangiogenic secretome from multiple hMSC lines. The results shown here were in agreement with previously published reports and identified HGF as a novel important factor that contributes to the angiogenic potency and further investigation is warranted. As postulated by Lehman et al. (2012), defining a panel of key angiogenic factors that could be measured in-line with manufacturing, will ensure the quality of the product is not adversely affected.

On the other hand, analysis of the hMSC secretome provides a non-destructive and reproducible method that could be applied for quality control and product manufacturing. Although the main clinical efficacy is attributed to the released cytokines it has also been shown that hMSCs could provide therapeutic effects through direct cell-cell interactions

and may warrant future investigations (Carrion et al. 2013; Pedersen et al. 2013).

6.5 Conclusions

The overall aims of this chapter was to develop a high-throughput assay to examine the angiogenic potency of hMSCs by using a HUVEC tube (vessel) formation method.

The first aims of this chapter was to evaluate the assay parameter and optimise the hMSC conditioned medium protocol. Initial experiments found that a basement membrane layer was required for HUVEC tube formation and it was enhanced in the presence of hMSC-CM. Further comparisons of basement membranes found GelTrex to be superior to another widely used alternative, Matrigel. Different conditioning protocols of hMSCs found regular culture conditions to be more effective than 20% dO_2 and serum-free cultures.

High-throughput technologies have emerged as a promising tool for basic and clinical investigations. Combining the Nikon Biostation CT and CL-Quant software provided an automated and accurate methodology to determine HUVEC tube formation from multiple hMSC line conditioned media. Novel data was thus generated for the formation and degradation of the HUVEC tube formation. Unlike previously described reports where the endothelial tube formation was only measured after 12-24 hours, this chapter highlights that at these time points the key metrics of nodes and branches have passed the optimal range and have noticeably degraded and thus are not as accurate as the methodology described here. The work here shows that the optimal time for observation is approximately 6 hours after seeding.

Next, conditioned medium from three individual hMSC donor lines were examined. It was found that M3, previously a poorer performing line in terms of growth rate (Chapter 3), was the best inducer of HUVEC tube formation when compared to the other tested

lines, M2 and M4. Further cytokine analysis revealed all lines secreted similar amounts of known pro-angiogenic cytokines except for M3 that produced HGF between passage 3 and 6. This correlated to the higher node and longer tube formation during these passages, therefore HGF may be an indicator of enhanced angiogenic potential.

High-content screening of the various cytokines has suggested HGF may be a key surrogate potency marker for angiogenesis due to its correlation to node formation. Likewise, VEGF was highly expressed throughout and is a known inducer of angiogenesis. In order to fully investigate the relationship of these proteins to the angiogenic potential of the hMSCs either knock-out or neutralisation antibody experiments could be performed to determine the key cytokines.

Chapter 7

Summary & Future Work

7.1 Summary

Cell therapy and regenerative medicine is the next significant development that will revolutionise modern healthcare. hMSCs are likely to play a large role in this success due to their proliferative potential and many areas of therapeutic application. With many late-stage clinical trials and treatments already taking place it is imperative the cells being administered are efficacious and will produce the desired outcome. Therefore, the aim of this thesis was to fully characterise multiple hMSCs lines then develop standardised potency assays that reflect the *in vivo* MoA.

Five individual donor hMSCs were isolated, expanded and characterised. Isolation was performed using their tissue culture plastic adherence properties and was successful in all five donors. From recent publications indicating a specific hMSC marker, isolation was also attempted using the low-affinity nerve growth factor receptor, CD271. However, after separation and flow cytometry analysis on thawed PBMCs there was no evidence of this marker on the samples tested here.

Next, more detailed characterisation was performed. Following isolation, the growth rate over five consecutive passages were compared. Here, M2 and M4 demonstrated a significantly higher growth rate when compared to the other three lines, when extrapolated and compared to current allogeneic therapies there were clear significant advantages of choosing a faster growing hMSC line due to the reduced number of days in continuous culture for a full treatment dose. Unsurprisingly, the faster growing lines also had greater glucose demands whilst also producing more metabolic waste products including lactate and ammonia. However, with the culture and medium exchange regime used in these experiments glucose or lactate concentrations did not approach inhibitory levels.

In accordance with the minimal criteria set by the ISCT to define an hMSC, tri-lineage differentiation into the adipogenic, osteogenic and chondroblast lineages was performed along with analysis of the canonical extracellular surface markers using a multiparameter flow cytometry technique developed in Chapter 4. All five hMSC were able to meet the minimal criteria. Table 7.1 summaries these characteristics.

Confirming cell identity/purity is a critical step for cell therapy regulations. Chapter 4 describes the method development of a multiparameter flow cytometry assay using the extracellular cell surface markers as suggested by the ISCT. This method allowed the simultaneous analysis of all markers on the same sample resulting in greater depth of information when compared to the more commonly used method of single marker analysis. From a practical standpoint the multiparameter method also provided savings in sample volume, reagent use, and time. This technique was then replicated on a different flow cytometry analyser and improved with further controls showing the method is transferable and adaptable.

Perhaps the most critical part developing a cell therapy is the quantification of the potency - a quantitative measure of the intended MoA. This will determine if the product will have a clinical benefit. The next two chapters in this thesis then went on develop potency assays that reflect their main clinical applications as identified by the trends in current clinical

Table 7.1: Summary of differentiation capability and cell surface marker expression of the five individual hMSC lines

hMSC line	Adpiocyte Differentiation	Chondrocyte Differentiation	Osteoblast Differenetiation	% complete surface marker expression profile
M1	Yes	Yes	Yes	98.87
M2	Yes	Yes	Yes	96.21
M3	Yes	Yes	Yes	98.19
M4	Yes	Yes	Yes	93.6
M5	Yes	Yes	Yes	98.14

trials.

For the remaining experiments, M2 and M4 hMSCs were chosen as 'good' quality lines as they both demonstrated rapid and consistent growth rates, whereas M3 was chosen as a poorer cell line due to its slower growth rate.

The immunosuppressive potency was first examined. Initially the cells were cultured under a chemically defined inflammatory environment using IFN-γ and TNF-α cytokines. Several factors such as IL-6 protein production; IDO gene expression and function; and metabolism were all compared over several passages as surrogate assays of suppression. In these conditions M4 produced the most IL-6, and M2 and M4 expressed the largest upregulation of IDO gene.

Next, the hMSCs were examined for their immunosuppressive capability by co-cultures with purified CD4+ T-cells. Initially, the hMSC:CD4 T-cell ratios, co-culture length and hMSC pre-treatment variables were first optimised. It was found that a 1:5 ratio was optimal as it allowed for accurate cell counting whereas higher ratios caused the T-cells to overtake the culture. Priming the hMSCs with IFN-γ to induce IDO expression did not have any significant effect on the suppression. When assessing the individual hMSC

lines, M4 showed the greatest amount of suppression when compared to M2 or M3. There was no difference in the amount of kynurenine produced although the concentrations were near the maximum level if there was full conversion of tryptophan in the medium. Another widely reported immunomodulatory assay is hMSC co-cultured with a mixed lymphocyte reaction (MLR). Under this system all hMSC lines showed the same level of suppression and amount of tryptophan to kynurenine conversion. They were also examined for their ability to induce a T-reg phenotype, M3 and M4 were found to induce a higher proportion of a CD4/CD25/FoxP3 expressing cells when compared to M2. With these results taken together it seems M4 is likely the better candidate for immunotherapies as it could effectively inhibit CD4 T-cell proliferation and induce a T-reg phenotype in MLRs. Table 7.2 summaries the immunomodulatory characteristics of the hMSCs and shows overall M4 performed better under the inflammatory conditions when compared to M2 and M3.

Angiogenesis is a key factor in the treatment of many cardiovascular diseases in including myocardial infarction and ischaemia. In a separate assay the hMSCs were examined for their pro-angiogenic effect using conditioned medium to induce HUVEC endothelial to tube (capillary) formation. By using time-lapse imaging over 24 hours it was possible to observe the tube formation and degradation, and quantify the results using image analysis software. In contrast to current literature that observe the cells after 24 hours, the data shown here shows the most tube formation occurs within 4 to 6 hours following plating.

Having identified the key factors for efficient angiogenesis and analysis, conditioned medium from the three hMSCs lines over several passages were examined in this potency assay. Whilst conditioned medium from all three lines was able to induce tube formation, M3 induced more nodes and a longer overall tube length when compared to M2 and M4. This effect was most noticeable in earlier passages as in later passages (p6-7) there was a significant decrease in both nodes and tube length from all hMSC lines. This suggests that the potency of hMSCs is greater in younger *in vitro* cells. As this work was conducted

on conditioned medium, this was then analysed for known pro-angiogenic cytokines. Unsurprisingly there was a high concentration of VEGF, FGF and IL-8 which are known to be secreted by hMSCs. Additionally M3 was found to produce HGF which correlated to its greater node and tube length formation suggesting this protein could be used to as a surrogate marker for angiogenesis. Table 7.3 summaries the key pro-angiogenic aspects of hMSCs and shows M3 outperformed M2 and M4 in all angiogenic potency assays.

In summary, this thesis shows the successful characterisation of five individual hMSC lines that all meet the ISCT minimal criteria, however, functionally they are significantly different. By examining the same cells under two different potency assays M4 was found to be the better cell line for immunosuppression and modulation. Whereas, M3 hMSCs, a line that was used as a 'poorer' quality line due to its slower growth rate was found to be the better inducer of angiogenesis. This shows that a 'one-fits-all' approach for hMSC allogeneic therapies is not appropriate and there must be a comparison into the potency for an effective treatment.

Table 7.2: Summary of immunomodulatory characteristics of the hMSC lines in Chapter 5, blue highlighted cells indicate the best performer

hMSC line	Maximum HLA-DR Expression	IL-6 Yield (pg/cell)	Kynurenine Concentration (nM/cell)	Fold increase IDO Expression (p3 D2)	% CD4 T-Cell proliferation inhibition	% Induction of T-reg
M1						
M2	94.55 ± 0.7	0.15 ± 0.01	0.015 ± 0.002	108848.3	75.9 ± 5.7	5.4 ± 0.98
M3	82.78 ± 2.9	0.18 ± 0.02	0.011 ± 0.004	756.6	69.9 ±2.5	21.2 ± 9.12
M4	10.67 ± 1.63	0.79 ± 0.07	0.013 ± 0.004	182803.3	87.2 ± 1.5	16.1 ± 3.6
M5						

Table 7.3: Summary of pro-angiogenic characteristics of the hMSC lines in Chapter 6, blue highlighted cells indicate the best performer

hMSC line	Maximum Node formed (p5)	Maximum Branch length (p5)	HGF production (fg/cell, p5)
M1			
M2	387.5 ± 140	149270 ± 30785	0.05 ± 0.009
M3	593.8 ± 106.8	223936 ± 89625	1.52 ± 0.2
M4	227.3 ± 70.65	128844 ± 22693	0.11 ± 0.01
M5			

7.2 Future Work

This thesis has started with the aim to develop standardised and robust assays to measure hMSCs quality and potency as defined by their MoA as a cell therapy. This aspect is just one part of a larger development process.

- The work in this thesis uses hMSCs that were cultured in medium containing fetal bovine serum (FBS). With advances in traditional bioprocess and cell culture there is an increasing use of serum-free and other chemically defined media. Currently there is no study into the effect of serum-free or chemically defined medium on the potency or efficacy of hMSCs. Therefore a comparison of hMSCs cultured in serum-containing and serum-free media in terms of potency would provide an indication into the utility of such media.

- The effect of cryopreservation on the potency of hMSC was only briefly examined. Chapter 5, Figure 5.13 showed that DMSO exposure did not affect the immuno-suppressive properties hMSCs on CD4 T-cells by way of overall cell counts, but the conversion of tryptophan to kynurenine was significantly lower than control hMSCs. This could be explored further by comparing freshly thawed cells to those in culture and to cells which have never been cryopreserved. The same principal can also be implemented in the angiogenesis assay in Chapter 6

- Microcarrier-based expansion within a stirred tank bioreactor is a promising method to gain the required number of hMSCs for a cell therapy treatment. This change in culture method may affect the quality and potency, therefore, both the immuno-suppression and angiogenesis assay can be used before, during, and after expansion to determine if the potency changes. Therefore, these assays could be deployed alongside the bioprocess manufacturing stage as quality control checks.

- For the angiogenic assay, the cytokines were screened from hMSC conditioned

medium and correlated to the potency. Future studies can look at selectively removing these cytokines via antibody deletion to determine the critical cytokines that lead to the tube/capillary formation.

This thesis has presented ways to characterise hMSCs based upon their extracellular surface markers, immunosuppressive potential and angiogenic potency. Continuing to develop these potency assays and implement them into a manufacturing process will be key to producing a successful cell therapy.

References

Acosta, María Lourdes, Asterio Sánchez, Francisco García, Antonio Contreras, and Emilio Molina (2007). "Analysis of kinetic, stoichiometry and regulation of glucose and glutamine metabolism in hybridoma batch cultures using logistic equations". In: *Cytotechnology* 54.3, pp. 189–200.

Adewumi, Oluseun, Behrouz Aflatoonian, Lars Ahrlund-Richter, Michal Amit, Peter W Andrews, Gemma Beighton, Paul A Bello, Nissim Benvenisty, Lorraine S Berry, Simon Bevan, Barak Blum, Justin Brooking, Kevin G Chen, Andre B H Choo, Gary A Churchill, Marie Corbel, Ivan Damjanov, Jon S Draper, Petr Dvorak, Katarina Emanuelsson, Roland A Fleck, Angela Ford, Karin Gertow, Marina Gertsenstein, Paul J Gokhale, Rebecca S Hamilton, Ales Hampl, Lyn E Healy, Outi Hovatta, Johan Hyllner, Marta P Imreh, Joseph Itskovitz-Eldor, Jamie Jackson, Jacqueline L Johnson, Mark Jones, Kehkooi Kee, Benjamin L King, Barbara B Knowles, Majlinda Lako, Franck Lebrin, Barbara S Mallon, Daisy Manning, Yoav Mayshar, Ronald D G Mckay, Anna E Michalska, Milla Mikkola, Masha Mileikovsky, Stephen L Minger, Harry D Moore, Christine L Mummery, Andras Nagy, Norio Nakatsuji, Carmel M OBrien, Steve K W Oh, Cia Olsson, Timo Otonkoski, Kye-Yoon Park, Robert Passier, Hema Patel, Minal Patel, Roger Pedersen, Martin F Pera, Marian S Piekarczyk, Renee A Reijo Pera, Benjamin E Reubinoff, Allan J Robins, Janet Rossant, Peter Rugg-Gunn, Thomas C Schulz, Henrik Semb, Eric S Sherrer, Henrike Siemen, Glyn N Stacey, Miodrag Stojkovic, Hirofumi Suemori, Jin Szatkiewicz, Tikva Turetsky, Timo Tuuri, Steineke van den Brink, Kristina Vintersten, Sanna Vuoristo, Dorien Ward, Thomas A Weaver, Lesley A Young,

and Weidong Zhang (2007). “Characterization of human embryonic stem cell lines by the International Stem Cell Initiative”. In: *Nat Biotechnol* 25.7, pp. 803–816.

Adusumilli, P. S., L. Cherkassky, J. Villena-Vargas, C. Colovos, E. Servais, J. Plotkin, D. R. Jones, and M. Sadelain (2014). “Regional delivery of mesothelin-targeted CAR T cell therapy generates potent and long-lasting CD4-dependent tumor immunity”. In: *Science Translational Medicine* 6.261, 261ra151–261ra151.

Agata, Hideki, Nobukazu Watanabe, Yumiko Ishii, Noriyuki Kubo, Satoshi Ohshima, Mika Yamazaki, Arinobu Tojo, and Hideaki Kagami (2009). “Feasibility and efficacy of bone tissue engineering using human bone marrow stromal cells cultivated in serum-free conditions.” In: *Biochemical and biophysical research communications* 382.2, pp. 353–8.

Akiyama, Kentaro, Chider Chen, DanDan Wang, Xingtian Xu, Cunye Qu, Takayoshi Yamaza, Tao Cai, WanJun Chen, Lingyun Sun, and Songtao Shi (2012). “Mesenchymal-stem-cell-induced immunoregulation involves FAS-ligand-/FAS-mediated T cell apoptosis.” In: *Cell stem cell* 10.5, pp. 544–55.

Alper, Joe (2009). “Geron gets green light for human trial of ES cell derived product”. In: *Nat Biotechnol* 27.3, pp. 213–214.

Alsalameh, Saifeddin, Rayya Amin, Takefumi Gemba, and Martin Lotz (2004). “Identification of mesenchymal progenitor cells in normal and osteoarthritic human articular cartilage”. In: *Arthritis & Rheumatism* 50.5, pp. 1522–1532.

Alvarez-Viejo, M (2013). “LNGFR (CD271) as Marker to Identify Mesenchymal Stem Cells from Different Human Sources: Umbilical Cord Blood, Wharton’s Jelly and Bone Marrow”. In: *J Bone Marrow ...* 1.4, pp. 1–6.

Andrae, Johanna, Radiosa Gallini, and Christer Betsholtz (2008). “Role of platelet-derived growth factors in physiology and medicine”. In: pp. 1276–1312.

Ankrum, James a, Joon Faii Ong, and Jeffrey M Karp (2014). “Mesenchymal stem cells: immune evasive, not immune privileged.” In: *Nature biotechnology* 32.3, pp. 252–60.

Ankrum, James A., Riddhi G. Dastidar, Joon Faii Ong, Oren Levy, and Jeffrey M. Karp (2014). “Performance-enhanced mesenchymal stem cells via intracellular delivery of steroids”. In: *Sci. Rep.* 4.

Arnaoutova, Irina and Hynda K Kleinman (2010). "In vitro angiogenesis: endothelial cell tube formation on gelled basement membrane extract". In: *Nat Protoc* 5.4, pp. 628–635.

Asari, Sadaki, Shin Itakura, Kevin Ferreri, Chih-Pin Liu, Yoshikazu Kuroda, Fouad Kandeel, and Yoko Mullen (2009). "Mesenchymal stem cells suppress B-cell terminal differentiation". In: *Experimental Hematology* 37.5, pp. 604–615.

Ascheim, D. D., A. C. Gelijns, D. Goldstein, L. A. Moye, N. Smedira, S. Lee, C. T. Klodell, A. Szady, M. K. Parides, N. O. Jeffries, D. Skerrett, D. A. Taylor, J. E. Rame, C. Milano, J. G. Rogers, J. Lynch, T. Dewey, E. Eichhorn, B. Sun, D. Feldman, R. Simari, P. T. OGara, W. C. Taddei-Peters, M. A. Miller, Y. Naka, E. Bagiella, E. A. Rose, and Y. J. Woo (2014). "Mesenchymal Precursor Cells as Adjunctive Therapy in Recipients of Contemporary Left Ventricular Assist Devices". In: *Circulation* 129.22, pp. 2287–2296.

Atala, A. (2011). "Tissue engineering of human bladder". In: *British Medical Bulletin* 97.1, pp. 81–104.

Attar, A., A. Ghalyanchi Langeroudi, A. Vassaghi, I. Ahrari, M. K. Maharlooei, and A. Monabati (2013). "Role of CD271 enrichment in the isolation of mesenchymal stromal cells from umbilical cord blood". In: *Cell Biol. Int.* 37.9, pp. 1010–1015.

Auerbach, Robert, Rachel Lewis, Brenda Shinners, Louis Kubai, and Nasim Akhtar (2003). "Angiogenesis assays: A critical overview". In: *Clinical Chemistry* 49, pp. 32–40.

Autissier, Patrick, Caroline Soulas, Tricia H. Burdo, and Kenneth C. Williams (2010). "Evaluation of a 12-color flow cytometry panel to study lymphocyte, monocyte, and dendritic cell subsets in humans". In: *Cytometry* 9999A, NA–NA.

Bahr, Lena Von, Berit Sundberg, L Lena, Birgitta Sander, Holger Karbach, H Hans, Per Ljungman, Britt Gustafsson, Helen Karlsson, Tbi-based Mac, and Busulfan-based Mac (2007). "Long-Term Complications , Immunologic Effects , and Role of Passage for Outcome in Mesenchymal Stromal Cell Therapy". In: pp. 557–564.

Bahramsoltani, Mahtab, Johanna Plendl, Pawel Janczyk, Pia Custodis, and Sabine Kaessmeyer (2009). "Quantitation of angiogenesis and antiangiogenesis in vivo, ex vivo and in

vitro - an overview." In: *ALTEX : Alternativen zu Tierexperimenten* 26.March, pp. 95–107.

Banchereau, Jacques and Ralph M. Steinman (1998). In: *Nature* 392.6673, pp. 245–252.

Bara, Jennifer J., Sarah Turner, Sally Roberts, Gareth Griffiths, Rod Benson, Jayesh M. Trivedi, and Karina T. Wright (2015). "High content and high throughput screening to assess the angiogenic and neurogenic actions of mesenchymal stem cells in vitro". In: *Experimental Cell Research*.

Bartholomew, A., C. Sturgeon, M. Siatskas, K. Ferrer, K. McIntosh, S. Patil, W. Hardy, S. Devine, D. Ucker, R. Deans, A. Moseley, and R. Hoffman (2002). "Mesenchymal stem cells suppress lymphocyte proliferation in vitro and prolong skin graft survival in vivo". In: *Exp. Hematol.* 30.1, pp. 42–48.

Basford, Christina, Nico Forraz, and Colin McGuckin (2010). "Optimized multiparametric immunophenotyping of umbilical cord blood cells by flow cytometry". In: *Nat Protoc* 5.7, pp. 1337–1346.

Basu, Joydeep and John W Ludlow (2014). "Cell-based therapeutic products: potency assay development and application." In: *Regenerative medicine* 9.4, pp. 497–512.

Baumgart, Daniel C and William J Sandborn (2012). "Crohn's disease". In: *The Lancet* 380.9853, pp. 1590–1605.

Benvenuto, Federica, Stefania Ferrari, Ezio Gerdoni, Francesca Gualandi, Francesco Frassoni, Vito Pistoia, Gianluigi Mancardi, and Antonio Uccelli (2007). "Human mesenchymal stem cells promote survival of T cells in a quiescent state." In: *Stem cells (Dayton, Ohio)* 25.7, pp. 1753–60.

Blanc, K Le, H Samuelsson, B Gustafsson, M Remberger, B Sundberg, J Arvidson, P Ljungman, H Lönnies, S Nava, and O Ringdén (2007). "Transplantation of mesenchymal stem cells to enhance engraftment of hematopoietic stem cells". In: *Leukemia* 21.8, pp. 1733–1738.

Blimkie, Darren, Edgardo S Fortuno, Francis Thommai, Lixin Xu, Elaine Fernandes, Juliet Crabtree, Annie Rein-Weston, Kirstin Jansen, R R Brinkman, and Tobias R Kollmann (2010). "Identification of B cells through negative gating-An example of the MIFlowCyt

standard applied." In: *Cytometry. Part A : the journal of the International Society for Analytical Cytology* 77.6, pp. 546–51.

Bloom, Debra D, John M Centanni, Neehar Bhatia, Carol A Emler, Diana Drier, Glen E Leverson, David H Mckenna, Adrian P Gee, Robert Lindblad, Derek J Hei, and Peiman Hematti (2015). "A reproducible immunopotency assay to measure mesenchymal stromal cell e mediated T-cell suppression". In: *Journal of Cytotherapy* 17.2, pp. 140–151.

Bonab, Mandana Mohyeddin, Kamran Alimoghaddam, Fatemeh Talebian, Syed Hamid Ghaffari, Ardeshir Ghavamzadeh, and Behrouz Nikbin (2006). "Aging of mesenchymal stem cell in vitro." In: *BMC cell biology* 7, p. 14.

Bonin, M von, F St Olzel, A Goedecke, K Richter, N Wuschek, K Holig, U Platzbecker, T Illmer, M Schaich, J Schetelig, A Kiani, R Ordemann, G Ehninger, M Schmitz, and M Bornhauser (2008). "Treatment of refractory acute GVHD with third-party MSC expanded in platelet lysate-containing medium". In: *Bone Marrow Transplant* 43.3, pp. 245–251.

Bravery, Christopher a, Jessica Carmen, Timothy Fong, Wanda Oprea, Karin H Hoogendoorn, Juliana Woda, Scott R Burger, Jon a Rowley, Mark L Bonyhadi, and Wouter Van't Hof (2013). "Potency assay development for cellular therapy products: an ISCT review of the requirements and experiences in the industry." In: *Cytotherapy* 15.1, pp. 9–19.

Breier, G. (2000). "Angiogenesis in Embryonic Development A Review". In: *Placenta* 21, S11–S15.

Brindley, David a, Natasha L Davie, Emily J Culme-Seymour, Chris Mason, David W Smith, and Jon a Rowley (2012). "Peak serum: implications of serum supply for cell therapy manufacturing." In: *Regenerative medicine* 7.1, pp. 7–13.

Bronckaers, Annelies, Petra Hilkens, Wendy Martens, Pascal Gervois, Jessica Ratajczak, Tom Struys, and Ivo Lambrichts (2014). "Mesenchymal stem/stromal cells as a pharmacological and therapeutic approach to accelerate angiogenesis". In: *Pharmacology and Therapeutics* 143.2, pp. 181–196.

Bunnell, B, M FLAAT, C GAGLIARDI, B PATEL, and C RIPOLL (2008). "Adipose-derived stem cells: Isolation, expansion and differentiation". In: *Methods* 45.2, pp. 115–120.

Campioni, Diana, Roberta Rizzo, Marina Stignani, Loredana Melchiorri, Luisa Ferrari, Sabrina Moretti, Antonio Russo, Gian Paolo Bagnara, Laura Bonsi, Francesco Alviano, Giacomo Lanzoni, Antonio Cuneo, Olavio R. Baricordi, and Francesco Lanza (2009). "A decreased positivity for CD90 on human mesenchymal stromal cells (MSCs) is associated with a loss of immunosuppressive activity by MSCs". In: *Cytometry Part B - Clinical Cytometry* 76.3, pp. 225–230.

Caplan, A. I. (1991). "Mesenchymal stem cells". In: *J. Orthop. Res.* 9.5, pp. 641–650.

Caplan, Arnold I. (2008). "All MSCs Are Pericytes?" In: *Cell Stem Cell* 3.3, pp. 229–230.

Caplan, Arnold I. and Diego Correa (2011). "The MSC: An Injury Drugstore". In: *Cell Stem Cell* 9.1, pp. 11–15.

Caplan, Arnold I and James E Dennis (2006). "Mesenchymal stem cells as trophic mediators." In: *Journal of cellular biochemistry* 98.5, pp. 1076–84.

Carmen, Jessica, Scott R Burger, Michael McCaman, and Jon a Rowley (2012). "Developing assays to address identity, potency, purity and safety: cell characterization in cell therapy process development." In: *Regenerative medicine* 7.1, pp. 85–100.

Carrion, Bita, Yen P. Kong, Darnell Kaigler, and Andrew J. Putnam (2013). "Bone marrow-derived mesenchymal stem cells enhance angiogenesis via their integrin receptor". In: *Experimental Cell Research* 319.19, pp. 2964–2976.

Chan, Jennifer L, Katherine C Tang, Anoop P Patel, Larissa M Bonilla, Nicola Pierobon, Nicholas M Ponzio, and Pranela Rameshwar (2006). "Antigen-presenting property of mesenchymal stem cells occurs during a narrow window at low levels of interferon-gamma." In: *Blood* 107.12, pp. 4817–24.

Chen, Lei, Yingbin Xu, Jingling Zhao, Zhaoqiang Zhang, Ronghua Yang, Julin Xie, Xusheng Liu, and Shaohai Qi (2014). "Conditioned Medium from Hypoxic Bone Marrow-Derived Mesenchymal Stem Cells Enhances Wound Healing in Mice". In: *PLoS ONE* 9.4. Ed. by Maurizio Pesce, pp. 96–161.

Chevalier, Fabien, Mélanie Lavergne, Elisa Negroni, Ségolène Ferratge, Gilles Carpentier, Marie Gilbert-Sirieix, Fernando Siñeriz, Georges Uzan, and Patricia Albanese (2014). "Glycosaminoglycan mimetic improves enrichment and cell functions of human endothelial progenitor cell colonies". In: *Stem Cell Research* 12.3, pp. 703–715.

Chullikana, Anoop, Anish Sen Majumdar, Sanjay Gottipamula, Sagar Krishnamurthy, a Sreenivas Kumar, V S Prakash, and Pawan Kumar Gupta (2014). "Randomized, double-blind, phase I/II study of intravenous allogeneic mesenchymal stromal cells in acute myocardial infarction." In: *Cytotherapy* 72.

Churchman, Sarah M, Frederique Ponchel, Sally a Boxall, Richard Cuthbert, Dimitrios Kouroupis, Tarek Roshdy, Peter V Giannoudis, Paul Emery, Dennis McGonagle, and Elena a Jones (2012). "Transcriptional profile of native CD271+ multipotential stromal cells: evidence for multiple fates, with prominent osteogenic and Wnt pathway signaling activity." In: *Arthritis and rheumatism* 64.8, pp. 2632–43.

Cooper, Max D. (2015). "The early history of B cells". In: *Nat Rev Immunol* 15.3, pp. 191–197.

Corcione, A. (2006). "Human mesenchymal stem cells modulate B-cell functions". In: *Blood* 107.1, pp. 367–372.

Corthay, a. (2009). "How do regulatory t cells work?" In: *Scandinavian Journal of Immunology* 70.4, pp. 326–336.

Cox, George, Sally a Boxall, Peter V Giannoudis, Conor T Buckley, Tarek Roshdy, Sarah M Churchman, Dennis McGonagle, and Elena Jones (2012). "High abundance of CD271(+) multipotential stromal cells (MSCs) in intramedullary cavities of long bones." In: *Bone* 50.2, pp. 510–7.

Crisan, Mihaela, Solomon Yap, Louis Casteilla, Chien-Wen Chen, Mirko Corselli, Tea Soon Park, Gabriella Andriolo, Bin Sun, Bo Zheng, Li Zhang, Cyrille Norotte, Pang-Ning Teng, Jeremy Traas, Rebecca Schugar, Bridget M. Deasy, Stephen Badylak, Hans-Jorg Buhring, Jean-Paul Giacobino, Lorenza Lazzari, Johnny Huard, and Bruno Peault (2008). "A Perivascular Origin for Mesenchymal Stem Cells in Multiple Human Organs". In: *Cell Stem Cell* 3.3, pp. 301–313.

Cross, Michael J. and Lena Claesson-Welsh (2001). "FGF and VEGF function in angiogenesis: Signalling pathways, biological responses and therapeutic inhibition". In: *Trends in Pharmacological Sciences* 22.4, pp. 201–207.

Cuerquis, Jessica, Raphaëlle Romieu-Mourez, Moïra François, Jean-Pierre Routy, Yoon Kow Young, Jing Zhao, and Nicoletta Eliopoulos (2014). "Human mesenchymal stromal cells transiently increase cytokine production by activated T cells before suppressing T-cell proliferation: effect of interferon-γ and tumor necrosis factor-α stimulation." In: *Cytotherapy* 16.2, pp. 191–202.

Dao, Mo, Ciara C Tate, Michael McGrogan, and Casey C Case (2013). "Comparing the angiogenic potency of naïve marrow stromal cells and Notch-transfected marrow stromal cells." In: *Journal of translational medicine* 11.1, p. 81.

Deans, Robert (2015). "Towards the creation of a standard MSC line as a calibration tool". In: *Cytotherapy* 17.9, pp. 1167–1168.

DeCicco-Skinner, Katie L., Gervaise H. Henry, Christophe Cataisson, Tracy Tabib, J. Curtis Gwilliam, Nicholas J. Watson, Erica M. Bullwinkle, Lauren Falkenburg, Rebecca C. ONeill, Adam Morin, and Jonathan S. Wiest (2014). "Endothelial Cell Tube Formation Assay for the In Vitro Study of Angiogenesis". In: *Journal of Visualized Experiments* 91.

Del Gaudio, Costantino, Silvia Baiguera, Margherita Boieri, Benedetta Mazzanti, Domenico Ribatti, Alessandra Bianco, and Paolo Macchiarini (2013). "Induction of angiogenesis using VEGF releasing genipin-crosslinked electrospun gelatin mats." In: *Biomaterials* 34.31, pp. 7754–65.

Deuse, Tobias, Christoph Peter, Paul W M Fedak, Tim Doyle, Hermann Reichenspurner, Wolfram H Zimmermann, Thomas Eschenhagen, William Stein, Joseph C Wu, Robert C Robbins, and Sonja Schrepfer (2009). "Hepatocyte growth factor or vascular endothelial growth factor gene transfer maximizes mesenchymal stem cell-based myocardial salvage after acute myocardial infarction." In: *Circulation* 120.11 Suppl, S247–S254.

Djouad, Farida, Louis-Marie Charbonnier, Carine Bouffi, Pascale Louis-Plence, Claire Bony, Florence Apparailly, Céline Cantos, Christian Jorgensen, and Danièle Noël (2007).

"Mesenchymal stem cells inhibit the differentiation of dendritic cells through an interleukin-6-dependent mechanism." In: *Stem cells (Dayton, Ohio)* 25.8, pp. 2025–32.

Dominici, M, K Le Blanc, I Mueller, I Slaper-Cortenbach, Fc Marini, Ds Krause, Rj Deans, A Keating, Dj Prockop, and Em Horwitz (2006). "Minimal criteria for defining multipotent mesenchymal stromal cells. The International Society for Cellular Therapy position statement." In: *Cytotherapy* 8.4, pp. 315–7.

Dreesmann, Lars, Michael Ahlers, and Burkhard Schlosshauer (2007). "The pro-angiogenic characteristics of a cross-linked gelatin matrix." In: *Biomaterials* 28.36, pp. 5536–43.

Duff, Sarah E, Chenggang Li, John M Garland, and Shant Kumar (2003). "CD105 is important for angiogenesis: evidence and potential applications." In: *The FASEB journal : official publication of the Federation of American Societies for Experimental Biology* 17.9, pp. 984–992.

Duffy, Michelle M, Thomas Ritter, Rhodri Ceredig, and Matthew D Griffin (2011). "Mesenchymal stem cell effects on T-cell effector pathways." In: *Stem cell research & therapy* 2.4, p. 34.

Duriancik, David M and Kathleen a Hoag (2009). "The identification and enumeration of dendritic cell populations from individual mouse spleen and Peyer's patches using flow cytometric analysis." In: *Cytometry. Part A : the journal of the International Society for Analytical Cytology* 75.11, pp. 951–9.

Eibes, Gemma, Francisco dos Santos, Pedro Z Andrade, Joana S Boura, Manuel M a Abecasis, Cláudia Lobato da Silva, and Joaquim M S Cabral (2010). "Maximizing the ex vivo expansion of human mesenchymal stem cells using a microcarrier-based stirred culture system." In: *Journal of biotechnology* 146.4, pp. 194–7.

Eming, S, B BRACHVOGEL, T ODORISIO, and M KOCH (2007). "Regulation of angiogenesis: Wound healing as a model". In: *Progress in Histochemistry and Cytochemistry* 42.3, pp. 115–170.

English, K, J M Ryan, L Tobin, M J Murphy, F P Barry, and B P Mahon (2009). "Cell contact, prostaglandin E(2) and transforming growth factor beta 1 play non-redundant

roles in human mesenchymal stem cell induction of CD4+CD25(High) forkhead box P3+ regulatory T cells." In: *Clinical and experimental immunology* 156.1, pp. 149–60.

English, Karen, Frank P. Barry, and Bernard P. Mahon (2008). "Murine mesenchymal stem cells suppress dendritic cell migration, maturation and antigen presentation". In: *Immunology Letters* 115.1, pp. 50–58.

English, Karen, Frank P Barry, Ciara P Field-Corbett, and Bernard P Mahon (2007). "IFN-gamma and TNF-alpha differentially regulate immunomodulation by murine mesenchymal stem cells." In: *Immunology letters* 110.2, pp. 91–100.

Fattori, E, M Cappelletti, P Costa, C Sellitto, Lavinia Cantoni, M Carelli, R Faggioni, G Fantuzzi, P Ghezzi, and V Poli (1994). "Defective inflammatory response in interleukin 6-deficient mice." In: *The Journal of experimental medicine* 180.4, pp. 1243–50.

Faulkner, Ashton, Robert Purcell, Andrew Hibbert, Sally Latham, Scott Thomson, Wendy L Hall, Caroline Wheeler-Jones, and David Bishop-Bailey (2014). "A thin layer angiogenesis assay: a modified basement matrix assay for assessment of endothelial cell differentiation". In: *BMC Cell Biology* 15.1, p. 41.

Ferrara, James LM, John E Levine, Pavan Reddy, and Ernst Holler (2009). "Graft-versus-host disease". In: *The Lancet* 373.9674, pp. 1550–1561.

Ferrara, Napoleone, Hans-Peter Gerber, and Jennifer LeCouter (2003). "The biology of VEGF and its receptors". In: *Nature Medicine* 9.6, pp. 669–676.

Figueroa, Fernando E, Flavio Carrion, Sandra Villanueva, and Maroun Khoury (2012). "Mesenchymal Stem Cell treatment for autoimmune diseases: a critical review". In: *Biol. Res.* 45.3, pp. 269–277.

Fishman, Jonathan M, Katherine Wiles, Mark W Lowdell, Paolo De Coppi, Martin J Elliott, Anthony Atala, and Martin A Birchall (2014). "Airway tissue engineering: an update". In: *Expert Opinion on Biological Therapy* 14.10, pp. 1477–1491.

Franco, Rodrigo and John a Cidlowski (2012). "Glutathione efflux and cell death." In: *Antioxidants & redox signaling* 17.12, pp. 1694–713.

François, Moïra, Ian B. Copland, Shala Yuan, Raphaëlle Romieu-Mourez, Edmund K. Waller, and Jacques Galipeau (2012). "Cryopreserved mesenchymal stromal cells dis-

play impaired immunosuppressive properties as a result of heat-shock response and impaired interferon-γ licensing". In: *Cytotherapy* 14.May 2011, pp. 147–152.

Fraser, John K., Kevin C. Hicok, Rob Shanahan, Min Zhu, Scott Miller, and Douglas M. Arm (2014). "The Celution ® System: Automated Processing of Adipose-Derived Regenerative Cells in a Functionally Closed System". In: *Advances in Wound Care* 3.1, pp. 38–45.

Freedman, L. P. (2015). "Know Thy Cells: Improving Biomedical Research Reproducibility". In: *Science Translational Medicine* 7.294, 294ed7–294ed7.

Freeman, Brian T, Nicholas A Kouris, and B. M. Ogle (2015). "Tracking Fusion of Human Mesenchymal Stem Cells After Transplantation to the Heart". In: *Stem Cells Translational Medicine* 4.6, pp. 685–694.

Friedenstein, A. J., R. K. Chailakhjan, and K. S. Lalykina (1970). "The development of fibroblast colonies in monolayer cultures of guinea-pig bone marrow and spleen cells". In: *Cell Tissue Kinet* 3.4, pp. 393–403.

Friedenstein, A. J., R. K. Chailakhyan, and U. V. Gerasimov (1987). "Bone marrow osteogenic stem cells: in vitro cultivation and transplantation in diffusion chambers". In: *Cell Proliferation* 20.3, pp. 263–272.

Friedenstein, A. J., K. V. Petrakova, A. I. Kurolesova, and G. P. Frolova (1968). "Heterotopic of bone marrow. Analysis of precursor cells for osteogenic and hematopoietic tissues". In: *Transplantation* 6.2, pp. 230–247.

Gabay, Cem (2006). "Interleukin-6 and chronic inflammation." In: *Arthritis research & therapy* 8 Suppl 2, S3.

Galipeau, Jacques (2013). "The mesenchymal stromal cells dilemma–does a negative phase III trial of random donor mesenchymal stromal cells in steroid-resistant graft-versus-host disease represent a death knell or a bump in the road?" In: *Cytotherapy* 15.1, pp. 2–8.

Galipeau, Jacques, Mauro Krampera, John Barrett, Francesco Dazzi, Robert J. Deans, Joost DeBruijn, Massimo Dominici, Willem E. Fibbe, Adrian P. Gee, Jeffery M. Gimble, Peiman Hematti, Mickey B.C. Koh, Katarina LeBlanc, Ivan Martin, Ian K. McNiece,

Michael Mendicino, Steve Oh, Luis Ortiz, Donald G. Phinney, Valerie Planat, Yufang Shi, David F. Stroncek, Sowmya Viswanathan, Daniel J. Weiss, and Luc Sensebe (2016). "International Society for Cellular Therapy perspective on immune functional assays for mesenchymal stromal cells as potency release criterion for advanced phase clinical trials". In: *Cytotherapy* 18.2, pp. 151–159.

Ghorashian, Sara, Martin Pule, and Persis Amrolia (2015). "CD19 chimeric antigen receptor T cell therapy for haematological malignancies". In: *British Journal of Haematology* 169.4, pp. 463–478.

Gieseke, Friederike, Burkhardt Schütt, Susanne Viebahn, Ewa Koscielniak, Wilhelm Friedrich, Rupert Handgretinger, and Ingo Müller (2007). "Human multipotent mesenchymal stromal cells inhibit proliferation of PBMCs independently of IFNgammaR1 signaling and IDO expression." In: *Blood* 110.6, pp. 2197–2200.

Glennie, Sarah, Inês Soeiro, Peter J Dyson, Eric W-F Lam, and Francesco Dazzi (2005). "Bone marrow mesenchymal stem cells induce division arrest anergy of activated T cells." In: *Blood* 105.7, pp. 2821–7.

Gnecchi, Massimiliano, Zhiping Zhang, Aiguo Ni, and Victor J. Dzau (2008). "Paracrine mechanisms in adult stem cell signaling and therapy". In: *Circulation Research* 103.11, pp. 1204–1219. arXiv: NIHMS150003.

Go, A. S., D. Mozaffarian, V. L. Roger, E. J. Benjamin, J. D. Berry, M. J. Blaha, S. Dai, E. S. Ford, C. S. Fox, S. Franco, H. J. Fullerton, C. Gillespie, S. M. Hailpern, J. A. Heit, V. J. Howard, M. D. Huffman, S. E. Judd, B. M. Kissela, S. J. Kittner, D. T. Lackland, J. H. Lichtman, L. D. Lisabeth, R. H. Mackey, D. J. Magid, G. M. Marcus, A. Marelli, D. B. Matchar, D. K. McGuire, E. R. Mohler, C. S. Moy, M. E. Mussolino, R. W. Neumar, G. Nichol, D. K. Pandey, N. P. Paynter, M. J. Reeves, P. D. Sorlie, J. Stein, A. Towfighi, T. N. Turan, S. S. Virani, N. D. Wong, D. Woo, and M. B. Turner (2013). "Heart Disease and Stroke Statistics–2014 Update: A Report From the American Heart Association". In: *Circulation* 129.3, e28–e292.

Grant, D.S., M.C. Kibbey, J.L. Kinsella, M.C. Cid, and H.K. Kleinman (1994). "The Role of Basement Membrane in Angiogenesis and Tumor Growth". In: *Pathology - Research and Practice* 190.9-10, pp. 854–863.

Gray, D (2006). "Thrombolysis: past, present, and future". In: *Postgraduate Medical Journal* 82.968, pp. 372–375.

Groeber, Florian, Monika Holeiter, Martina Hampel, Svenja Hinderer, and Katja Schenke-Layland (2011). "Skin tissue engineering In vivo and in vitro applications". In: *Advanced Drug Delivery Reviews* 63.4-5, pp. 352–366.

Gronthos, S., J. Brahim, W. Li, L.W. Fisher, N. Cherman, A. Boyde, P. DenBesten, P. G. Robey, and S. Shi (2002). "Stem Cell Properties of Human Dental Pulp Stem Cells". In: *Journal of Dental Research* 81.8, pp. 531–535.

Gupta, Pawan K, Anoop Chullikana, Rajiv Parakh, Sanjay Desai, Anjan Das, Sanjay Gottipamula, Sagar Krishnamurthy, Naveen Anthony, Arun Pherwani, and Anish S Majumdar (2013). "A double blind randomized placebo controlled phase I/II study assessing the safety and efficacy of allogeneic bone marrow derived mesenchymal stem cell in critical limb ischemia". In: *Journal of Translational Medicine* 11.1, p. 143.

Guzman, Camilo, Manish Bagga, Amanpreet Kaur, Jukka Westermarck, and Daniel Abankwa (2014). "ColonyArea: An ImageJ Plugin to Automatically Quantify Colony Formation in Clonogenic Assays". In: *PLoS ONE* 9.3. Ed. by Rossella Rota, e92444.

Haleem, A. M., A. A. E. Singergy, D. Sabry, H. M. Atta, L. A. Rashed, C. R. Chu, M. T. E. Shewy, A. Azzam, and M. T. A. Aziz (2010). "The Clinical Use of Human Culture-Expanded Autologous Bone Marrow Mesenchymal Stem Cells Transplanted on Platelet-Rich Fibrin Glue in the Treatment of Articular Cartilage Defects: A Pilot Study and Preliminary Results". In: *Cartilage* 1.4, pp. 253–261.

Hare, J M, J E Fishman, G Gerstenblith, and Et Al (2012). "Comparison of Allogeneic vs Autologous Bone Marrow–Derived Mesenchymal Stem Cells Delivered by Transendocardial Injection in Patients With Ischemic . . . " In: *JAMA: the journal . . .* Icm, pp. 1–11.

Hare, Joshua M., Jay H. Traverse, Timothy D. Henry, Nabil Dib, Robert K. Strumpf, Steven P. Schulman, Gary Gerstenblith, Anthony N. DeMaria, Ali E. Denktas, Roger S. Gammon, James B. Hermiller, Mark a. Reisman, Gary L. Schaer, and Warren Sherman (2009). "A Randomized, Double-Blind, Placebo-Controlled, Dose-Escalation Study of Intravenous Adult Human Mesenchymal Stem Cells (Prochymal) After Acute Myocardial Infarction". In: *Journal of the American College of Cardiology* 54.24, pp. 2277–2286.

Hashemi, S. M., S. Ghods, F. D. Kolodgie, K. Parcham-Azad, M. Keane, D. Hamamdzic, R. Young, M. K. Rippy, R. Virmani, H. Litt, and R. L. Wilensky (2007). "A placebo controlled, dose-ranging, safety study of allogenic mesenchymal stem cells injected by endomyocardial delivery after an acute myocardial infarction". In: *European Heart Journal* 29.2, pp. 251–259.

Haynesworth, S E, M A Baber, and A I Caplan (1996). "Cytokine expression by human marrow-derived mesenchymal progenitor cells in vitro: effects of dexamethasone and IL-1 alpha." In: *Journal of cellular physiology* 166.3, pp. 585–92.

Hentze, Hannes, Poh Loong Soong, Siew Tein Wang, Blaine W. Phillips, Thomas C. Putti, and N. Ray Dunn (2009). "Teratoma formation by human embryonic stem cells: Evaluation of essential parameters for future safety studies". In: *Stem Cell Research* 2.3, pp. 198–210.

Hess, David C, Cathy a Sila, Anthony J Furlan, Larry R Wechsler, Jeffrey a Switzer, and Robert W Mays (2014). "A double-blind placebo-controlled clinical evaluation of MultiStem for the treatment of ischemic stroke." In: *International journal of stroke : official journal of the International Stroke Society* 9.3, pp. 381–6.

Hoch, Allison I., Bernard Y. Binder, Damian C. Genetos, and J. Kent Leach (2012). "Differentiation-Dependent Secretion of Proangiogenic Factors by Mesenchymal Stem Cells". In: *PLoS ONE* 7.4. Ed. by Antonio Paolo Beltrami, e35579.

Hu, B.-Y., J. P. Weick, J. Yu, L.-X. Ma, X.-Q. Zhang, J. A. Thomson, and S.-C. Zhang (2010). "Neural differentiation of human induced pluripotent stem cells follows develop-

mental principles but with variable potency". In: *Proceedings of the National Academy of Sciences* 107.9, pp. 4335–4340.

Hung, Shih-Chieh, Radhika R Pochampally, Sy-Chi Chen, Shu-Ching Hsu, and Darwin J Prockop (2007). "Angiogenic effects of human multipotent stromal cell conditioned medium activate the PI3K-Akt pathway in hypoxic endothelial cells to inhibit apoptosis, increase survival, and stimulate angiogenesis." In: *Stem cells (Dayton, Ohio)* 25.9, pp. 2363–70.

inAnker, Pieternella S., Sicco A. Scherjon, Carin Kleijburg van der Keur, Godelieve M.J.S. de Groot-Swings, Frans H.J. Claas, Willem E. Fibbe, and Humphrey H.H. Kanhai (2004). "Isolation of Mesenchymal Stem Cells of Fetal or Maternal Origin from Human Placenta". In: *Stem Cells* 22.7, pp. 1338–1345.

Isakova, Iryna A., Jason Dufour, Calvin Lanclos, Julie Bruhn, and Donald G. Phinney (2010). "Cell-dose-dependent increases in circulating levels of immune effector cells in rhesus macaques following intracranial injection of allogeneic MSCs". In: *Experimental Hematology* 38.10, 957–967.e1.

Janeczek Portalska, Karolina, Anne Leferink, Nathalie Groen, Hugo Fernandes, Lorenzo Moroni, Clemens van Blitterswijk, and Jan de Boer (2012). "Endothelial Differentiation of Mesenchymal Stromal Cells". In: *PLoS ONE* 7.10, e46842.

Jeong, Ju Ah, Kyung-Min Ko, Sohyun Bae, Choon-Ju Jeon, Gou Young Koh, and Hoeon Kim (2007). "Genome-Wide Differential Gene Expression Profiling of Human Bone Marrow Stromal Cells". In: *Stem Cells* 25.4, pp. 994–1002.

Jiang, Chen yang, Chun Gui, Ai na He, Xin yang Hu, Jie Chen, Yun Jiang, and Jian an Wang (2008). "Optimal time for mesenchymal stem cell transplantation in rats with myocardial infarction". In: *J. Zhejiang Univ. Sci. B* 9.8, pp. 630–637.

Jiang, Y., B. N. Jahagirdar, R. L. Reinhardt, R. E. Schwartz, C. D. Keene, X. R. Ortiz-Gonzalez, M. Reyes, T. Lenvik, T. Lund, M. Blackstad, J. Du, S. Aldrich, A. Lisberg, W. C. Low, D. A. Largaespada, and C. M. Verfaillie (2002). "Pluripotency of mesenchymal stem cells derived from adult marrow". In: *Nature* 418.6893, pp. 41–49.

Jin, Hye, Yun Bae, Miyeon Kim, Soon-Jae Kwon, Hong Jeon, Soo Choi, Seong Kim, Yoon Yang, Wonil Oh, and Jong Chang (2013). "Comparative Analysis of Human Mesenchymal Stem Cells from Bone Marrow, Adipose Tissue, and Umbilical Cord Blood as Sources of Cell Therapy". In: *International Journal of Molecular Sciences* 14.9, pp. 17986–18001.

Jones, Ben J. and Steven J. McTaggart (2008). "Immunosuppression by mesenchymal stromal cells: From culture to clinic". In: *Experimental Hematology* 36.6, pp. 733–741.

Jones, E, a English, S M Churchman, D Kouroupis, S a Boxall, S Kinsey, P G Giannoudis, P Emery, and D McGonagle (2010). "Large-scale extraction and characterization of CD271+ multipotential stromal cells from trabecular bone in health and osteoarthritis: implications for bone regeneration strategies based on uncultured or minimally cultured multipotential stromal cells." In: *Arthritis and rheumatism* 62.7, pp. 1944–54.

Jones, Elena and Richard Schäfer (2015). "Where is the common ground between bone marrow mesenchymal stem/stromal cells from different donors and species?" In: *Stem Cell Research & Therapy* 6.1, p. 143.

Jones, Elena a, Sally E Kinsey, Anne English, Richard a Jones, Liz Straszynski, David M Meredith, Alex F Markham, Andrew Jack, Paul Emery, and Dennis McGonagle (2002). "Isolation and characterization of bone marrow multipotential mesenchymal progenitor cells." In: *Arthritis and rheumatism* 46.12, pp. 3349–60.

Jones, S., N. Horwood, a. Cope, and F. Dazzi (2007). "The Antiproliferative Effect of Mesenchymal Stem Cells Is a Fundamental Property Shared by All Stromal Cells". In: *The Journal of Immunology* 179.5, pp. 2824–2831.

Josefowicz, Steven Z., Li-Fan Lu, and Alexander Y. Rudensky (2012). "Regulatory T Cells: Mechanisms of Differentiation and Function". In: *Annual Review of Immunology* 30.1, pp. 531–564.

Jung, Sunghoon, Krishna M. Panchalingam, Lawrence Rosenberg, and Leo a. Behie (2012). "Ex vivo expansion of human mesenchymal stem cells in defined serum-free media". In: *Stem Cells International* 2012.

Kalinski, P. (2011). "Regulation of Immune Responses by Prostaglandin E2". In: *The Journal of Immunology* 188.1, pp. 21–28.

Kano, Mitsunobu R, Yasuyuki Morishita, Caname Iwata, Shigeru Iwasaka, Tetsuro Watabe, Yasuyoshi Ouchi, Kohei Miyazono, and Keiji Miyazawa (2005). "VEGF-A and FGF-2 synergistically promote neoangiogenesis through enhancement of endogenous PDGF-B-PDGFRbeta signaling." In: *Journal of cell science* 118.Pt 16, pp. 3759–3768.

Karussis, Dimitrios, Panayiota Petrou, Urania Vourka-Karussis, and Ibrahim Kassis (2013). "Hematopoietic stem cell transplantation in multiple sclerosis". In: *Expert Review of Neurotherapeutics* 13.5, pp. 567–578.

Katsube, Yoshihiro, Motohiro Hirose, Chikashi Nakamura, and Hajime Ohgushi (2008). "Correlation between proliferative activity and cellular thickness of human mesenchymal stem cells". In: *Biochemical and Biophysical Research Communications* 368, pp. 256–260.

Kebriaei, Partow, Luis Isola, Erkut Bahceci, Kent Holland, Scott Rowley, Joseph McGuirk, Marcel Devetten, Jan Jansen, Roger Herzig, Michael Schuster, Rod Monroy, and Joseph Uberti (2009). "Adult Human Mesenchymal Stem Cells Added to Corticosteroid Therapy for the Treatment of Acute Graft-versus-Host Disease". In: *Biology of Blood and Marrow Transplantation* 15.7, pp. 804–811.

Kern, Susanne, Hermann Eichler, Johannes Stoeve, Harald Kluter, and Karen Bieback (2006). "Comparative analysis of mesenchymal stem cells from bone marrow, umbilical cord blood, or adipose tissue." In: *Stem cells* 24.5, pp. 1294–1301.

Keyser, Kirsten A., Karen E. Beagles, and Hans-Peter Kiem (2007). "Comparison of Mesenchymal Stem Cells From Different Tissues to Suppress T-Cell Activation". In: *ct* 16.5, pp. 555–562.

Kinnaird, T, E Stabile, M S Burnett, C W Lee, S Barr, S Fuchs, and S E Epstein (2004). "Marrow-derived stromal cells express genes encoding a broad spectrum of arteriogenic cytokines and promote in vitro and in vivo arteriogenesis through paracrine mechanisms." In: *Circulation research* 94.5, pp. 678–85.

Klyushnenkova, Elena, Joseph D Mosca, Valentina Zernetkina, Manas K Majumdar, Kirstin J Beggs, Donald W Simonetti, Robert J Deans, and Kevin R McIntosh (2005). "T cell responses to allogeneic human mesenchymal stem cells: immunogenicity, tolerance, and suppression". In: *J Biomed Sci* 12.1, pp. 47–57.

Kochenderfer, J. N., M. E. Dudley, S. A. Feldman, W. H. Wilson, D. E. Spaner, I. Maric, M. Stetler-Stevenson, G. Q. Phan, M. S. Hughes, R. M. Sherry, J. C. Yang, U. S. Kammula, L. Devillier, R. Carpenter, D.-A. N. Nathan, R. A. Morgan, C. Laurencot, and S. A. Rosenberg (2011). "B-cell depletion and remissions of malignancy along with cytokine-associated toxicity in a clinical trial of anti-CD19 chimeric-antigen-receptor-transduced T cells". In: *Blood* 119.12, pp. 2709–2720.

Kochenderfer, J. N., M. E. Dudley, S. H. Kassim, R. P. T. Somerville, R. O. Carpenter, M. Stetler-Stevenson, J. C. Yang, G. Q. Phan, M. S. Hughes, R. M. Sherry, M. Raffeld, S. Feldman, L. Lu, Y. F. Li, L. T. Ngo, A. Goy, T. Feldman, D. E. Spaner, M. L. Wang, C. C. Chen, S. M. Kranick, A. Nath, D.-A. N. Nathan, K. E. Morton, M. A. Toomey, and S. A. Rosenberg (2014). "Chemotherapy-Refractory Diffuse Large B-Cell Lymphoma and Indolent B-Cell Malignancies Can Be Effectively Treated With Autologous T Cells Expressing an Anti-CD19 Chimeric Antigen Receptor". In: *Journal of Clinical Oncology* 33.6, pp. 540–549.

Krampera, Mauro, Lorenzo Cosmi, Roberta Angeli, Annalisa Pasini, Francesco Liotta, Angelo Andreini, Veronica Santarlasci, Benedetta Mazzinghi, Giovanni Pizzolo, Fabrizio Vinante, Paola Romagnani, Enrico Maggi, Sergio Romagnani, and Francesco Annunziato (2006). "Role for interferon-gamma in the immunomodulatory activity of human bone marrow mesenchymal stem cells." In: *Stem cells (Dayton, Ohio)* 24.2, pp. 386–98.

Krampera, Mauro, Jacques Galipeau, Yufang Shi, Karin Tarte, and Luc Sensebe (2013). "Immunological characterization of multipotent mesenchymal stromal cells-The International Society for Cellular Therapy (ISCT) working proposal." In: *Cytotherapy* 15.9, pp. 1054–1061.

Krinner, Axel, Martin Hoffmann, Markus Loeffler, Dirk Drasdo, and Joerg Galle (2010). "Individual fates of mesenchymal stem cells in vitro." In: *BMC Systems biology* 4, p. 73.

Kuçi, Selim, Zyrafete Kuçi, Hermann Kreyenberg, Erika Deak, Kathrin Pütsch, Sabine Huenecke, Chandrasekhar Amara, Stefanie Koller, Eva Rettinger, Manuel Grez, Ulrike Koehl, Hatixhe Latifi-Pupovci, Reinhard Henschler, Torsten Tonn, Dorothee von Laer, Thomas Klingebiel, and Peter Bader (2010). "CD271 antigen defines a subset of multipotent stromal cells with immunosuppressive and lymphohematopoietic engraftment-promoting properties." In: *Haematologica* 95.4, pp. 651–9.

Kuo, Catherine K, Wan-Ju Li, Robert L Mauck, and Rocky S Tuan (2006). "Cartilage tissue engineering: its potential and uses". In: *Current Opinion in Rheumatology* 18.1, pp. 64–73.

Kurtzberg, Joanne, Susan Prockop, Pierre Teira, Henrique Bittencourt, Victor Lewis, Ka Wah Chan, Biljana Horn, Lolie Yu, Julie-an Talano, Eneida Nemecek, Charles R Mills, and Sonali Chaudhury (2014). "Allogeneic Human Mesenchymal Stem Cell Therapy Refractory Acute Graft-versus-Host Disease in Pediatric Patients". In: *Biology of Blood and Marrow Transplantation* 20.2, pp. 229–235.

Kwon, Hyuk Min, Sung Mo Hur, Keon Young Park, Chun Ki Kim, Yong Man Kim, Hyun Soo Kim, Ha Cheol Shin, Moo Ho Won, Kwon Soo Ha, Young Guen Kwon, Dong Heon Lee, and Young Myeong Kim (2014). "Multiple paracrine factors secreted by mesenchymal stem cells contribute to angiogenesis". In: *Vascular Pharmacology* 63.1, pp. 19–28.

Lamers, C. H. J., R. Willemsen, P. van Elzakker, S. van Steenbergen-Langeveld, M. Broertjes, J. Oosterwijk-Wakka, E. Oosterwijk, S. Sleijfer, R. Debets, and J. W. Gratama (2010). "Immune responses to transgene and retroviral vector in patients treated with ex vivo-engineered T cells". In: *Blood* 117.1, pp. 72–82.

Le Blanc, Katarina, Ida Rasmusson, Berit Sundberg, Cecilia Götherström, Moustapha Hassan, Mehmet Uzunel, and Olle Ringdén (2004). "Treatment of severe acute graft-versus-host disease with third party haploidentical mesenchymal stem cells." In: *Lancet* 363.9419, pp. 1439–41.

Le Blanc, Katarina, Francesco Frassoni, Lynne Ball, Franco Locatelli, Helene Roelofs, Ian Lewis, Edoardo Lanino, Berit Sundberg, Maria Ester Bernardo, Mats Remberger,

Giorgio Dini, R Maarten Egeler, Andrea Bacigalupo, Willem Fibbe, and Olle Ringdén (2008). "Mesenchymal stem cells for treatment of steroid-resistant, severe, acute graft-versus-host disease: a phase II study." In: *Lancet* 371.9624, pp. 1579–86.

LeBlanc, K., L. Tammik, B. Sundberg, S. E. Haynesworth, and O. Ringden (2003). "Mesenchymal Stem Cells Inhibit and Stimulate Mixed Lymphocyte Cultures and Mitogenic Responses Independently of the Major Histocompatibility Complex". In: *Scand J Immunol* 57.1, pp. 11–20.

Lee, Eun Ju, Hwan-Woo Park, Hyo-Jin Jeon, Hyo-Soo Kim, and Mi-Sook Chang (2013). "Potentiated therapeutic angiogenesis by primed human mesenchymal stem cells in a mouse model of hindlimb ischemia." In: *Regenerative medicine* 8.3, pp. 283–93.

Lee, Jamie A., Josef Spidlen, Keith Boyce, Jennifer Cai, Nicholas Crosbie, Mark Dalphin, Jeff Furlong, Maura Gasparetto, Michael Goldberg, Elizabeth M. Goralczyk, Bill Hyun, Kirstin Jansen, Tobias Kollmann, Megan Kong, Robert Leif, Shannon McWeeney, Thomas D. Moloshok, Wayne Moore, Garry Nolan, John Nolan, Janko Nikolich-Zugich, David Parrish, Barclay Purcell, Yu Qian, Biruntha Selvaraj, Clayton Smith, Olga Tchuvatkina, Anne Wertheimer, Peter Wilkinson, Christopher Wilson, James Wood, Robert Zigon, Richard H. Scheuermann, and Ryan R. Brinkman (2008). "MIFlowCyt: The minimum information about a flow cytometry experiment". In: *Cytometry* 73A.10, pp. 926–930.

Lee, O. K. (2004). "Isolation of multipotent mesenchymal stem cells from umbilical cord blood". In: *Blood* 103.5, pp. 1669–1675.

Lehman, Nicholas, Rochelle Cutrone, Amy Raber, Robert Perry, Wouter Van't Hof, Robert Deans, Anthony E Ting, and Juliana Woda (2012). "Development of a surrogate angiogenic potency assay for clinical-grade stem cell production." In: *Cytotherapy* 14.8, pp. 994–1004.

Li, Aihua, Seema Dubey, Michelle L Varney, Bhavana J Dave, and Rakesh K Singh (2003). "IL-8 directly enhanced endothelial cell survival, proliferation, and matrix metalloproteinases production and regulated angiogenesis." In: *Journal of immunology (Baltimore, Md. : 1950)* 170.6, pp. 3369–3376.

Li, Zhe, Tiejun Qu, Chen Ding, Chi Ma, Hongchen Sun, Shirong Li, and Xiaohua Liu (2015). "Injectable gelatin derivative hydrogels with sustained vascular endothelial growth factor release for induced angiogenesis". In: *Acta Biomaterialia* 13, pp. 88–100.

Lin, Ching-Shwun, Hongxiu Ning, Guiting Lin, and Tom F Lue (2012). "Is CD34 truly a negative marker for mesenchymal stromal cells?" In: *Cytotherapy* 14.10, pp. 1159–63.

Liu, Linqi, Jianhua Gao, Yi Yuan, Qiang Chang, Yunjun Liao, and Feng Lu (2013). "Hypoxia preconditioned human adipose derived mesenchymal stem cells enhance angiogenic potential via secretion of increased VEGF and bFGF". In: *Cell Biology International* 37.6, pp. 551–560.

Luckheeram, Rishi Vishal, Rui Zhou, Asha Devi Verma, and Bing Xia (2012). "CD4+T Cells: Differentiation and Functions". In: *Clinical and Developmental Immunology* 2012, pp. 1–12.

Luetzkendorf, Jana, Katrin Nerger, Julian Hering, Angelika Moegel, Katrin Hoffmann, Christiane Hoefers, Carsten Mueller-Tidow, and Lutz P Mueller (2015). "Cryopreservation does not alter main characteristics of Good Manufacturing Process-grade human multipotent mesenchymal stromal cells including immunomodulating potential and lack of malignant transformation." In: *Cytotherapy* 17.2, pp. 186–198.

Luttun, Aernout, Marc Tjwa, Lieve Moons, Yan Wu, Anne Angelillo-Scherrer, Fang Liao, Janice A. Nagy, Andrea Hooper, Josef Priller, Bert De Klerck, Veerle Compernolle, Evis Daci, Peter Bohlen, Mieke Dewerchin, Jean-Marc Herbert, Roy Fava, Patrick Matthys, Geert Carmeliet, Désiré Collen, Harold F. Dvorak, Daniel J. Hicklin, and Peter Carmeliet (2002). "Revascularization of ischemic tissues by PlGF treatment, and inhibition of tumor angiogenesis, arthritis and atherosclerosis by anti-Flt1". In: *Nature Medicine*.

Luz-Crawford, Patricia, Monica Kurte, Javiera Bravo-Alegría, Rafael Contreras, Estefania Nova-Lamperti, Gautier Tejedor, Danièle Noël, Christian Jorgensen, Fernando Figueroa, Farida Djouad, and Flavio Carrión (2013). "Mesenchymal stem cells gener-

ate a CD4+/CD25+/Foxp3+ regulatory T cell population during the differentiation process of Th1 and Th17 cells". In: *Stem Cell Research & Therapy* 4.3, p. 65.

Maccario, Rita, Marina Podestà, Antonia Moretta, Angela Cometa, Patrizia Comoli, Daniela Montagna, Liane Daudt, Adalberto Ibatici, Giovanna Piaggio, Sarah Pozzi, Francesco Frassoni, and Franco Locatelli (2005). "Interaction of human mesenchymal stem cells with cells involved in alloantigen-specific immune response favors the differentiation of CD4+ T-cell subsets expressing a regulatory/suppressive phenotype." In: *Haematologica* 90.4, pp. 516–25.

Mandal, Arundhati and Chandra Viswanathan (2015). "Natural killer cells: In health and disease". In: *Hematology/Oncology and Stem Cell Therapy* 8.2, pp. 47–55.

Mason, Chris, David a Brindley, Emily J Culme-Seymour, and Natasha L Davie (2011). "Cell therapy industry: billion dollar global business with unlimited potential". In: *Regenerative Medicine* 6.3, pp. 265–272.

Maziarz, R.T., T. Devos, C. Bachier, S.C. Goldstein, J. Leis, K.R. Cooke, R. Perry, R.J. Deans, W.J. Van't Hof, and H.M. Lazarus (2012). "Prophylaxis of Acute GVHD Using Multistem® Stromal Cell Therapy: Preliminary Results After Administration of Single or Multiple Doses in a Phase 1 Trial". In: *Biology of Blood and Marrow Transplantation* 18.2, S264–S265.

Meisel, Roland, Andree Zibert, Maurice Laryea, Ulrich Göbel, Walter Däubener, and Dagmar Dilloo (2004). "Human bone marrow stromal cells inhibit allogeneic T-cell responses by indoleamine 2,3-dioxygenase-mediated tryptophan degradation." In: *Blood* 103.12, pp. 4619–21.

Melief, Sara Marie, Sacha Brigitte Geutskens, Willem Fibbe, and Helene Roelofs (2013). "Multipotent stromal cells skew monocytes towards an anti-inflammatory IL-10 producing phenotype by production of IL-6." In: *Haematologica*.

Moffett, John R and Ma Aryan Namboodiri (2003). "Tryptophan and the immune response." In: *Immunology and cell biology* 81.4, pp. 247–65.

Mohyeldin, Ahmed, Tomás Garzón-Muvdi, and Alfredo Quiñones Hinojosa (2010). "Oxygen in stem cell biology: A critical component of the stem cell niche". In: *Cell Stem Cell* 7.Figure 1, pp. 150–161.

Moll, Guido, Jessica J. Alm, Lindsay C. Davies, Lena von Bahr, Nina Heldring, Lillemor Stenbeck-Funke, Osama A. Hamad, Robin Hinsch, Lech Ignatowicz, Matthew Locke, Helena Lönnies, John D. Lambris, Yuji Teramura, Kristina Nilsson-Ekdahl, Bo Nilsson, and Katarina Le Blanc (2014). "Do Cryopreserved Mesenchymal Stromal Cells Display Impaired Immunomodulatory and Therapeutic Properties?" In: *STEM CELLS* 32.9, pp. 2430–2442.

Morishita, Ryuichi, Motokuni Aoki, Naotaka Hashiya, Keita Yamasaki, Hitomi Kurinami, Shiro Shimizu, Hirofumi Makino, Yasushi Takesya, Junya Azuma, and Toshio Ogihara (2004). "Therapeutic Angiogenesis using Hepatocyte Growth Factor (HGF)". In: *CGT* 4.2, pp. 199–206.

Mota, Carlos, Dario Puppi, Federica Chiellini, and Emo Chiellini (2012). "Additive manufacturing techniques for the production of tissue engineering constructs". In: *J Tissue Eng Regen Med* 9.3, pp. 174–190.

Mushtaq, Muzammil, Darcy L. DiFede, Samuel Golpanian, Aisha Khan, Samirah A. Gomes, Adam Mendizabal, Alan W. Heldman, and Joshua M. Hare (2014). "Rationale and Design of the Percutaneous Stem Cell Injection Delivery Effects on Neomyogenesis in Dilated Cardiomyopathy (The POSEIDON-DCM Study)". In: *Journal of Cardiovascular Translational Research* 7.9, pp. 769–780.

Nagaya, Noritoshi, Takafumi Fujii, Takashi Iwase, Hajime Ohgushi, Takefumi Itoh, Masaaki Uematsu, Masakazu Yamagishi, Hidezo Mori, Kenji Kangawa, Soichiro Kitamura, Masakazu Yama, and Soichiro Kitamura Intra (2004). "Intravenous administration of mesenchymal stem cells improves cardiac function in rats with acute myocardial infarction through angiogenesis and myogenesis". In: *Am J Physiol Heart Circ Physiol.* 287.6, pp. 5–7.

Najar, Mehdi, Gordana Raicevic, Hicham Id Boufker, Hussein Fayyad Kazan, Cécile De Bruyn, Nathalie Meuleman, Dominique Bron, Michel Toungouz, and Laurence

Lagneaux (2010). "Mesenchymal stromal cells use PGE2 to modulate activation and proliferation of lymphocyte subsets: Combined comparison of adipose tissue, Wharton's Jelly and bone marrow sources". In: *Cellular Immunology* 264.2, pp. 171–179.

Nakajima, Kazuaki, Jun Fujita, Makoto Matsui, Shugo Tohyama, Noriko Tamura, Hideaki Kanazawa, Tomohisa Seki, Yoshikazu Kishino, Akinori Hirano, Marina Okada, Ryota Tabei, Motoaki Sano, Shinya Goto, Yasuhiko Tabata, and Keiichi Fukuda (2015). "Gelatin Hydrogel Enhances the Engraftment of Transplanted Cardiomyocytes and Angiogenesis to Ameliorate Cardiac Function after Myocardial Infarction". In: *Plos One* 10.7, e0133308.

Nakamura, Toshikazu and Shinya Mizuno (2010). "The discovery of Hepatocyte Growth Factor (HGF) and its significance for cell biology, life sciences and clinical medicine". In: *Proc. Jpn. Acad., Ser. B* 86.6, pp. 588–610.

Nauta, A. J. (2006). "Donor-derived mesenchymal stem cells are immunogenic in an allogeneic host and stimulate donor graft rejection in a nonmyeloablative setting". In: *Blood* 108.6, pp. 2114–2120.

Nauta, A. J., A. B. Kruisselbrink, E. Lurvink, R. Willemze, and W. E. Fibbe (2006). "Mesenchymal Stem Cells Inhibit Generation and Function of Both CD34 Derived and Monocyte-Derived Dendritic Cells". In: *The Journal of Immunology* 177.4, pp. 2080–2087.

Nawrot, Maria, David H. McKenna, Darin Sumstad, John D. McMannis, Zbigniew M. Szczepiorkowski, Helen Belfield, Elke Grassman, Toni Temples, Deanna Nielsen, Ning Yuan, Bert Wognum, and Jo-Anna Reems (2011). "Interlaboratory assessment of a novel colony-forming unit assay: a multicenter study by the cellular team of Biomedical Excellence for Safer Transfusion (BEST) collaborative". In: *Transfusion* 51.9, pp. 2001–2005.

Nicola, M. Di (2002). "Human bone marrow stromal cells suppress T-lymphocyte proliferation induced by cellular or nonspecific mitogenic stimuli". In: *Blood* 99.10, pp. 3838–3843.

Nilsson, Alexandra Rundberg, David Bryder, and Cornelis J. H. Pronk (2013). "Frequency determination of rare populations by flow cytometry: A hematopoietic stem cell perspective". In: *Cytometry* 83A.8, pp. 721–727.

Noh, Hye Bin, Hee-Jin Ahn, Woo-Jung Lee, KyuBum Kwack, and Young Do Kwon (2010). "The molecular signature of in vitro senescence in human mesenchymal stem cells". In: *Genes Genom* 32.1, pp. 87–93.

Nold, Philipp, Cornelia Brendel, Andreas Neubauer, Gregor Bein, and Holger Hackstein (2013). "Good manufacturing practice-compliant animal-free expansion of human bone marrow derived mesenchymal stroma cells in a closed hollow-fiber-based bioreactor". In: *Biochemical and Biophysical Research Communications* 430.1, pp. 325–330.

Ode, Andrea, Janosch Schoon, Annett Kurtz, Marcel Gaetjen, Jan E. Ode, Sven Geissler, and Georg N. Duda (2012). "CD73/5'-ecto-nucleotidase acts as a regulatory factor in osteo-/chondrogenic differentiation of mechanically stimulated mesenchymal stromal cells". In: *European Cells and Materials* 25.030, pp. 37–47.

O'Donnell, Erika a, David N Ernst, and Ravi Hingorani (2013). "Multiparameter flow cytometry: advances in high resolution analysis." In: *Immune network* 13.2, pp. 43–54.

ONS (2015). *What are the top causes of death by age and gender?* URL: `http://visual.ons.gov.uk/what-are-the-top-causes-of-death-by-age-and-gender/`.

Oswald, Joachim, Sabine Boxberger, Birgitte Jø rgensen, Silvia Feldmann, Gerhard Ehninger, Martin Bornhäuser, and Carsten Werner (2004). "Mesenchymal stem cells can be differentiated into endothelial cells in vitro." In: *Stem cells (Dayton, Ohio)* 22.3, pp. 377–84.

Otte, Anna, Vesna Bucan, Kerstin Reimers, and Ralf Hass (2013). "Mesenchymal stem cells maintain long-term in vitro stemness during explant culture." In: *Tissue engineering. Part C, Methods* 19.12, pp. 1–42.

Owen, M. and A. J. Friedenstein (1988). "Stromal stem cells: marrow-derived osteogenic precursors". In: *Ciba Found. Symp.* 136, pp. 42–60.

Park, C. W., K. S. Kim, S. Bae, H. K. Son, P. K. Myung, H. J. Hong, and H. Kim (2009). "Cytokine secretion profiling of human mesenchymal stem cells by antibody array". In: *Int J Stem Cells* 2.1, pp. 59–68.

Pedersen, Torbjorn O, Anna L Blois, Zhe Xing, Ying Xue, Yang Sun, Anna Finne-Wistrand, Lars A Akslen, James B Lorens, Knut N Leknes, Inge Fristad, and Kamal Mustafa (2013). "Endothelial microvascular networks affect gene-expression profiles and osteogenic potential of tissue-engineered constructs". In: *Stem Cell Research Therapy* 4.3, p. 52.

Phinney, D G, G Kopen, W Righter, S Webster, N Tremain, and D J Prockop (1999). "Donor variation in the growth properties and osteogenic potential of human marrow stromal cells." In: *Journal of cellular biochemistry* 75.3, pp. 424–36.

Pineault, Nicolas and Ahmad Abu-Khader (2015). "Advances in umbilical cord blood stem cell expansion and clinical translation". In: *Experimental Hematology* 43.7, pp. 498–513.

Pittenger, M. F. (1999). "Multilineage Potential of Adult Human Mesenchymal Stem Cells". In: *Science* 284.5411, pp. 143–147.

Plumas, J, L Chaperot, M-J Richard, J-P Molens, J-C Bensa, and M-C Favrot (2005). "Mesenchymal stem cells induce apoptosis of activated T cells." In: *Leukemia* 19.9, pp. 1597–604.

Polchert, David, Justin Sobinsky, GW Douglas, Martha Kidd, Ada Moadsiri, Eduardo Reina, Kristyn Genrich, Swati Mehrotra, Suman Setty, Brett Smith, and Amelia Bartholomew (2008). "IFN-g activation of mesenchymal stem cells for treatment and prevention of graft versus host disease". In: *European Journal of Immunology* 38.6, pp. 1745–1755.

Potian, J. a., H. Aviv, N. M. Ponzio, J. S. Harrison, and P. Rameshwar (2003). "Veto-Like Activity of Mesenchymal Stem Cells: Functional Discrimination Between Cellular Responses to Alloantigens and Recall Antigens". In: *The Journal of Immunology* 171.7, pp. 3426–3434.

Prasad, Vinod K, Kenneth G Lucas, Gary I Kleiner, Julie An M Talano, David Jacobsohn, Gloria Broadwater, Rod Monroy, and Joanne Kurtzberg (2011). "Efficacy and safety of ex vivo cultured adult human mesenchymal stem cells (Prochymal^{TM}) in pediatric

patients with severe refractory acute graft-versus-host disease in a compassionate use study." In: *Biology of blood and marrow transplantation : journal of the American Society for Blood and Marrow Transplantation* 17.4, pp. 534–41.

Prasanna, S Jyothi, Divya Gopalakrishnan, Shilpa Rani Shankar, and Anoop Babu Vasandan (2010). "Pro-inflammatory cytokines, IFNgamma and TNFalpha, influence immune properties of human bone marrow and Wharton jelly mesenchymal stem cells differentially." In: *PloS one* 5.2, e9016.

Premer, Courtney, Arnon Blum, Michael A. Bellio, Ivonne Hernandez Schulman, Barry E. Hurwitz, Meela Parker, Christopher R. Dermarkarian, Darcy L. DiFede, Wayne Balkan, Aisha Khan, and Joshua M. Hare (2015). "Allogeneic Mesenchymal Stem Cells Restore Endothelial Function in Heart Failure by Stimulating Endothelial Progenitor Cells". In: *EBioMedicine* 2.5, pp. 467–475.

Prevosto, Claudia, Marta Zancolli, Paolo Canevali, Maria Raffaella Zocchi, and Alessandro Poggi (2007). "Generation of CD4+ or CD8+ regulatory T cells upon mesenchymal stem cell-lymphocyte interaction." In: *Haematologica* 92.07, pp. 881–8.

Quevedo, Henry C, Konstantinos E Hatzistergos, Behzad N Oskouei, Gary S Feigenbaum, Jose E Rodriguez, David Valdes, Pradip M Pattany, Juan P Zambrano, Qinghua Hu, Ian McNiece, Alan W Heldman, and Joshua M Hare (2009). "Allogeneic mesenchymal stem cells restore cardiac function in chronic ischemic cardiomyopathy via trilineage differentiating capacity." In: *Proceedings of the National Academy of Sciences of the United States of America* 106.33, pp. 14022–7.

Ra, J. C., S. K. Kang, I. S. Shin, H. G. Park, S. A. Joo, J. G. Kim, B. C. Kang, Y. S. Lee, K. Nakama, M. Piao, B. Sohl, and A. Kurtz (2011). "Stem cell treatment for patients with autoimmune disease by systemic infusion of culture-expanded autologous adipose tissue derived mesenchymal stem cells". In: *J Transl Med* 9, p. 181.

Ranganath, Sudhir H, Oren Levy, Maneesha S Inamdar, and Jeffrey M Karp (2012). "Harnessing the mesenchymal stem cell secretome for the treatment of cardiovascular disease." In: *Cell stem cell* 10.3, pp. 244–58.

Ren, Guangwen, Liying Zhang, Xin Zhao, Guangwu Xu, Yingyu Zhang, Arthur I. Roberts, Robert Chunhua Zhao, and Yufang Shi (2008). "Mesenchymal Stem Cell-Mediated Immunosuppression Occurs via Concerted Action of Chemokines and Nitric Oxide". In: *Cell Stem Cell* 2.2, pp. 141–150.

Ren, Guangwen, Xin Zhao, Liying Zhang, Jimin Zhang, Andrew L'Huillier, Weifang Ling, Arthur I Roberts, Anh D Le, Songtao Shi, Changshun Shao, and Yufang Shi (2010). "Inflammatory cytokine-induced intercellular adhesion molecule-1 and vascular cell adhesion molecule-1 in mesenchymal stem cells are critical for immunosuppression." In: *Journal of immunology (Baltimore, Md. : 1950)* 184.5, pp. 2321–8.

Ringden, O., M. Uzunel, I. Rasmusson, M. Remberger, B. Sundberg, H. Lonnies, H. U. Marschall, A. Dlugosz, A. Szakos, Z. Hassan, B. Omazic, J. Aschan, L. Barkholt, and K. Le Blanc (2006). "Mesenchymal stem cells for treatment of therapy-resistant graft-versus-host disease". In: *Transplantation* 81.10, pp. 1390–1397.

Ryan, J M, F Barry, J M Murphy, and B P Mahon (2007). "Interferon-gamma does not break, but promotes the immunosuppressive capacity of adult human mesenchymal stem cells." In: *Clinical and experimental immunology* 149.2, pp. 353–63.

Sadelain, M., R. Brentjens, and I. Riviere (2013). "The Basic Principles of Chimeric Antigen Receptor Design". In: *Cancer Discovery* 3.4, pp. 388–398.

Sakaguchi, S., K. Wing, Y. Onishi, P. Prieto-Martin, and T. Yamaguchi (2009). "Regulatory T cells: how do they suppress immune responses?" In: *International Immunology* 21.10, pp. 1105–1111.

Samsonraj, Rebekah M., Bina Rai, Padmapriya Sathiyanathan, Kia Joo Puan, Olaf Rötzschke, James H. Hui, Michael Raghunath, Lawrence W. Stanton, Victor Nurcombe, and Simon M. Cool (2015). "Establishing Criteria for Human Mesenchymal Stem Cell Potency". In: *STEM CELLS* 33.6, pp. 1878–1891.

Schallmoser, Katharina, Christina Bartmann, Eva Rohde, Simone Bork, Christian Guelly, Anna C. Obenauf, Andreas Reinisch, Patrick Horn, Anthony D. Ho, Dirk Strunk, and Wolfgang Wagner (2010). "Replicative senescence-associated gene expression changes

in mesenchymal stromal cells are similar under different culture conditions". In: *Haematologica* 95.6, pp. 867–874.

Schellenberg, Anne, Thomas Stiehl, Patrick Horn, Sylvia Joussen, Norbert Pallua, Anthony D. Ho, and Wolfgang Wagner (2012). "Population dynamics of mesenchymal stromal cells during culture expansion". In: *Cytotherapy* 14.4, pp. 401–411.

Scheuermann, R. H. and E. Racila (1995). "CD19 Antigen in Leukemia and Lymphoma Diagnosis and Immunotherapy". In: *Leukemia & Lymphoma* 18.5-6, pp. 385–397.

Schneider, Markus, Ian W. Marison, and Urs Von Stockar (1996). "The importance of ammonia in mammalian cell culture." In: *Journal of biotechnology* 46.3, pp. 161–185.

Schop, Deborah, Frank W Janssen, Linda D.S. van Rijn, Hugo Fernandes, Rolf M Bloem, Joost D. de Bruijn, and Riemke van Dijkhuizen-Radersma (2009). "Growth, Metabolism, and Growth Inhibitors of Mesenchymal Stem Cells". In: *Tissue Engineering Part A* 15.8, pp. 1877–1886.

Schwartz, Steven D, Jean-Pierre Hubschman, Gad Heilwell, Valentina Franco-Cardenas, Carolyn K Pan, Rosaleen M Ostrick, Edmund Mickunas, Roger Gay, Irina Klimanskaya, and Robert Lanza (2012). "Embryonic stem cell trials for macular degeneration: a preliminary report". In: *The Lancet* 379.9817, pp. 713–720.

Selmani, Zohair, Abderrahim Naji, Ines Zidi, Benoit Favier, Emilie Gaiffe, Laurent Obert, Christophe Borg, Philippe Saas, Pierre Tiberghien, Nathalie Rouas-Freiss, Edgardo D Carosella, and Frederic Deschaseaux (2008). "Human leukocyte antigen-G5 secretion by human mesenchymal stem cells is required to suppress T lymphocyte and natural killer function and to induce CD4+CD25highFOXP3+ regulatory T cells." In: *Stem cells (Dayton, Ohio)* 26.1, pp. 212–22.

Sharpe, N, H Smith, J Murphy, S Greaves, H Hart, and G Gamble (1991). "Early prevention of left ventricular dysfunction after myocardial infarction with angiotensin-converting-enzyme inhibition". In: *The Lancet* 337.8746, pp. 872–876.

Shen, Chongyang, Puchang Lie, Tianyu Miao, Meixing Yu, Qiao Lu, Ting Feng, Jinrong Li, Tingting Zu, Xiaohuan Liu, and Hong Li (2015). "Conditioned medium from um-

bilical cord mesenchymal stem cells induces migration and angiogenesis". In: *Molecular Medicine Reports*, pp. 20–30.

Siddappa, Ramakrishnaiah, Ruud Licht, Clemens van Blitterswijk, and Jan de Boer (2007). "Donor variation and loss of multipotency during in vitro expansion of human mesenchymal stem cells for bone tissue engineering". In: *Journal of Orthopaedic Research* 25.8, pp. 1029–1041.

Siegel, Georg, Torsten Kluba, Ursula Hermanutz-Klein, Karen Bieback, Hinnak Northoff, and Richard Schäfer (2013). "Phenotype, donor age and gender affect function of human bone marrow-derived mesenchymal stromal cells." In: *BMC medicine* 11, p. 146.

Silva, Meirelles da, Arnold I. Caplan, and Nance Beyer Nardi (2008). "In Search of the In Vivo Identity of Mesenchymal Stem Cells". In: *Stem Cells* 26.9, pp. 2287–2299.

Silva, W. A. (2003). "The Profile of Gene Expression of Human Marrow Mesenchymal Stem Cells". In: *Stem Cells* 21.6, pp. 661–669.

Sotiropoulou, Panagiota A., Sonia A. Perez, Angelos D. Gritzapis, Constantin N. Baxevanis, and Michael Papamichail (2006). "Interactions Between Human Mesenchymal Stem Cells and Natural Killer Cells". In: *Stem Cells* 24.1, pp. 74–85.

Spaggiari, G. M., A. Capobianco, H. Abdelrazik, F. Becchetti, M. C. Mingari, and L. Moretta (2007). "Mesenchymal stem cells inhibit natural killer-cell proliferation, cytotoxicity, and cytokine production: role of indoleamine 2, 3-dioxygenase and prostaglandin E2". In: *Blood* 111.3, pp. 1327–1333.

Sreeramkumar, Vinatha, Manuel Fresno, and Natalia Cuesta (2011). "Prostaglandin E2 and T cells: friends or foes?" In: *Immunology and Cell Biology* 90.6, pp. 579–586.

Staton, Carolyn A., Malcolm W. R. Reed, and Nicola J. Brown (2009). "A critical analysis of current in vitro and in vivo angiogenesis assays". In: *International Journal of Experimental Pathology* 90.3, pp. 195–221.

Stroncek, David F, Ping Jin, Ena Wang, and Betsy Jett (2007). "Potency analysis of cellular therapies: the emerging role of molecular assays". In: *Journal of Translational Medicine* 5.1, p. 24.

Suni, Maria A, Holli S Dunn, Patricia L Orr, Rian de Laat, Elizabeth Sinclair, Smita A Ghanekar, Barry M Bredt, John F Dunne, Vernon C Maino, and Holden T Maecker (2003). "Performance of plate-based cytokine flow cytometry with automated data analysis". In: *BMC Immunol* 4.1, p. 9.

Sutton, M. G. St. J. and N. Sharpe (2000). "Left Ventricular Remodeling After Myocardial Infarction : Pathophysiology and Therapy". In: *Circulation* 101.25, pp. 2981–2988.

Sylvester, Paul W. (2011). "Optimization of the Tetrazolium Dye (MTT) Colorimetric Assay for Cellular Growth and Viability". In: pp. 157–168.

Tabera, S., J. A. Perez-Simon, M. Diez-Campelo, L. I. Sanchez-Abarca, B. Blanco, A. Lopez, A. Benito, E. Ocio, F. M. Sanchez-Guijo, C. Canizo, and J. F. San Miguel (2008). "The effect of mesenchymal stem cells on the viability, proliferation and differentiation of B-lymphocytes". In: *Haematologica* 93.9, pp. 1301–1309.

Takahashi, Kazutoshi and Shinya Yamanaka (2006). "Induction of Pluripotent Stem Cells from Mouse Embryonic and Adult Fibroblast Cultures by Defined Factors". In: *Cell* 126.4, pp. 663–676.

Tan, Kah Yong, Kim Leng Teo, Jessica F.Y. Lim, Allen K.L. Chen, Shaul Reuveny, and Steve Kw Oh (2015). "Serum-free media formulations are cell line–specific and require optimization for microcarrier culture". In: *Cytotherapy* 17.8, pp. 1152–1165.

Tan, P. K. (2003). "Evaluation of gene expression measurements from commercial microarray platforms". In: *Nucleic Acids Research* 31.19, pp. 5676–5684.

Tanavde, Vivek, Candida Vaz, Mahendra S. Rao, Mohan C. Vemuri, and Radhika R. Pochampally (2015). "Research using Mesenchymal Stem/Stromal Cells: quality metric towards developing a reference material". In: *Cytotherapy* 17.9, pp. 1169–1177.

Tarca, Adi L., Roberto Romero, and Sorin Draghici (2006). "Analysis of microarray experiments of gene expression profiling". In: *American Journal of Obstetrics and Gynecology* 195.2, pp. 373–388.

Terness, P., T. M. Bauer, L. Rose, C. Dufter, A. Watzlik, H. Simon, and G. Opelz (2002). "Inhibition of Allogeneic T Cell Proliferation by Indoleamine 2, 3-Dioxygenase-

expressing Dendritic Cells: Mediation of Suppression by Tryptophan Metabolites". In: *Journal of Experimental Medicine* 196.4, pp. 447–457.

Thomson, J. A. (1998). "Embryonic Stem Cell Lines Derived from Human Blastocysts". In: *Science* 282.5391, pp. 1145–1147.

Timmers, Leo, Sai Kiang Lim, Imo E. Hoefer, Fatih Arslan, Ruenn Chai Lai, Angelique A.M. van Oorschot, Marie Jose Goumans, Chaylendra Strijder, Sui Kwan Sze, Andree Choo, Jan J. Piek, Pieter A. Doevendans, Gerard Pasterkamp, and Dominique P.V. de Kleijn (2011). "Human mesenchymal stem cell-conditioned medium improves cardiac function following myocardial infarction". In: *Stem Cell Research* 6.3, pp. 206–214.

Tondreau, Tatiana, Nathalie Meuleman, Alain Delforge, Marielle Dejeneffe, Rita Leroy, Martine Massy, Christine Mortier, Dominique Bron, and Laurence Lagneaux (2005). "Mesenchymal Stem Cells Derived from CD133-Positive Cells in Mobilized Peripheral Blood and Cord Blood: Proliferation, Oct4 Expression, and Plasticity". In: *Stem Cells* 23.8, pp. 1105–1112.

Tonnesen, M. G., X. Feng, and R. a F Clark (2000). "Angiogenesis in wound healing". In: *Journal of Investigative Dermatology Symposium Proceedings* 5.1, pp. 40–46.

Uccelli, Antonio, Lorenzo Moretta, and Vito Pistoia (2006). "Immunoregulatory function of mesenchymal stem cells". In: *European Journal of Immunology* 36.10, pp. 2566–2573.

Vaes, Bart, Wouter Van't Hof, Robert Deans, and Jef Pinxteren (2012). "Application of MultiStem Allogeneic Cells for Immunomodulatory Therapy: Clinical Progress and Pre-Clinical Challenges in Prophylaxis for Graft Versus Host Disease". In: *Front. Immun.* 3.

Vailhé, B, D Vittet, and J J Feige (2001). "In vitro models of vasculogenesis and angiogenesis." In: *Laboratory investigation; a journal of technical methods and pathology* 81.4, pp. 439–452.

Veeraputhiran, Muthu, Lakshmikanth Katragadda, Appathurai Balamurugan, and Michele Cottler-Fox (2011). "Aldehyde dehydrogenase as an alternative to enumeration of total and viable CD34 cells in autologous hematopoietic progenitor cell transplantation". In: *Cytotherapy* 13.10, pp. 1256–1258.

Vertès, Alain A. (2016). "Deployment of stem cell technologies in industry and healthcare". In: *Science, regulation and business strategies*. Wiley-Blackwell, pp. 693–722.

Viswanathan, Sowmya, Armand Keating, Robert Deans, Peiman Hematti, Darwin Prockop, David F. Stroncek, Glyn Stacey, Dan J. Weiss, Christopher Mason, and Mahendra S. Rao (2014). "Soliciting Strategies for Developing Cell-Based Reference Materials to Advance Mesenchymal Stromal Cell Research and Clinical Translation". In: *Stem Cells and Development* 23.11, pp. 1157–1167.

Wagner, Wolfgang, Patrick Horn, Mirco Castoldi, Anke Diehlmann, Simone Bork, Rainer Saffrich, Vladimir Benes, Jonathon Blake, Stefan Pfister, Volker Eckstein, and Anthony D Ho (2008). "Replicative senescence of mesenchymal stem cells: a continuous and organized process." In: *PloS one* 3.5, e2213.

Waltz, Emily (2013). "Mesoblast acquires Osiris' stem cell business". In: *Nature Biotechnology* 31.12, pp. 1061–1061.

Wang, Hwai-Shi, Shih-Chieh Hung, Shu-Tine Peng, Chun-Chieh Huang, Hung-Mu Wei, Yi-Jhih Guo, Yu-Show Fu, Mei-Chun Lai, and Chin-Chang Chen (2004). "Mesenchymal Stem Cells in the Whartons Jelly of the Human Umbilical Cord". In: *Stem Cells* 22.7, pp. 1330–1337.

Wang, Y, Z Zhang, Y Chi, Q Zhang, F Xu, Z Yang, L Meng, S Yang, S Yan, A Mao, J Zhang, Y Yang, S Wang, J Cui, L Liang, Y Ji, Z-B Han, X Fang, and Z C Han (2013). "Long-term cultured mesenchymal stem cells frequently develop genomic mutations but do not undergo malignant transformation". In: *Cell Death Dis* 4.12, e950.

Watson, J. T., T. Foo, J. Wu, B. R. Moed, M. Thorpe, L. Schon, and Z. Zhang (2013). "CD271 as a marker for mesenchymal stem cells in bone marrow versus umbilical cord blood". In: *Cells Tissues Organs (Print)* 197.6, pp. 496–504.

Wilkie, Scott, May C I Van Schalkwyk, Steve Hobbs, David M. Davies, Sjoukje J C Van Der Stegen, Ana C Parente Pereira, Sophie E. Burbridge, Carol Box, Suzanne A. Eccles, and John Maher (2012). "Dual targeting of ErbB2 and MUC1 in breast cancer using chimeric antigen receptors engineered to provide complementary signaling". In: *Journal of Clinical Immunology* 32.5, pp. 1059–1070.

Williams, Adam R. and Joshua M. Hare (2011). "Mesenchymal stem cells: Biology, pathophysiology, translational findings, and therapeutic implications for cardiac disease". In: *Circulation Research* 109.8, pp. 923–940. arXiv: NIHMS150003.

Williams, Adam R., Konstantinos E. Hatzistergos, Benjamin Addicott, Fred McCall, Decio Carvalho, Viky Suncion, Azorides R. Morales, Jose Da Silva, Mark A. Sussman, Alan W. Heldman, and Joshua M. Hare (2012). "Enhanced Effect of Combining Human Cardiac Stem Cells and Bone Marrow Mesenchymal Stem Cells to Reduce Infarct Size and to Restore Cardiac Function After Myocardial InfarctionClinical Perspective". In: *Circulation* 127.2, pp. 213–223.

Xin, Xiaohua, Suya Yang, Gladys Ingle, Constance Zlot, Linda Rangell, Joe Kowalski, Ralph Schwall, Napoleone Ferrara, and Mary E. Gerritsen (2001). "Hepatocyte Growth Factor Enhances Vascular Endothelial Growth Factor-Induced Angiogenesis in Vitro and in Vivo". In: *The American Journal of Pathology* 158.3, pp. 1111–1120.

Xing, Z, J Gauldie, G Cox, H Baumann, M Jordana, X F Lei, and M K Achong (1998). "IL-6 is an antiinflammatory cytokine required for controlling local or systemic acute inflammatory responses." In: *The Journal of clinical investigation* 101.2, pp. 311–20.

Yang, F, S.-W. Cho, S M Son, S R Bogatyrev, D Singh, J J Green, Y Mei, S Park, S H Bhang, B.-S. Kim, R Langer, and D G Anderson (2010). "Genetic engineering of human stem cells for enhanced angiogenesis using biodegradable polymeric nanoparticles". In: *Proceedings of the National Academy of Sciences* 107.8, pp. 3317–3322.

Yao, Yongwei, Fumin Zhang, Liansheng Wang, Guohui Zhang, Zhaojun Wang, Jianmei Chen, and Xiang Gao (2009). "Lipopolysaccharide preconditioning enhances the efficacy of mesenchymal stem cells transplantation in a rat model of acute myocardial infarction". In: *Journal of Biomedical Science* 16.1, p. 74.

Yoo, Keon Hee, In Keun Jang, Myoung Woo Lee, Hyo Eun Kim, Mal Sook Yang, Youngwoo Eom, Jong Eun Lee, Young Jin Kim, Seong Kyu Yang, Hye Lim Jung, Ki Woong Sung, Cheol Woo Kim, and Hong Hoe Koo (2009). "Comparison of immunomodulatory properties of mesenchymal stem cells derived from adult human tissues". In: *Cellular Immunology* 259.2, pp. 150–156.

Young, Henry E., Timothy A. Steele, Robert A. Bray, John Hudson, Julie A. Floyd, Kristina Hawkins, Karen Thomas, Troy Austin, Chris Edwards, Jeremy Cuzzourt, Mary Duenzl, Paul A. Lucas, and Asa C. Black (2001). "Human reserve pluripotent mesenchymal stem cells are present in the connective tissues of skeletal muscle and dermis derived from fetal, adult, and geriatric donors". In: *Anat. Rec.* 264.1, pp. 51–62.

Zanella, Fabian, James B. Lorens, and Wolfgang Link (2010). "High content screening: seeing is believing". In: *Trends in Biotechnology* 28.5, pp. 237–245.

Zimmerlin, Ludovic, Vera S. Donnenberg, Melanie E. Pfeifer, E. Michael Meyer, Bruno Péault, J. Peter Rubin, and Albert D. Donnenberg (2010). "Stromal vascular progenitors in adult human adipose tissue". In: *Cytometry Part A* 77A.1, pp. 22–30.

Zimmerlin, Ludovic, Vera S. Donnenberg, J. Peter Rubin, and Albert D. Donnenberg (2013). "Mesenchymal markers on human adipose stem/progenitor cells". In: *Cytometry Part A* 83A.1, pp. 134–140.

Appendix A

Appendix

Table A.1: Number of bone marrow-derived hMSC clinical trials from 2011 to 2015 grouped into treatment area

	Year			
Area	**2011-2012**	**2012-2013**	**2013-2014**	**2014-2015**
Immune System Diseases	4	8	8	9
Wounds and Injuries	0	2	2	0
Muscle, Bone, and Cartilage Repair	16	10	11	8
Heart and Vascular Diseases	10	10	10	6
Digestive System Diseases	0	0	0	3
Respiratory Tract (Lung and Bronchial) Diseases	1	3	4	2
Ear, Nose, and Throat Diseases	2	0	0	1
Eye Diseases	0	0	0	2
Nervous System Diseases	4	9	9	9
Nutritional and Metabolic Diseases	7	2	2	3
Skin and Connective Tissue Diseases	0	1	1	0
Symptoms and General Pathology	0	0	0	1
Urinary Tract, Sexual Organs, and Pregnancy Conditions	0	1	1	5
Total	**44**	**46**	**48**	**49**

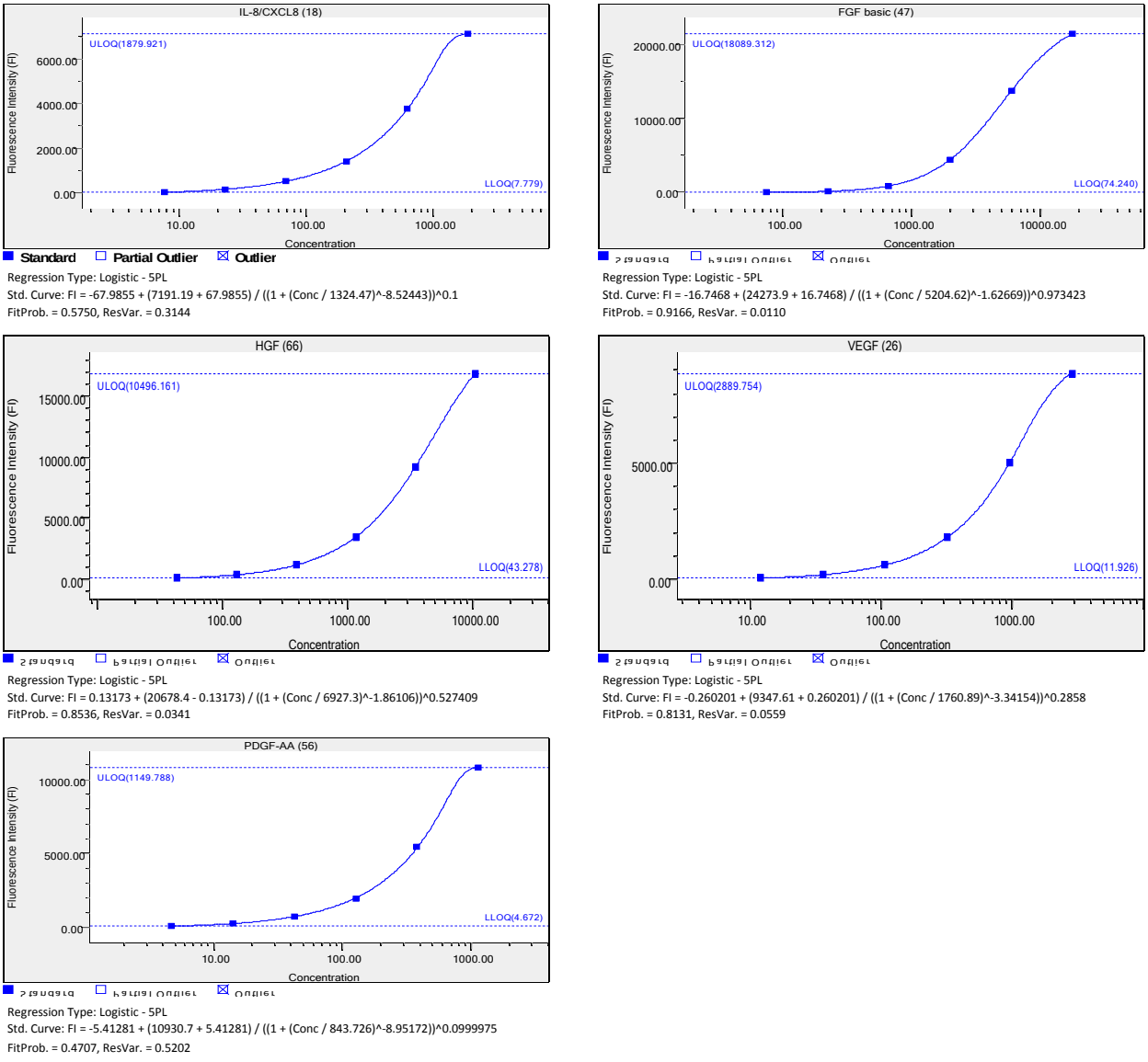

Figure A.1: Standard curves generated for IL-8, FGF-basic, HGF, VEGF and PDGF-AA for the Luminex assay